



Kent Academic Repository

de Sousa Loreto Aresta Branco, Mafalda (2020) *Drug delivery model to inform investigations into bladder pathophysiology: potential role for suburothelial pericyte cells*. Doctor of Philosophy (PhD) thesis, University of Kent,.

Downloaded from

<https://kar.kent.ac.uk/80942/> The University of Kent's Academic Repository KAR

The version of record is available from

This document version

UNSPECIFIED

DOI for this version

Licence for this version

CC BY-NC (Attribution-NonCommercial)

Additional information

Versions of research works

Versions of Record

If this version is the version of record, it is the same as the published version available on the publisher's web site. Cite as the published version.

Author Accepted Manuscripts

If this document is identified as the Author Accepted Manuscript it is the version after peer review but before type setting, copy editing or publisher branding. Cite as Surname, Initial. (Year) 'Title of article'. To be published in *Title of Journal*, Volume and issue numbers [peer-reviewed accepted version]. Available at: DOI or URL (Accessed: date).

Enquiries

If you have questions about this document contact ResearchSupport@kent.ac.uk. Please include the URL of the record in KAR. If you believe that your, or a third party's rights have been compromised through this document please see our [Take Down policy](https://www.kent.ac.uk/guides/kar-the-kent-academic-repository#policies) (available from <https://www.kent.ac.uk/guides/kar-the-kent-academic-repository#policies>).

Drug delivery model to inform
investigations into bladder
pathophysiology: potential role for
suburothelial pericyte cells

MAFALDA DE SOUSA LORETO ARESTA BRANCO

A thesis submitted in partial fulfilment of the requirements of the
University of Kent and the University of Greenwich for the Degree of
Doctor of Philosophy

This research programme was carried out in collaboration with
Cardiff University

February 2020

DECLARATION

I certify that this work has not been accepted in substance for any degree, and is not concurrently being submitted for any degree other than that of Doctor of Philosophy being studied at the Universities of Greenwich and Kent. I also declare that this work is the result of my own investigations except where otherwise identified by references and that I have not plagiarised the work of others.

Mafalda Aresta Branco
.....

Mafalda Aresta Branco

February, 2020

ACKNOWLEDGMENTS

First, I would like to give a special thank you to my supervisors Scott P. Wildman, Claire Peppiatt-Wildman and Jenna Bowen. All the amazing support, wisdom and words of encouragement you have provided me with throughout this project meant a great deal to me. I am also very grateful to Kirsti Taylor for her support, time and dedication.

Many thanks to Dave Havard and Neil James who kindly donated pig bladders for this project. In addition, I would like to thank Derek Scarborough for his histology work.

A massive thank you goes to my lab colleagues (and good friends): Rebecca, Will, Danny, Elena and Nikos. I had a fantastic time with all of you in (and out of) the lab, not only exchanging ideas and knowledge related to work but also having fun socialising. A special thank you also to Kar Lai, who was an amazing help in the delivery studies of ketamine.

I would also like to thank a few friends outside of work who made my PhD journey much more enjoyable. Living abroad would have been ten times more challenging without their friendship and support. A big thank you to all my friends from Cardiff, in particular Steffy, Joana, Adi, Shakil and Alex and to all my friends from Medway, specially Kwan and Adam. Also, thank you to Sanne, Josep, Carmen, Christian and Francisco, because with you by my side Erasmus never ends.

And finally, to my family: Obrigada por tudo! A distância não é fácil e as saudades são muitas mas mesmo de longe senti que estiveram sempre comigo, com apoio e amor incondicional. Obrigada por acreditarem sempre em mim, beijinhos com muito amor.

ABSTRACT

Pathologies affecting the bladder, such as overactive bladder, interstitial cystitis/bladder pain syndrome and ketamine-induced cystitis have a dramatic effect on quality of life. Unfortunately, the pathological mechanisms are poorly understood and therefore treatment is mostly empirical, often ineffective or with intolerable side effects.

Intravesical drug delivery is a therapeutic strategy that provides direct delivery of drugs into the bladder, minimizing systemic side effects associated with oral therapies. However, there is limited knowledge regarding drug distribution across the different bladder layers when an effect beyond the superficial layer is desired. In a proof of concept study, an *ex vivo* porcine whole bladder model was used to investigate the bladder wall distribution of lidocaine after intravesical instillation with clinically relevant solutions. It was demonstrated that concentrations within all layers of the bladder are dependent on the pH and concentration of the solution administered. Alkalinised lidocaine resulted in higher concentrations within the bladder and was less affected by urine dilution but was also associated with severe urothelial changes.

In a subsequent study, the aim was to estimate the concentrations of ketamine accumulated in the urine following recreational use and investigate if urinary ketamine penetrates the bladder wall to achieve harmful concentrations, which ultimately lead to the development of ketamine-induced cystitis. Higher concentration and longer exposure to ketamine were associated with urothelial damage, supporting the hypothesis that urinary ketamine has a direct toxic effect. It has also been proposed that the pathophysiological mechanism involves microvascular changes induced by ketamine. To investigate this further, a viable murine bladder tissue model was developed to study microvascular blood flow regulation, with a particular focus on the role of pericyte cells. Using this model, it was observed that ketamine evoked pericyte-mediated constriction of the suburothelial capillaries of the bladder, which may translate *in vivo* into reduction of blood flow to the tissue and eventually lead to bladder dysfunction.

Overall, this thesis highlights that changes to the barrier function and microvascular blood flow can have an important role in bladder pathophysiology.

CONTENTS

DECLARATION	2
ACKNOWLEDGMENTS	3
ABSTRACT	4
CONTENTS.....	5
FIGURES	10
TABLES	13
CHAPTER 1 - GENERAL INTRODUCTION	14
1.1. Overview of the bladder.....	14
1.2. Bladder wall structure	16
1.3. Bladder innervation and control of micturition	19
1.3.1. Micturition cycle	20
1.3.2. Mucosa sensory and contractile properties.....	22
1.4. Microvasculature	25
1.5. Lower urinary tract symptoms (LUTS).....	29
1.5.1. Overactive bladder	29
1.5.2. Interstitial cystitis/ bladder pain syndrome	31
1.5.3. Ketamine-induced cystitis	33
1.6. Intravesical drug delivery	39
1.7. Models to study bladder physiology and dysfunction	41
1.8. Aims and objectives.....	45
Chapter 2 – General methodology	47
2.1. Drug delivery studies	47
2.1.1. Reagents and solvents.....	47
2.1.2. Tissue preparation.....	47
2.1.3. Cryosectioning	49

2.1.4. Drug extraction, analysis and quantification.....	49
2.1.5. Histology.....	49
2.2. Murine tissue model to study the microvasculature properties and function <i>in situ</i>	51
2.2.1. Tissue preparation.....	51
2.2.2. Tissue viability.....	51
2.2.3. DIC imaging and functional experiments	52
2.2.4. Immunohistochemistry	54
2.3. Statistical analysis.....	57
Chapter 3 – Intravesical drug delivery studies – Lidocaine.....	58
3.1. Introduction.....	58
3.1.1. Clinical relevance of intravesical delivery of lidocaine.....	58
3.1.2. Hypothesis and aims.....	63
3.2. Methods.....	65
3.2.1. Intravesical instillation of lidocaine hydrochloride (LH).....	65
3.2.2. Cryosectioning	65
3.2.3. Lidocaine extraction	66
3.2.4. Quantification of lidocaine in the bladder wall.....	66
3.2.5. Histology.....	67
3.2.6. Statistical analysis.....	67
3.3. Results.....	68
3.3.1. Quantification of lidocaine in the bladder wall.....	68
3.3.3. Histology.....	73
3.4. Discussion	76
3.5. Conclusions.....	82
Chapter 4 – Intravesical drug delivery studies – Ketamine hydrochloride.....	83

4.1. Introduction	83
4.1.1. Historical perspective	83
4.1.2. Recreational use of ketamine – global panorama.....	83
4.1.3. Complications of ketamine use	84
4.1.4. Chemical properties of ketamine and pharmacokinetics	89
4.1.6. Hypothesis and aims.....	91
4.2. Methods.....	93
4.2.1. Intravesical delivery of ketamine hydrochloride (KH).....	93
4.2.2. Cryosectioning	94
4.2.3. Ketamine extraction	95
4.2.4. Quantification of ketamine in the bladder wall	95
4.2.5. Histology.....	95
4.2.6. Statistical analysis.....	96
4.3. Results.....	97
4.3.1. Pharmacokinetic modelling.....	97
4.3.1. Quantification of ketamine in the bladder wall	99
4.3.2 Histology	105
4.4. Discussion	108
4.5. Conclusions	111
Chapter 5 – Establishing an <i>ex-vivo</i> murine tissue model to investigate microvasculature properties and function in the bladder	112
5.1. Introduction.....	112
5.1.1. The role of vascular changes in bladder dysfunction	112
5.1.2. Investigating blood flow through capillaries in live bladder tissue.....	116
5.1.3. Hypothesis and aims.....	122
5.2. Methods.....	122

5.2.1. Tissue preparation	122
5.2.2. Tissue viability.....	122
5.2.3. DIC imaging and pericyte functional experiments	122
5.2.4. α -SMA and NG2 immunoreactivity of perivascular cells.....	123
5.2.5. Statistical analysis	123
5.3. Results.....	124
5.3.1. Tissue viability.....	124
5.3.2. DIC imaging and pericyte functional experiments	126
5.3.3. α -SMA and NG2 immunoreactivity of perivascular cells.....	138
5.4. Discussion	140
5.4.1. Tissue viability.....	140
5.4.2. DIC imaging and pericyte functional experiments	141
5.4.3. α -SMA and NG2 immunoreactivity of perivascular cells.....	145
5.5. Conclusions.....	146
Chapter 6 – Ketamine effect in microvasculature.....	147
6.1 Introduction	147
6.1.1. Pharmacodynamics of ketamine	147
6.1.1.2. Ketamine effect on vascular reactivity or tone	149
6.1.2. Hypotheses and aims.....	150
6.2. Methods.....	152
6.2.1. Tissue preparation	152
6.2.2. DIC imaging and pericyte functional experiments	152
6.2.3 NG2/GS-IB4 co-staining	152
6.2.4 Statistical analysis	152
6.3. Results.....	153
6.3.1. Functional experiments	153

6.3.2 Immunohistochemical features (NG2/IB4)	158
6.4 Discussion	161
6.4.1. DIC imaging and pericyte functional experiments	161
6.4.2. Immunohistochemical features (NG2/IB4)	163
6.5. Conclusions.....	166
GENERAL OVERVIEW OF THE THESIS.....	167
REFERENCES.....	173

FIGURES

Figure 1. Anatomy of the urinary system and frontal sections of the male and female urinary bladders.....	14
Figure 2. Anterior view of the frontal section of the female and male urinary bladder.	15
Figure 3. Cross-section of urinary bladder wall.....	16
Figure 4. Efferent innervation and neurotransmitters involved in regulation of the urinary bladder.	21
Figure 5. Neural circuits that control the micturition cycle.	22
Figure 6. Mucosa sensory role.....	24
Figure 7. Suburothelial capillary networks.....	26
Figure 8 Diagram showing the heterogeneity of mural cells along the microvasculature	27
Figure 9 Morphological features of mural cells in the suburothelial microvasculature of mouse bladder.....	28
Figure 10 Empty porcine bladder.	47
Figure 11 Experimental set up.....	48
Figure 12 Cryosectioning	49
Figure 13 Mouse bladder full of urine.....	51
Figure 14 DIC imaging.....	53
Figure 15 Dissection of murine bladder tissue.....	54
Figure 16 Chemical structure of lidocaine hydrochloride	58
Figure 17 Calibration curve of lidocaine hydrochloride (LH).....	68
Figure 18 HPLC chromatograms of lidocaine hydrochloride (LH)	68
Figure 19 Profiles of intravesical delivery of lidocaine hydrochloride (LH) - undiluted set.	70
Figure 20 Profiles of intravesical delivery of lidocaine hydrochloride (LH) - undiluted and urine-diluted sets.....	72
Figure 21 Photomicrographs of histological porcine bladder sections stained with Masson's Trichrome	74

Figure 22 Photomicrographs of histological porcine bladder sections stained with Masson’s Trichrome	75
Figure 23 Histological section of porcine bladder sample stained with haematoxylin eosin.	77
Figure 24 Correlations between symptom scores and duration of ketamine abuse.....	88
Figure 25 Chemical structure of ketamine hydrochloride	89
Figure 26 Estimated cumulative amount of ketamine in urine over 24 h	98
Figure 27 (a) Estimated cumulative mass of ketamine in urine in 4 h (b) estimated concentration of ketamine in urine in 4 h.....	99
Figure 28. Calibration curve of ketamine hydrochloride (KH).....	99
Figure 29. HPLC chromatogram of ketamine hydrochloride (KH).....	100
Figure 30 Profiles of intravesical delivery of ketamine hydrochloride (KH) 3mM and 6 mM.....	101
Figure 31 Intravesical delivery of KH 0.3 mM.....	102
Figure 32 Profiles of intravesical delivery of ketamine hydrochloride (KH) gradient concentration	104
Figure 33 Photomicrographs of histological porcine bladder sections stained with Masson’s Trichrome	105
Figure 34 Photomicrographs of histological porcine bladder sections stained with Masson’s Trichrome	107
Figure 35 Arterial supply of the male bladder.....	112
Figure 36 Fluorescence images of bladder tissue labelled with Hoechst 33342 and propidium iodide (PI).....	124
Figure 37 Representative fluorescence images of bladder tissue stained at different time points after animal dissection	125
Figure 38– Functional experiments - Angiotensin II (Ang II)	127
Figure 39 Functional experiments – Endothelin-1 (ET-1).....	129
Figure 40 Functional experiments – Noradrenaline (NA)	131
Figure 41 Functional experiments – Prostaglandin E ₂ (PGE ₂).....	134
Figure 42 Functional experiments – Prostaglandin E ₂ (PGE ₂).....	135
Figure 43 Functional experiments – Indomethacin.....	137

Figure 44 α -SMA/NG2/Hoechst immunohistochemical staining of the suburothelial microvasculature of the bladder)	139
Figure 45 NMDA receptor	148
Figure 46 Functional experiments – Ketamine (KH).....	155
Figure 47 Functional experiments – Glycine	157
Figure 48 Confocal image of a mouse bladder mucosa preparation (where urothelium was not removed) stained with GS-IB4 conjugated with Alexa Fluor® 488.....	158
Figure 49 Representative confocal images of the capillary network.....	159
Figure 50 Pericyte density (number of pericytes/10 000 μm^2 , a), distance between pericytes (b), capillary diameter at pericyte sites (c) and non-pericyte sites (d) and pericyte morphology (cell body height, e), width, f) and processes along vessel's length (g) after incubation for 4 h with Krebs buffer, KH 10 $\mu\text{g}/\text{mL}$, 30 $\mu\text{g}/\text{mL}$ and 100 $\mu\text{g}/\text{mL}$	160

TABLES

Table 1 Masson's trichrome protocol	50
Table 2 Summary of pharmacokinetic parameters of racemic ketamine.....	91
Table 3 Solutions of KH prepared in artificial urine were added every 20 min with a variable concentration	94
Table 4. Pharmacokinetic parameters of racemic ketamine for nasal administration and values assumed for the present study	98
Table 5 DIC imaging of live bladder tissue demonstrates pericyte-mediated regulation of capillary diameter in response to angiotensin II (Ang II; 10 nM, 100 nM and 300 nM).	126
Table 6 Summary of main findings from DIC experiments to study capillary functional responses to endothelin-1 (ET-1; 1 nM, 10 nM)	128
Table 7 Summary of main findings from DIC experiments to study capillary functional responses to noradrenaline (NA; 10nM).....	130
Table 8 Summary of main findings from DIC experiments to study capillary functional responses to Prostaglandin E ₂ (PGE ₂ ; 10 μM, 30 μM and 100 μM).	133
Table 9 Summary of main findings from DIC experiments to study capillary functional responses to ketamine (KH; 10 μg/mL, 100 μg/mL and 300 μg/mL)	154

CHAPTER 1 - GENERAL INTRODUCTION

1.1. Overview of the bladder

The urinary bladder (Figure 1) is a hollow muscular organ located anteriorly in the pelvic cavity. (Miftahof and Nam, 2013) Urine generated in the kidneys is transported through the ureters and collected in the bladder, where it is stored prior to voluntary voiding. (Hill, 2015) This organ is highly distensible, being able to accommodate on average 300 - 600 mL of urine, with low intravesical pressure during the filling stage. However, a first urge to void often occurs with a urine volume of between 150 and 300 mL (25 – 50% of the bladder maximum capacity). (Wyndaele and Wachter, 2002; Andersson and Arner, 2004; GuhaSarkar and Banerjee, 2010; Fry and Vahabi, 2016) Micturition (urination) is under neurohormonal control as is discussed in greater detail in 1.3. Bladder innervation and control of micturition.

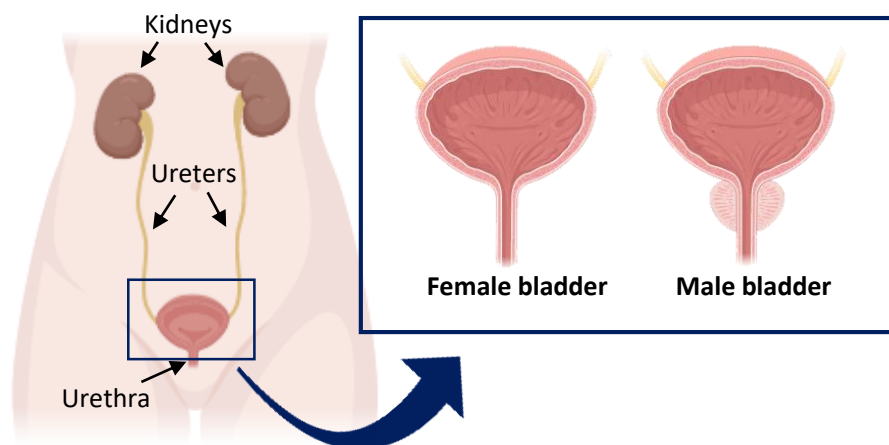


Figure 1. Anatomy of the urinary system and frontal sections of the male and female urinary bladders. The urinary bladder is located anteriorly in the pelvic cavity. Urine produced in the kidneys is transported through the ureters into the bladder. Urine is stored inside the bladder until voluntary voiding, when it is excreted through the urethra. (Hill, 2015) Images were created with BioRender.

Urine composition, osmolality and pH differ greatly from the blood. In physiological conditions, urine osmolality ranges from 50 - 1300 mOsm/Kg H₂O whereas serum osmolality varies between 280 - 300 mOsm/Kg H₂O. (Cahill, Fry and Foxall, 2003) Also, urine pH can assume a broad range of values, typically from 4.5 to 8, which contrasts with plasma, the pH of which is tightly regulated to 7.4. (GuhaSarkar and Banerjee, 2010) To maintain the gradient, the bladder wall constitutes a very efficient urine-blood barrier. Accordingly, the urothelium (the apical membrane of the bladder wall, section

1.2. Bladder wall structure) has the highest transepithelial electrical resistance (TEER, a measure of ion permeability) of all epithelial membranes reported to date. (Lewis, 2000) As such, urine can be held for several hours inside the bladder without significant movement of water, urea, ammonia or other solutes and electrolytes present in the urine back to the bloodstream. (Negrete *et al.*, 1996)

Anatomical features of the bladder include the apex, body and fundus (or base), where the trigone and neck are located. Urine enters the bladder through the ureteral orifices and is eliminated through the urethra, upon relaxation of the internal urethral sphincter and contraction of the detrusor muscle. These three orifices demark the trigone, a triangular region with smooth muscle walls that connects with the neck in the proximities of the internal urinary sphincter (Figure 2). (Miftahof and Nam, 2013)

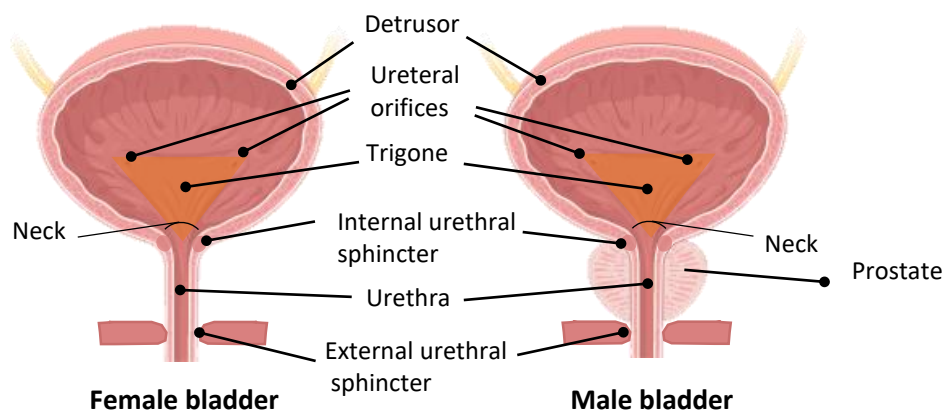


Figure 2. Anterior view of the frontal section of the female and male urinary bladder. The urinary bladder is a hollow muscular organ. The ureteral and urethra orifices demark the trigone region, which connects with the neck in the proximities of the internal urinary sphincter. Urine enters through the ureter orifices and is stored in the bladder until voluntary voiding. During voiding, the detrusor muscle contracts and the internal and external (voluntary) sphincters relax for the urine to be excreted through the urethra. (Miftahof and Nam, 2013) Image was created with BioRender.

1.2. Bladder wall structure

The bladder wall can be differentiated histologically into the mucosa, which is comprised of the urothelium and lamina propria, the detrusor and the serosa/adventitia, as evidenced in Figure 3. Even though these layers have distinct morphology and functional roles, the normal physiology of the bladder relies on their complex communication, through paracrine, neuro and hormonal mechanisms. (Birder and Andersson, 2013; Fry and Vahabi, 2016)

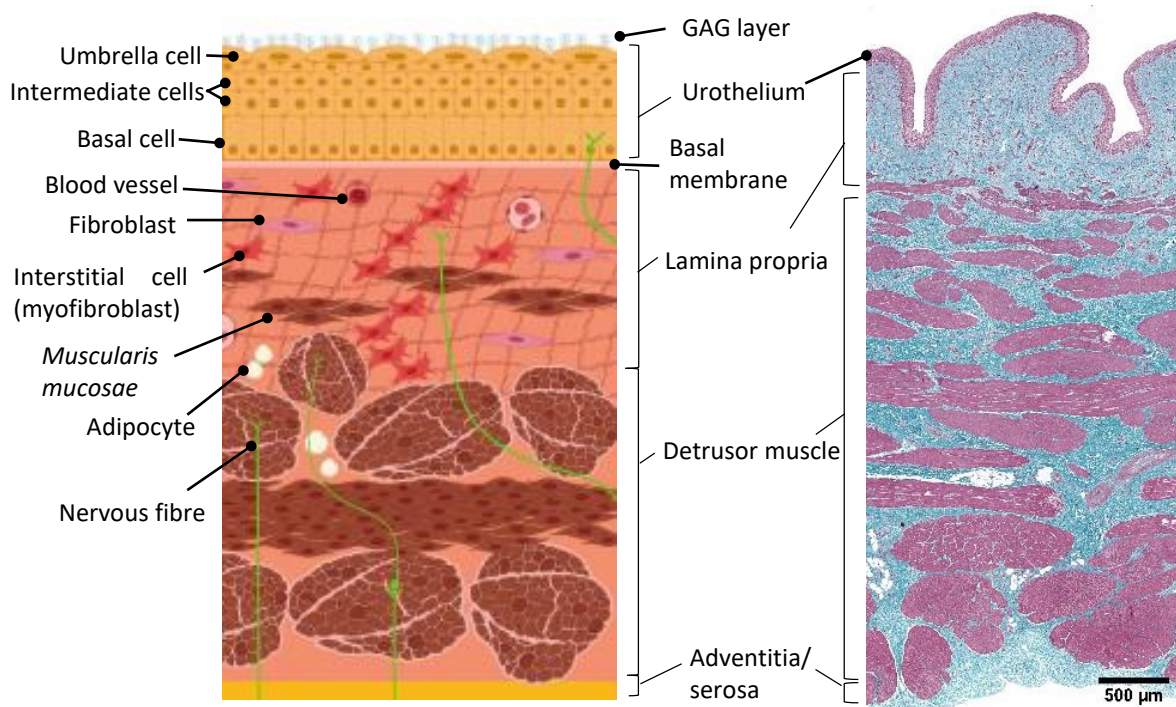


Figure 3. Cross-section of urinary bladder wall. A diagram of the bladder wall (on the left) shows the distinct layers and cell types found in this organ (not to scale). Created with BioRender. A cross-section of a porcine bladder (on the right) stained with Masson's Trichrome. Masson's Trichrome stains nuclei in black, collagen and mucin in blue, muscle, some cytoplasmic granules and red blood cells in red. Represents own work. The bladder wall is composed of mucosa, which includes urothelium and lamina propria, detrusor and serosa/adventitia. The urothelium is a transitional epithelium comprised of basal, intermediate and umbrella cells. The latter are specialized cells involved in the barrier function. A mucus layer of glycosaminoglycans (GAGs) and proteoglycans coats the urothelium contributing to the urothelial barrier function. The lamina propria lies beneath the urothelium and has an extracellular matrix with various types of cells, including interstitial cells (or myofibroblasts), fibroblasts and adipocytes. This layer is well vascularized and is innervated by afferent and efferent nerves. A *muscularis mucosae* can also be present. The detrusor muscle has muscular fibres orientated longitudinally in the outer and inner layers that surround a layer of muscular fibres with a circumferential orientation. Externally, the bladder is coated by adventitia or serosa layer. (Birder and Andersson, 2013)

The urothelium is histologically described as transitional epithelium. (Lewis, 2000) Its thickness depends on the level of distension of the bladder (~2-7 cells thick in the human

bladder). (Chaux, 2011) It comprises three layers of cells: a basal cell line, with germinal cells presenting diameters of 5 to 10 μm ; an intermediate cell line, in which cells have an approximate diameter of 20 μm ; and a luminal layer of large specialized cells, with diameters of 50 to 120 μm , with hexagonal shape. (Lewis, 2000) These cells are commonly designated “umbrella cells”, have a high density of polygonal-shaped uroplakin plaques in their apical membrane and are firmly connected to each other by tight junctions. Such morphological features are particularly important to limit the permeability of the bladder wall. (Lewis, 2000)

A highly hydrophilic mucus layer composed of glycosaminoglycans (GAGs) and proteoglycans coats the luminal side of the urothelium and further contributes to the urothelial barrier function. (Janssen *et al.*, 2013) GAGs are anionic sulphated polysaccharides that can covalently bond to core proteins, also negatively charged due to the presence of sialic acid, to form proteoglycans. (Janssen *et al.*, 2013) Hydrogen bonds are established with water, forming a stationary water layer that helps to prevent the movement of small molecules to the urothelial cells, protecting the bladder wall from exposure to toxins, irritative substances and electrolytes present in the urine. (GuhaSarkar and Banerjee, 2010; Parsons, 2011) Additionally, this layer is thought to impair bacterial adhesion to the bladder wall. (Damiano *et al.*, 2011)

The lamina propria is positioned below the urothelium and comprises of an extracellular matrix with different types of cells, including interstitial cells (or myofibroblasts), fibroblasts and adipocytes. This layer is highly vascularized and is innervated by both afferent and efferent nerves. Also, a *muscularis mucosae*, constituted by disperse groups of muscular fibres isolated from the detrusor layer, can be present. (Andersson and McCloskey, 2014; Fry and Vahabi, 2016)

The detrusor muscle has muscular fibres arranged in a longitudinal orientation in the outer and inner layers that surround a layer of muscular fibres disposed in circumferential orientation. (Miftahof and Nam, 2013) Neurohormonal regulation of contraction and relaxation will be further discussed in 1.3. Bladder innervation and control of micturition.

The serosa layer coats the superior surface and upper part of the lateral surfaces of the bladder wall. Where serosa is absent, a loose connective tissue named adventitia covers the external bladder wall. (Merrill *et al.*, 2016)

An average bladder wall thickness of 3.35 mm (SD \pm 1.15) in normal adults was determined by subrapubic ultrasonography.(Hakenberg *et al.*, 2000)

1.3. Bladder innervation and control of micturition

The normal filling and voiding of the bladder is organized in “on-off switch-like” patterns and depends on complex coordination of striated and smooth muscle activity, neurohormonal control and urothelial regulation. (Fowler, Griffiths and de Groat, 2008; Miftahof and Nam, 2013)

Neurohormonal control involves both the central nervous system (CNS) – spinal cord and brain - and peripheral nervous system (PNS) – including autonomic (sympathetic and parasympathetic nerves) and somatic. (Fowler, Griffiths and de Groat, 2008; Miftahof and Nam, 2013)

Pre-ganglionic sympathetic nerve fibres exit the spinal cord in the T11-L2 and synapse at ganglia with post-ganglionic (hypogastric) sympathetic nerves. These release noradrenaline (NA) and activate β -adrenergic inhibitory receptors in the detrusor muscle, to relax the bladder, and α -adrenergic excitatory receptors in the proximal urethra and the bladder neck, promoting its contraction during bladder filling. Parasympathetic (pelvic) nerves and somatic (pudendal) nerves originate in the sacral spinal cord S2-S4. Parasympathetic nerves innervate the detrusor muscle and release cholinergic (acetylcholine) and nonadrenergic–noncholinergic (mainly ATP) transmitter substances stimulating its contraction during the voiding stage. Parasympathetic nerves also provide an inhibitory input to the urethral smooth muscle mediated by the release of nitric oxide (NO). The somatic fibres, responsible for the voluntary control of micturition, innervate the external sphincter. This voluntary control in humans is developed at the age of 3 to 5 years. (Fowler, Griffiths and de Groat, 2008; Miftahof and Nam, 2013)

Afferent pathways include A δ -fibres and C-fibres. Thin myelinated A δ -fibres are predominantly distributed in the detrusor and communicate the sensation of bladder fullness in response to distension. Unmyelinated C-fibres, present mostly in urothelium and lamina propria, are considered silent under physiological conditions. However, these respond to higher degrees of bladder distension and to noxious stimuli, such as chemical irritants and cooling, and convey the sensation of pain and urgency. The cell bodies of A δ -fibres and C-fibres are found in the spinal cord in S2–S4 and T11–L2. (Fowler, Griffiths and de Groat, 2008; Miftahof and Nam, 2013)

In the brain, distinct groups of neurons are implicated in the control of the bladder and bladder outlet. These can be organised in non-specific or specific areas. The pontine micturition centre (PMC), also designated as Barrington's nucleus, and periaqueductal grey (PAG) are examples of the latter. (Fowler, Griffiths and de Groat, 2008; Miftahof and Nam, 2013)

1.3.1. Micturition cycle

Bladder filling is primarily coordinated by spinal reflex pathways (Figure 5). During this stage, distention of the bladder results in low-level vesical afferent firing, leading to activation of sympathetic outflow and inhibition of parasympathetic outflow. Sympathetic neurons release NA, which activates β_3 -adrenoceptors in the detrusor muscle and promotes its relaxation. Detrusor relaxation together with the viscoelastic properties of the bladder enable storage of urine with little increase in intravesical pressure. On the other hand, sympathetic innervation stimulates muscular contraction of the bladder neck and internal urethral sphincter, mediated by NA activation of α_1 -adrenoceptors. Contraction of striated muscle in the external urethral sphincter and pelvic floor is achieved by somatic (voluntary) innervation, mediated by acetylcholine (ACh) interaction with nicotinic receptors. This coordination is essential to prevent involuntary urine drainage during bladder storage. (Fowler, Griffiths and de Groat, 2008; Miftahof and Nam, 2013; Gonzalez, Arms and Vizzard, 2014) Efferent innervation and neurotransmitters involved in regulation of the urinary bladder are illustrated in Figure 4.

In contrast with the filling stage, voiding is mediated by a spinalbulbospinal pathway which is coordinated by the pontine micturition centre. When the distension of the bladder wall achieves a critical level, A δ -fibres communicate to the brain the sensation of fullness and switch the nervous system to maximal activity. Nevertheless, micturition is largely voluntary in humans and, despite sensations of bladder filling, elimination of urine can be temporarily delayed. When voiding is intended, excitation of the pontine micturition centre activates the parasympathetic pathways. Cholinergic and non-adrenergic/non-cholinergic neurotransmission stimulate detrusor contraction, resulting in a fast increase of intravesical pressure. The bladder expresses different muscarinic receptors (M₁-M₅) but the contraction of the detrusor muscle occurs predominantly via

ACh activation of the M_3 muscarinic receptor. Additionally, ATP released by parasympathetic nerves interacts with P2X purinergic receptors in the detrusor, further contributing to its contraction. On the other hand, relaxation of the sphincters is accomplished by the release of NO, mediated by parasympathetic innervation, and suppression of sympathetic and somatic inputs. These actions occur in a fast and synchronized manner, resulting in an efficient elimination of urine. (Fowler, Griffiths and de Groat, 2008; Miftahof and Nam, 2013; Gonzalez, Arms and Vizzard, 2014)

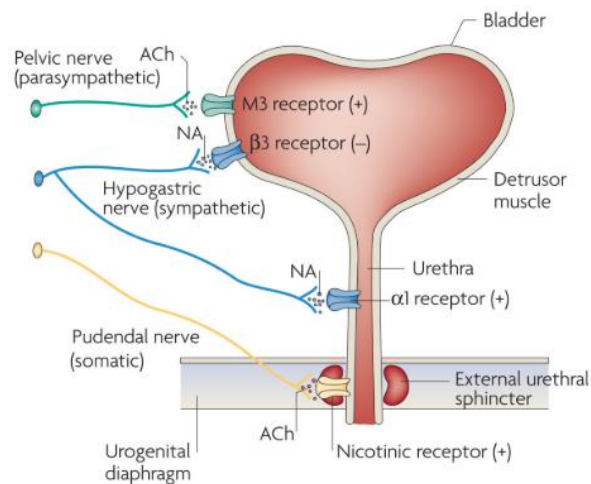


Figure 4. Efferent innervation and neurotransmitters involved in regulation of the urinary bladder. Parasympathetic postganglionic neurons (pelvic nerve) release acetylcholine (ACh), which mediates contraction of the detrusor muscle via M_3 muscarinic receptors. Sympathetic postganglionic neurons (hypogastric nerve) release noradrenaline (NA), which relaxes the detrusor muscle via β_3 adrenergic and contracts urethral smooth muscle via α_1 adrenergic receptors. Somatic neurons (pudendal nerve) also release ACh, which mediates contraction of the external sphincter striated muscle via nicotinic cholinergic receptors. Parasympathetic postganglionic neurons also release ATP, stimulating detrusor muscle contraction, and nitric oxide (NO), which relaxes urethral smooth muscle (not shown). Reused from (Fowler, Griffiths and de Groat, 2008) with permission.

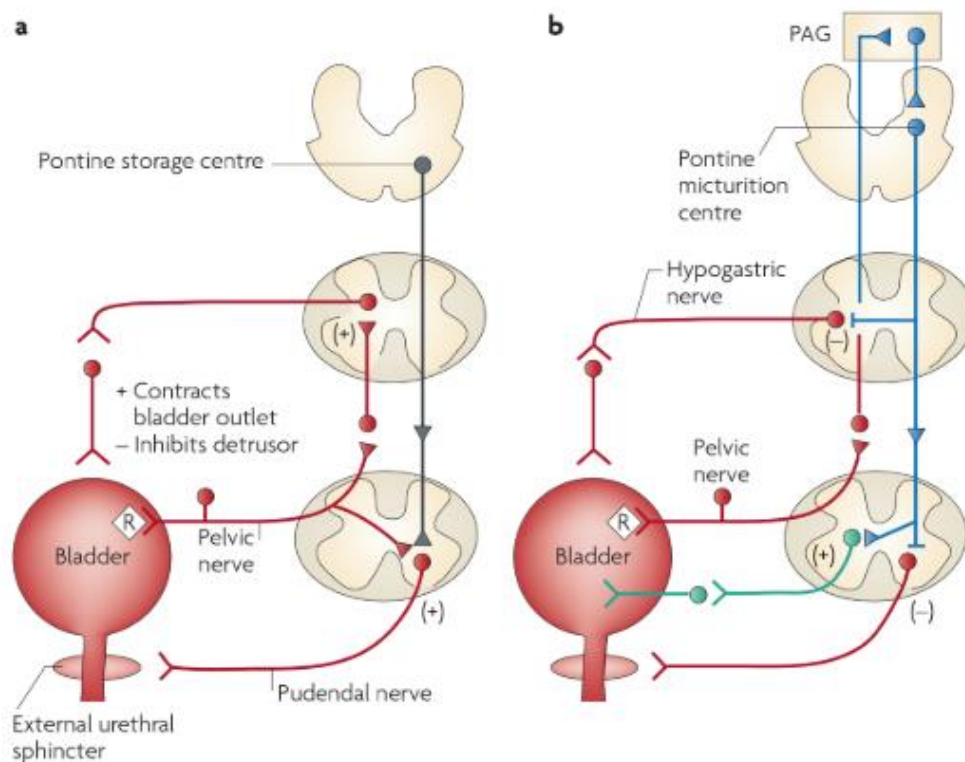


Figure 5. Neural circuits that control the micturition cycle. (a) Bladder filling. During this stage, distention of the bladder produces low-level vesical afferent firing, which stimulates the sympathetic outflow (hypogastric nerve) to the bladder outlet and the somatic (pudendal) outflow to the external urethral sphincter. In addition, activation of sympathetic outflow facilitates detrusor muscle relaxation. These responses occur via spinal reflex pathways that ensure continence. The pontine storage centre might promote striated urethral sphincter activity. (b) Bladder voiding. During the elimination of urine, intense bladder-afferent firing (via pelvic nerve) activates spinobulbospinal reflex pathways (represented in blue) that pass through the pontine micturition centre. Subsequently the parasympathetic outflow (represented in green) is activated and the sympathetic and pudendal outflow are inhibited (represented in red), leading to contraction of the detrusor muscle and relaxation of the bladder outlet. Spinobulbospinal reflex pathways may also involve the periaqueductal grey (PAG). These diagrams do not illustrate conscious bladder sensations, nor the mechanisms involved in the shift from storage to voiding phase, which are likely to involve cerebral circuits above the PAG. R represents receptors on afferent nerve terminals. Reused with permission (Fowler, Griffiths and de Groat, 2008).

1.3.2. Mucosa sensory and contractile properties

The relevance of the urothelium is not limited to its role as a tight barrier, to provide protection to the bladder wall and bloodstream from the noxious environment of the urine. Remarkably, the urothelium is also known to have an important sensory and transducer role, being involved in the reciprocal communication with different cell types, namely sensory afferent fibres and interstitial cells present in the lamina propria (Figure 6). (Fry and Vahabi, 2016)

The urothelium expresses different receptors important for cell to cell communication, such as muscarinic (Mansfield *et al.*, 2005; S. Tyagi *et al.*, 2006), nicotinic (Beckel *et al.*, 2006), tachykinin (Azadzoi, Radisavljevic and Siroky, 2008), purinergic (Lee, Bardini and Burnstock, 2000), adrenergic (Ishihama *et al.*, 2006; Yanase *et al.*, 2008; Tyagi *et al.*, 2009), bradykinin and transient-receptor-potential vanilloid receptors (TRPV) (Birder *et al.*, 2001). Also, in response to changes in urine composition (e.g. increase in urine concentration of K⁺ or H⁺), physical (e.g. stretch and torsion), chemical (e.g. capsaicin) and/or pathogenic (e.g. bacteria) stimuli, this layer is able to secrete potent mediators. These include ATP (Ferguson, Kennedy and Burton, 1997; Lewis and Lewis, 2006; Sadananda *et al.*, 2009), NO (Birder, G Apodaca, *et al.*, 1998; Giglio *et al.*, 2005), ACh (Yoshida *et al.*, 2006; Hanna-Mitchell *et al.*, 2007) and prostaglandins (Brown, Zenser and Davis, 1980; Jeremy *et al.*, 1987; de Jongh *et al.*, 2009). These mediators can then act in a paracrine or autocrine way to stimulate the release of additional mediators, to convey the sensation of fullness to afferent nerves, to influence detrusor contractibility and/or to locally modulate vascular tone. (Fry and Vahabi, 2016)

Evidence of this interaction is the physical proximity of the urothelium to the sensory nerves. The latter are present in a high density in the suburothelial layer, in intimate contact with the urothelium, and some terminations of afferent sensory neurons project into the urothelial layer. However, the distribution of afferent nerves is not uniform across the bladder, with higher expression observed in the neck region. (Gosling and Dixon, 1974; Dixon and Gilpin, 1987; Wakabayashi *et al.*, 1993; Gabella, 1995; Gabella and Davis, 1998; Birder *et al.*, 2001; Wiseman *et al.*, 2002)

On the other hand, interstitial cells (also denominated as interstitial cells of Cajal or myofibroblasts) are present in the lamina propria and were found to communicate through gap junctions. This may be a means of long-distance transmission from the urothelium to the detrusor cells. (Sui *et al.*, 2002; Wiseman, Fowler and Landon, 2003; Neuhaus *et al.*, 2018)

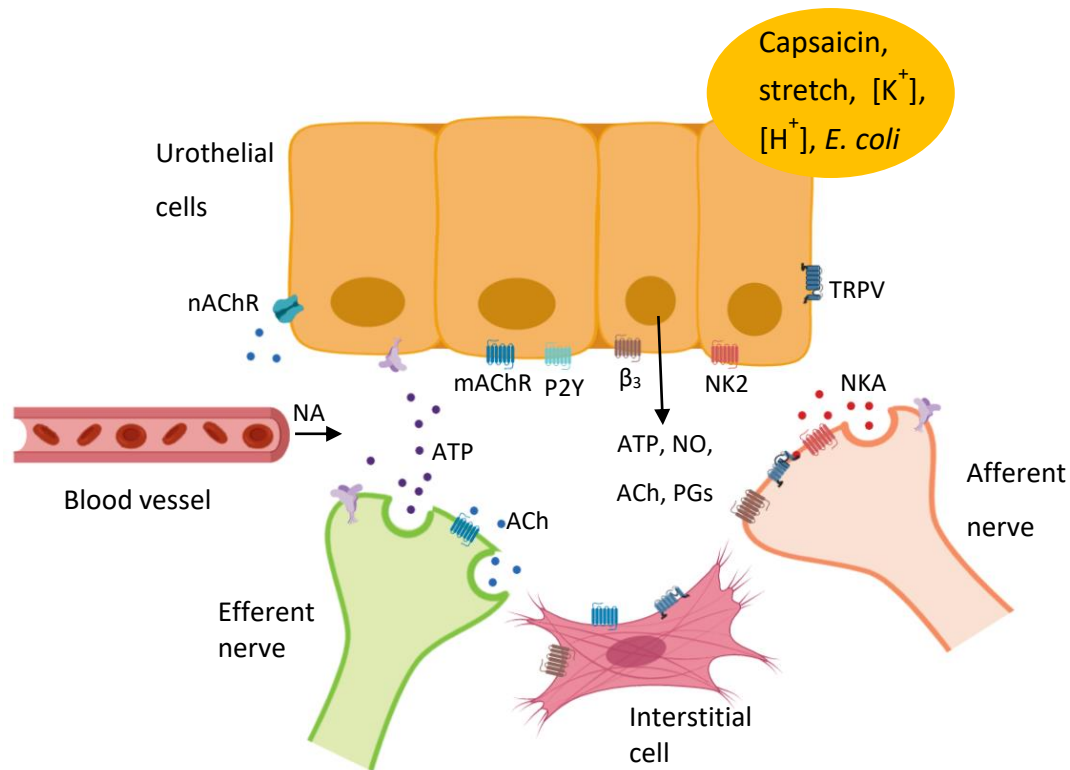


Figure 6. Mucosa sensory role Possible interactions between urothelial cells, afferent and efferent nerves, interstitial cells and blood vessels in the urinary bladder. In response to different stimuli, including bladder distension, capsaicin, concentration of K^+ ($[K^+]$), concentration of H^+ ($[H^+]$) and/or pathogens, urothelial cells are able to secrete various mediators such as ATP, nitric oxide (NO), acetylcholine (ACh) and prostaglandins (PGs). These mediators can target adjacent nerves, interstitial cells, blood vessels or urothelial cells, acting in an autocrine or paracrine way, to stimulate the release of additional mediators, to convey the sensation of fullness to afferent nerves, to influence detrusor contractibility and/or to locally modulate vascular tone. Urothelial cells express different receptors important for cell to cell communication, such as muscarinic (mAChR), nicotinic (nAChR), tachykinin (e.g. NK2), purinergic (P2X and P2Y), adrenergic (e.g. β_2) and transient-receptor-potential vanilloid receptors (TRPV). Image was created with BioRender.

Moreover, isolated mucosal strips of pig and guinea pig bladders have been shown to develop spontaneous phasic contractions and to contract in response to various agonists (Sadananda, Chess-Williams and Burcher, 2008; Moro and Chess-Williams, 2012; Moro, Leeds and Chess-Williams, 2012; Kushida and Fry, 2016). These studies also show that the mucosa and detrusor have a distinct profile of response to diverse pharmacological agents in regards to contractile activity, demonstrating that mucosa contractile activity in these preparations is not merely a result of residual detrusor muscle fibres. (Kushida and Fry, 2016). The origin of spontaneous contractibility in the mucosa is still unclear, but the *muscularis mucosae*, interstitial cells (or myofibroblasts) and pericytes have been suggested to play a role (Kushida and Fry, 2016).

1.4. Microvasculature

Functioning as a unit, the microvasculature is essential to secure tissue demands of oxygen and nutrients and remove toxins resulting from the normal cellular metabolic activity. The microvasculature includes arterioles, capillaries, and venules. (Hashitani *et al.*, 2018) The bladder is a highly distensible organ, therefore the microvasculature is structurally and functionally designed to accommodate differences in pressure and distension experienced during the micturition cycle. (Miodoński and Litwin, 1999) Nevertheless, changes in blood flow in the bladder during the filling stage have been reported in various studies, with both an increase and decrease in flow being described. Distinct methods and species contribute to the lack of consensus regarding this matter. (F. Brading, J. E. Greenland, I. W., 1999; Kershen, Azadzi and Siroky, 2002)

Miodoński and Litwin, 1999 describe in great detail the microvascular architecture of human urinary bladder. Accordingly, the human bladder embodies two vascular plexuses of larger diameter vessels present in the adventitial/serosa and mucosa layers, and two capillary plexuses found in the detrusor muscle and lamina propria. Vessels from the adventitial/serosa plexus communicate with the poorly developed capillary network in the detrusor muscle, by supplying and draining blood, and further communicates with the mucosal larger vessel plexus. The latter communicates with the capillary network in the lamina propria, which lays in intimate contact with urothelium. These capillaries anastomose to form a dense network, with multiple interconnections. They have diameters ranging from 10 to 20 μm and exhibit irregular contours, with the presence of constrictions and dilations (Figure 7 a). These features and a characteristic tortuosity and the coiling ability of larger vessels, are important adaptations to the structural changes that occur during the filling and voiding stage. (Miodoński and Litwin, 1999)

Similar features have been described for other mammal species, such as mouse (Figure 7 b) (Hossler *et al.*, 2013), rat (Tatematsu *et al.*, 1978; Inoue and Gabella, 1991), rabbit (Hossler and Monson, 1995), dog (Hossler and Kao, 2007), guinea pig and pig (Figure 7 c) (Hossler, Kao and Monson, 2005).

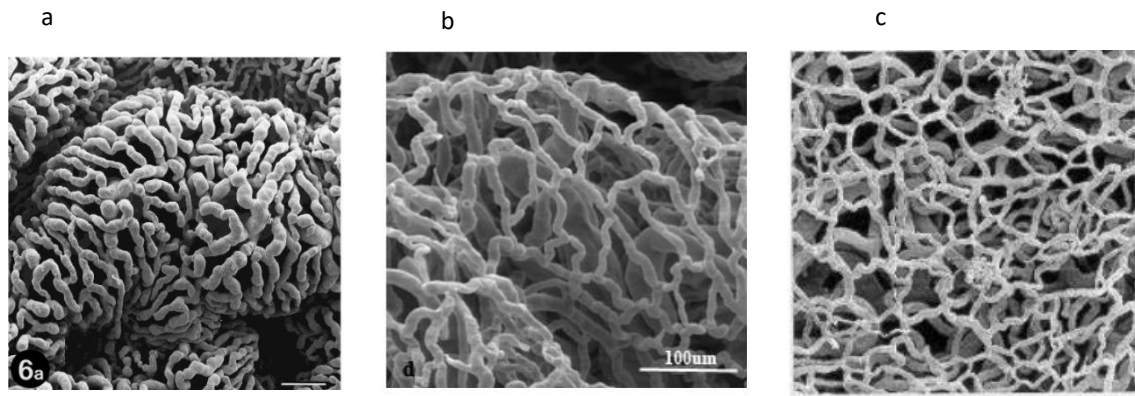


Figure 7. Suburothelial capillary networks . Extensive intercapillary connections can be observed in the bladders of (a) human (scale bar: 1,000 μm ; reused [Miodoński and Litwin, 1999] with permission), (b) mouse (reused [Hossler *et al.*, 2013] with permission) and (c) pig (magnification: x100; reused [Hossler, Kao and Monson, 2005] with permission).

Microvasculature blood flow has conventionally been associated with modulation by arterioles and precapillary valves. Arterioles are surrounded by smooth muscle cells (SMCs) that influence microvascular blood flow by exerting their contractile activity to induce vessel diameter changes.(Hashitani *et al.*, 2011; Shimizu *et al.*, 2014) Current knowledge however, suggests regulation of tissue perfusion is not limited to the arterioles. Suburothelial venules in the bladder of rat (Hashitani *et al.*, 2011; Shimizu *et al.*, 2014) and mouse (Hashitani *et al.*, 2012) develop spontaneous phasic constrictions, mediated by SMCs and stellate-shaped pericyte cells (pericytes), thus suggesting their role in maintaining microcirculation drainage even during bladder filling. Similar findings were reported for other distensible visceral organs such as the stomach (Mitsui and Hashitani, 2015, 2016) and colon (Mitsui and Hashitani, 2016). This spontaneous rhythmic activity was not observed in bladder arterioles in mouse and rat, suggesting their constrictions are dependent exclusively on neurohormonal control.(Hashitani *et al.*, 2011, 2012; Shimizu *et al.*, 2014)

Increasing attention is being given to pericytes, perivascular cells with a typical 'bump-on-a-log' morphology, which have been shown to play a role in angiogenesis, vessel stabilisation (Bergers and Song, 2005) and regulation of blood flow in various capillary beds, for example in the CNS (Peppiatt *et al.*, 2006; Fernandez-Klett *et al.*, 2010; Hall *et al.*, 2014) and kidney (Crawford *et al.*, 2012). Pericytes are heterogenous cells that can evidence distinct morphological features and protein expression, suggestive of possible divergent functional roles. These can be identified by their expression of the platelet-

derived growth factor receptor beta (PDGFR β) or neuron-gial antigen 2 (NG2, a chondroitin sulfate proteoglycan used as a marker for mesenchimal cells). Other molecular markers include desmin and alpha-smooth muscle actin (α -SMA), contractile filaments.(Bergers and Song, 2005) Some authors further classify pericytes based on their location, morphology and protein expression, by differentiating pericytes located in pre-capillary arterioles (PCA), capillaries and post-capillary venules (PCV) (Figure 8) (Borysova *et al.*, 2013; Hartmann *et al.*, 2015; Hashitani *et al.*, 2018). However, this classification is not consensual (Attwell *et al.*, 2016; Borysova and Dora, 2018; Grant *et al.*, 2019).

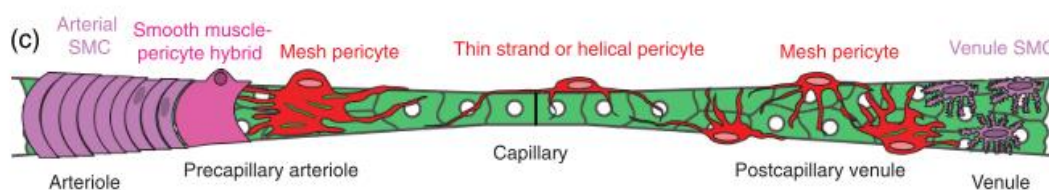


Figure 8 Diagram showing the heterogeneity of mural cells along the microvasculature Reused from. (Hartmann *et al.*, 2015). Smooth muscle cells (SMC) are densely packed around arteries and arterioles. According to Hartmann *et al.* nomenclature, transitional forms between SMCs and pericyte cells, designated as smooth muscle pericyte hybrids and mesh pericytes, reside in pre-capillary arterioles. Pericytes located in the abluminal side of capillaries have a protruding cell body and long thin processes. Mesh pericytes and stellate-shaped SMCs reside in post-capillary venules and venules, respectively.

A comparative study of human, pig and guinea pig bladder shows expression of α -SMA in pericytes of suburothelial microvasculature in all species. (Steiner *et al.*, 2018) Differentiation between PCA, capillary and PCV pericytes is not addressed in this study.

According to the immunohistochemistry studies of Hashitani *et al.*, pericytes located at suburothelial PCAs of rat and mouse bladder express NG2 and α -SMA. Pericytes positioned in the bladder capillary bed of rats and mice are positive for NG2, however positive expression of α -SMA was only observed for rat. On the contrary, pericytes on suburothelial PCVs in the bladder of these species express α -SMA but have reduced or no expression of NG2. (Mitsui and Hashitani, 2013; Hashitani *et al.*, 2018) Regarding morphology (Figure 9), PCA pericytes presented a typical ‘bump-on-a-log’ with an oval cell body and processes arranged circumferentially. Capillary pericytes presented a ‘bump-on-a-log’ cell body and bipolar processes, running longitudinally in relation to the capillary. On the other hand, PCV pericytes had a stellate shape.(Hashitani *et al.*, 2018)

Similar observations were described for the ureteric microvasculature. (Borysova *et al.*, 2013) Moreover, NG2(+) pericytes in PCAs, capillaries and PVCs have been shown to develop spontaneous Ca²⁺ transients in a murine lamina propria preparation, however, only in PCAs was this accompanied by diameter reduction (~15%). (Hashitani *et al.*, 2018)

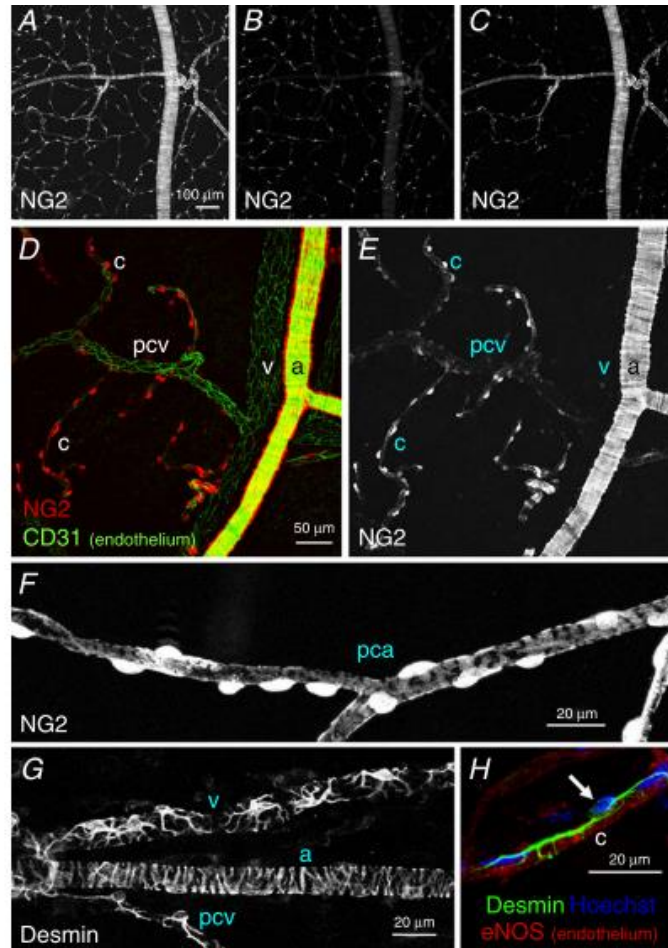


Figure 9 Morphological features of mural cells in the suburothelial microvasculature of mouse bladder. (A-C) NG2-expressing mural cell in the microvascular network. (D and E) Lamina propria stained for endothelial marker CD31, showing NG2⁺ arteriolar smooth muscle cells (a) and no NG2 signal surrounding venules (v). Capillary (c) pericytes also expressed NG2, whereas pericytes located in the postcapillary venule (pcv) exhibited faint NG2 signals. (F) Lamina propria preparation showing NG2⁺ pericytes in the precapillary arteriole (pca) with an oval cell body and extended circumferentially arranged processes. (G) Desmin immunoreactivity revealing the stellate shaped morphology of pericytes in a venule (v) and a postcapillary venule (pcv). (H) A capillary pericyte identified with desmin (green) situated in the abluminal side of a capillary, identified by endothelial expression of eNOS (red). The pericyte cell body (arrow) was stained with Hoechst (blue) and extends longitudinally-oriented bipolar long processes. Reused (Hashitani *et al.*, 2018) with permission.

1.5. Lower urinary tract symptoms (LUTS)

LUTS are common in a diverse range of bladder disorders and have a profound effect on the quality of life. These disorders comprise of *disturbances in storage* function, also commonly described as irritative, such as increased frequency, nocturia, urgency and urge incontinence; *voiding dysfunctions*, frequently described as obstructive, namely hesitancy, reduced flow, intermittency, dribbling and incomplete voiding; *sensory symptoms* like pelvic pain and dysuria; and *stress urinary incontinence*. (Abrams *et al.*, 2003; Haylen *et al.*, 2009) Overlapping of symptoms in patients with different bladder pathologies is usual and a differential diagnosis is required for a better therapeutic approach. Current knowledge suggests, regardless of the aetiology, some common features in the underlying pathophysiological mechanisms. In the context of the present study, more detail is provided for overactive bladder, interstitial cystitis and ketamine-induced cystitis.

1.5.1. Overactive bladder

Overactive bladder (OAB) is a storage disorder clinically defined by the International Continence Society and International Urogynecological Association as a symptom-based syndrome with the presence of urinary urgency with or without urge-incontinence, typically accompanied with increased urinary frequency and nocturia. Urinary tract infection (UTI) or other underlying pathologies like bladder cancer or bladder calculus should be excluded prior to a diagnosis being made. (Abrams *et al.*, 2003; Haylen *et al.*, 2009)

OAB has an estimated prevalence of 11-17%, which increases with age. It has a major negative impact on the quality-of-life and represents a relevant economic burden. (Wein *et al.*, 2003; Irwin *et al.*, 2006, 2011; Lawrence *et al.*, 2008; Milsom *et al.*, 2014)

Urodynamic observation of involuntary detrusor contractions, spontaneous or triggered, during the filling phase of the micturition cycle is designated as detrusor overactivity (DO). Although these terms are not synonyms, DO is closely related to the manifestation of OAB symptoms. It is important to note, however, that only a portion of patients with OAB reveal DO on urodynamic testing (Hashim and Abrams, 2006). DO can be idiopathic (IDO), when no obvious cause can be identified, or neurogenic (NDO),

when associated with a neurological condition, such as multiple sclerosis, cerebrovascular disease, Parkinson's or spinal injury. (Abrams *et al.*, 2003)

In relation to idiopathic OAB, the underlying pathological mechanism is, as the name suggests, not entirely understood and requires further debate and research. Nevertheless, myogenic and urothelial-based theories prevail in the literature. (Chapple, 2014)

The myogenic hypothesis proposes that upregulated involuntary contractions of detrusor myocytes may contribute to the pathophysiology of idiopathic OAB. (Brading, 1997) Denervation of detrusor muscle in unstable human bladders has been reported (Mills *et al.*, 2000) and it was suggested it could increase the excitability of detrusor muscle cells. Moreover, Drake *et al.* described localized contractions in the human bladder which were accompanied by afferent activity, manifested by urinary urgency. (Drake *et al.*, 2005)

Dysfunction of the mucosa sensory role, as supported by the urothelium-based hypothesis, can enhance afferent activity. This heightens the sensation of bladder fullness, subsequently eliciting the perception of urinary urgency and possibly promoting activation of the micturition reflex. Hence, changes in urothelial receptor function (e.g. TRPV1 [L.A. Birder *et al.*, 2002; Daly *et al.*, 2007]) and release of neurohormonal mediators (e.g. ATP [Kumar *et al.*, 2010; Contreras-Sanz *et al.*, 2016]), as well as changes in sensitivity and coupling of myofibroblasts (or interstitial cells) (Biers *et al.*, 2006; Ikeda *et al.*, 2007; Sui *et al.*, 2008; Roosen *et al.*, 2009) can contribute to increased afferent activity.

First-line treatment for OAB comprises lifestyle changes, behavioural therapy and pelvic floor muscle exercises. Pharmacological management with oral antimuscarinic medication or oral β_3 -adrenergic receptor agonist (Mirabegron[®]) is frequently recommended, to partially block the efferent pathway. (Gormley *et al.*, 2012; NICE, 2013; Corcos *et al.*, 2017) However, many patients are refractory to this therapeutic approach or experience adverse effects to these pharmacological agents such as blurred vision, dry mouth, and/or constipation. (Vouri *et al.*, 2017) Current alternative treatments include intravesical injections of botulinum toxin A (BoNT-A), peripheral

tibial nerve stimulation (PTNS) and sacral neuromodulation (SNM). (Gormley *et al.*, 2012; NICE, 2013; Corcos *et al.*, 2017) Additionally, for postmenopausal women with vaginal atrophy and OAB symptoms therapy with intravaginal oestrogens is recommended. (NICE, 2013)

1.5.2. Interstitial cystitis/ bladder pain syndrome

Interstitial cystitis/bladder pain syndrome (IC/BPS) is a debilitating chronic condition characterized by pelvic pain, pressure or discomfort, often accompanied by urinary urgency and frequency. (Vij, Srikrishna and Cardozo, 2012) For diagnostic purposes, other pathologies, with similar symptomatology, should be ruled out, including ITU, endometriosis and carcinoma *in situ*. As there are no definitive diagnostic tests, IC/BPS is mainly a diagnosis of exclusion.

Different terms have been used overtime to designate this syndrome such as interstitial cystitis, bladder pain syndrome, painful bladder syndrome, chronic pelvic pain syndrome (CPPS) and IC/BPS. This lack of consensus is also extended to the definition, diagnosis and therapeutic approach as illustrated by Malde *et al.*, which compares the most relevant guidelines on this topic, highlighting their differences. Overall, the terms of bladder pain syndrome or IC/BPS is preferred over interstitial cystitis. (Malde *et al.*, 2018)

A classic IC/BPS with the presence of Hunner's lesions (inflammatory infiltrate, with granulation tissue), as firstly described by Guy Hunner in 1915 (Hunner, 1915), and glomerulations can be identified by cystoscopy with hydrodistension. However, its presence is associated with a different prognosis and requires different therapeutic strategies, therefore in some guidelines is treated as a separate disease. (Malde *et al.*, 2018)

The estimated prevalence of IC/BPS varies greatly depending on the diagnostic criteria used and whether it is diagnosed by a physician or self-reported, ranging from 18 to 1,400 per 100,000 women. (Oravisto, 1975; Curhan *et al.*, 1999; Leppilahti *et al.*, 2002; Roberts *et al.*, 2003; Clemens *et al.*, 2005) The estimated female-to-male proportion varies from 10:1 to 5:1. (Oravisto, 1975; Clemens *et al.*, 2005)

Although its aetiology and pathophysiology are yet to be fully elucidated, a dysfunctional urothelial and mucus layer resulting in an increased bladder wall permeability is thought to be the most likely cause of the symptoms. Accordingly, studies report an altered pattern of gene expression in explanted bladder urothelial cells from patients with IC/BPS, with a reduction in tight junctions and adherens protein expression observed. (Keay *et al.*, 2003; Zhang *et al.*, 2005) Also, a GAG layer deficiency is believed to play an important role in the course of the disease (Lokeshwar *et al.*, 2005; Lv *et al.*, 2012), providing the rationale for the use of mucus enhancers (e.g. heparin [Parsons *et al.*, 2012], hyaluronic acid [Riedl *et al.*, 2008; Engelhardt *et al.*, 2011], pentosane polysulphate [Bade *et al.*, 1997; Hwang *et al.*, 1997; Sant *et al.*, 2003] and chondroitin sulphate [Steinhoff, Ittah and Rowan, 2002]) as a treatment, to restore the integrity of the GAG layer. Furthermore, these alterations in the GAG layer result in a defective barrier function and expose the bladder wall to the noxious environment of the urine, facilitating the activation of sensory C-fibres thereby resulting in pain sensation. Evidence shows that potassium, present in the urine in high concentrations, diffuses into the bladder in GAG defective walls and depolarizes nerves and muscle, resulting in the symptoms described (reviewed (Parsons, 2007, 2011)).

Other pathophysiological mechanisms that may contribute to this condition, as reviewed by Davis *et al.*, (Davis, Brady and Creagh, 2014) include an enhanced inflammatory response with mast cell activation (Theoharides, Kempuraj and Sant, 2001; Sant *et al.*, 2007); altered NO metabolism (Smith *et al.*, 1996) and a defective Tamm–Horsfall Protein (THP) (Stein, Rajasekaran and Parsons, 2005); and an autoimmune mechanism (Smith *et al.*, 1996).

Similar to OAB, the first-line therapeutic approach focuses on behavioural modification strategies and lifestyle changes. Oral pharmacological therapy can include amitriptyline, cimetidine, hydroxyzine, pentosane polysulphate or quercetin, with different degrees of recommendation depending on the guidelines. Additionally, intravesical instillation of anti-inflammatory agents, analgesics and mucus layer enhancers, have shown to be beneficial in some patients, with fewer side effects observed as a consequence of the limited systemic distribution of the drug associated with their site-specific delivery. Examples of agents delivered intravesically include lidocaine, lidocaine/sodium

bicarbonate, hyaluronic acid, pentosane polysulphate, heparin, chondroitin sulphate and DMSO. Despite the numerous therapeutic drugs described here, treatment remains mainly empirical and in many cases fails to provide both acute and sustained relief of symptoms.(Nickel *et al.*, 2009; Matsuoka *et al.*, 2012)

1.5.3. Ketamine-induced cystitis

Ketamine-induced cystitis (KIC) was first identified as a clinical condition by Shahani *et al.* in 2007, who established causality between the illicit consumption of ketamine and the onset of lower urinary tract symptoms.(Shahani *et al.*, 2007) Other case studies in the following years further supported this relationship and helped to characterise the disease. (Chu *et al.*, 2008; Oxley *et al.*, 2009; Tsai *et al.*, 2009; Mason *et al.*, 2010; Lai *et al.*, 2012; Baker *et al.*, 2013; Lee, Jiang and Kuo, 2013; Huang *et al.*, 2014) In addition, there are occasional case reports of patients taking therapeutic doses of ketamine that have subsequently developed LUTS. (Storr and Quibell, 2009; Vickers, Lee and Hunsberger, 2017)

Ketamine is a phencyclidine derivative for human and veterinary use with analgesic and anaesthetic activity. (Pai and Heining, 2007) More recently, this drug has gained a new clinical interest for its antidepressant effect. (Chen *et al.*, 2018) However, ketamine is known to cause dissociative and hallucinogenic side effects that make this drug attractive for recreational misuse. (Muetzelfeldt *et al.*, 2008) Abuse of ketamine is particularly problematic among young adults and its consumption has increased over the years possibly due to lower cost, easier access and general perception that ketamine causes less adverse effects than other drugs of abuse.

KIC shares common features with the bladder pathologies described above, particularly with IC/BPS (Lu, Jiang and Kuo, 2015), with symptoms such as frequency, urgency, dysuria and urge incontinence. However, in this case, the clinical presentation is usually more severe, with the presence of haematuria being commonly described. (Fan *et al.*, 2017; Sihra, Ockrim and Wood, 2018) Additionally, reduced bladder capacity has been reported, following urodynamic evaluation and a thickening of the bladder wall by CT scans are frequently reported in these patients. (Mason *et al.*, 2010; Huang *et al.*, 2014; Jhang *et al.*, 2018; Sihra, Ockrim and Wood, 2018) Histological investigation reveals signs of mucosal inflammation, with infiltration of lymphocytes, eosinophils and neutrophils,

fibrosis, nerve hyperplasia and in some cases urothelial denudation. (Fan *et al.*, 2017; Lin, Yang and Lin, 2017; Jhang *et al.*, 2018; Sihra, Ockrim and Wood, 2018) Similar histological changes can be observed in the ureters and in severe cases hydronephrosis (swelling of the kidney as a result of a build-up of urine) can be found. (Chu *et al.*, 2008; Huang *et al.*, 2014; Lin *et al.*, 2016; Yee *et al.*, 2017; Jhang *et al.*, 2018; Sihra, Ockrim and Wood, 2018)

A clear relationship between consumption history (dose, frequency and duration of abuse) with severity and onset of symptoms has not yet been established. (Chen *et al.*, 2017; Jhang *et al.*, 2018) Additionally, the pathophysiological mechanism is poorly understood. Current knowledge is mostly provided by bladder biopsies of KIC patients (Baker *et al.*, 2013; Lee, Jiang and Kuo, 2013; Jhang *et al.*, 2014; Lu, Jiang and Kuo, 2015; Lin *et al.*, 2015; Kidger *et al.*, 2016; Lin, Yang and Lin, 2017), KIC rodent models (Yeung *et al.*, 2009; Meng *et al.*, 2011; Chuang *et al.*, 2013; Gu *et al.*, 2014; Juan *et al.*, 2015; Liu *et al.*, 2015; Song *et al.*, 2016; Kim *et al.*, 2016; Duan *et al.*, 2017; Wang *et al.*, 2017; Lee *et al.*, 2017; Rajandram *et al.*, 2017; W.-C. Lee *et al.*, 2018; S. W. Lee *et al.*, 2018) and cell culture models (Bureau *et al.*, 2015; Shen *et al.*, 2015; Baker *et al.*, 2016; Lin, Yang and Lin, 2017; Wang *et al.*, 2017; Shan *et al.*, 2018). Some hypotheses advanced for the pathological mechanism include a direct cytotoxic effect on the mucosa, neurogenic inflammation, immunogenic inflammation and microvascular change. (Chu *et al.*, 2008; Jhang, Hsu and Kuo, 2015; Tsai and Kuo, 2015)

Ketamine and its metabolites (norketamine and hydroxynorketamine) are excreted in the urine (Moore *et al.*, 2001) following illicit use. Changes in the bladder wall elicited by the accumulation of these compounds in the urine stored in the bladder are thereby plausible. A case report of a KIC patient with a rare urachal cyst showed denuded urothelium in areas in direct contact with urine but healthy urothelium in areas covered by the cyst (therefore not exposed to urine), which supports the hypothesis that urinary / local, rather than systemic factors, are likely involved in the pathological mechanism. (Kidger *et al.*, 2016)

Ketamine is a non-competitive antagonist of glutamatergic N-methyl-D-aspartate receptors (NMDAR). NMDAR subunits have been previously identified in the male human and rat urinary bladder. (Gonzalez-Cadavid *et al.*, 2000) In this study,

administration of NMDA induced contraction in detrusor muscle strips, while administration of ketamine failed to evoke a contractile response. Furthermore, ketamine elicited complete relaxation in tissue pre-contracted with bethanechol, in a NO-independent manner (confirmed with the addition of an inhibitor of guanylyl cyclase). Similar findings were observed for dextromethorphan and MK-801 (other antagonists of NMDAR). This suggests ketamine's harmful effects are not a result of direct action on detrusor muscle.

Urothelial barrier dysfunction has also been associated with KIC, with significant denuded urothelium being commonly reported (Lin *et al.*, 2015; Fan *et al.*, 2017). In human biopsies, a reduced expression of E-cadherin and zonula occludens-1 (ZO-1) has been described. (Lee, Jiang and Kuo, 2013; lu, Jiang and Kuo, 2015; Tsai, Birder and Kuo, 2016) Decreased or abnormal distribution of tight junction proteins (ZO-1 and claudin-4), adhesion proteins (E-cadherin) and umbrella cell markers (UPKII) in rodents have also been observed. (Gu *et al.*, 2014; Liu *et al.*, 2015; Duan *et al.*, 2017; Lee *et al.*, 2017; W.-C. Lee *et al.*, 2018) Furthermore, Baker *et al.* showed high concentrations of ketamine (> 1 mM) were toxic to a human urothelial cell line, in an NMDAR independent pathway. A sustained increase of cytosolic calcium was observed in these cells, leading to mitochondrial-mediated apoptosis. (Baker *et al.*, 2016) Similarly, ketamine induced apoptosis has been observed in human urothelial cells in monolayer and on a 3D tissue-engineered vesical equivalents in another study. (Bureau *et al.*, 2015) Additional studies have shown increased apoptosis in human (Lee, Jiang and Kuo, 2013; lu, Jiang and Kuo, 2015; Tsai, Birder and Kuo, 2016) and rodent (Liu *et al.*, 2015; Song *et al.*, 2016; S. W. Lee *et al.*, 2018) bladders as well as cell culture (Shen *et al.*, 2015; Wang *et al.*, 2017). In agreement with these studies, a proteomic study has shown increased markers of apoptosis in bladder biopsies from KIC patients. (Yang, Zhai and Kuo, 2017) Interestingly, Rajandram *et al.*, reported a mouse model treated with ketamine that exhibited voiding dysfunction without changes in the urothelial barrier, suggesting urothelial dysfunction may not be the triggering pathological event leading to KIC. (Rajandram *et al.*, 2016)

Inflammation of the mucosa plays a part in the course of the disease with infiltration of inflammatory cells and fibrosis commonly reported both in humans (Lee, Jiang and Kuo, 2013; lu, Jiang and Kuo, 2015; Lin *et al.*, 2016; Tsai, Birder and Kuo, 2016; Fan *et al.*,

2017; Jhang *et al.*, 2018; Sihra, Ockrim and Wood, 2018) and rodent models (Yeung *et al.*, 2009; Chuang *et al.*, 2013; Liu *et al.*, 2015; Kim *et al.*, 2016; Song *et al.*, 2016; Duan *et al.*, 2017; Lee *et al.*, 2017; Rajandram *et al.*, 2017; Wang *et al.*, 2017). Moreover, the severity of inflammation has been shown to be positively correlated with the severity of symptoms. (Jhang *et al.*, 2018) In addition, serum levels of immunoglobulin (Ig) E, interleukin (IL)-6 and interferon (IFN)- γ as well as effector T helper (T_H1, T_H2 and T_H17) cells were found to be increased in KIC patients when compared to controls, while TGF- β was decreased. (Jhang *et al.*, 2014, 2016; Fan *et al.*, 2017) Fan and colleagues proposed that the immunologic response initiates through a T_H1 pathway with increased production of IL-6 leading to differentiation of T_H17 cells and further amplified expression of T_H1, T_H2. Also, it was suggested possible suppression of T_{REG} by IL-6 causing an imbalance of T_H/T_{REG} worsens the inflammatory process. Increased expression of inflammatory mediators (e.g. IL-6, IL-1 β , tumour necrosis factor [TNF]- α , transforming growth factor [TGF]- β 1, nuclear factor [NF]- κ B and cyclooxygenase [COX]-2) and fibrosis markers (fibronectin and type I collagen) has also been described in rodent models (Chuang *et al.*, 2013; Gu *et al.*, 2014; Juan *et al.*, 2015; Lee *et al.*, 2017; Wang *et al.*, 2017; W.-C. Lee *et al.*, 2018). In the study of Juan *et al.*, a group of rats treated with ketamine and a COX-2 inhibitor presented better bladder function and less histological changes than rats treated with ketamine alone, further implicating COX-2 in the development of KIC. However, it is important to note that an opposite response to ketamine (e.g. reduced expression of IL-6 and iNOS) is observed in other cell types and tissues. (Huang *et al.*, 2018; Xu *et al.*, 2018)

Neurohormonal imbalance also appears to play a role in the pathophysiology. Nerve hyperplasia has been reported in human biopsies, possibly mediating the sensation of pain in this pathology. (Baker *et al.*, 2013; Jhang *et al.*, 2018) Decrease in cholinergic innervation (Yeung *et al.*, 2009), increased expression of TRPV1 receptors (W.-C. Lee *et al.*, 2018) in the mucosa, and increased expression of purinergic receptors (P2X1) (Meng *et al.*, 2011) and muscarinic receptors (M₂ and M₃) (Chuang *et al.*, 2013) in detrusor and nitric oxide synthase (NOS) have also been reported in rodent models.

Chu *et al.*, 2008 first proposed that the pathophysiological mechanism of KIC involves microvascular changes induced by ketamine and its metabolites. It was hypothesized

that endothelial cell injury of small blood vessels could compromise microcirculation or affect microvascular density in the lamina propria. Resulting bladder ischemia would prompt fibrosis over time. Neovascularization and fibrosis are common histological findings that support this hypothesis. A study by Lin *et al.*, 2016 has evidenced significant microvascular changes in bladders from KIC patients, including thickening of the basal membrane in greater and small blood vessels, structural changes of the vascular lumen and reduced endothelial cell count. Also, this study demonstrated a reduced expression of NMDAR-1 in endothelial cells and increased expression of endothelial-mesenchymal-transition markers in the vessels of bladders from KIC patients, when compared to normal human bladders. Lin and colleagues proposed that ketamine-mediated activation of NMDAR-1 in the endothelial cells could lead to the thickening of the basal membrane and chronic inflammation and further contribute to the development of fibrosis, through an endothelial-mesenchymal-transition mechanism. A following study (Lin, Yang and Lin, 2017) has evidenced overexpression of S6RP (end product of the mammalian target of rapamycin (mTOR) pathway) in endothelial cells of urinary bladders of KIC patients. In addition, this study has shown activation of mTOR signalling pathway in a time-dependent manner and increased expression of NMDAR-1 and fibroblast specific protein 1 (FSP-1, mesenchymal marker) in cultured human bladder microvascular endothelial cells (HBdMECs) incubated with ketamine. Activation of mTOR pathway in the brain had previously been shown in a rat model with low-dose ketamine, associated with an antidepressant effect. (Li *et al.*, 2010)

Currently, there are no official guidelines regarding diagnosis and therapeutic approaches to help health professionals deal with KIC. Therefore, the diagnosis will depend mainly on self-reported history of ketamine consumption with the clinical presentation of lower urinary tract symptoms, having excluded other bladder pathologies. Therapeutic strategies are mostly empirical and lacking clinical evidence, as pathogenesis is poorly understood. Since ketamine and/or its metabolites (norketamine and hydroxynorketamine) are considered the causative element, cessation of ketamine intake is recommended in a first instance. (Tsai and Kuo, 2015; Yee *et al.*, 2016) The physical and psychological dependence associated with this drug should be dealt by a multidisciplinary team. In addition, as ketamine has an analgesic

effect, it helps to mask the pain present with this type of cystitis, therefore in order to cease abuse of this drug patients should be given alternatives to manage the pain. Whether cessation on its own can lead to mucosa recovery is unknown, as persistence of symptoms after cessation is often reported. (Winstock *et al.*, 2012) Moreover, in case of drug abuse relapse the lower urinary symptoms normally recur. (Hong *et al.*, 2018) In addition to analgesic and anti-inflammatory drugs, other options can be considered in line with available therapies for OAB and IC/BPS, such as anticholinergics, GAG layer enhancers and intravesical injections of botulinum toxin. (Tsai and Kuo, 2015; Yee *et al.*, 2015; Hong *et al.*, 2018) For severe cases, refractory to other therapies, surgical intervention, such as augmentation enterocystoplasty (AE) and cystectomy followed by neobladder implantation, is an option (Sihra, Ockrim and Wood, 2018)

1.6. Intravesical drug delivery

Intravesical drug delivery describes the instillation of a therapeutic drug through the urethra, following catheterisation (GuhaSarkar and Banerjee, 2010). It can be an option for different pathologies affecting the bladder, either to locally target bladder tumours with chemotherapy or for the administration of therapeutic solutions to treat/mitigate the symptoms of OAB, IC/BPS and ketamine induced-cystitis. (GuhaSarkar and Banerjee, 2010; Tyagi *et al.*, 2016) Additionally, it has been used as a diagnostic tool, as exemplified by the Potassium Sensitivity Test (PST), which can be used as an indicator of epithelial dysfunction (Parsons *et al.*, 1994; Parsons, 2007, 2011), or a study by Yokoyama *et al.*, which used lidocaine to help distinguish neurogenic overactive bladder resulting from spinal injury or brain injury (Yokoyama *et al.*, 2000).

This therapeutic approach offers both valuable advantages and difficult challenges. (P. Tyagi *et al.*, 2006; GuhaSarkar and Banerjee, 2010) Although the access to most internal organs requires invasive surgical procedures, this is fortunately not the case for the urinary bladder. Benefiting from its particular anatomical features, the lumen of the urinary bladder can be easily accessed by inserting a catheter through the urethra. In addition, the bladder wall is an extremely efficient barrier and high concentrations can be instilled intravesically with small concentrations reaching the systemic circulation, which minimizes the occurrence of side effects and improves efficacy. This contrasts with conventional treatments that rely on the systemic distribution of therapeutic drugs, which can affect efficacy, as only reduced amounts of the drug reach the bladder, and tolerability, considering patients often experience systemic adverse effects. However, whilst inner layers can be easily targeted through intravesical drug delivery, it can be harder to predict concentrations in the deeper layers. Also, urine production decreases drug concentration throughout time and elimination of the instilled solution occurs when voiding happens, thus reducing drug residence time. Some strategies including voiding right before treatment and limiting patient fluid intake can be helpful. However, multiple sessions involving catheterisation are needed for a better therapeutic outcome, which can affect patient adherence and compliance. This is less likely to represent a problem in patients with neurogenic overactive bladder in result of spinal or brain injury,

as intermittent catheterisation is already a common need. (P. Tyagi *et al.*, 2006; GuhaSarkar and Banerjee, 2010)

Movement of molecules across membranes depends on many parameters, some intrinsic to the substance such as molecular weight, chemical structure, partition coefficient, ionization degree at urine pH, while others are patient dependent for example residence time, concentration gradient and voiding frequency. Different approaches have been studied to improve permeation and ensure minimum effective concentrations reach the target layer. Those can be broadly grouped in physical methods and chemical methods to enhance permeation. (GuhaSarkar and Banerjee, 2010) Physical methods affect temporarily the transepithelial resistance as it is the case of electromotive drug administration (EMDA) (Giannantoni *et al.*, 2006), which associates iontophoresis and electrophoresis to increase the rate of drug penetration. Chemical permeation enhancers interact with the urothelial barrier to promote permeation and include, for example, protamine sulphate, dimethyl sulfoxide (DMSO) and chitosan. Protamine sulphate is important as an experimental model of urothelial injury but has limited clinical relevance considering urothelial damage recovery can take days. On the other hand, DMSO can penetrate the urothelium without severe damage and has beneficial anti-inflammatory and antibacterial properties, hence the rationale for its use alone (Perez-Marrero, Emerson and Feltis, 1988; Peeker *et al.*, 2000; Sairanen *et al.*, 2009) or in association with other drugs in a multimodal regimen (See and Xia, 1992; Petrou *et al.*, 2009). This solvent was approved by the US Food and Drug Administration (FDA) in 1978 to treat IC/BPS, however it remains unlicensed in the UK (National Institute for Health and Care Excellence, 2014).

1.7. Models to study bladder physiology and dysfunction

Studies in humans to investigate bladder dysfunction are limited due to legal, ethical and moral implications. (Parsons and Drake, 2011) Although human bladder tissue samples can be obtained from cystectomies performed in patients with invasive bladder cancer, this access is limited. Therefore, *in vitro* studies using animal-derived tissue and *in vivo* animal models are valuable tools to study bladder physiology, inform pathophysiological mechanisms and test therapeutic options. Several species have been used for this purpose, including pig, guinea pig, rabbit, rat, mouse, cat, dog and non-human primates. (Westropp and Buffington, 2002; Parsons and Drake, 2011) It is therefore important to recognise inter-species differences and similarities and understand which model is the most appropriate for a particular investigation. Special focus will be given to porcine and murine bladders in comparison to human bladders (when possible) for their relevance in the present study.

Mice are widely studied experimental models for biomedical research, they are easier to maintain, have a short generation time and can be easily manipulated genetically, to develop transgenic and knock-out mice. (Perlman, 2016) Mice are phylogenetically related and physiologically similar to humans; however, caution is necessary when translating findings as inter-species differences go beyond size. For example, the contractibility of detrusor muscle of most mammalian species is regulated by both cholinergic and purinergic innervation. However, purinergic innervation predominates in rodents, whereas in humans the contraction of detrusor is mostly mediated by cholinergic neurotransmission, with purinergic neurotransmission only accounting for ~3% of neuronal responses (in health). In pathological states this percentage can increase up to ~40%. (Burnstock, 2013) Also, Gevaert *et al.* have described a similar organisation of interstitial cells (IC) in each layer of human, rat and mouse bladders. Although some phenotypic similarities have been observed, this study highlights differences in the phenotype of IC in the upper lamina propria, with less expression of microfilaments (α -SMA) in small rodents when compared to human. (Gevaert *et al.*, 2017)

Pigs provide a good animal model for translational research as they are anatomically and physiologically more comparable to humans than most other species used as biomedical

models. (Kuzmuk and Schook, 2010; Kobayashi *et al.*, 2012) This is also true for the particular case of the porcine urological system, with analogous anatomic, histological and physiological features to humans. (A. L. Dalmoose, J. J. Hvistendahl, 2000) Similar type, distribution and functional response of receptors in porcine and human bladder has been reported in various studies (Crowe and Burnstock, 1989; Goepel *et al.*, 1998; Templeman *et al.*, 2003; Andersson and Arner, 2004; Kumar, Chapple and Chess-Williams, 2004) A comparative immunohistochemistry study of IC in the lamina propria of the urinary bladder of human and pig also evidenced distribution and phenotypic profile of IC in this species. (Steiner *et al.*, 2018)

Despite obvious size differences, the microvasculature of several mammalian species (including human, pig and mouse) is structurally similar as evidenced by vascular corrosion casting studies (Tatematsu *et al.*, 1978; Inoue and Gabella, 1991; Hossler and Monson, 1995; Miodoński and Litwin, 1999; Hossler, Kao and Monson, 2005; Hossler and Kao, 2007; Hossler *et al.*, 2013) Hashitani *et al.* further characterized the suburothelial microvasculature of rat and mouse, particularly regarding morphological, phenotypic and functional properties of mural cells. (Hashitani *et al.*, 2012, 2018; Mitsui and Hashitani, 2013; Shimizu *et al.*, 2014). These studies have been previously discussed in greater detail in section 1.4. Microvasculature. To date, no comparable human studies have been published. Most functional studies on the microvasculature of different organs have been performed in *ex-vivo* live tissue or *in-vivo* rodents. (Kawamura *et al.*, 2004; Peppiatt *et al.*, 2006; Fernandez-Klett *et al.*, 2010; Crawford *et al.*, 2012, 2013; Hall *et al.*, 2014; Hashitani *et al.*, 2015; Bertlich *et al.*, 2017; Canis *et al.*, 2017) It is important to note that available transgenic mice such as NG2 DsRed (red fluorescent labelling of NG2 expression) (Steiner *et al.*, 2018) offer an advantage in the study of pericytes and their functional role.

In vivo pre-clinical intravesical drug delivery studies have been performed in different animal models including mice (Hsieh *et al.*, 2011; Peng *et al.*, 2016; Ren *et al.*, 2016; Pan *et al.*, 2017), rats (Hwang *et al.*, 2009; Karavana *et al.*, 2018), rabbits (Lee and Cima, 2011), dogs (Song, Wientjes and Au, 1997; Chen *et al.*, 2003) and pigs (Harrison *et al.*, 1996; Leakakos *et al.*, 2003; Arentsen *et al.*, 2011). Porcine bladders are considered a better model as their capacity is approximately 500 mL (Sibley, 1985) (volume equivalent

to human [GuhaSarkar and Banerjee, 2010]), whereas in mice and rats the bladder capacity is just ~0.15 mL and ~1 mL, respectively (Andersson and Arner, 2004). In addition, *ex-vivo* studies use rabbit/leporine (Negrete *et al.*, 1996), bovine (Karavana *et al.*, 2018), porcine (Kerec *et al.*, 2002; Di Stasi *et al.*, 2003; Grabnar, Bogataj and Mrhar, 2003; Grabnar *et al.*, 2006; Tsallas, Jackson and Burt, 2011; Williams *et al.*, 2014) and human tissue (S M Di Stasi *et al.*, 1997; Savino M. Di Stasi *et al.*, 1997) and are commonly performed using diffusion apparatus. *Ex-vivo* whole bladder models (Tammela *et al.*, 1993; Tringali *et al.*, 2008; Williams *et al.*, 2015, 2016) have also been reported and a study by Williams *et al.*, further simulated the effect of urine dilution on drug delivery.

Animal models described in the literature to investigate IC/BPS and OAB (or DO) have been previously reviewed (Westropp and Buffington, 2002; Parsons and Drake, 2011) IC/BPS pathology is usually reproduced in these models by exposing healthy animals to noxious intravesical, systemic or environmental stimuli. (Westropp and Buffington, 2002; Birder and Andersson, 2018) However, a similar pathology occurs naturally in domestic cats (feline interstitial cystitis), with features highly comparable to those of IC/BPS in humans, and as such better suited to investigate the disease. (Westropp and Buffington, 2002; Birder and Andersson, 2018) OAB is inheritably difficult to model, considering its symptom-based definition. As such there is no suitable animal model for human idiopathic OAB, that is able to represent the natural progression of the disease and depict the subjective nature of the symptoms (e.g. urinary urgency). (Parsons and Drake, 2011) Animal models to study OAB normally evidence urodynamic changes compatible with DO that are easier to assess. This can be induced in healthy animals with exposure to noxious stimuli (in a similar manner to IC/BPS) or through neuronal injury (relevant for research of NDO). DO can also be present in genetic (e.g. spontaneous hypertensive rat) and transgenic (e.g. purinergic receptor knock-out mouse) animal models. (Parsons and Drake, 2011) Rat and mouse models for KIC have been developed by administering enteric or parenteral ketamine to these animals. Histological features and urodynamic observations are comparable to those reported in human. (Yeung *et al.*, 2009; Meng *et al.*, 2011; Chuang *et al.*, 2013; Gu *et al.*, 2014; Juan *et al.*, 2015; Liu *et al.*, 2015; Song *et al.*, 2016; Kim *et al.*, 2016; Duan *et al.*, 2017; Wang *et al.*, 2017; Lee *et al.*, 2017; Rajandram *et al.*, 2017; W.-C. Lee *et al.*, 2018; S. W. Lee *et*

al., 2018) To my knowledge, no other species have been reported with this condition, despite the common veterinary use of ketamine. It is possible that KIC has not been observed in the veterinary setting considering the dose used is adjusted to the species and therefore not high enough to cause bladder damage. Also, KIC is thought to result from prolonged exposure to ketamine (Middela and Pearce, 2011) and veterinary use of ketamine is often short-term, for restraint or anaesthesia. On the other hand, it cannot be ruled out that KIC develops in other species and is potentially overlooked, as manifestations of this condition are difficult to identify.

1.8. Aims and objectives

OAB, IC/BPS and KIC are bladder pathologies that dramatically affect the quality of life of patients and represent an important economic burden for society. As mentioned before, there is a significant overlap between these bladder conditions, however, an adequate diagnosis is necessary to ensure that patients receive appropriate therapeutic care. Unfortunately, therapeutic options are limited, often ineffective or have side effects that are poorly tolerated by patients. We need to understand better the physiology of the bladder and the pathophysiological mechanisms underlying these conditions to develop targeted and tolerated therapies.

As stated earlier, the bladder wall is an extremely efficient barrier. Given its low permeability to several substances, it is relevant to investigate:

- 1) what concentrations are achieved within the bladder wall following intravesical delivery of a therapeutic drug relevant in the treatment of IC/BPS - lidocaine hydrochloride (Chapter 3; *development of an experimental model*);
- 2) how these are influenced by factors such as the concentration of solution administered, pH and dilution resultant from urine production (Chapter 3; *further development of the experimental model*).
- 3) if ketamine accumulates in the urine and stored in the bladder following drug abuse can permeate into the bladder and achieve potential noxious concentrations (Chapter 4; *using said established experimental model*);
- 4) is the behaviour of ketamine and lidocaine comparable, considering these substances are weak bases with similar molecular weights (Chapter 4).

Informed by these drug delivery studies investigate whether the detrimental effect of ketamine in the bladder is caused by changes in the microvasculature. In that context, it is essential to investigate:

- 5) how blood flow is regulated through the suburothelial capillaries of the bladder and investigate a potential role of pericyte cells in this regulation (chapter 5);
- 6) if ketamine has a vasoactive effect on the suburothelial capillaries and whether this is mediated through NMDAR (Chapter 6);

- 7) if exposure to this drug results in changes in pericyte morphology and density, plausibly leading to bladder dysfunction (Chapter 6).

Taken all together, I propose to:

- 1) Use an establish ex-vivo whole bladder model to study the effect of concentration, pH and urine dilution on intravesical drug delivery (IDD) of lidocaine hydrochloride (Chapter 3).
- 2) Repurpose this IDD model to study the permeation of ketamine through the bladder wall. Firstly, evaluate the effect of ketamine urine concentration (single intravesical instillation) in bladder wall concentration-depth profiles. Later, simulate predicted physiological accumulation of ketamine in urine after consumption and develop bladder wall concentration-depth profiles (Chapter 4).
- 3) Develop and validate a live mouse bladder tissue model to visualise *in situ* microvessels in the bladder and study the mechanisms by which the vasculature is regulated by pericytes (Chapter 5).
- 4) Using this live mouse bladder tissue model investigate the effect of ketamine on the microvasculature, to further elucidate the pathological mechanism of ketamine.

Chapter 2 – General methodology

2.1. Drug delivery studies

These studies were conducted at the School of Pharmacy and Pharmaceutical Sciences, Cardiff University.

2.1.1. Reagents and solvents

Lidocaine hydrochloride (LH) monohydrate, (\pm)-ketamine hydrochloride (KH) and protamine sulfate were acquired from Sigma-Aldrich Company, Dorset, UK. Acetonitrile (HPLC grade), acetic acid glacial, sodium chloride (NaCl), sodium bicarbonate (NaHCO_3), calcium chloride (CaCl_2), magnesium sulphate (MgSO_4), potassium chloride (KCl), monopotassium phosphate (KH_2PO_4), D-glucose, monosodium dihydrogen orthophosphate (NaH_2PO_4), sodium citrate tribasic dehydrate ($\text{Na}_3\text{C}_6\text{H}_5\text{O}_7 \cdot 2\text{H}_2\text{O}$) and sodium sulphate (Na_2SO_4) were purchased from Fisher Scientific, Leicestershire, UK. Sodium oxalate ($\text{Na}_2\text{C}_2\text{O}_4$) and sodium nitrate (NaNO_3) were purchased from Acros Organics, UK. All reagents were of analytical grade or superior. Solutions were prepared with deionised water ($\sim 18\text{m}\Omega\cdot\text{cm}$, supplied by a Purite Select Fusion 160 system).

2.1.2. Tissue preparation

Fresh porcine bladders (Figure 10) were acquired from two local abattoirs and transported to the laboratory in ice-cold oxygenated Krebs-Henseleit buffer. This buffer was composed of 118.3 mM NaCl, 25 mM NaHCO_3 , 2.5 mM CaCl_2 , 1.2 mM MgSO_4 , 4.7 mM KCl, 1.2 mM KH_2PO_4 and 11 mM D-glucose. Prior to use, the buffer was purged with 5% CO_2 and 95% O_2 to pH 7.4. When necessary, the pH was adjusted with either NaOH 1 M or HCl 1 M.

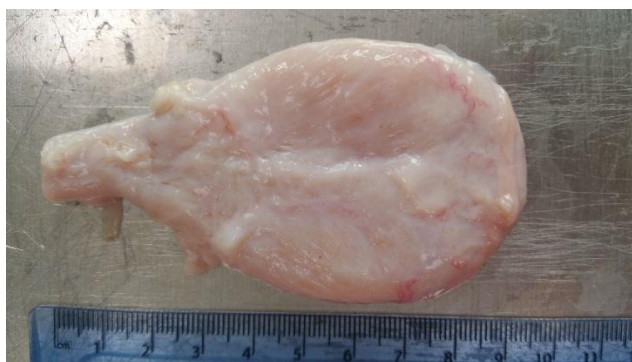


Figure 10 Empty porcine bladder.

Bladders were prepared in similar way to what was previously described by Williams *et al.* (Williams *et al.*, 2015) Excess perivesical fat was removed with the help of ophthalmic scissors, and bladders were filled with saline solution and drained to eliminate any remaining urine. The relevant drug solutions were then instilled into the bladder via the urethra, as specified in 3.2.1. Intravesical instillation of lidocaine hydrochloride (LH) and 4.2.1. Intravesical delivery of ketamine hydrochloride (KH). To prevent solution outflow, bladders were clamped above the vesical trigone and maintained partially submerged in an oxygenated Krebs-Henseleit buffer bath, thermostatically controlled at 37°C, for a set time. Subsequently, clamps were removed, and the solution was discarded. Through a single sagittal cut, the bladders were opened to expose the lumen and rinsed three times with saline solution to eliminate any surface-bound drug. Three samples of full wall thickness ($\varnothing \sim 1\text{cm}$) per bladder were removed, with the help of a cork borer and a scalpel, from areas exposed to the drug solution and promptly snap-frozen between two metal plates with liquid nitrogen. The serosal surface was attached to cork mounts with optimal cutting temperature (OCT) medium (Tissue-Tek™, CRYO-OCT Compound, Fisher Scientific UK, Leicestershire, UK), leaving the mucosa facing upwards. To ensure the concentration gradient throughout the bladder wall was preserved, time between discarding the solution and freezing the samples was less than to 5 min.

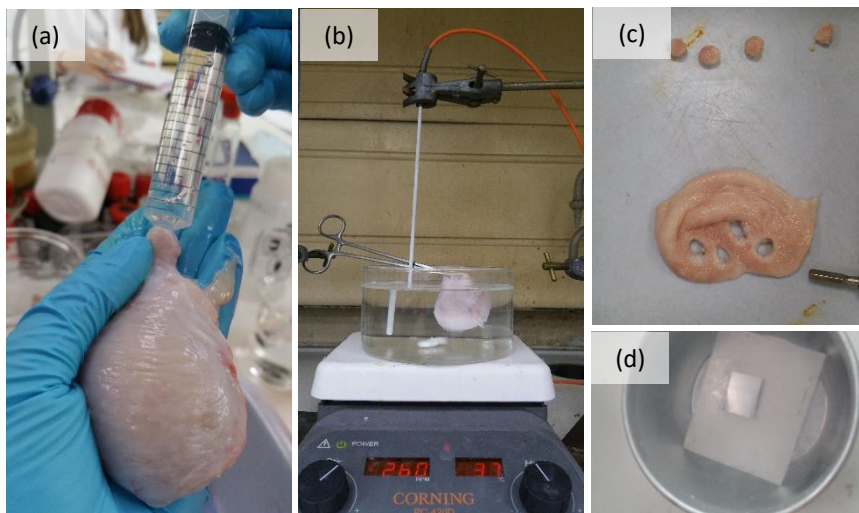


Figure 11 Experimental set up. Bladders were instilled through the urethra with one of the drug solutions in the study (a), clamped and maintained in a Krebs-Henseleit buffer bath, thermostatically controlled at 37°C (b). After a set time, the solution was drained, bladders were cut open and mucosa was rinsed to remove surface-bound drug. Full thickness samples of bladder wall were excised with a cork borer and a scalpel (c) and immediately snap frozen between two metal plates with liquid nitrogen (d).

2.1.3. Cryosectioning

Samples were serially sectioned, with a cutting plane parallel to the urothelium, using a Leica CM3050 cryostat (Leica Microsystems, UK; Figure 12). Slices of 50 μm thickness were obtained and collected in pre-weighed 1.5 mL microcentrifuge tubes. Slices were grouped differently depending on the drug being studied, as specified in 3.2.2. Cryosectioning and 4.2.2 Cryosectioning.

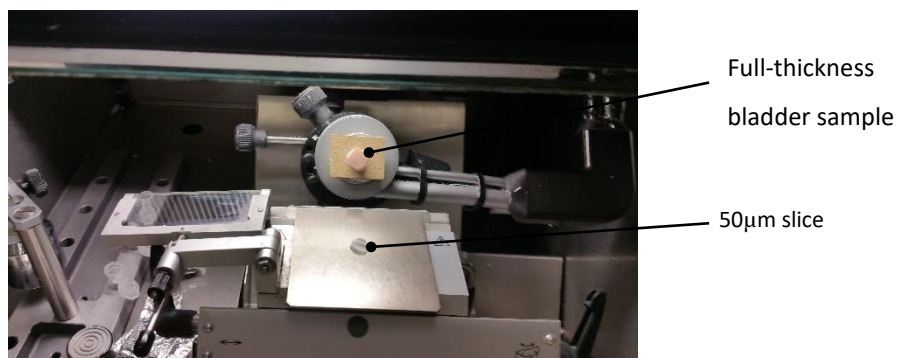


Figure 12 Cryosectioning Slices of 50 μm thickness were obtained from full-thickness bladder samples using a cryostat.

2.1.4. Drug extraction, analysis and quantification

Substances studied were extracted with the respective mobile phase and quantified using HPLC-UV. Considering differences inherent to the drugs studied, drug extraction, analysis and quantification will be addressed in greater detail in 3.2.3. Lidocaine extraction, 3.2.4. Quantification of lidocaine in the bladder wall, 4.2.4 Ketamine extraction, and 4.2.5 Ketamine quantification.

2.1.5. Histology

Samples of tissue were excised from bladders treated with each of the drug solutions used in the study and fixed in 4% buffered formaldehyde (Fisher Scientific, UK) for 48 h at room temperature (RT). Samples were paraffin waxed processed, sectioned at 5 μm thickness and stained with Masson's trichrome by Technical Staff at the Cardiff School of Biosciences, Cardiff University, using the protocol in Table 1.

Stained tissue sections were mounted under a coverslip using D.P.X mountant.

Whole slide images of histological tissue sections were obtained using an objective imaging semi-automated slide scanning system - Olympus BX41 brightfield microscope (20x objective), QImaging QICAM Fast 1394 colour digital camera (associated to a PC) and an OASIS motorised XYZ stage controlled directly via Surveyor software.

Table 1 Masson's trichrome protocol

STEP	REAGENT	TIME
1	Xylene	2 min
2	Xylene	2 min
3	100% Alcohol	2 min
4	100% Alcohol	2 min
5	100% Alcohol	2 min
6	95% Alcohol	1 min
7	70% Alcohol	1 min
8	Running water	2 min
9	Saturated picric acid to enhance stain overnight	Overnight
10	Running water	5 min
11	Iron alum	10 min
12	Running water	2 min
13	Mayer's haemalum	10 min
14	Running water	5 min
15	Ponceau/Fuchsin stain	5 min
16	Running water	1 min
17	1% phosphomolybdic acid	3 min
18	Light green stain	2 min
19	Running water	1 min
20	95% alcohol	20 s
21	100 % alcohol	1 min
22	100% alcohol	2 min
23	100% alcohol	2 min
24	Xylene	2 min
25	Xylene	2 min
26	Xylene	2 min

2.2. Murine tissue model to study the microvasculature properties and function *in situ*

These studies were conducted at the School of Pharmacy, University of Kent.

2.2.1. Tissue preparation

Male C57BL/6J mice (Charles River, UK), aged 8 to 9 weeks old, were killed by cervical dislocation in accordance to Schedule 1 of the Animals Scientific Act of 1986. Bladders (Figure 13) were immediately excised and collected to a container with ice-cold Krebs-Henseleit buffer, freshly prepared as described in 2.1.2. Tissue preparation and oxygenated with 95% O₂/ 5% CO₂. In a petri dish filled with Krebs-Henseleit buffer, continuously bubbled with 95% O₂/ 5% CO₂, two to four full thickness samples were taken per bladder, with the help of a scalpel and tweezers.

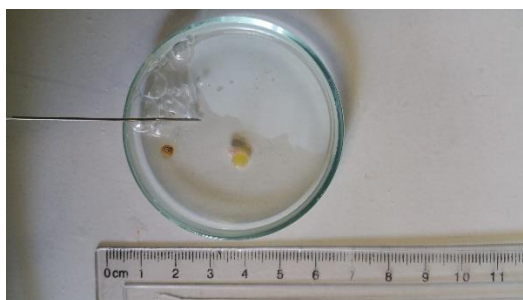


Figure 13 Mouse bladder full of urine.

2.2.2. Tissue viability

Tissue viability for the bladder samples was assessed using a propidium iodide (Invitrogen™, Thermo Fisher Scientific, UK) and Hoechst 33342 (Invitrogen™, Thermo Fisher Scientific, UK) counterstaining protocol. In order to determine the period of time tissue is viable after bladder excision, three full thickness samples from different mice (n=3) were analysed following a defined time from animal dissection to end of staining (45 min, 1 h 45 min, 2 h 45 min, 3 h 45 min or 4 h 45 min). One sample per well was placed in a Nunclon™ 4 well plate (Nunc™, Thermo Fisher Scientific, UK) and filled with Krebs-Henseleit buffer. This plate was enclosed in an oxygen dye-loading chamber, kept oxygenated until tissue fixation and was continuously shaken on top of a shaker table. Samples were incubated with propidium iodide at a working concentration of 40 μM and Hoechst 33342 10 μM for 20 min. After incubation, samples were washed three times with Krebs-Henseleit buffer, 5 min per wash. Bladder samples were fixed with 4% (w/v)

paraformaldehyde (PFA) (Sigma-Aldrich, UK) made in 0.1 M phosphate buffer solution (PBS) (Sigma-Aldrich, UK) for 15 min, followed by three washes with 0.1 M PBS for 10 min each. Samples were mounted on a slide using CitiFluor™AF1 (Agar Scientific) and protected with a coverslip, sealed with nail varnish and stored in the dark at 2 °C.

Slides were imaged using a Nikon 50i Epifluorescence microscope associated with a QI imaging camera. Six images per slice were captured with a 40x objective separately with a DAPI (blue) filter, allowing detection of Hoechst 33342 stained cells (excitation/emission: 350 nm/461 nm) and Texas Red (red) filter for identification of propidium iodide stained cells (excitation/emission: 535 nm/617 nm). Using Fiji software, the two images obtained per field were merged and the number of dead cells (counterstained by Hoechst and propidium iodide) and the total number of cells (stained by Hoechst) was counted. Cell viability (%) was calculated as follows (Equation 1):

[Equation 1]
$$Cell\ viability\ (\%) = 100 - \frac{Number\ of\ dead\ cells}{Total\ number\ of\ cells} \times 100$$

That is:

$$Cell\ viability\ (\%) = 100 - \frac{Number\ of\ cells\ counterstained\ by\ Hoechst\ 33342\ and\ Propidium\ iodide}{Number\ of\ cells\ stained\ by\ Hoechst\ 33342} \times 100$$

2.2.3. DIC imaging and functional experiments

Capillary diameter changes mediated by pericytes in response to physiological relevant vasoactive drugs were recorded in video using differential interference contrast (DIC) microscopy as reported in by Crawford *et al.* (Crawford *et al.*, 2012) Samples prepared as described in 2.2.1. Tissue preparation were imaged in an upright Olympus BX51WI microscope, positioned in a lens dish filled with Krebs-Henseleit buffer bath (~1.5 mL), with the mucosa facing upwards and kept in place with the help of a harp pin. Tissue samples were continuously superfused with oxygenated Krebs-Henseleit buffer at a rate of 2.5 mL min⁻¹, using a Watson Marlow 120s perfusion pump. Images were obtained with an Olympus x60 water immersion objective, with a Rolera XR CCD camera (QImaging, Surrey, Canada), and a video was produced as a succession of images were captured at 1 frame per second, for a total of 1200 frames (unless otherwise stated).



Figure 14 DIC imaging. Full-thickness bladder samples were imaged using an upright Olympus BX51WI microscope, positioned in a lens dish filled with Krebs-Henseleit buffer bath, with the mucosa facing upwards and kept in place by a harp pin. Tissue samples were continuously superfused with oxygenated Krebs-Henseleit buffer at a rate of 2.5 mL min^{-1} . Images were obtained with an Olympus x60 water immersion objective with a Rolera XR CCD camera.

Functional experiments to validate the model were performed with physiologically relevant vasoactive drugs to assess pericyte-mediated changes. For each bladder sample, one capillary with a pericyte site (where the cell body was observed with a 'bump-on-a-log morphology' (Crawford *et al.*, 2012)) and a non-pericyte site was identified in the lamina propria. A baseline of the inner capillary diameter at those sites was established during superfusion of the bladder tissue with Krebs-Henseleit buffer (~ 150 frames). This was typically followed by superfusion with one of the vasoactive drugs for a defined period (~ 500 frames) and washed away with Krebs-Henseleit buffer. The following drugs were used to evoke diameter changes: angiotensin II (Ang-II: 1nM, 10nM, 100nM and 300nM; Sigma-Aldrich, UK), indomethacin (30 μM and 100 μM ; Sigma-Aldrich, UK), endothelin-1 (ET-1, 1 nM and 10 nM, Tocris, UK), noradrenaline (NA: 10 nM; Sigma-Aldrich, UK), prostaglandin E₂ (PGE₂: 10 μM , 30 μM and 100 μM ; Tocris, UK), glycine (Gly: 10 μM and 1 mM; Sigma-Aldrich, UK), L-glutamic acid (Glu: 10 μM and 1 mM; Sigma-Aldrich, UK) and ketamine hydrochloride (KH: 10 $\mu\text{g/mL}$, 30 $\mu\text{g/mL}$ and 100 $\mu\text{g/mL}$; Tocris, UK). Drugs were prepared into stock aliquots according to the respective data sheets. Working concentrations were prepared in oxygenated Krebs-Henseleit buffer prior to imaging.

Analysis of the videos was performed off-line with Fiji software. In these experiments, each capillary acted as its own control. The inner diameter of the capillaries was measured (47 pixels of the images is equivalent to 10 μm) in a straight-line every 5 frames of the video at a pericyte site and in a non-pericyte site. Resting baseline of the inner diameter was calculated as an average of the first 5 measurements of each video (whilst the tissue had been exposed to oxygenated Krebs-Henseleit buffer only) and was

expressed as 100% diameter. All subsequent measurements of the inner diameter of the capillaries were expressed as a percentage of the baseline diameter (Equation 2). A maximum constriction or dilation per pericyte site and non-pericyte site of each capillary was determined as shown in Equation 2.

$$\text{[Equation 2]} \quad \% \Delta \text{ vessel diameter} = \frac{\text{Measured diameter}}{\text{Mean baseline diameter}} \times 100$$

$$\% \text{ constriction or dilation} = 100\% (\text{baseline} - \% \Delta \text{ vessel diameter})$$

Only changes in capillary diameter superior to 5% of the baseline were considered as a response to the drug applied, to reduce the risk of bias during analysis.

2.2.4. Immunohistochemistry

2.2.4.1 α -SMA/NG2/Hoechst immunohistochemical staining

Bladder tissue was pinned to a Sylgard® 184 dissection disc with insect pins and mucosa was carefully separated from the detrusor with the help of a brush, tweezers and an ophthalmic scissor (Figure 15).

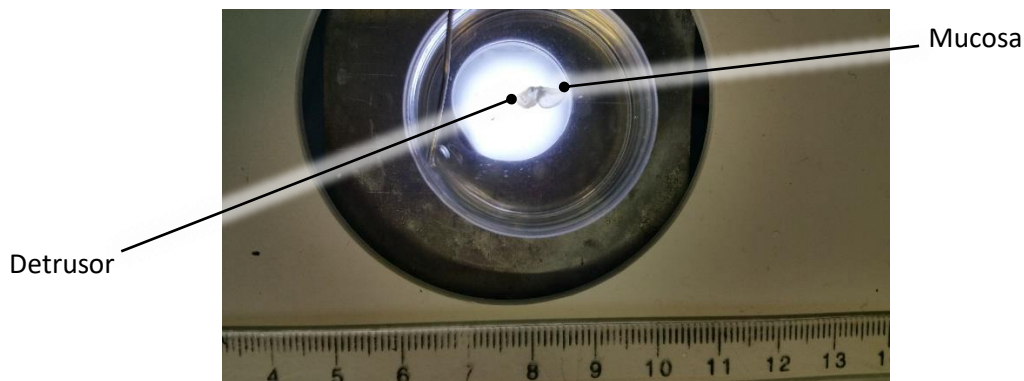


Figure 15 Dissection of murine bladder tissue Bladder tissue pinned to a dissection disc showing separation of mucosa from detrusor.

Mucosal preparations were placed in a Nunclon®4 well plate, one per well filled with Krebs-Henseleit buffer, which was positioned in an oxygen dye-loading chamber. Mucosal preparations were incubated for 20 min with Hoechst 33342, to stain the nucleus of all cells, with a working concentration of 5 μ M, followed by 3 washes with Krebs-Henseleit buffer for 5 min each. Slices were then fixed with PFA for 15 min and

PFA was washed away with PBS (3 washes of 10 min). After this period, tissue cells were permeabilised using 0.1% triton x100 (Acros Organics, UK; prepared in PBS 0.1M) at RT for 10 min on shaker table and blocked with 10% donkey serum (prepared in 0.1% triton x100) at RT for 2 h. Mucosal preparations were then incubated with primary antibodies – goat polyclonal anti- α -SMA (abcam, Cambridge, UK), to detect mural cells in the microvasculature expressing α -SMA, and rabbit anti-NG2 polyclonal antibody (Millipore UK Ltd, Watford, UK), to identify NG2⁺ mural cells in the microvasculature - for 16 h at 2 °C followed by 3 washes of 10 min each with PBS 0.1 M. Subsequently, slices were incubated for 2 h with donkey anti-rabbit IgG (H+L), Alexa Fluor 555[®] (1/200) (Thermo Fisher Scientific, UK) and donkey anti-goat IgG (H+L), Alexa Fluor[®] 488 (Abcam, Cambridge, UK) (1/200) prepared in 10% donkey serum. After the incubation with the secondary antibodies, mucosal preparations were washed 3 times with PBS 0.1 M. Mucosal preparations were mounted on a slide with CitiFluor™AF1 and protected by a coverslip, sealed with nail varnish and stored in the dark at 2 °C. For control, mucosal preparations were treated as described but incubated with each one of the primary or secondary antibodies on its own.

Slides were imaged with use of a Carl Zeiss LSM 800 confocal microscope with a Plan-Apochromat 40x oil immersion lens (Carl Zeiss Ltd, Oberkochen, Germany), using immersion oil (#518F, Carl Zeiss Ltd, Oberkochen, Germany). Alexa Fluor[®] 488 was excited at 488 nm and detected in a range of 490-570 nm, Alexa Fluor[®] 555 was excited at 561 nm and detected between 566-697 nm and Hoechst 33342 was excited at 405 nm and detected at 410-498 nm. At least 6 images per slide were obtained of regions of interest, showing the capillary network, arterioles and/or venules.

2.2.4.2 NG2/GS-IB4 co-staining

Full thickness tissue preparations were obtained as described in 2.2.1 Tissue preparation. These were placed in a Nunclon[®]4 well plate, one per well filled with Krebs-Henseleit buffer, which was positioned in an oxygen dye-loading chamber. Full thickness tissue preparations were incubated for 4 h with either Krebs-Henseleit buffer (acting as control) or ketamine hydrochloride 10 μ g/mL, 30 μ g/mL or 100 μ g/mL, prepared in Krebs-Henseleit buffer. During incubation the chamber was kept oxygenated. After

incubation, tissue preparations were fixed with paraformaldehyde 4% prepared in 0.1 M of PBS, for 15 min, followed by three washes of 10 min each with 0.1M PBS. These were pinned to a Sylgard® 184 dissection disc with insect pins with the urothelium facing up. With the help of a scalpel blade the urothelium was carefully scraped off followed by separation of the lamina propria from the detrusor.

Each lamina propria preparation was placed back in the Nunclon®4 well plate for immunohistochemical staining. Lamina propria preparations were permeabilised using 0.1% triton x100 (Acros Organics, UK, prepared in PBS 0.1 M) at RT for 10 min on a shaker table and blocked with 10% donkey serum (prepared in 0.1% triton x100) at RT for 2 h. Slices were then incubated with rabbit anti-NG2 polyclonal antibody (1/200) (primary antibody) GS-IB4 conjugated with Alexa Fluor® 488 (10 µg/mL) (Invitrogen™, Thermo Fisher Scientific, UK) in 10% donkey serum (prepared in 0.1% triton x100) for 16 h at 2°C. On the following day, slices were washed three times (10 min each) with PBS 0.1M, followed by incubation for 2 h with anti-rabbit IgG (H+L), Alexa Fluor 555® (1/200) prepared in 10% donkey serum. After incubation with the secondary antibody, lamina propria preparations were washed 3 times with PBS 0.1 M. Lamina propria preparations were mounted in a slide with CitiFluor™AF1 and protected by a coverslip, sealed with nail varnish and stored in the dark at 2 °C. NG2 antibodies are well-established in our research laboratory (Crawford *et al.*, 2012) and therefore additional tests for specificity of these antibodies used were not conducted.

Slides were imaged using a Carl Zeiss LSM 800 confocal microscope with a Plan-Apochromat 63x oil immersion lens (Carl Zeiss Ltd, Oberkochen, Germany), using immersion oil (#518F, Carl Zeiss Ltd, Oberkochen, Germany). Alexa Fluor® 488 was excited at 488 nm and detected in the range of 490-570 nm, whereas Alexa Fluor® 555 was excited at 561 nm and detected between 566-697 nm. Six regions per slice were randomly selected and imaged.

Images were analysed with Fiji software. Mean pericyte density (number of perivascular NG2⁺cells/10,000 µm²), number of pericytes along 100 µm of capillary, distance between pericyte cell bodies, height and width of pericyte cell body and length of processes along the capillaries were determined for each treatment and compared.

2.3. Statistical analysis

All data values are presented as the mean \pm standard error of the mean (SEM), determined from experiments conducted using a number of animals (n is specified in each experimental section). Statistical significance was calculated with the appropriate test (*t*-test or ANOVA, as specified in each experimental section), using IBM® SPSS® Statistics or GraphPad PRISM 8.0 software. Values of $p < 0.05$ were considered statistically significant. The rationale for each statistical test conducted is provided in 3.2.6. Statistical analysis, 4.2.6. Statistical analysis, 5.2.5. Statistical analysis and 6.2.4. Statistical analysis.

Chapter 3 – Intravesical drug delivery studies – Lidocaine

3.1. Introduction

3.1.1. Clinical relevance of intravesical delivery of lidocaine

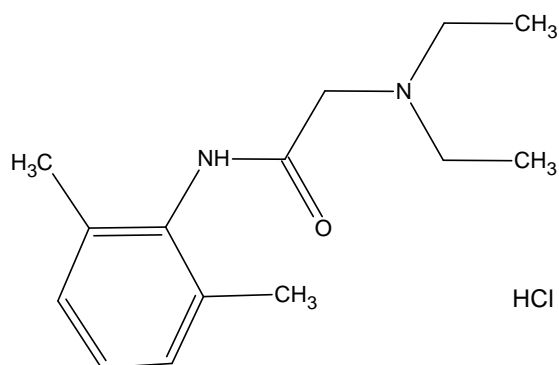


Figure 16 Chemical structure of lidocaine hydrochloride

Lidocaine (Figure 16) is one of the most commonly employed local anaesthetics, to prevent or treat acute and chronic pain and manage neuropathic pain. It has several therapeutic applications in medicine, including infiltration anaesthesia, epidural anaesthesia, spinal anaesthesia and intravenous regional anaesthesia. (Golzari *et al.*, 2014) It reversibly binds to neuronal voltage-gated sodium channels, thus inhibiting the initiation and propagation of action potentials in both nerve and muscle cells. Lidocaine is indicated not only for anaesthesia but also as an antiarrhythmic drug. (Golzari *et al.*, 2014) This compound is characterized by a fast onset of action and an intermediate duration of activity. Additional effects of lidocaine include blockage of muscarinic and dopamine receptors and anti-inflammatory properties, with suppression of migration, exocytosis, and phagocytosis. (Hollmann and Durieux, 2000; Henry, Morales and Cahill, 2015)

Intravesical administration of lidocaine has long been used for local anaesthesia, with or without electromotive drug administration (EMDA), prior to painful procedures, such as bladder biopsies (Pode, Zylber-Katz and Shapiro, 1992; Thrasher *et al.*, 1993; Holmäng, Aldenborg and Hedelin, 1994; Lugnani *et al.*, 2008), hydrodistension (Fontanella, Rossi and Stephen, 1992; Riedl *et al.*, 1997; Rosamilia, Dwyer and Gibson, 1997), botulinum toxin injections (Nambiar *et al.*, 2016) and intravesical instillation of irritative substances like capsaicin (Dasgupta, Fowler and Stephen, 1998; De Sèze *et al.*, 2004).

Additionally, lidocaine has been suggested to have some diagnostic value. Yokoyama *et al.* have proposed that lidocaine can be used to distinguish detrusor overactivity resultant from spinal cord injuries or other lesions. Bladder overactivity in patients with chronic spinal cord injuries may be explained by a reorganisation of the afferent connections, with afferent C-fibres contributing for the micturition cycle. In healthy individuals or patients with detrusor overactivity secondary to brain lesions or benign prostatic hyperplasia (BPH) the afferent signalling is mainly mediated by A δ fibres (although some individual differences can be observed). Accordingly, it was observed that lidocaine, which blocks afferent C fibres, increases bladder capacity more significantly in patients with detrusor overactivity secondary to spinal cord injuries than patients with BPH or brain lesions. (Yokoyama *et al.*, 1997, 2000) Other studies have suggested intravesical instillation of lidocaine can be useful in differentiating between pain originating from urinary bladder or from conditions affecting other organs, including endometriosis, colitis, diverticulitis, vaginosis and cervicitis. (Teichman, Nielsen-Omeis and McIver, 1997; Taneja, 2010)

An important advantage of intravesical lidocaine when compared to other analgesic therapies is that it achieves a therapeutic effect without the rebound effect experienced upon withdrawal of narcotics or the detrimental effect of neurotoxins. (Nickel *et al.*, 2009)

In pathophysiological conditions affecting the bladder, including OAB, IC/BPS, the afferent C-fibres, which are silent in physiological conditions, assume an important role in micturition as these are often overstimulated, conveying the sensation of pain and urgency. (Fowler, Griffiths and de Groat, 2008) Local anaesthetics act primarily by blocking the conduction of afferent C-fibres, which are smaller unmyelinated fibres and therefore easier to block than larger and myelinated afferent A δ -fibres. Intravesical instillation of local anaesthetics was shown to reduce pain, increase functional bladder capacity and inhibit detrusor contractions (Yokoyama *et al.*, 1997).

It has been argued however that lidocaine is poorly absorbed by the bladder tissue and therefore can only provide superficial mucosal anaesthesia. Birch *et al.* studied the systemic absorption of the drug following retention of a 1% (w/v) lidocaine solution in the bladder for 1 or 2 h. The maximum plasma concentration achieved was 121 ng/ml

with a time to maximum concentration of 60-90 min. (Birch and Miller, 1994) Podes *et al.* reported a mean serum lidocaine concentration of 160 ng/ml following 30 min retention of intravesical instillation of 1.5% (w/v) lidocaine hydrochloride solution. (Pode, Zylber-Katz and Shapiro, 1992)

Considering these studies, a number of strategies to improve lidocaine penetration into the bladder tissue have been explored, including EMDA and alkalisation of the lidocaine solution.

EMDA is a technique used to enhance the penetration of ionic drugs into the bladder tissue in the presence of an electric field. (Rosamilia, Dwyer and Gibson, 1997) Preliminary studies using EMDA with intravesical administration of lidocaine prior to hydrodistension report effective mucosal anaesthesia and persistent improvement of voiding symptoms in roughly two-thirds of IC patients. It was not however clear in these studies whether symptomatic relief was a direct consequence of lidocaine instillation, as hydrodistension procedures alone have been shown to benefit IC patients. (Fontanella, Rossi and Stephen, 1992; Gürpınar, Wong and Griffith, 1996; Riedl *et al.*, 1997; Rosamilia, Dwyer and Gibson, 1997) In another study by Gürpınar *et al.*, blood lidocaine values ranged from undetectable (<0.1 µg/dL) to 0.6 µg/dL. (Gürpınar *et al.*, 1996) More recently, the results of an open-label study have shown multiple intravesical EMDA of lidocaine can improve both quality-of-life and sexuality in patients with therapy-refractory chronic OAB, with significant improvement in bladder capacity and reduction in daily micturition observed. However, in this study patients were hospitalised with circulatory monitoring as a cautionary measure; 17% of the patients experienced reactive hypertension during treatment, which resolved without intervention. (Burmester *et al.*, 2008)

Lidocaine is a weak base (pKa ~7.8) and is usually administered as a water-soluble, ionized hydrochloride salt, with a pH in aqueous solution ranging from 5 to 7. (Di Stasi *et al.*, 2003) Notably, drug absorption of local anaesthetics is directly proportional to lipid solubility and concentration and inversely proportional to molecular weight and ionized fraction. (Henry, Morales and Cahill, 2015) Lidocaine has a poor lipid solubility, however, that impact on absorption can be counterbalanced by using higher concentrations in solution. More importantly, the ionized and non-ionized fractions are

markedly dependent on pH. The non-ionized form of lidocaine has a higher lipophilicity and therefore better penetration across the mucosa. When administered into the bladder, the presence of urine (pH 5 to 6) means the majority (~98%) of lidocaine remains in the ionized form. This “ion-trapping” effect limits permeation through the bladder wall and restricts its use.(Henry, Morales and Cahill, 2015) The effect of intravesical alkalinised lidocaine on detrusor instability was first studied by Higson *et al.* (Higson, Smith and Hills, 1979) One intravesical instillation of 40 ml of 1% (w/v) lidocaine solution with 40 ml of 8.4% (w/v) sodium bicarbonate solution in 20 patients resulted in augmented bladder capacity and a reduction of the maximum detrusor pressure during bladder filling in most patients. However, the effect was short-lived, lasting less than 24 h in most patients. Lapointe *et al.* have retrospectively studied the effects of intravesical lidocaine on bladder urodynamics in children with neurogenic bladder secondary to myelomeningocele. Instillation of alkalinised lidocaine (7.5 to 15 mL lidocaine 2% [w/v] plus 35 mL of sodium bicarbonate 4% [w/v] in physiological saline) for up to 8 min has shown to improve significantly bladder capacity in 70.8% of the urodynamic studies in children and decrease the number of uninhibited contractions during bladder filling in 56.8% of the urodynamic studies in children, suggesting an improvement in bladder dynamics in children with neurogenic bladder. (Lapointe *et al.*, 2001) The pharmacokinetics of alkalinised lidocaine were studied by Henry *et al.* in a small group of healthy volunteers and patients with IC. Intravesical instillation of 4, 5 and 6 mg/kg lidocaine buffered with 8.4% (w/v) sodium bicarbonate (1 to 2% final concentration of lidocaine) resulted in a serum peak concentration of ~1 µg/ml within 30 to 60 min. Buffering the anaesthetic solution with sodium bicarbonate (to a pH~8), where the non-ionized fraction is estimated to be around 61%, showed safe and increased lidocaine serum levels in both groups and it decreased pain scores in the group of patients with IC. However, urethral discomfort after voiding the buffered lidocaine was experienced in all patients. (Henry *et al.*, 2001) A later multi-centre, placebo-controlled trial with a larger number of patients (~100) with interstitial cystitis revealed that a 5-day treatment with alkalinised intravesical lidocaine was effective in reducing overall bladder symptoms, when compared to placebo. The peak serum lidocaine concentration during this study was less than 2 µg/mL, and below the toxic level (>5 µ g/mL). The effect persisted beyond the end of the treatment. (Nickel *et al.*, 2009)

As dysfunction of the glycosaminoglycan layer (GAG) is believed to be an important feature of IC/BPS pathophysiology (Parsons, 2007), the combination of alkalinised lidocaine with glycosaminoglycans has also been studied. It was hypothesised that lidocaine could provide an immediate sense of relief whilst the mucus layer enhancers could provide positive long-term effects by restoring the barrier function of the mucus. Therapy with mucus layer enhancers alone showed positive long-term results following multiple instillations (Morales *et al.*, 1996; Riedl *et al.*, 2008; Engelhardt *et al.*, 2011), however, these failed to provide immediate relief of symptoms, which can potentially lead to early patient withdrawal. Parsons tested the efficacy of 40,000 U heparin, 8 mL 1%(w/v) lidocaine (group 1) or 2% (w/v) lidocaine (group 2), and 3 mL 8.4% (w/v) sodium bicarbonate administered intravesically in patients with newly diagnosed IC in a small open-label non-randomized trial. (Parsons, 2005) Significant immediate symptom relief was experienced after one instillation in 75% of patients from group 1 and 94% from group 2. Sustained relief was experienced by 80% of patients in group 2 after 2 weeks with multiple instillations. Based on the results of this study, Parsons also proposed that lidocaine has a capacity to downregulate nerves beyond the duration of its anaesthetic activity. A subsequent study by Welk *et al.* studied the effect of multiple instillation of a similar therapeutic cocktail in IC patients with complaints of dyspareunia. Most patients experienced an improvement of symptoms and reduction in dyspareunia was experienced in roughly half. (Welk and Teichman, 2008) Furthermore, Lv *et al.* reported a non-randomized controlled open-label trial to study the effect of a therapeutic protocol with multiple instillations of alkalinised lidocaine and hyaluronic acid (40 mg hyaluronic acid, 10 ml of 2% [w/v] lidocaine and 5 ml of 8.4% [w/v] sodium bicarbonate) when compared to alkalinised lidocaine or hyaluronic acid alone. The group receiving combination therapy was shown to yield short-term and long-term symptomatic benefits, whereas alkalinised lidocaine alone only provided symptomatic improvement in the first weeks and hyaluronic acid in later stages. This further supports the use of a 'cocktail' therapy for benefit of the patient throughout treatment. (Lv *et al.*, 2012) Randomized controlled blinded trials are necessary to confirm this effect.

One of the disadvantages of IDD is the low drug residence time, leading to the necessity of multiple instillations for the maintenance of an effective drug concentration within

the bladder. (Lee and Cima, 2011) Recently, a continuous lidocaine-releasing intravesical system (LiRIS®) was developed for IC/BPS patients. This device, designed to be retained in the bladder for 2 weeks, was shown in Phase I clinical trial to be well tolerated and reduce bladder pain and urinary urgency. The effect on bladder pain was maintained months after removal of the device and an unexpected effect on urothelial healing of IC/BPS lesions was observed, suggesting an anti-inflammatory action. (Nickel *et al.*, 2012) Informed by the latter, a randomized Phase II study to assess the safety and efficacy of LiRIS® in females with IC with Hunner's lesions was recently completed and revealed a significant reduction in number of Hunner's lesions but not a significant reduction in daily average bladder pain when compared to placebo. (ClinicalTrials.gov, 2018)

Despite the studies described, there is limited knowledge regarding the concentration of lidocaine present in the bladder tissue following an intravesical instillation and how it distributes across the different layers. As stated previously, serum or plasma concentrations were reported in some studies and are valuable to confirm safe values of lidocaine systemic concentration following intravesical delivery. Moreover, those values reinforce that bladder absorption occurs. As lidocaine is believed to act in the bladder wall, estimating this anaesthetic concentration within the bladder might provide further understanding of the effect of distinct solutions used in the clinic and provide rationale for future drug design and formulation.

In this study we use a previously established *ex vivo* whole bladder model of IDD, as first reported by Williams *et al.* 2015, to describe in detail the concentration of lidocaine per layer of tissue after instillation with clinically relevant solutions of lidocaine (2% [w/v] and 4% [w/v] saline and 2% [w/v] alkalised). Moreover, urine flow was simulated to address the effect of pH and dilution on the permeation of the instilled solutions expected in physiological conditions.

3.1.2. Hypothesis and aims

It was hypothesised that lidocaine concentrations within the bladder wall would depend on the concentration and pH of the solution administered intravesically and would be further affected by urine production, due to dilution and change of pH.

The aim of the present section of work was to study these effects on concentrations of lidocaine achieved within the bladder wall, using clinically relevant solutions of lidocaine. To accomplish the aims, the key objectives were:

1. Establish and compare concentration-depth profiles throughout the bladder wall following 1 h retention of intravesically instilled lidocaine 2% (w/v) and 4% (w/v) saline solutions and 2% (w/v) alkalised.
2. Simulate urine production and establish concentration-depth profiles and concentration per layer after 1h of intravesical instillation of lidocaine 2% (w/v) saline and 2% (w/v) alkalised. Compare with the urine-undiluted bladders treated with the same solutions.
3. Compare histological features of bladders treated with each solution and bladders treated with saline alone (control).

3.2. Methods

3.2.1. Intravesical instillation of lidocaine hydrochloride (LH)

Porcine bladders were collected and prepared as described in 2.1.2. Tissue preparation. To study the effect of concentration and pH on LH penetration through the bladder wall, with or without the influence of urine production, two different sets of experiments were conducted.

In the first set – here designated **urine-undiluted set** – bladders were instilled with one of the following solution: 20 mL of LH 2% (w/v) prepared in saline solution (8 bladders); 20 mL of LH 4% (w/v) prepared in saline solution (8 bladders); or 10 mL of LH 4% (w/v) aqueous followed by 10 mL of sodium bicarbonate 8.4% (w/v) (8 bladders), resulting in a final concentration of LH 2% (w/v).

In the second set - here designated **urine-diluted set** – synthetic urine (composed of NaCl 105.5 mM, NaH₂PO₄ 3.2 mM, Na₃C₆H₅O₇·2H₂O 3.2 mM, MgSO₄ 3.9 mM, CaCl₂ 4.0 mM, Na₂SO₄ 17 mM, KCl 64 mM, Na₂C₂O₄ 0.3 mM and NaNO₃ 1.0 mM, pH 5.8, pre-equilibrated at 37 °C (Williams *et al.*, 2015)) was administered at a rate of 10 mL/10 min to bladders for the duration of the experiment to bladders instilled either with 20 mL of LH 2% (w/v) saline (6 bladders) or LH 2% (w/v) alkalised (6 bladders).

As a negative control, two bladders were instilled with 20 mL of saline solution, NaCl 0.9% (w/v).

Solutions were retained within the bladders for 60 min. After this period, bladders were treated as described in 2.1.2. Tissue preparation.

3.2.2. Cryosectioning

Full-thickness samples of bladder wall were serially sectioned parallelly to urothelium, with a defined thickness of 50 µm, and collected to pre-weighed microcentrifuge tubes as described in

2.1.3. Cryosectioning. Similar to what was previously described (Williams *et al.*, 2015) the first 5 slices, comprising the urothelium (0-250 µm), were collected separately; six groups of four slices were collected from lamina propria (250-1450 µm) and four groups

of ten slices from detrusor muscle (1450-3450 μm). After collection, microcentrifuge tubes containing sliced tissue were weighed.

3.2.3. Lidocaine extraction

LH was extracted with 1 mL of mobile phase (please refer to 3.2.4. Quantification of lidocaine in the bladder wall) per microcentrifuge tube for a period of 24 h, with 10 min of sonication. This was followed by centrifugation at 14000 rpm for 10 min to sediment the tissue residues and isolate supernatant for high-performance liquid chromatography (HPLC) associated with ultraviolet (UV) detection. Slices of tissue were not further homogenised as preliminary studies showed that such process would require additional steps of separation (e.g. filtration) to avoid impurities in the HPLC system, which was viewed as potential source of error, without relevant changes in extraction efficiency. Furthermore, a second extraction with mobile phase did not produce peaks above LOQ, therefore a single extraction was considered sufficient.

3.2.4. Quantification of lidocaine in the bladder wall

Identification and quantification of LH were achieved with HPLC-UV, using a Thermo Scientific Spectra SYSTEM AS3000 equipped with a Kromasil column (5 μm , C18, 250 mm x 4.6 mm i.d.) (Sigma-Aldrich, Dorset, UK) and associated with a Thermo Scientific Spectra SYSTEM UV1000 set at 254 nm. ChromQuest 5.0 software was used to operate the chromatographic system and analyse chromatograms obtained. The mobile phase was acetonitrile/water with 5% acetic acid, pH 3.4 (20:80), as specified in the lidocaine monograph of the United States Pharmacopeia (USP) (Pharmacopeial Convention, 2016). The injection volume was 20 μL and the flow rate was maintained at 1 mL/min. Measurements were performed at room temperature (RT). External standard calibration curves were developed to determine the integrated peak areas (AUC) as a function of LH concentrations (5, 15, 25, 100, 200 $\mu\text{g}/\text{mL}$) prepared in mobile phase. Limit of detection (LOD) and limit of quantification (LOQ) were based on the signal-to-noise-ratios of 3:1 and 10:1, respectively.

Tissue concentrations of LH for each individual or grouped sections were determined by dividing the total amount of drug extracted by the total weight of tissue collected per microcentrifuge tube. Similarly, average concentrations of LH in urothelium, lamina propria, detrusor muscle and full thickness bladder wall after treatment were

determined by dividing the total amount of drug extracted by the total weight of tissue in that layer.

3.2.5. Histology

Please refer to 2.1.5. Histology.

3.2.6. Statistical analysis

Statistical analysis was performed using IBM® SPSS® Statistics and GraphPad Prism software. One-way ANOVA with Tukey post hoc test was used to compare the mean concentration for each layer following intravesical instillation with LH 2% (w/v) saline, LH 4% (w/v) saline and LH 2% (w/v) alkalised (undiluted sets). This test was used considering that: the dependent variable (concentration) is continuous; the independent variable consists of three categorical and independent groups (bladders treated with LH 2% saline, LH 4 % saline and LH 2% alkalised), and concentration is approximately normally distributed for each treatment (confirmed using D'Agostino-Pearson normality test). Tukey post hoc test was used to indicate which tests differed from each other. Unpaired *t*-tests were conducted to compare undiluted and diluted sets treated with same solution. This test was conducted as it allows comparison of the means between two independent groups (LH 2% saline undiluted and LH 2% saline urine-diluted; LH2 % alkalised undiluted and LH 2% alkalised urine-diluted) on the same continuous, dependent variable (concentration). Assumptions were as described above. Although normality was not confirmed for urine-diluted treatments, due to the small sample size, it was extrapolated that urine-diluted sets would show a normal distribution as observed for the undiluted sets.

3.3. Results

3.3.1. Quantification of lidocaine in the bladder wall

3.3.1.1. LH detection and analysis

External calibration curves were linear for the range of concentrations studied (Figure 17). The retention time for LH was ~7 min (Figure 18). LOD and LOQ were 1 and 5 $\mu\text{g mL}^{-1}$ respectively. Samples from bladders instilled with saline solution had no peaks in the proximity of the LH retention time. All samples from bladders instilled with one of LH solutions exhibited peaks above LOQ.

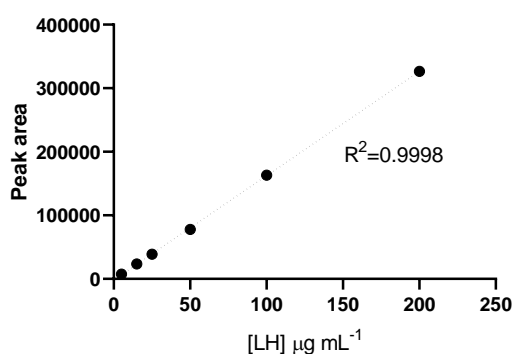


Figure 17 Calibration curve of lidocaine hydrochloride (LH) Example of an external calibration curve for lidocaine hydrochloride (LH). Linearity was observed over the range of concentrations studied (5, 15, 25, 100, 200 $\mu\text{g/mL}$). The calibration curve was used to extrapolate concentration of LH in solution extracted from bladder samples.

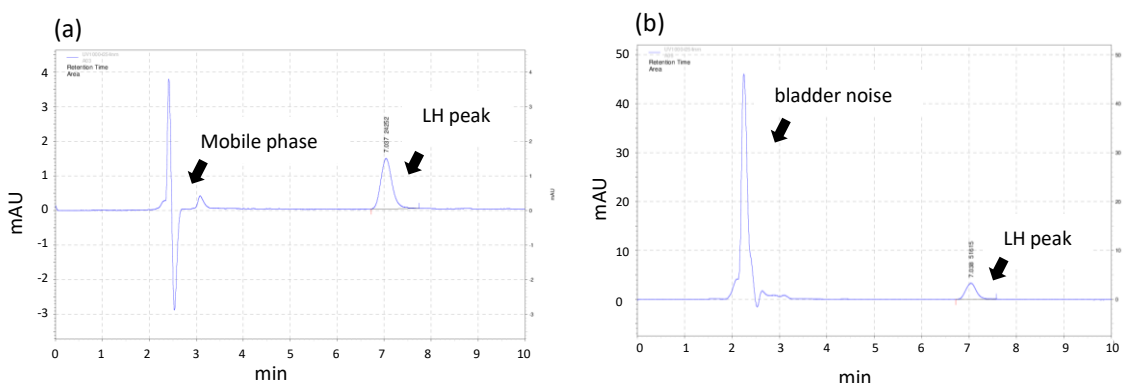


Figure 18 HPLC chromatograms of lidocaine hydrochloride (LH) Examples of HPLC chromatograms showing detection of LH in a calibration standard (a) and in solution extracted from bladder samples (b). Retention time for LH was ~7 min.

3.3.1.2. Static experiments – undiluted set

Concentration-depth and log-concentration-depth profiles and mean concentration per layer following intravesical instillation with LH 2% (w/v) saline, LH 4% (w/v) saline and LH 2% (w/v) alkalised (please note that for simplification w/v will be omitted hereafter) for 60 min (undiluted set) are shown in Figure 19. Concentrations of LH decreased as a logarithmic function of the distance from the lumen for all the solutions studied.

Average concentrations \pm SEM (mg of LH/g of wet tissue) after intravesical instillation of LH 2% saline were 5.03 ± 0.47 in the urothelium, 2.80 ± 0.31 in the lamina propria, 0.86 ± 0.10 in the detrusor and 1.78 ± 0.18 in the full thickness bladder (n=8 bladders). Following instillation with LH 4% saline average concentrations \pm SEM (mg of LH/g of wet tissue) were 11.12 ± 1.04 in the urothelium, 6.32 ± 0.50 in the lamina propria, 2.11 ± 0.21 in the detrusor and 4.09 ± 0.35 in the full thickness (n=8 bladders). After instillation with LH 2% alkalised the average concentrations \pm SEM (mg of LH/g of wet tissue) were 10.47 ± 1.45 in the urothelium, 5.40 ± 0.57 in the lamina propria, 1.87 ± 0.21 in the detrusor and 3.55 ± 0.38 in the full thickness bladder (n=8 bladders). Average concentrations in bladders treated with LH 2% saline were significantly different from those in bladders treated with LH 4% saline and LH 2% alkalised ($p < 0.01$, as calculated by one-way ANOVA with Tukey posthoc test). However, no statistically significant difference was determined when comparing the groups instilled with LH 4% saline and LH 2% alkalised. LH saline solutions collected from the bladders after completion of the experiment had a pH that ranged between 4.6 to 6, whereas those collected from bladders treated with LH 2% alkalised had a pH of ~ 8 .

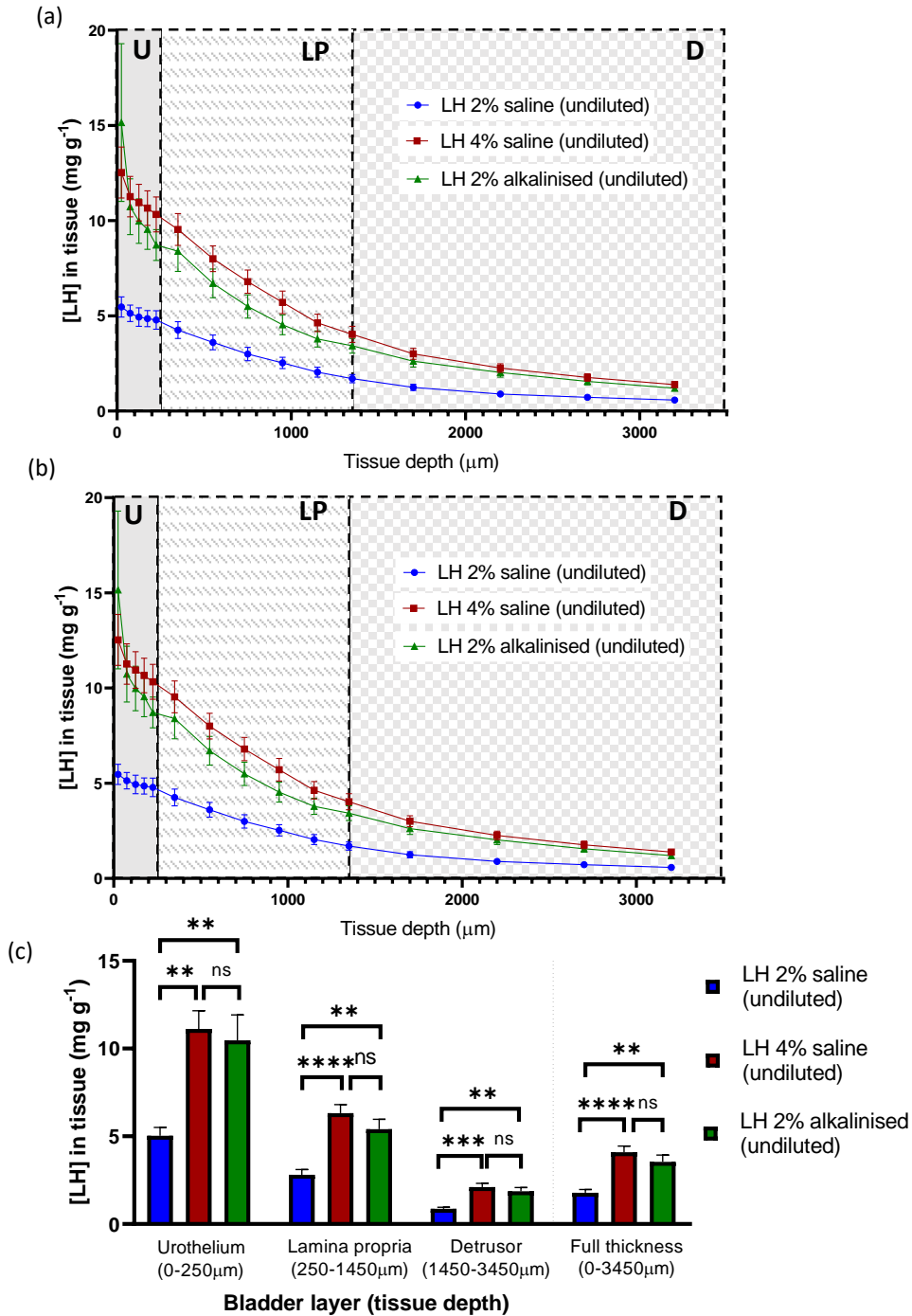


Figure 19 Profiles of intravesical delivery of lidocaine hydrochloride (LH) - undiluted set. (a) Concentration-depth profile and (b) log-concentration-depth profile showing average concentrations \pm SEM of LH determine in the bladder wall in function of tissue depth following 60 min of instillation with LH 2% saline (n=8), LH 4% saline (n=8) and LH2% alkalised (n=8). Concentrations of LH decreased as a logarithmic function of the distance from the lumen as evidenced in (b). U-urothelium, LP-lamina propria, D-detrusor. (c) Average LH concentrations \pm SEM achieved in the different layers of the bladder wall following 60 min instillation with LH 2% saline (n=8), LH 4% saline (n=8) and LH 2% alkalised (n=8). ****p<0.0001, **p<0.01, ns – non-significant p>0.05, calculated by one-way ANOVA.

3.3.1.3. Consideration of urine dilution effects – urine-diluted set

Concentration-depth and log-concentration-depth profiles and average concentration per layer of the group of bladders instilled with LH 2% saline and LH 2% alkalised, with and without reproducing urine dilution, are illustrated in Figure 20.

When urine accumulation in the bladder was simulated the average concentrations \pm SEM (mg of LH/g of wet tissue) in the urothelium, lamina propria, detrusor and full thickness bladder wall following instillation of LH2% saline were 2.68 ± 0.10 , 1.77 ± 0.12 , 0.72 ± 0.05 and 1.18 ± 0.18 , respectively. Concentrations were statistically significantly lower in the urothelium ($p < 0.01$), lamina propria ($p < 0.05$) and full thickness bladder ($p < 0.05$) when urine flow was simulated than in bladders treated with LH 2% only (undiluted), as determined by unpaired *t*-tests. Nevertheless, no statistically significant difference ($p > 0.05$) was observed for the average concentrations of the detrusor. Average concentrations \pm SEM (mg of LH/g of wet tissue) following intravesical instillation with LH 2% alkalised and simulation of urine flow were 6.52 ± 0.58 in the urothelium, 4.99 ± 0.44 in the lamina propria, 2.08 ± 0.30 in the detrusor and 3.37 ± 0.35 in the full thickness bladder. Only in the urothelium was the difference shown to be statistically significant between the bladders instilled with LH 2% alkalised alone (undiluted) and bladders instilled with LH 2% alkalised followed by urine-flow simulation ($p < 0.05$, determined by unpaired *t*-test). LH saline solutions plus synthetic urine instilled and collected after experiment had a pH that ranged between 5 and 6, whereas those collected from bladders treated with LH 2% alkalised had a pH of 7.5-8.

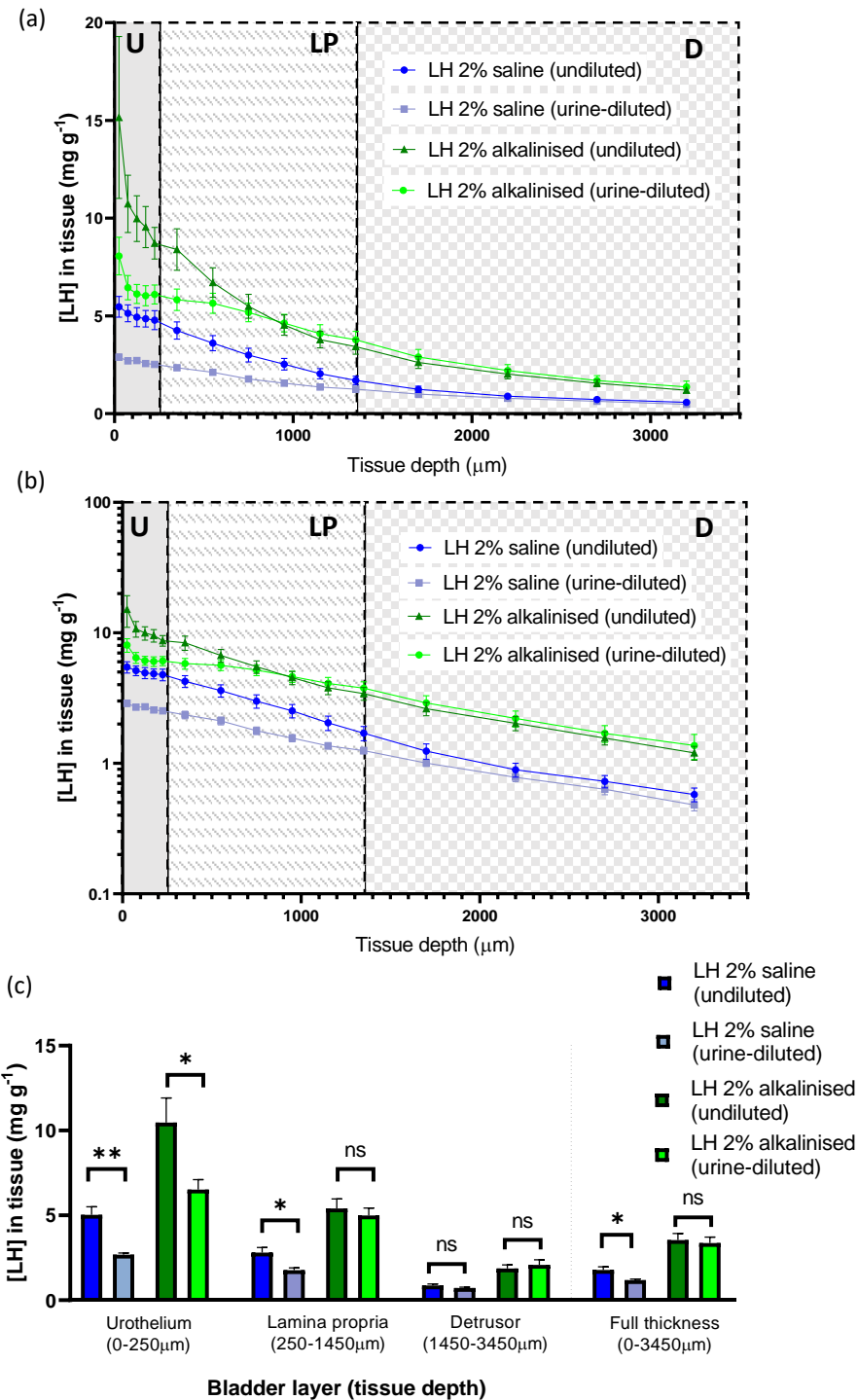


Figure 20 Profiles of intravesical delivery of lidocaine hydrochloride (LH) - undiluted and urine-diluted sets (a) Concentration-depth profile and (b) log-concentration-depth profile showing average concentrations \pm SEM of LH determine in the bladder wall in function of tissue depth following 60 min of instillation with LH 2% saline alone (undiluted, n=8), LH 2% saline urine-diluted (n=6), LH 2% alkalised alone (undiluted, n=8) and LH 2% alkalised urine-diluted (n=6). Concentrations of LH decreased as a logarithmic function of the distance from the lumen for most instilled solutions as evidenced in (b), however not for LH 2% alkalised urine diluted in the mucosa. U-urothelium, LP-lamina propria, D-detrusor. (c) Average LH concentrations \pm SEM achieved in the different layers of the bladder wall following 60 min instillation with LH 2% saline alone (undiluted, n=8), LH 2% saline urine-diluted (n=6), LH 2% alkalised alone (undiluted, n=8) and LH 2% alkalised urine-diluted (n=6). **p<0.01, *p<0.05, ns – non-significant p>0.05, calculated by unpaired *t*-tests.

3.3.3. Histology

Representative histological sections of bladders instilled with saline (control), LH 2% saline (undiluted), LH 4% saline (undiluted), LH 2% alkalised (undiluted and urine-diluted) for 60 min are illustrated in Figures 21 and 22. Normal morphology of the bladder wall with a typical multicellular (2-7 cells thick) tightly organised urothelium, submucosa with abundant collagen, and detrusor layer with organised muscle fascicles connected with interfascicular collagen can be observed in bladders treated with saline (control), LH 2% saline (undiluted), LH 4% saline (undiluted). On the other hand, bladders treated with LH 2% alkalised, either undiluted or urine-diluted, revealed extensive damage of the urothelium, with some areas deprived of this layer or with a reduced number of cells remaining. In cases where some urothelial cells are present, these are not tightly organised in the same manner as for bladders treated with saline. Previous work by Williams *et al.* has shown simulation of urine accumulation does not produce histological changes. (Williams *et al.*, 2015)

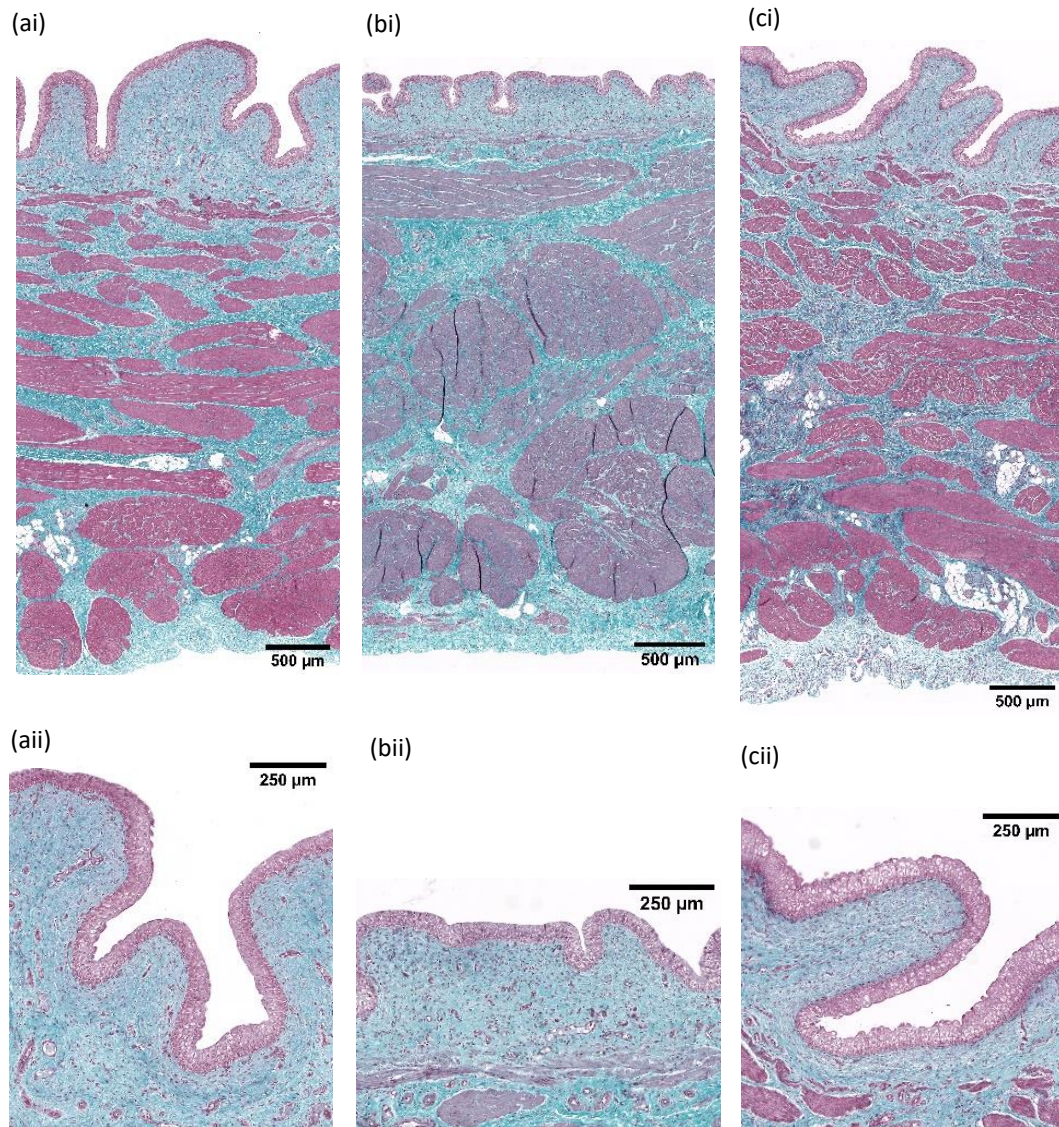


Figure 21 Photomicrographs of histological porcine bladder sections stained with Masson's Trichrome after instillation for 60 min with (a) saline solution, (b) LH 2% saline (undiluted) and (c) LH 4% saline (undiluted). Full thickness bladder wall (a-ci) and a close up of the mucosa (a-cii) are shown for these treatments. Masson's Trichrome stains nuclei in black, collagen and mucin in blue, muscle, some cytoplasmic granules and red blood cells in red. Normal morphology of the bladder wall with a typical multicellular (2-7 cells thick) tightly organised urothelium can be observed in bladders treated with saline (control, a), LH 2% saline (undiluted, b) and LH 4% saline (undiluted, c).

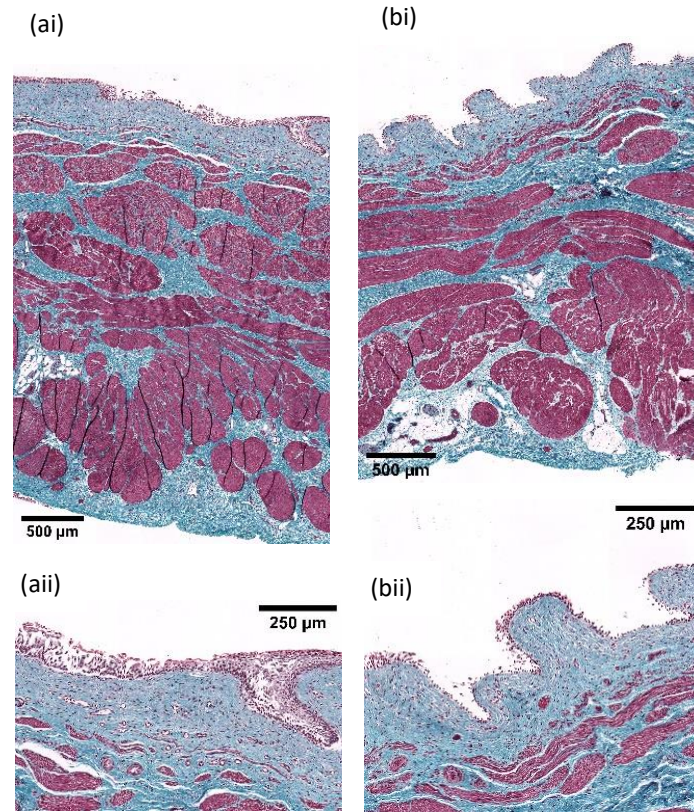


Figure 22 Photomicrographs of histological porcine bladder sections stained with Masson's Trichrome after instillation for 60 min with (a) LH 2% alkalinised (undiluted) and (b) LH 2% alkalinised (urine-diluted). Full thickness bladder wall (a-bi) and a close up of the mucosa (a-bii) are shown for these treatments. Masson's Trichrome stains nuclei in black, collagen and mucin in blue, muscle, some cytoplasmic granules and red blood cells in red. Urothelial changes can be observed in bladders treated with LH 2% alkalinised (undiluted, d, and urine-diluted, e), with some areas with denuded urothelium or remaining urothelial cells poorly organised.

3.4. Discussion

Several studies have reported serum levels of LH post intravesical instillation and confirmed circulatory LH is within the safety margin following intravesical administration. (Birch and Miller, 1994; Henry *et al.*, 2001; Nickel *et al.*, 2009; Parsons *et al.*, 2012) However, concentrations within the bladder tissue remain largely unknown. LH administered intravesically is intended to act locally in the bladder wall to exert its mechanism of action. Therefore, estimating concentration within the bladder wall can provide a better rationale for drug design and formulation.

Di Stasi *et al.* have studied the transport rate of lidocaine with passive diffusion for comparison with electromotive administration, using an LH 2% solution with 1% adrenaline. The concentrations in the bladder tissue at the time points studied did not follow a clear relation with time and a maximum of 0.50 mg g⁻¹ of wet tissue was reported at the end of experiment (45 min). (Di Stasi *et al.*, 2003) According to the authors, Fick's first law did not apply for the time considered; in order to take further conclusions on lidocaine permeation behaviour a longer duration of experiment would have been required. Also, the vasoconstrictor effect of adrenaline might have had an effect on the permeation of lidocaine. (Tanaka *et al.*, 2016)

Furthermore, Moch *et al.* have studied the bladder tissue permeability and transport of LH using three experimental setups. (Moch *et al.*, 2014) In these studies, however, the bladder tissue was stored at -18 °C and rehydrated for the bladder permeability studies. The group reports a membrane thickness of 200 µm, far below the thickness here observed and described in other studies. (Li *et al.*, 2014; Williams *et al.*, 2016) Moreover, the histological image provided (Figure 23) reveals a membrane almost deprived of urothelium, therefore the viability of the tissue and preservation of the barrier function is questionable.

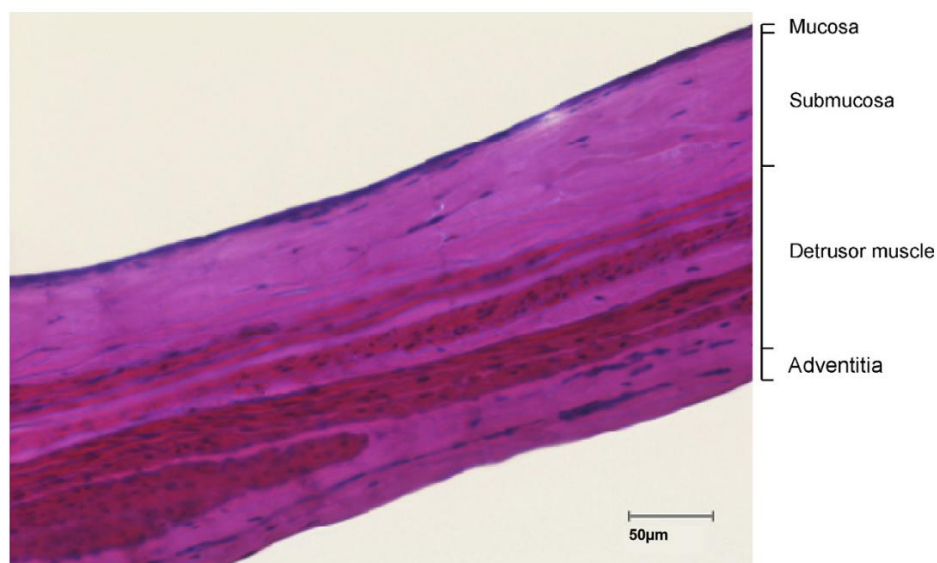


Figure 23 Histological section of porcine bladder sample stained with haematoxylin eosin. This represents work from Moch *et al.*, where bladder tissue was frozen and rehydrated prior to permeability studies. The small thickness (200 µm) of the section and the mucosa almost deprived of urothelium suggest the barrier function of the bladder may be affected. Image reused with permission. (Moch *et al.*, 2014)

In the present study, a pre-established *ex-vivo* whole bladder model of IDD (Williams *et al.*, 2015) was used to study the permeation of LH through the bladder wall. Tissue viability for similar experimental conditions was previously investigated and shown suitable by the same group. (Williams *et al.*, 2014)

The concentrations of LH within the tissue layers of bladders treated with LH 2% saline, LH 4% saline and LH 2% alkalised solutions were analysed and compared. Concentration - depth profiles (Figures 19 and 20) were in line with those determined for other compounds (Williams *et al.*, 2014, 2015), with a higher drug concentration in the urothelium than in the underlying layers. The concentration of LH found in the tissue was shown to be dependent on the concentration instilled intravesically. As such, bladders instilled with LH 4% saline had approximately double the concentration of LH within all layers of the bladder when compared to those instilled with LH 2% saline. This agrees with Fick's first law (Fick, 1995) that states that flux is proportional to concentration gradient. A similar observation has been previously documented for dermal tissue, where an increase in the concentration applied resulted in a proportional increment of concentrations in underlying layers. (Singh and Roberts, 1994) Bladders

treated with LH 2% saline and LH 4% saline shared normal histological features with bladders treated with saline solution only. This suggests urothelial barrier function was preserved following exposure to these solutions.

Permeation of LH was also shown to be influenced by pH, as instillation of LH 2% alkalised resulted in concentrations within the bladder that were approximately twice the concentration for LH 2% saline. This result is in agreement with studies by Henry *et al.* (Henry *et al.*, 2001; Nickel *et al.*, 2009) Lidocaine is a weak base ($pK_a \pm 7.8$) and has a pH ranging from 5 to 7 in aqueous solution, with its ionized form prevailing in these conditions. Drug absorption of local anaesthetics is directly proportional to lipid solubility and concentration and inversely proportional to molecular weight and ionized fraction. (Henry, Morales and Cahill, 2015) Therefore, alkalizing the solution instilled into the bladder can increase the fraction of non-ionized form of Lidocaine and subsequently increase tissue absorption. (Henry *et al.*, 2001) In the present study, however, significant changes in the urothelial layer were observed in bladders instilled with LH 2% alkalised solution, which are likely to have had a detrimental effect on barrier function, resulting in augmented LH permeation. These changes were observed for all four bladders instilled with LH 2% alkalised solution and for which histological features were investigated, having these experiments been performed over different days. Although LH 2% alkalised has a high osmolarity (1150 mOsm), its value is within the range of osmolarity for urine (50 to 1200 mOsm/L) (Apodaca, 2004) and is therefore unlikely to be the factor causing urothelial damage. A study from Recker *et al.*, has shown that a 24h continuous irrigation of a solution of sodium bicarbonate (pH 7.6) in an *in vivo* rabbit model does not produce changes in the urothelium. (Reckler *et al.*, 1986) It is worth noting though that in a study with healthy volunteers and interstitial cystitis patients treated with 1 h intravesical instillation of alkalised lidocaine, urgency and dysuria were common complaints upon voiding. These adverse effects were resolved within 3 h in healthy volunteers but persisted for days in interstitial cystitis patients. (Henry *et al.*, 2001) However, a subsequent placebo-controlled study reported comparable occurrence of bladder pain in the placebo (intravesical saline solution) and treated (alkalised lidocaine) group. (Nickel *et al.*, 2009) Parsons *et al.* combined heparin and lidocaine alkalised and did not report relevant side effects resulting from

the treatment. (Parsons, 2005; Parsons *et al.*, 2012) Moreover, a randomized, double-blind cross-over study has shown there was no statistically significant difference in pain scores on instilling an acidic-buffered solution (pH 5.0) or sodium- phosphate buffered saline (pH 7.5) in patients with IC. Clinical symptom changes with alkaline intravesical environments of pH 8.0 or higher were not evaluated.(Nguan *et al.*, 2005) Whether the histological observations in the present study translate to human patients is unclear; the potentially detrimental effect of sodium bicarbonate on the human bladder mucosa requires further investigation.

The IDD model used here provides an advantage when compared to the widely used Franz-cell set-up, as it prevents contact with the delicate urothelial surface prior to instillation of the drug whilst also allowing the effect of urine-dilution on the instilled drug to be explored. Furthermore, it is possible to instil solutions that have both similar volume and concentration to that used in clinical settings. (Williams *et al.*, 2015) Although in physiological conditions urine is continuously produced, in the present study urine was instilled intravesically every 10 min for practical reasons as has been described by Williams *et al.* In the future using a pre-loaded syringe driver set at a rate of 1 ml min⁻¹ could improve this experimental model.

Accordingly, urine production was simulated in a group of bladders instilled with LH 2% saline and LH 2% alkalinised, to account for the pH change and dilution effect expected in clinical applications. Tissue concentrations were significantly lower when urine dilution was considered with an LH 2% saline instillation but barely altered the amount delivered when the instillation solution had been alkalinised. Even though dilution was present in both situations, the non-ionized fraction of lidocaine was superior in the alkalinised solution, resulting in increased tissue absorption. However, as described earlier severe urothelial changes observed in those bladders exposed to the alkalinised LH solution, likely had a negative impact on barrier function resulting in increased Lidocaine penetration into the tissue. Histological analysis for the urine-diluted set of bladders treated with LH 2% and 4% saline was not completed for this study; the bladder is functionally designed for accumulation and retention of urine and simulation of urine flow was previously shown not to cause changes in the bladder tissue by Williams *et al.* in a similar experimental setting. (Williams *et al.*, 2015)

As previously described, LH can produce effective local anaesthesia in the bladder mucosa, increase functional bladder capacity and inhibit detrusor contractions. This action is mainly mediated through blockage of the conduction of unmyelinated C fibres that innervate the bladder, by reversible binding to neuronal voltage-gated sodium channels.(Juszczak *et al.*, 2009) These fibres are mostly found in the bladder mucosa. (Fowler, Griffiths and de Groat, 2008; Miftahof and Nam, 2013) Several animal models have shown inhibition of bladder afferent activity resultant of lidocaine administration (Juszczak *et al.*, 2009; Aizawa and Wyndaele, 2010; Xiao *et al.*, 2014)

To the extent of my knowledge, the minimum effective concentration of lidocaine within the bladder remains undetermined and relation between bladder tissue concentration and serum levels is not well established. The minimum effective interstitial fluid concentration of lidocaine to produce dermal anaesthesia against the sensation of pinprick is 1 to 20 µg/mL (~4 – 80 µM) according to Kopacz *et al.* (Kopacz and Bernard, 2001) Half-maximal inhibitory concentration (IC₅₀) of lidocaine at the sodium neuronal channel can vary between 50 and 200 µM depending on the sensitivity of specific channel subtype and study preparation.(Scholz *et al.*, 1998) The concentration of LH found within the bladder wall in the current study were largely superior to these reported values (for comparison purposes 1 g of tissue was considered 1 mL).

It is known however that the therapeutic effects of LH go beyond the blockage of neuronal sodium channels. Effects reported include, but are not limited to, anti-nociceptive effects, by blockage of neuronal sodium channels and potassium currents, blockage of muscarinic and dopamine receptors and anti-inflammatory properties. (Hollmann and Durieux, 2000; Henry, Morales and Cahill, 2015).

Oh *et al.* has investigated the effects of local anaesthetics in isolated detrusor strips from human bladder and reported that these increase phasic and tonic spontaneous contractibility of the detrusor muscle in a dose-dependent way (1-500 µM) but eliminate phasic activity above 1 mM. Additionally, this study has shown local anaesthetics have a dose-dependent inhibitory effect on nerve mediated and non-nerve mediated muscle contraction, induced by KCl, carbachol and long pulse electrical field stimulation. (Oh *et al.*, 2005) Oh *et al.* studies suggest the effect of lidocaine may not be confined to an effect in the sensory nerves present in the mucosa, but also involve motor nerves and

detrusor muscle. In the present study, concentrations achieved in the detrusor with LH 2% alkalised (urine-diluted and undiluted) and LH 4% saline are superior to the IC_{50} for the detrusor contraction to the various stimuli reported in Oh *et al.* study, therefore it seems feasible that an inhibitory effect would be possible. An instillation of LH 2% saline, however, would only be likely to inhibit nerve-mediated contractions and KCl induced *in situ*, however not contractions induced by other stimuli studied (e.g. carbachol).

In the present study, only one time point was studied therefore it is not possible to calculate the rate of delivery or the transurothelial permeability coefficient.

3.5. Conclusions

A comprehensive analysis of the bladder tissue concentrations after intravesical instillation with clinically relevant solutions of lidocaine is reported. Concentration within the bladder was shown to be dependent on the pH and concentration of the solution administered, which was expected and in line with observations in other studies. (Henry *et al.*, 2001; Nickel *et al.*, 2009) Furthermore, the effect of urine flow, expected under physiological conditions, was simulated. It was observed that bladders instilled with a buffered solution of LH were less affected by this factor than bladders instilled with a LH saline solution of similar concentration. Concentration-depth profiles were established for the different relevant clinical solutions; these can inform future investigation on the minimum effective concentration of lidocaine within the bladder, which remains largely unknown. Normal histological features were observed in sections from bladders treated with lidocaine saline solutions, which were comparable to those treated with saline alone. Surprisingly, however, histological changes of the urothelial layer were observed for bladders treated with alkalinised lidocaine solution, which needs to be further investigated to understand if there are real implications for the clinical application in humans.

While the whole bladder model was here used to study the delivery of a drug with therapeutic interest (*i.e.* lidocaine), it was considered that this model could also be relevant if applied to the study of a drug associated with a bladder pathology, as is the case of ketamine, discussed in Chapter 4.

Chapter 4 – Intravesical drug delivery studies – Ketamine hydrochloride

4.1. Introduction

4.1.1. Historical perspective

Ketamine was first synthesised in 1962, as an alternative to its related compound – phencyclidine, which was associated with strong psychedelic and excitatory effects. Shortly after, ketamine was introduced as an analgesic and anaesthetic for human and veterinary use with a promising therapeutic margin and with less cardiorespiratory depressive effects. Nevertheless, this compound soon revealed dissociative effects, accompanied by a description of hallucinogenic/psychedelic side effects in some patients, however to a lesser degree than phencyclidine. It is not surprising therefore that ketamine is liable to recreational abuse. The first reports of recreational exploitation of ketamine started in US during the Vietnam War, where it had been widely used for an analgesic therapy in soldiers. (Mion, 2017) Since then, recreational use has risen as a consequence of its relatively low cost and easy access, together with the general perception that ketamine has less adverse effects and lower potential for addiction than other drugs do. (Wood *et al.*, 2011) More recently, ketamine is gaining interest as a fast-acting antidepressant; in US a ketamine nasal spray for treatment-resistant depression was approved by the FDA in March 2019 (U.S. Food and Drug Administration, no date). To date, in the UK ketamine is only licensed as an analgesic and anaesthetic although it has been used ‘off-label’ for treatment-resistant depression. (Oxford Health NHS Foundation Trust, no date)

4.1.2. Recreational use of ketamine – global panorama

Ketamine is commercially available as an injectable liquid for medical use. (Tyler *et al.*, 2017) Ketamine for recreational use can have origin in clandestine laboratories or be diverted from licit channels. Typically, sellers evaporate the liquid to obtain a powder, that can be snorted or compressed into a pill and sold under several designations, such as ‘special K’, ‘Dorothy’, ‘K’, ‘K powder’, ‘kit-kat’, ‘vitamin k’ and ‘cat Valium’. (Sihra, Ockrim and Wood, 2018; *World Drug Report*, 2019) Ketamine street prices in UK range from £20-30 per gram whereas cocaine can cost £30-80 per gram depending on purity.

(DrugWise, 2017) Abuse of this substance is of concern primarily in East and South-East Asia; in the period of 2013-2019 authorities in Asia were responsible for 89% of all ketamine seized globally. Most of the ketamine seized was reported, in descending order of quantity seized, by mainland China, Taiwan, Hong Kong, Malaysia, Myanmar, Thailand, the United Kingdom, India and the Netherlands. Reports of illicit use also show abuse of this substance prevails in Asia, as a recreational or club drug. (*World Drug Report*, 2019) According to the World Drug Report 2019 the amount of ketamine seized increased until 2015 (23 tons seized), falling to 12 tons in 2017. Ketamine accounts for 87% of the quantity of hallucinogens seized in the past five years, although if adjusted to dose rather than weight LSD would represent 95% of the hallucinogens seized from 1998-2017. In addition, data from the Global Drug Survey 2019 shows that 12.8% of respondents reported misuse of ketamine in the last year with 0.8% seeking emergency medical treatment following use of ketamine. Respondents were mostly young adults with access to the internet, therefore this online survey should not be seen as representative of the world population. (Winstock, 2019) Despite the alarming increase in recreational use of ketamine, this drug is not under international control to avoid the restriction of its accessibility and availability for medical purposes, which is viewed as particularly important in low-income countries. (Liao, Tang and Hao, 2017) However, the legal status of ketamine differs in several jurisdictions and in the UK the non-medical use of this substance has been illegal since 2006 when it was classified as a Class C drug and rescheduled as a Class B drug in 2014. (Liao, Tang and Hao, 2017; *World Drug Report*, 2019) Data provided by the Crime Survey for England and Wales 2018/2019 show ketamine abuse in these countries has fluctuated over the last decade among adults aged 16 to 59, showing an overall trend to increase, from an estimation of 0.5% in 2008/19 to 0.8% in 2017/2018. (Home Office, 2018, 2019) The increase was particularly noticeable among adolescents and young adults (16-25 years old) with an overall increase from 1.9% in 2008/2009 to 2.9% in 2018/2019 in this age group, with a more dramatic rise between 2016/2017 (1.3%) and 2017/2018 (3.1%).

4.1.3. Complications of ketamine use

Ketamine has a favourable safety margin, with scarce lethal cases described, even in overdose situations. (Schifano *et al.*, 2008) Side effects associated with its therapeutic

and recreational use affect the neurologic, cardiovascular, urologic and gastrointestinal systems. Psychoactive side effects experienced comprise the dissociative and psychotomimetic effects already described along with other memory and cognitive dysfunctions (Ke *et al.*, 2018). Ketamine has a sympathomimetic effect which can disturb the cardiovascular system, resulting in tachycardia, hypertension and palpitations. (Zanos *et al.*, 2018) Gastrointestinal complications, including abdominal pain, nausea and vomiting, are also a common reason for ketamine abusers to seek medical help and often co-exist with urologic complications. (Ng *et al.*, 2010; Liu *et al.*, 2017) The latter is the focus of the current study.

4.1.3.1. Ketamine abuse and lower urinary tract symptoms (LUTS)

Shahani *et al.* reported the first case series of ketamine-induced cystitis (KIC) in 2007, followed by several other cases described in the literature. (Shahani *et al.*, 2007; Chu *et al.*, 2008; Oxley *et al.*, 2009; Tsai *et al.*, 2009; Mason *et al.*, 2010; Lai *et al.*, 2012; Baker *et al.*, 2013; Lee, Jiang and Kuo, 2013; Huang *et al.*, 2014)

Nevertheless, the prevalence of KIC is difficult to characterise considering the illicit nature of ketamine use and that associated symptoms are not easily perceived until progression to a late stage of the disease. An initial study from Muetzfeldt *et al.*, which provides interview-based narratives from recreational users of ketamine, has suggested a prevalence of 20% on frequent users. (Muetzfeldt *et al.*, 2008) Similarly, a small-scale survey in Hong Kong estimated an incidence of LUTS in 30% of ketamine users. (Chu *et al.*, 2008)

An outreach programme in Hong Kong collected data from 66 adolescents and young adults with a history of ketamine abuse using a mobile medical assessment service established at youth community centres. In this study, frequent users (using ketamine 3 or more times a week for at least 2 years) demonstrated a dysfunction of the lower urinary tract. This was associated with lower voided volume and higher scores in the Pelvic Pain, Urgency and Frequency (PUF) questionnaire, which assesses self-reported urinary frequency, urinary urgency, pelvic pain, nocturia (*i.e.* waking up during the night to urinate) and dyspareunia (*i.e.* pain during sexual intercourse). Furthermore, the study suggested that symptoms (measured through PUF scoring) may persist for up to 1 year

following cessation of ketamine abuse. Multidrug use was reported by 80% of participants and was considered a confounding variable. (Mak *et al.*, 2011)

A cross-sectional study using an online survey has investigated the patterns of ketamine abuse and prevalence of LUTS among recreational drug users in a dance music setting. From those reporting having used ketamine in the previous year (1285 people), 34% have used 1 g or more during a typical session. Regarding maximum dose, roughly half have used 1 g or more and almost a quarter 3 g or more. Intranasal administration was the most reported route. Around a quarter reported having experienced at least one urinary symptom, with higher doses and frequency of abuse correlating positively with the development of LUTS. Cessation of ketamine consumption has improved symptoms in 51% but symptoms have worsened in 3.8% of those reporting experience with ketamine use over time. Almost 15% of those subjects with LUTS had sought medical help. Abuse of other drugs alongside ketamine was widely reported, which was identified as a confounding factor. (Winstock *et al.*, 2012)

Another cross-sectional survey study, which included almost 12,000 students randomly selected from 45 secondary schools in Hong Kong over a period of 2 years, 2.5% of students self-reported consuming psychotropic substances. Ketamine was the most used substance (45.6% of substance abusers). With reference to the control subjects, other substance users and ketamine users were 2.8-fold and 6.2-fold respectively more likely to develop LUTS according to this study. (Tam *et al.*, 2016)

A further cross-sectional survey conducted in Taichung City investigated the risk factors for LUTS resultant from ketamine abuse, such as duration of use, dosage, comorbidities and depression. Of the 143 ketamine users recruited from police detention and outpatient urology departments to participate in this study, 17.5% reported LUTS. In a similar way to other studies concomitant use of ketamine and other psychotropic drugs was commonly reported (44.8% of all participants). Depression and long duration of abuse were significantly related to the onset of LUTS among ketamine recreational users, whereas dosage showed no clear relationship with development of LUTS in this study. (Chen *et al.*, 2017)

A survey-based study which included 106 ketamine abusers from rehabilitation centres in Taiwan showed that on average LUTS develop following 2 years of consumption, with improvement of symptoms being reported by most of the abusers after cessation of ketamine. (Li *et al.*, 2019) In this study, most abusers reported consuming ketamine multiples times a day, sometimes in association with other drugs, with an average of 10 mg a day either by snorting or smoking. LUTS such as increased urinary frequency and urgency, nocturia, urethral pain, and incomplete emptying were reported by more than half of the respondents. All the symptom scores investigated in this study (interstitial cystitis problem index [ICPI]; interstitial cystitis symptom index [ICSI]; international prostate symptom score-storage [IPSS-S]; overactive bladder symptom score [OABSS]; visual analogue scale [VAS]) correlated positively (Figure 24) with the duration of ketamine abuse. Snorting was associated with more severe LUTS than smoking. (Li *et al.*, 2019)

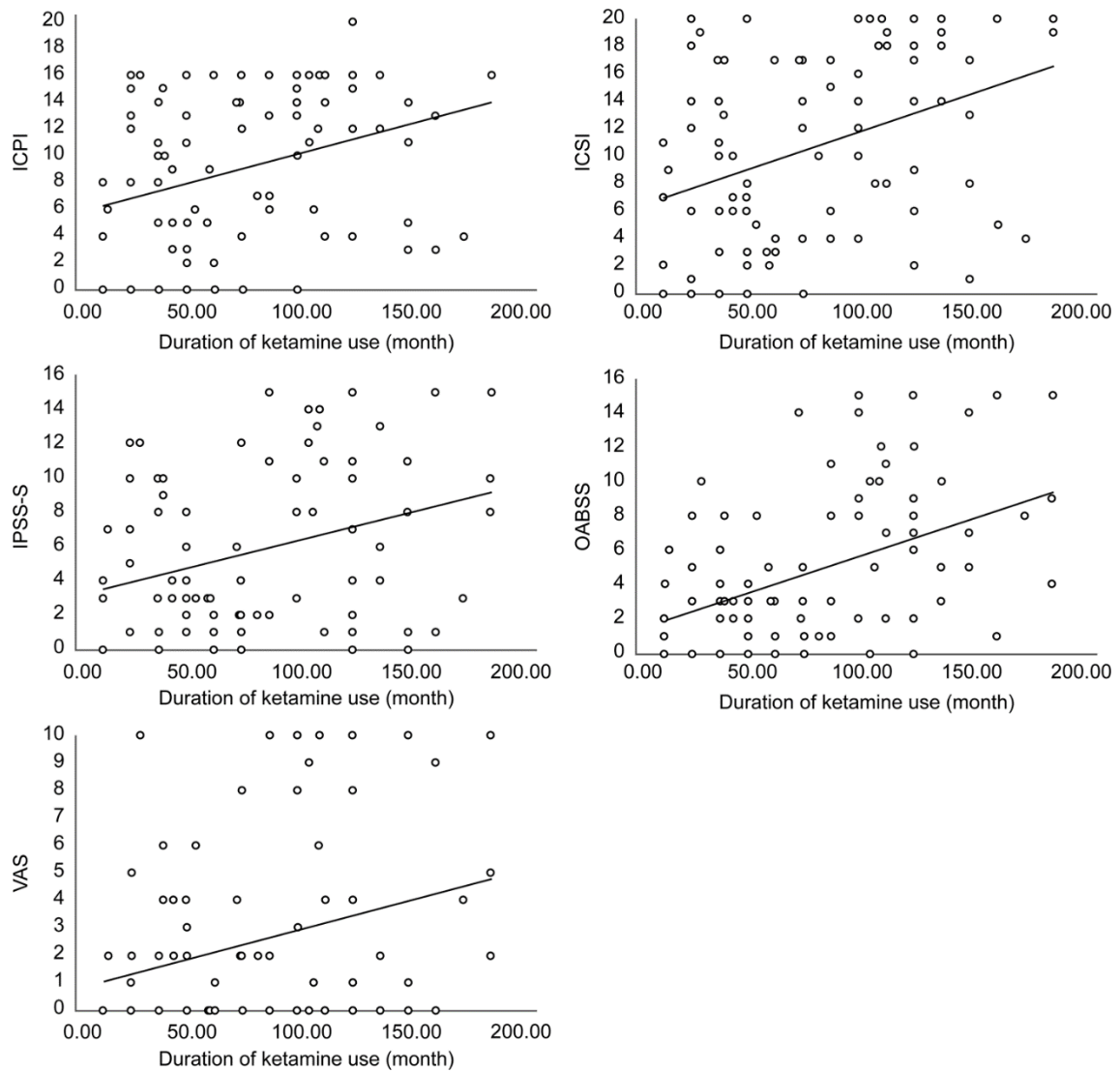


Figure 24 Correlations between symptom scores and duration of ketamine abuse. All the symptom scores were positively correlated with the duration of ketamine abuse according to the study of Li *et al.* ICPI: interstitial cystitis problem index; ICSI: interstitial cystitis symptom index; IPSS-S: international prostate symptom score-storage; OABSS: overactive bladder symptom score; VAS: visual analogue scale. Image reused with permission (Li *et al.*, 2019)

4.1.4. Chemical properties of ketamine and pharmacokinetics

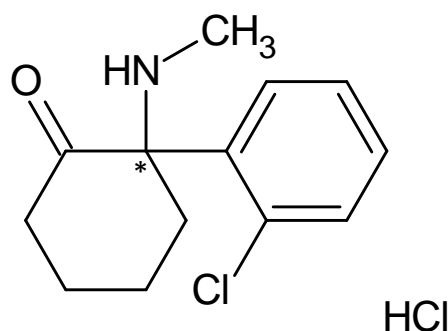


Figure 25 Chemical structure of ketamine hydrochloride * represents the chiral centre

Ketamine (Figure 25) is chemically designated as 2-(2-chlorophenyl)-2-(methylamino)-cyclohexan-1-one with a molecular weight of 274.18 (hydrochloride salt) (National Center for Biotechnology Information, no date). Ketamine has a chiral structure, giving rise to two optical isomers, S(+) and R(-) enantiomers. The pharmacokinetics of ketamine have been extensively reviewed. (Peltoniemi *et al.*, 2016; Zanos *et al.*, 2018). Most studies focus on the pharmacokinetics of racemic ketamine, although more recently the pharmacokinetics of each enantiomer has also been studied with increasing interest in S(+)-ketamine, which is postulated to be a more potent analgesic and anaesthetic than R(-)-ketamine. (Peltoniemi *et al.*, 2016) In cases of drug abuse, ketamine is normally consumed as a racemic mixture, and therefore the present section of work will focus primarily on the pharmacokinetic properties of (R,S)-ketamine, hereafter designated ketamine.

For therapeutic purposes ketamine can be administered via multiple routes: intravenous (i.v.), intramuscular (i.m.), oral, intranasal, epidural and intrarectal. Bioavailability differs greatly depending on the route of administration. (Zanos *et al.*, 2018) .Intravenous infusion is the most common route of administration, as it achieves fast maximum plasma concentrations. Intramuscular administration has a high bioavailability (93%) and is mostly used in emergency cases with uncooperative patients and children. Oral bioavailability is poor (16-29%) due to extensive first-pass metabolism. In the liver ketamine is metabolized by cytochrome P450 (CYP) 3A and CYP2B6 enzymes. converting

ketamine to norketamine via N-demethylation. Norketamine is further metabolized to hydroxynorketamines (HNKs) and dehydronorketamine (DHNK). (Peltoniemi *et al.*, 2016; Zanos *et al.*, 2018) Intranasal administration bypasses first-pass hepatic metabolism and has a better bioavailability (25-50%) than oral intake, reaching maximum concentration within 10-17 min (Pai and Heining, 2007; Peltoniemi *et al.*, 2016; Zanos *et al.*, 2018) Also, it is less invasive and is, therefore, an attractive alternative to i.v. administration. (Peltoniemi *et al.*, 2016; Zanos *et al.*, 2018) This is also the preferred route for drug abusers. (Winstock *et al.*, 2012) Distribution of ketamine into well-perfused tissues (including the brain) occurs rapidly (distribution half-life, $t_{1/2\alpha} = 2 - 4$ min), resulting in a high volume of distribution ($V_d = 160-550$ L/kg). (Peltoniemi *et al.*, 2016) Plasma protein binding ranges from 10% to 50%. Ketamine has a high rate of systemic clearance ($Cl = 60 - 147$ L/70kg) and a short elimination half-life ($t_{1/2} = 2 - 4$ h). Elimination occurs through the kidneys, with a low fraction excreted unchanged in urine for ketamine ($f_u = 2 - 4\%$), norketamine ($f_u = 2\%$) and DHNK ($f_u = 16\%$). A summary of the main pharmacokinetic parameters is provided in Table 2. Most of the drug (80%) is excreted as the glucuronic acid-labile conjugates of HK and HNK, which are eliminated in urine and bile. (Peltoniemi *et al.*, 2016; Zanos *et al.*, 2018) The dose used in pharmacokinetic studies usually varies between 10 and 50 mg. (Peltoniemi *et al.*, 2016) Drug abusers however regularly take 1 g or more of ketamine. (Winstock *et al.*, 2012) Possible changes to the pharmacokinetic profile resulting from enzyme saturation for example have not been studied. Normally these studies are conducted in healthy volunteers or neuropathic pain patients and higher doses would raise ethical concerns.

It has been suggested that urinary ketamine or its metabolites are involved in the pathological mechanism of KIC (Kidger *et al.*, 2016). Urinary data showing the variation of ketamine concentration over time, however, is scarce, as most studies focus on plasma concentration of ketamine. Some have reported detection of ketamine in urine up to 48 – 72 h following administration. (Adamowicz and Kala, 2005) Urinary concentrations ranging from 29 to 1410 ng/mL have been detected up to 2 days after a single administration of ketamine (0.75 to 1.59 mg/Kg) in children. (Adamowicz and Kala, 2005) A study by Parkin *et al.* shows detection of ketamine and norketamine in urine up to 72 h and reports 800 (± 400) ng/mL (~ 3 μ M) of ketamine quantified in the urine 2 h

after a 50 mg oral dose. (Parkin *et al.*, 2008). Concentrations of ketamine ranging from 6 to 7744 ng/mL in urine after illicit consumption have been reported, however it is important to note that limited patient history is provided in these cases, with doses nor route of administration reported. Also, collection of urine samples was often performed 3-36 h after a “drug bust”. (Moore *et al.*, 2001)

Table 2 Summary of pharmacokinetic parameters of racemic ketamine. Adapted from (Pai and Heining, 2007; Peltoniemi *et al.*, 2016; Zanos *et al.*, 2018)

<i>Ketamine (racemic)</i>	
<i>Molecular weight (MW, hydrochloride salt)</i>	274.18 g/mol
<i>Bioavailability (F):</i>	
<i>IM</i>	93%
<i>Oral</i>	16-29%
<i>Intranasal</i>	25-50%
<i>Protein binding (%Pt)</i>	10-30%
<i>Distribution half-life ($t_{1/2\alpha}$)</i>	2-4 min
<i>Elimination half-life ($t_{1/2\beta}$)</i>	2-4 h
<i>Distribution volume in the steady-state (V_{ss})</i>	160-550L/70 kg
<i>Systemic Clearance (Cl)</i>	60-147L/h/70 Kg

4.1.6. Hypothesis and aims

It was hypothesised that ketamine accumulated in the urine following illicit consumption could penetrate into the bladder wall and achieve tissue concentrations sufficient to lead to bladder dysfunction. The aim of the present section of work was to estimate the urinary accumulation of ketamine following intranasal administration and simulate it using a previously established *ex vivo* whole bladder model of IDD (Williams *et al.*, 2015) to inform on the concentrations of ketamine achieved per layer and inform future functional experiments. To accomplish these aims the key objectives were:

1. Establish and compare concentration-depth profiles and concentration per layer following 1h intravesical instillation with ketamine 3 mM and 6 mM in artificial urine.

2. Determine concentration per layer after 4h of intravesical instillation with ketamine 0.3 mM in artificial urine.
3. Establish concentration-depth profile and concentration per layer after 4h of intravesical instillation with various concentrations of ketamine (starting concentration ~3 mM) in artificial urine.
4. Compare histological features of bladders treated with each solution or treated with artificial urine alone (control).

4.2. Methods

4.2.1. Intravesical delivery of ketamine hydrochloride (KH)

Porcine bladders were collected and prepared as described in 2.1.2. Tissue preparation.

4.2.1.2. *Static experiments*

The effect of concentration of ketamine hydrochloride (KH) present in urine on ketamine permeation through the bladder wall was studied. A 50 mL solution of either 3 mM or 6 mM KH prepared in synthetic urine (composition described in 3.2.1. Intravesical instillation of lidocaine hydrochloride (LH)), pre-equilibrated at 37°C, was delivered intravesically through the urethra to a group of 7 and 6 bladders, respectively. Solutions were maintained inside the bladders for 60 min. After this period bladders were treated as described in 2.1.2. Tissue preparation.

In a similar way, 3 bladders were instilled intravesically with 50 mL of KH 0.3 mM prepared in synthetic urine, pre-equilibrated at 37 °C, but the solution was left in place for 4 h, to mimic the period between voiding times. (Lukacz *et al.*, 2011) After this period bladders were treated as described in 2.1.2. Tissue preparation.

One additional bladder was instilled intravesically with synthetic urine only and the solution was retained for 4 h.

4.2.1.3. *Gradient experiments*

A simple pharmacokinetic model was developed to determine the variation in concentration of urinary ketamine throughout time after nasal administration (route commonly used by ketamine abusers), as described in 4.3.1. Pharmacokinetic modelling. Based on those results, to simulate the accumulation of ketamine in urine after nasal administration various concentrations of ketamine were instilled intravesically. All solutions were prepared in synthetic urine. Due to limitations on the detection method of ketamine used (problem identified during quantification of ketamine in the bladder wall of bladders treated with 50 mL of KH 0.3 mM for 4 h) concentrations of ketamine 10-fold higher than estimated were used. A maximum of 90 mL of solution was added and a group of 6 bladders was instilled every 20 min with 7.5 mL of different concentration of KH as described in Table 3.

After these 4 h bladders were treated as described in 2.1.2. Tissue preparation

Table 3 Solutions of KH prepared in artificial urine were added every 20 min with a variable concentration

<i>t (min)</i>	<i>mg/mL</i>	<i>mM</i>
0-20	0.88	3.2
21-40	0.83	
41-60	0.78	
61-80	0.74	
81-100	0.70	
101-120	0.66	
121-140	0.62	
141-160	0.59	
161-180	0.56	
181-200	0.53	
201-220	0.51	
221-240	0.49	

4.2.2. Cryosectioning

Full-thickness samples of bladder wall were serially sectioned parallelly to urothelium, with a defined thickness of 50 μm , and collected to pre-weighed microcentrifuge tubes as described in

2.1.3. Cryosectioning.

To ensure later detection of ketamine above the LOQ, slices of bladders instilled with ketamine 3 mM and 6 mM for 1 h and gradient concentration for 4 h were grouped by this order: groups of 2 and 3 slices were collected from urothelium (0-250 μm), 4 groups of 4 slices and 1 group of 8 slices were collected from the lamina propria (250-1450 μm) and 4 groups of 10 slices were collected from the detrusor (1450-3450 μm).

Preliminary data showed the concentration of ketamine was below LOQ for some slices grouped as above from bladders instilled with 0.3 mM for 4 h. For that reason, slices were collected in the following manner: 5 slices from urothelium (0-250 μm) were collected together, 2 groups of 12 slices were collected from lamina propria (250-1450 μm) and 2 groups of 20 slices were collected from detrusor (1450-3450 μm).

4.2.3. Ketamine extraction

KH was extracted with 650 μ L of mobile phase (please refer to 4.2.4 Quantification of ketamine in the bladder wall) per microcentrifuge tube for a period of 24 h, with 10 min of sonication. This was followed by centrifugation at 14000 rpm for 10 min to sediment the tissue residues and isolate supernatant for high-performance liquid chromatography (HPLC) associated to ultraviolet (UV) detection.

4.2.4. Quantification of ketamine in the bladder wall

Analysis and quantification of KH were achieved with HPLC-UV, using a Thermo Scientific SpectraSYSTEM AS3000 equipped with a Kromasil column (5 μ m, C18, 250 mm x 4.6 mm i.d.) (Sigma-Aldrich, Dorset, UK) and associated with a Thermo Scientific SpectraSYSTEM UV1000 set at 220 nm. The mobile phase was prepared by dissolving 0.95 g of sodium 1-hexanesulfonate (Sigma-Aldrich, UK) in 1 L of a water : acetonitrile (3 : 1) solution, followed by the addition of 4 mL of acetic acid as specified in the ketamine monograph of USP (United States Pharmacopeia and National Formulary, 2006). The injection volume was 20 μ L and the flow rate was maintained at 1 mL/min. Measurements were performed at room temperature (RT). External standard calibration curves were developed for the integrated peak areas (AUC) as a function of KH concentrations (1.5, 2.5, 5, 10, 15 and 25 μ g/mL) prepared in mobile phase. Limit of detection (LOD) and limit of quantification (LOQ) were determined based on the signal-to noise-ratio 3:1 and 10:1, respectively.

Tissue concentrations of KH for each individual or grouped sections were determined as described for lidocaine in 3.2.4. Quantification of lidocaine in the bladder wall. In a similar way, depth-concentration profiles were established and average concentrations of KH in urothelium, lamina propria, detrusor muscle and full thickness bladder wall after treatment were determined and compared.

4.2.5. Histology

Please refer to 2.1.5. Histology.

2.1.5. Histology

4.2.6. Statistical analysis

Statistical analysis was performed using IBM® SPSS® Statistics and GraphPad Prism software. Whenever appropriate, unpaired *t*-tests were conducted to compare the mean concentration for each layer following intravesical instillation with KH 3 mM and KH 6 mM. As described in 3.2.6. Statistical analysis, *t*-test was conducted to compare means between two independent groups (treatment) on the same continuous, dependent variable (concentration). Normality was assumed, considering that a similar distribution to lidocaine should be expected, however this was not possible to confirm due to the small sample size.

4.3. Results

4.3.1. Pharmacokinetic modelling

Ketamine and its metabolites are excreted in the urine following administration. (Zanos *et al.*, 2018)

The cumulative mass of ketamine in urine in function of time is given by Equation 3:

[Equation 3]
$$U = fu \times F \times D \times (1 - e^{-K_{el} \times t})$$

Where U is the cumulative amount (mass) of ketamine in urine, f_u is excreted fraction unchanged in bladder, F is bioavailability, D is dose, K_{el} is the constant of elimination and t is time. (Bourne, 2016) Considering nasal administration of ketamine has a high absorption rate (maximum concentration within 10-17 min) the equation presented is simplified and does not address absorption phase.

Assuming the excretion rate of the drug is first order, K_{el} is given by equation 4:

[Equation 4]
$$K_{el} = \frac{Cl}{V}$$

Where Cl is clearance and V volume of distribution.

Therefore, U is given by equation 5:

[Equation 5]
$$U = fu \times F \times D \times (1 - e^{-\frac{Cl \times t}{V}})$$

To simulate the accumulation of ketamine in urine after nasal administration (route commonly used by ketamine abusers), the pharmacokinetic (PK) parameters values in Table 4 were considered. Values assumed for simulation are also present in Table 4.

Table 4. Pharmacokinetic parameters of racemic ketamine for nasal administration and values assumed for the present study Adapted from (Pai and Heining, 2007; Peltoniemi *et al.*, 2016; Zanos *et al.*, 2018)

PK parameter	Range	Value assumed
Dose (D)	>1000 mg	1000 mg
Excreted fraction unchanged in the bladder (f_u)	2%-4%	3%
Nasal bioavailability (F)	25-50%	50%
Systemic Clearance (Cl)	60-147 L/h/70 Kg	105 L/h/70 Kg
Distribution volume (V)	160-550 L/70 Kg	280 L/70 Kg

Considering the assumptions described a graphic representation of the estimated cumulative amount of ketamine in urine in function of time can be observed in Figure 26.

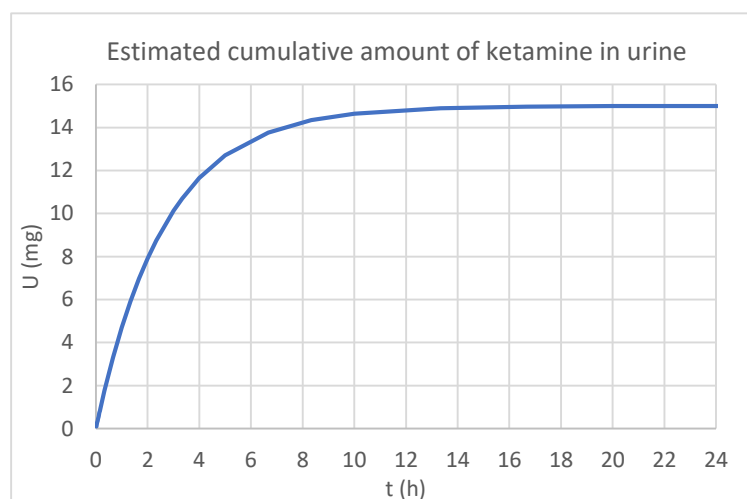


Figure 26 Estimated cumulative amount of ketamine in urine over 24 h assuming intranasal administration of 1 g dose. Assumed pharmacokinetic values follow: excreted fraction unchanged in the bladder (f_u) – 3%; bioavailability (F) – 50%; systemic clearance (Cl) - 105 L/h/70 Kg; distribution volume (V) - 280 L/70Kg.

In addition, to estimate the concentration of ketamine in urine stored in the bladder, it was assumed (1) initial bladder volume: 0 mL; (2) voiding time: every 4 h; (3) urine rate: 1mL/min. A graphic representation of the variation of cumulative amount and estimated concentration of ketamine in urine for 4h can be seen Figure 27.

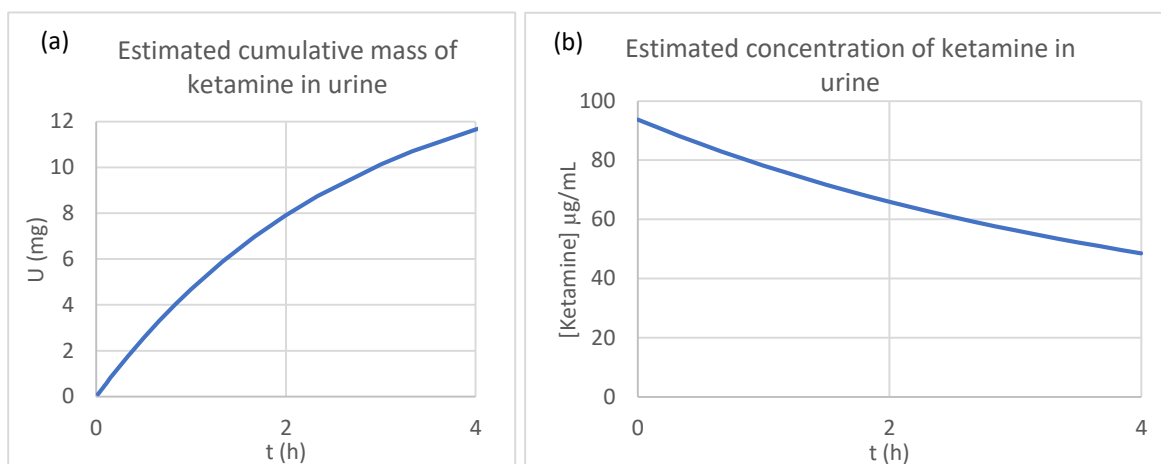


Figure 27 (a) Estimated cumulative mass of ketamine in urine in 4 h (b) estimated concentration of ketamine in urine in 4 h after intake considering no residual volume of urine at $t=0$ and urine rate production of $1\text{mL}/\text{min}$.

4.3.1. Quantification of ketamine in the bladder wall

4.3.1.1. Ketamine detection and analysis

Linear external calibration curves were obtained for the range of concentrations studied (Figure 28). Retention time for KH was ~ 7.2 min (Figure 29). LOD and LOQ were respectively 1 and $0.35 \mu\text{g mL}^{-1}$. Samples from bladders instilled with saline solution showed no peaks in the proximities of KH retention time. A second extraction with mobile phase showed no peaks above LOQ in preliminary measurements, thus a single extraction was considered sufficient.

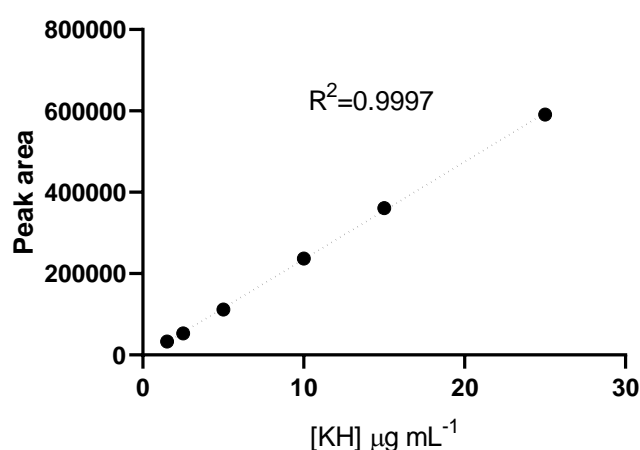


Figure 28. Calibration curve of ketamine hydrochloride (KH) Example of an external standard calibration curve for ketamine hydrochloride (KH) established for the integrated peak areas (AUC) as a function of KH concentrations. Linearity was observed over the range of concentrations studied ($1.5, 2.5, 5, 10, 15$ and $25 \mu\text{g}/\text{mL}$). The calibration curve was used to extrapolate concentration of KH in solution extracted from bladder samples.

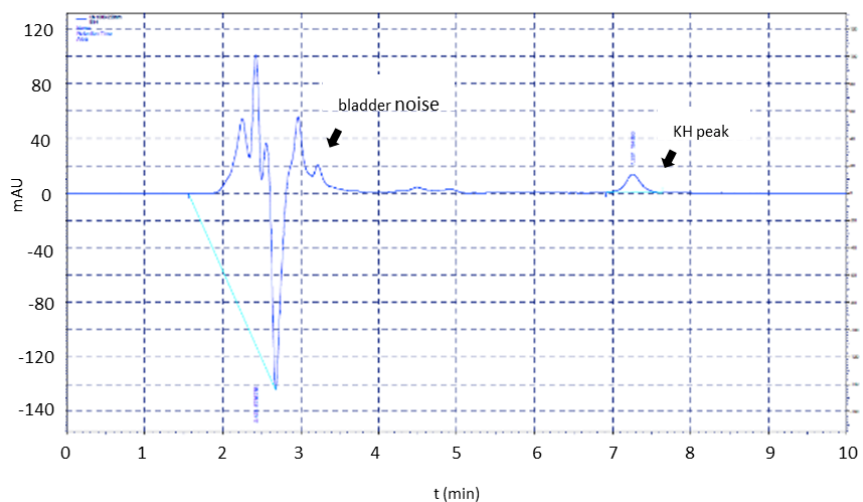


Figure 29. HPLC chromatogram of ketamine hydrochloride (KH) Examples of HPLC chromatogram showing detection of KH in solution extracted from bladder samples. Retention time for KH was ~ 7.2 min.

4.3.1.2. Static experiments

Concentration-depth, log-concentration-depth profiles and mean concentration per layer following intravesical instillation with KH 3mM and 6 mM for 60 min are shown in Figure 30. Concentrations of KH investigated show the same trend, steadily decreasing as a logarithmic function of the distance from the lumen for both solutions.

Average concentrations \pm SEM (μg of KH/g of wet tissue) following intravesical instillation of KH 3 mM in artificial urine were 183.76 ± 30.82 in the urothelium, 87.55 ± 12.05 in the lamina propria, 39.20 ± 5.48 in the detrusor and 66.28 ± 9.22 in the full thickness bladder ($n = 7$ bladders). Following instillation with KH 6 mM in artificial urine concentrations \pm SEM (μg of LH/g of wet tissue) were 333.71 ± 36.95 in the urothelium, 172.45 ± 21.31 in the lamina propria, 76.91 ± 6.55 in the detrusor and 129.66 ± 26.47 in the full thickness ($n = 6$ bladders). Mean concentrations in bladders treated with KH 3 mM and 6 mM were significantly different ($p < 0.01$, as calculated by unpaired t -test). Solutions contained in the bladder were collected after the experiment and had a pH that ranged between 5.61 and 5.85.

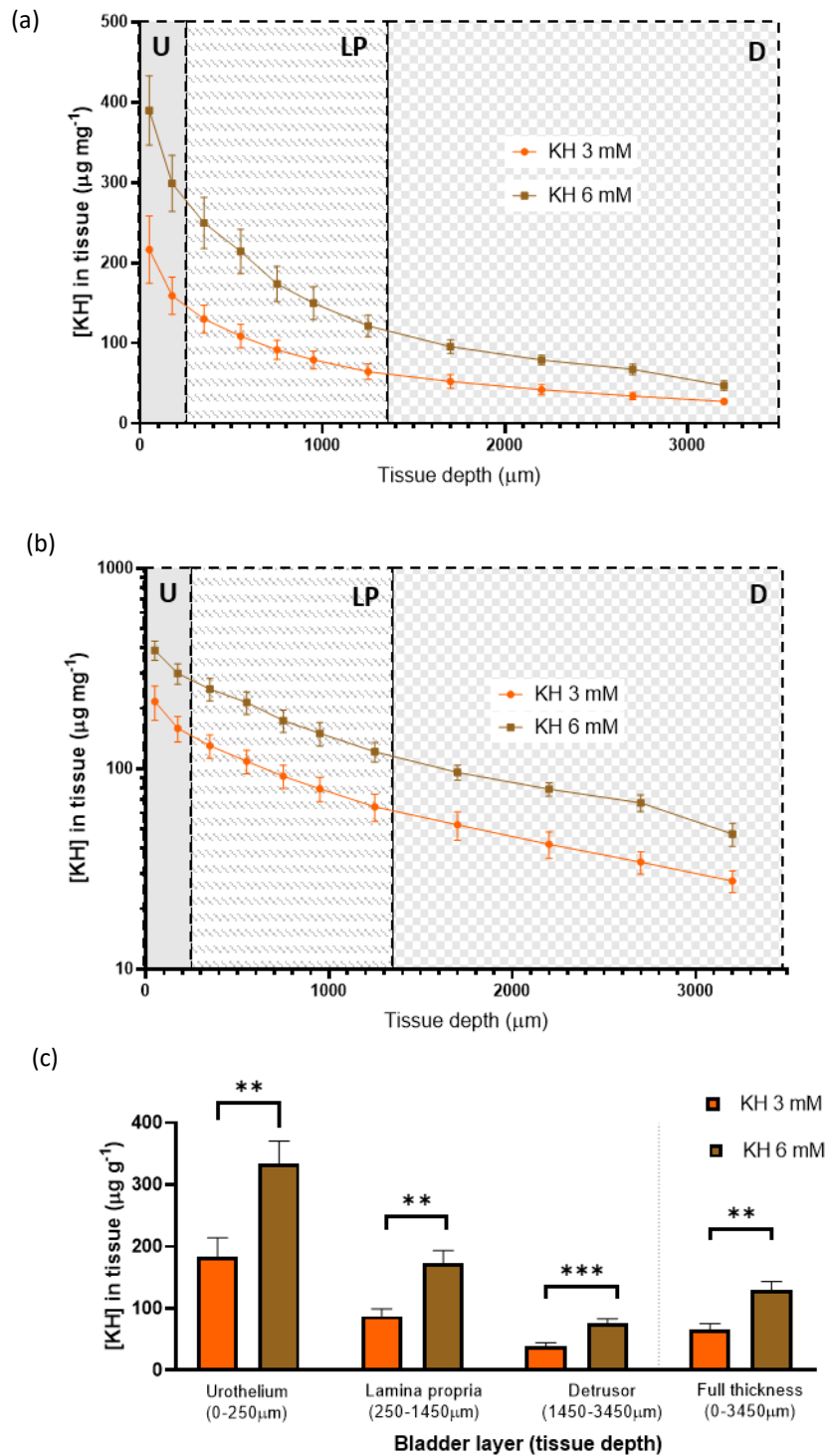


Figure 30 Profiles of intravesical delivery of ketamine hydrochloride (KH) 3mM and 6 mM (a) Concentration-depth profile and (b) log-concentration-depth profile showing average concentrations \pm SEM of KH determined in the bladder wall as a function of tissue depth following 60 min of instillation with KH 3 mM in artificial urine ($n = 7$) and KH 6 mM ($n = 6$) in artificial urine. Concentrations of KH declined as a logarithmic function of the distance from the lumen as evidenced in (b). U - urothelium, LP - lamina propria, D - detrusor. (c) Average KH concentrations \pm SEM achieved in the different layers of the bladder wall following 60 min instillation with KH 3 mM in artificial urine ($n = 7$) and KH 6 mM ($n = 6$) in artificial urine. *** $p < 0.001$, ** $p < 0.01$, calculated with unpaired t -tests.

Mean concentration per layer following intravesical instillation with KH 0.3 mM for 4 h are shown in Figure 31. Slices were grouped differently for this experiment as a consequence of preliminary data showing some extracted solutions with concentrations of KH below LOQ. For that reason, concentration-depth profile is not shown. Average concentrations \pm SEM (μg of KH/g of wet tissue) following intravesical instillation of KH 0.3 mM in artificial urine for 4 h were 37.79 ± 5.98 in the urothelium, 28.87 ± 5.44 in the lamina propria, 14.40 ± 2.47 in the detrusor and 20.88 ± 3.53 in the full thickness bladder (n = 3 bladders).

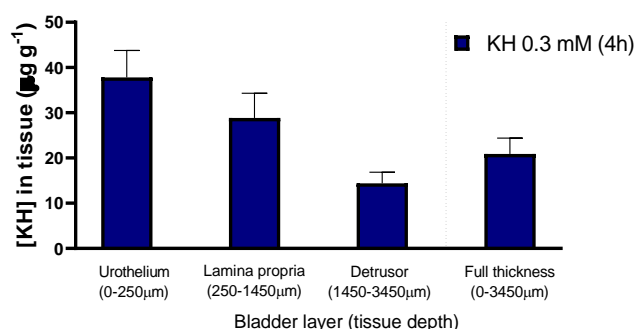


Figure 31 Intravesical delivery of KH 0.3 mM Average KH concentrations \pm SEM achieved in the different layers of the bladder wall following 4 h instillation of KH 0.3 mM in artificial urine (n = 3).

4.3.1.3 Gradient experiments

To avoid further problems in detection of KH, concentrations of ketamine 10-fold higher than estimated were used. Please note that a relation between concentration of ketamine in urine and concentration of ketamine in the bladder wall was established in a first instance. Although *in vivo* bladders can hold ~ 500 mL without a significant increase on intravesical pressure, in this *ex-vivo* whole bladder model high volumes of solution instilled can result in leakage of solution. For this reason, a maximum of 90 mL of solution was added to a group of 6 bladders, which were instilled every 20 min with 7.5 mL of various concentrations of KH as provided in Table 3 in 4.2.1. Intravesical delivery of ketamine hydrochloride (KH). The concentrations presented in Table 3 should have been the final concentration and not the concentration added every 20 min, however when the volume was adjusted to 7.5 mL the cumulative effect was not properly accounted for. This means the variation of concentration was inferior (0.88-0.65mg/mL) to what was estimated.

Concentration-depth and log-concentration-depth profiles and mean concentration per layer following intravesical instillation of these concentrations (Table 3) are shown in Figure 32.

Intravesical instillation of a gradient concentration of KH (initial concentration of 3.2 mM) resulted in average concentrations \pm SEM (μg of KH/g of wet tissue) of 168.67 ± 9.10 in urothelium, 122.33 ± 15.82 in lamina propria, 70.57 ± 16.50 in detrusor and 94.84 ± 14.36 in the full-thickness bladder ($n = 6$ bladders). The average concentration in the urothelium was not statistically different than to that observed in bladders instilled with 3 mM of KH for 1 h (Figure 32), however the concentration of KH in the lamina propria, detrusor and full-thickness bladder were significantly higher for this treatment ($p < 0.05$), calculated with unpaired t -tests.

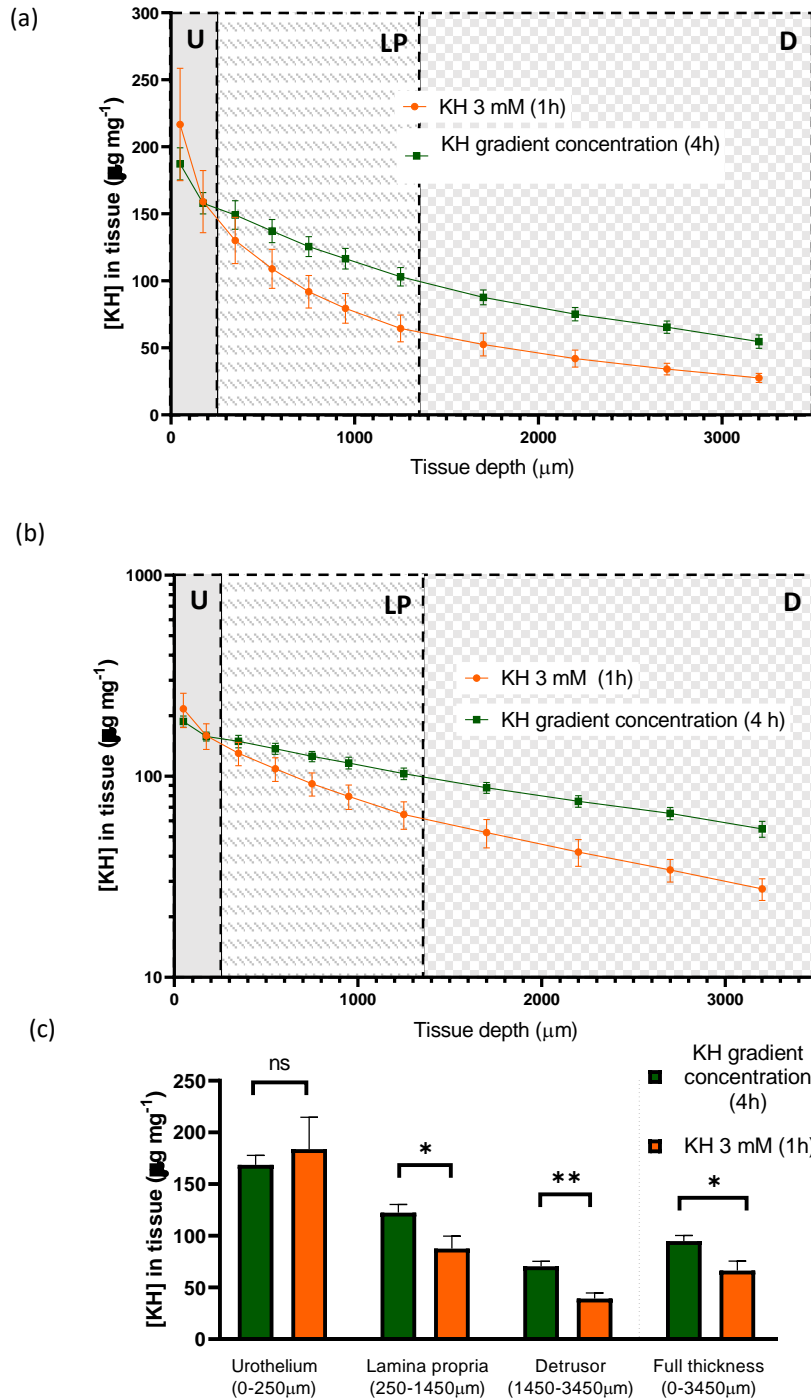


Figure 32 Profiles of intravesical delivery of ketamine hydrochloride (KH) gradient concentration (a) Concentration-depth profile and (b) log-concentration-depth profile showing average concentrations \pm SEM of KH determined in the bladder wall in function of tissue depth following 7.5 mL every 20 min for a total of 4 h with a variable concentration of KH ($n = 6$) and 50 mL of KH 3 mM (1 h, $n = 7$) in artificial urine. Concentrations of KH declined as a logarithmic function of the distance from the lumen as evidenced in (b). U-urothelium, LP-lamina propria, D-detrusor. (c) Average KH concentrations \pm SEM achieved in the different layers of the bladder wall following 7.5 mL every 20 min for a total of 4 h with various concentrations of KH ($n = 6$) and 50 mL of KH 3 mM (1 h, $n = 7$). ** $p < 0.01$, * $p < 0.05$, ns $p > 0.05$, calculated with unpaired t -tests.

4.3.2 Histology

Representative histological sections of bladders instilled with KH 3 mM or 6 mM in synthetic urine for 60 min are shown in Figure 33. The bladder wall of these sections exhibited a normal morphology with a typical multicellular tightly organised urothelium, submucosa rich in collagen, and detrusor layer with organised muscle fascicles connected with interfascicular collagen.

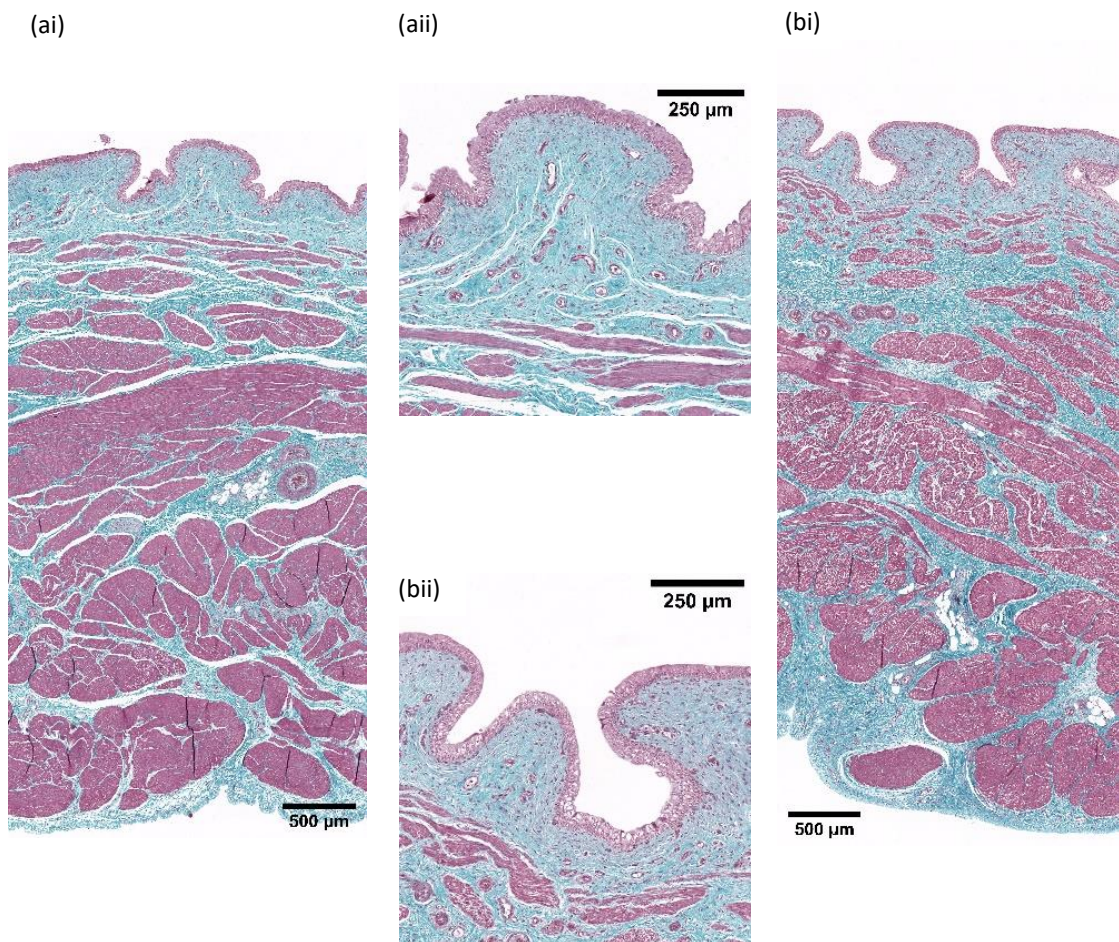


Figure 33 Photomicrographs of histological porcine bladder sections stained with Masson's Trichrome after instillation for 60 min with (a) KH 3mM and (b) KH 6mM Full thickness bladder wall (ai, bi) and a close up of the mucosa (aii, bii) are shown for these treatments. Masson's Trichrome stains nuclei in black, collagen and mucin in blue, muscle, some cytoplasmic granules and red blood cells in red. Normal morphology of the bladder wall with a typical multicellular tightly organised urothelium can be observed in bladders treated with KH 3 mM and KH 6 mM for 60 min.

Photomicrographs of sections of bladders instilled with artificial urine, ketamine 0.3 mM or a variable concentration of ketamine (starting concentration ~3 mM) over 4 h can be seen in Figure 34. Bladders treated with urine show a normal morphology, with only occasional cytoplasmic vacuolation of urothelial cells, whereas bladders treated with ketamine 0.3 mM showed regions with significant cytoplasmic vacuolation of urothelial cells, but urothelial structure preserved. On the other hand, bladders instilled with a variable concentration of ketamine revealed extensive cytoplasmic vacuolation of urothelial cells with some areas with denuded urothelium or severe damage of the basal/intermediate urothelial layer.

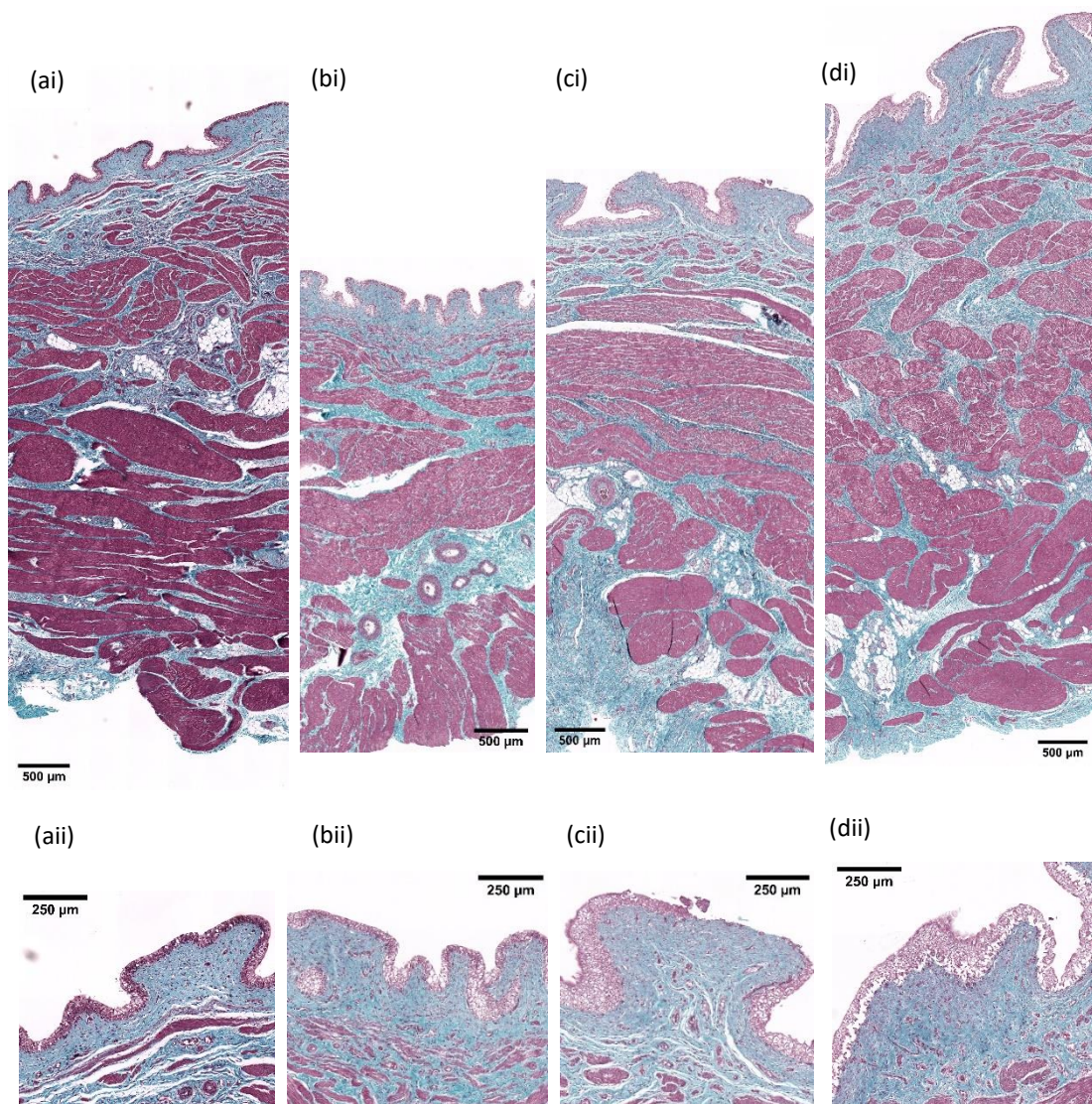


Figure 34 Photomicrographs of histological porcine bladder sections stained with Masson's Trichrome after instillation for 4 h (a) artificial urine, (b) KH 0.3 mM in artificial urine and (c,d) KH gradient concentration in artificial urine. Full thickness bladder wall (a-di) and a close up of the mucosa (a-dii) are shown for these treatments. Masson's Trichrome stains nuclei in black, collagen and mucin in blue, muscle, some cytoplasmic granules and red blood cells in red. Normal morphology of the bladder wall with a typical multicellular tightly organised urothelium can be observed in bladders treated with artificial urine (ai, aii). In bladders treated with KH 0.3 mM (bi, bii) cytoplasmic vacuolation of urothelial cells can be observed in some areas of the urothelium. Severe cytoplasmic vacuolation of urothelial cells can be seen in bladders treated with KH gradient concentration, with some areas with denuded urothelium (ci, cii) and extensive damage of the basal/intermediate urothelial layer in some portions of the mucosa (di, dii).

4.4. Discussion

Various studies have suggested that urinary ketamine or its metabolites stored in the bladder following ketamine abuse elicit changes in the bladder wall leading to bladder dysfunction. (Lee, Jiang and Kuo, 2013; Bureau *et al.*, 2015; Lu, Jiang and Kuo, 2015; Kidger *et al.*, 2016; Tsai, Birder and Kuo, 2016) Nevertheless, urinary data following ketamine drug abuse is scarce. (Moore *et al.*, 2001) Also, to my knowledge, there are no studies showing concentration of ketamine within the bladder wall or focusing on the bladder permeability to ketamine.

In the present section of work, a well-established *ex-vivo* whole bladder model of IDD (Williams *et al.*, 2015) was used to study the permeation of ketamine through the bladder wall.

The concentration of KH within the tissue layers of bladders instilled with KH 3 mM and 6 mM was analysed and compared to assess the effect of concentration in a similar way to what was described for LH intravesical delivery studies (chapter 3). Concentration-depth profiles followed a similar trend to LH and other intravesically administered compounds (Williams *et al.*, 2014, 2015), exhibiting a reduction in concentration with distance from bladder lumen. The concentration of KH was shown to be dependent on the concentration of the solution instilled. KH 6 mM resulted in concentrations within the bladder that were roughly double than those resulting from ketamine 3 mM (Figure 30). This behaviour is in agreement with Fick's first law (Fick, 1995) and is also similar to what was observed for LH, which is not surprising as KH and LH have similar molecular weight (respectively 274.18 g/mol and 270.8 g/mol). However, the pKa of KH is closer to physiological (pKa = 7.5), hence a higher non-ionized fraction than lidocaine (pKa = 7.8) is available in urine for membrane penetration. Histological features for exposition to ketamine over 60 min in these concentrations did not result in significant bladder damage.

Accumulation of ketamine in urine was estimated based on pharmacokinetic data available in the literature. (Pai and Heining, 2007; Peltoniemi *et al.*, 2016; Zanos *et al.*, 2018) Values assumed were within the range described in these studies and the profile of accumulation only represents a prediction of multiple possibilities. Concentration in urine will also depend on volume of urine stored in the bladder before drug intake and

voiding times, however for the purpose of this study was assumed that there was no urine in the bladder at the point of administration. This can lead to an overestimation of the concentration of ketamine in urine. In our study we did not validate our assumptions with pharmacokinetic studies in human population. It is also important to note that pharmacokinetic studies normally use low doses and possible changes in the pharmacokinetic profile of drug abusers cannot be unraveled.

It was not possible to obtain a concentration-depth profile for bladders instilled with KH 0.3 mM over 4h, as samples had to be grouped differently to ensure detection of ketamine above LOQ. Still, concentration per layer is provided and it is possible to see a reduction on ketamine concentration as the distance from the lumen increases, as was observed for the higher concentrations of KH. Cytoplasmic vacuolization of urothelium was observed which is considered as a nonspecific lesion (Frazier *et al.*, 2012) plausibly resultant from exposure to ketamine. Vacuolisation can also result from autolysis, which is a process of cell degradation that occurs due to autophagy or hydrolytic activity of enzymes present in cytosol, subsequent to disrupted blood circulation following tissue excision. (Erman and Veranič, 2011) However, presence of vacuoles was not pronounced in bladder tissue exposed to urine alone for 4 h, which suggests these lesions are resultant from direct exposure to ketamine, although the exact mechanism is not understood. An urinary concentration of ketamine of 0.3 mM is theoretically possible after 1 g dose (nasal administration) as previously demonstrated, as such the histological observations may have clinical relevance and support the hypothesis that urinary ketamine can have a direct detrimental effect in the urothelium, possibly involved in the mechanism of Ketamine-induced cystitis. Also, it is important to note that this effect was not observed for exposure over 1 h to higher concentrations of ketamine (3 mM and 6 mM), indicating that the effect is time dependent.

To simulate accumulation of ketamine stored in the bladder and considering the limitations with ketamine detection for bladders instilled with KH 0.3 mM for 4 h, concentrations 10-fold higher than initially estimated were used. The volume was also adjusted to avoid leakage during multiple additions of solutions of ketamine with variable concentration (initial concentration ~3.2 mM). The variation of concentrations administered was inferior to what was estimated, however the differences will be less

relevant in future functional studies, as concentrations used vary in the logarithmic scale. Solutions were instilled through the urethra, although after recreational use of ketamine this substance is transported from the kidneys to the bladder through the ureters, the concentration in the bladder lumen should be the same regardless of the access and the urethra guaranteed an easier administration. A solution of ketamine was prepared in artificial to mimic the excretion of ketamine in urine and account for the effect of pH in the proportion of non-ionized form of ketamine. The concentration within the urothelium was similar to that observed following instillation KH 3 mM for 1 h but was significantly superior in the other layers. This would be expected given the longer period of drug residence. If solutions 10-fold less concentrated had been administered as initially estimated, concentrations within the bladder wall would be roughly 10-fold less (around 10 µg/g of wet tissue), taking into consideration that concentration of KH appears directly dependent on the concentration of the solution instilled (additional concentrations would be required to confirm). An important limitation of this simulation is that it does not consider ketamine distributed or cleared through the bladder vasculature upon systemic distribution. Also, possible effect of metabolites was not investigated in this study. Histologically bladders exposed to these concentrations of ketamine showed a damaged urothelium, with signs of vacuolisation and loss of integrity more evident in the basal/intermediate layers of the urothelium. The deleterious effect was clearer when higher concentrations were used for a longer period (gradient concentration 3.2 mM and below over 4 h). Several intercellular junctions were disconnected and in some areas of the urothelial the superficial layer was detached. Bureau *et al.* had previously shown that ketamine mainly affected the intermediate layer of an urothelium tissue-engineered vesical equivalents model. This could be explained by the greater cohesion between cells in the superficial layer, making it less susceptible to ketamine in a first instance. The tissue-engineered model was exposed to various concentrations of ketamine (0.5 mM to 10 mM) over 48 h and the effect was dose dependent, with higher concentrations resulting in greater damage. (Bureau *et al.*, 2015) These findings suggest a direct harmful effect of ketamine in the urothelium layer, which is in line with clinical observation of significant denuded urothelium in bladders of recreational users of ketamine (Lin *et al.*, 2015; Fan *et al.*, 2017) and description of a

reduced expression of E-cadherin and zonula occludens-1 (ZO-1) in human bladder biopsies (Lee, Jiang and Kuo, 2013; Lu, Jiang and Kuo, 2015; Tsai, Birder and Kuo, 2016).

4.5. Conclusions

Bladder tissue concentrations were shown to be dependent on the concentration of ketamine solution stored in the bladder. Accumulation of ketamine in urine after intranasal administration was estimated and bladders were instilled with variable concentrations 10 times superior to the estimated value to ensure detection. Limitations of the method have been identified and should be considered when interpreting these results. Values here presented are an indication of plausible concentrations for future physiological work but do not replace pharmacokinetic studies in humans. Histological features compatible with urothelial damage were observed for bladders treated with ketamine for a longer period, which are in line with the hypothesis that urinary ketamine has a direct toxic effect on the urothelium, possibly contributing for the development of ketamine-induced cystitis. In addition, as ketamine distributes into the suburothelial layer, it is also plausible that it can induce changes in the microvasculature leading to bladder dysfunction, as will be further discussed in Chapter 6.

Chapter 5 – Establishing an *ex-vivo* murine tissue model to investigate microvasculature properties and function in the bladder

5.1. Introduction

5.1.1. The role of vascular changes in bladder dysfunction

The main blood supply in the bladder arrives from the superior and inferior vesical arteries (Figure 35). (Andersson, Boedtkjer and Forman, 2017) The metabolic needs of the bladder wall are satisfied at the microvascular level by two capillary beds: a dense capillary network in intimate contact with the urothelium, and a less organised capillary bed in the detrusor muscle. (Miodoński and Litwin, 1999) An overview of bladder microvascular features can be read in 1.4. Microvasculature.

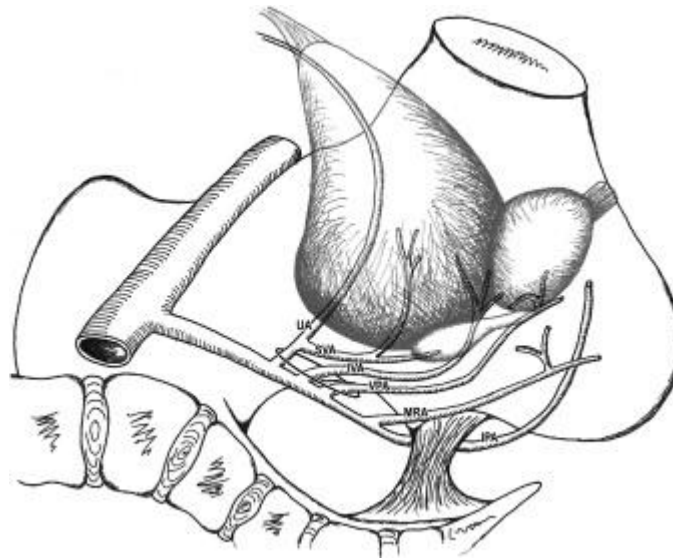


Figure 35 Arterial supply of the male bladder. The superior vesical artery (SVA) originates from the proximal portion of the umbilical artery and its branches supply the antero-lateral wall of the bladder and the seminal vesicles; the inferior vesical artery supplies the lower part of the ureter, the bladder base and seminal vesicles; the vesico-prostatic artery (VPA) supplies the prostate and seminal vesicles; and the middle rectal artery (MRA) has an ascendant branch that supplies the bladder and a descendant that supplies the prostate. (Simonato *et al.*, 2003)

Current knowledge suggests chronic ischemia has an important role in the development of LUTS. Age-related pelvic arterial insufficiency and bladder outlet obstruction, often secondary to benign prostatic hyperplasia (BPH) in male patients, might result in ischemia and subsequent tissue hypoxia, leading to structural, molecular and functional changes in the bladder. (Camões *et al.*, 2015; Andersson, Boedtkjer and Forman, 2017) Also, risk factors for vascular disease (Ponholzer *et al.*, 2006), and erectile dysfunction

(Tarcan *et al.*, 1998; Rosen *et al.*, 2003) have been implicated in the development of LUTS.

A relation between the ageing process, bladder ischemia and LUTS have been previously reviewed. (Camões *et al.*, 2015; Andersson, Boedtkjer and Forman, 2017) LUTS and vascular diseases are more prevalent and often co-exist in the elderly population. Pinggera *et al.* 2008 reported lower perfusion of the bladder neck in elderly patients with LUTS in both genders when compared to asymptomatic younger subjects. (Germar-Michael Pinggera *et al.*, 2008) Furthermore, a study of Uzun *et al.* has shown arterial stiffness and carotid intima-media thickness, indicators of vascular impairment related to atherosclerotic process, correlate positively with OAB symptoms, irrespectively of age. (Uzun *et al.*, 2013)

Several animal models have been used to study bladder ischemia leading to bladder dysfunction. Ischemia in these studies has been produced by ligating or clamping arteries (Koroäec and Jezernik, 2000; Juan *et al.*, 2009) or injuring bladder arteries with balloon or feeding animals with a high cholesterol diet. (Azadzoï *et al.*, 2004, 2011; Nomiya *et al.*, 2012, 2014; Zhang *et al.*, 2014) These studies suggest detrusor overactivity develops in response to the ischemic process and that it can progress to detrusor underactivity depending on the severity or duration of ischemia. (Azadoï *et al.*, 2003; Azadzoï *et al.*, 2004, 2011; Nomiya *et al.*, 2012, 2014; Zhang *et al.*, 2014; Zhao *et al.*, 2016) Arterial and arteriolar wall thickening leading to occlusion and reduction in bladder blood flow, changes in innervation and fibrosis are commonly observed in these models. (Azadzoï, Radisavljevic and Siroky, 2008; Azadzoï *et al.*, 2010, 2011; Nomiya *et al.*, 2012, 2014; Zhang *et al.*, 2014; Zhao *et al.*, 2016) Mitochondrial injury and increased expression of markers of oxidative stress and change in expression of muscarinic, purinergic and neurokinin receptors have been also reported (Azadzoï, Radisavljevic and Siroky, 2008; Azadzoï *et al.*, 2010, 2011; Zhang *et al.*, 2014; Zhao *et al.*, 2016) Azadzoï *et al.* has shown increased expression of COX-I, COX-II and 5-lipoxygenase with a marked increase release of leukotrienes B₄, E₄ and C₄, prostaglandin F_{2α} and thromboxane A₂ in response to moderate ischemia (Azadoï *et al.*, 2003; Azadzoï *et al.*, 2004). Furthermore, bladder mucosa has been shown to respond to the ischemic insult with increase in vimentin⁺ interstitial cells in the lamina propria, increased permeability and increased

expression of gap-junction proteins (connexin [Cx] 26 and Cx43) and tight junction protein (Zona occludens [ZO]-1) (Korošec and Jezernik, 2000; Sunagawa *et al.*, 2015). It is plausible the mucosa is more readily affected by ischemia considering it is more active metabolically than the detrusor muscle. (Hypolite *et al.*, 1993) To study a more gradual development of ischemia genetically modified or heritable animal models prone to atherosclerosis and vascular disease have also been used. (Shenfeld *et al.*, 2005; Yoshida *et al.*, 2010; Bschleipfer *et al.*, 2015) Bschleipfer *et al.* demonstrated that a hyperlipoproteinemic mouse model (apoE/LDLR double knockout) develops systemic atherosclerosis and causes detrusor overactivity. In this model, vascularization was reduced and changes in the microvasculature included a reduced lumen in capillaries, due to media thickening and activation of endothelial cells, accompanied of inflammatory cells infiltration (Bschleipfer *et al.*, 2015). However, Shenfeld *et al.* did not observe changes in detrusor contractibility using an apoE knockout mice model. Changes in bladder vasculature were not investigated in this model. (Shenfeld *et al.*, 2005) In addition, Yoshida *et al.* has shown that Watanabe Heritable Hyperlipidemic rabbits develop atherosclerosis, leading to bladder ischemia, and exhibit detrusor overactivity with decreased detrusor contraction. Histologically relevant changes in innervation and fibrosis were observed (Yoshida *et al.*, 2010) Bladder outlet obstruction has also been investigated in pig models and has revealed a reduction in bladder blood flow and oxygen tension with detrusor instability. During the micturition cycle repeated episodes of detrusor ischemia might result in ischemia-reperfusion injury. (Greenland *et al.*, 2000; Greenland and Brading, 2001)

As described in 1.5.3 Ketamine-induced cystitis, microvascular changes in response to ketamine or its metabolites have been proposed to be involved in the pathophysiological mechanism that leads to KIC. (Chu *et al.*, 2008; Lin *et al.*, 2016) These microvascular changes can result in local ischemia, induce fibrosis and promote an inflammatory response. Histological observations of basal membrane thickening in greater and small blood vessels, structural changes of the vascular lumen and reduced endothelial count have been documented by Lin *et al.* (Lin *et al.*, 2016) Fibrosis, neovascularisation and presence of inflammatory cells are also commonly reported in bladder biopsies of KIC patients. (Lee, Jiang and Kuo, 2013; Lu, Jiang and Kuo, 2015; Lin

et al., 2016; Tsai, Birder and Kuo, 2016; Fan *et al.*, 2017; Jhang *et al.*, 2018; Sihra, Ockrim and Wood, 2018) Although the histological features are compatible with an ischemic insult, changes in bladder microvascular blood flow in response to ketamine or its metabolites need to be further researched.

Possible therapeutic approaches for LUTS resulting from the ischemic process include α 1-adrenoceptor antagonists, phosphodiesterase type 5 (PDE5) inhibitors, β 3-adrenoceptor agonist and antioxidant agents. (Nomiya, Andersson and Yamaguchi, 2015) α 1-adrenoceptor antagonists (e.g. silodosin, tamsulosin, doxazosin) are effective to treat LUTS in patients with benign prostatic hyperplasia (BPH), a common cause of bladder outlet obstruction (BOO). (Djavan and Marberger, 1999; Rossi *et al.*, 2001) Although α 1-adrenoceptor antagonists have an important effect in prostatic smooth muscle tone thereby reducing prostatic urethral resistance, extra-prostatic effects also include increased blood perfusion in the bladder. Tamsulosin has been shown to increase bladder perfusion during filling and maximum cystometric capacity in male patients with LUTS (Germar-M. Pinggera *et al.*, 2008) Improvement of bladder blood flow and function in response to α 1-adrenoceptor antagonists has been also shown in several animal models. (Das *et al.*, 2002; Inoue *et al.*, 2012; Goi *et al.*, 2016) The therapeutic effect of PDE5 inhibitors (e.g. tadalafil, sildenafil, and vardenafil), alone or in association with α 1-adrenoceptor antagonists, in LUTS secondary to BPH, has been studied in several clinical trials and has been shown to improve the International Prostate Symptom Score (IPSS). (Soler *et al.*, 2013) The suggested mechanism involves inhibition of PDE5 with augmented nitric oxide-cyclic guanosine monophosphate (cGMP) mediated muscle relaxation and vasodilation. (Nomiya, Burmeister, Sawada, Campeau, Zarifpour, Keys, *et al.*, 2013; Pinggera *et al.*, 2014) Nomiya and colleagues have shown tadalafil has a prophylactic effect in bladder function of a chronic ischemia rat model. (Nomiya, Burmeister, Sawada, Campeau, Zarifpour, Keys, *et al.*, 2013) Nevertheless, a randomized placebo-controlled trial has found no differences in bladder and prostatic perfusion between patients with LUTS secondary to BPH treated with tadalafil when compared to controls (Pinggera *et al.*, 2014) Mirabegron, a β 3-adrenoceptor agonist used in the treatment of OAB, has also shown to have a protective effect in a rat model of chronic ischemia, resulting in reduced detrusor overactivity.

(Sawada *et al.*, 2013) In addition, antioxidant agents, such as Coenzyme Q10, lipoic acid and melatonin, also protect bladder function and morphology in animal models of bladder ischemia. (Radu *et al.*, 2011; Kim *et al.*, 2013; Nomiya, Burmeister, Sawada, Campeau, Zarifpour, Yamaguchi, *et al.*, 2013) Further studies are necessary to evidence this effect in humans.

5.1.2. Investigating blood flow through capillaries in live bladder tissue

As described in 1.4. Microvasculature, Hashitani and colleagues have investigated select immunohistochemical and functional features of the suburothelial microvasculature in rat and mouse bladder. (Hashitani *et al.*, 2011, 2012, 2018; Mitsui and Hashitani, 2013; Shimizu *et al.*, 2014; Hashitani and Lang, 2016) According to these studies arterioles are constricted in response to release of noradrenaline by sympathetic fibres but do not exhibit spontaneous activity. On the other hand, vasoconstriction of venules occurs spontaneously and is further stimulated by α -adrenergic stimulation and inhibited by β -adrenergic stimulation. Moreover, several biorelevant substances (e.g. ACh, SIN-1, ATP, CGRP, Substance P) were found to modulate venular diameter. This diameter regulation occurs through vascular smooth cells and stellate-shaped pericytes (Hashitani *et al.*, 2011, 2012; Shimizu *et al.*, 2014) Spontaneous Ca^{2+} transients in NG2(+) pericytes in PCAs, capillaries and PVCs have been observed but only elicited vasoconstriction on PCAs. (Hashitani *et al.*, 2018) Hashitani *et al.* argued that pericytes in capillaries of the mouse are not likely to be contractile as these cells are not immunoreactive for α -SMA and therefore lack the contractile machinery to exert vasoconstriction. (Mitsui and Hashitani, 2013)

The debate concerning contractile activity of capillary pericytes based on immunohistochemical studies extends to the microvascular networks of other organs (Mazzoni, Cutforth and Agalliu, 2015; Attwell *et al.*, 2016; Alarcon-Martinez *et al.*, 2018; Borysova and Dora, 2018) Several studies have reported detectable α -SMA expression in PCAs and PCVs but absence or reduced expression in the capillaries retina, brain and mesentery for example. (Nehls, 1991; Bandopadhyay *et al.*, 2001; Kur, Newman and Chan-Ling, 2012; Kornfield and Newman, 2014; Hill *et al.*, 2015) Functional studies showing pericyte-mediated changes of capillary diameter in response to various vasoactive agents in retina, brain and kidney challenge the argument against capillary

pericytes contractibility. (Peppiatt *et al.*, 2006; Fernandez-Klett *et al.*, 2010; Crawford *et al.*, 2012; Hall *et al.*, 2014) Furthermore, Alarcon-Martinez *et al.* have elegantly demonstrated the way samples are treated in immunohistochemical studies can result in different degrees of depolymerization of α -SMA, thereby affecting detection. This group used distinct methods to fix and preserve capillaries and pericytes in retina samples from mice and compared α -SMA immunoreactivity. Tissue samples readily frozen in ice-cold methanol allowed higher detection of α -SMA than fixation with formaldehyde. Also, tissue treated with phalloidin or jasplakinolide, which stabilizes filaments of actin, improved detection of α -SMA. This study evidenced α -SMA is expressed in half of NG2 (+) pericytes on high order retinal capillaries in the intermediate and deeper retinal microvascular network, although expression is inferior to upstream vessels and therefore more readily affected by degradation. (Alarcon-Martinez *et al.*, 2018)

Informed by these studies and to clarify the role of pericytes in the suburothelial capillaries in the bladder it is important to establish a viable tissue model that allows visualising capillaries and pericytes in the lamina propria of the bladder.

Such a model would make possible to evaluate pericyte-mediated diameter changes in response to vasoactive compounds, in a similar way to the live kidney slice model developed by Crawford *et al.* (Crawford *et al.*, 2012) Krska has previously reported a lamina propria preparation from mice bladder to investigate the role of pericytes in infection, however tissue viability was severely affected in this study, therefore, raising concerns regarding method validation and interpretation of results. (Krska, 2017)

Crawford *et al.* have shown pericyte-mediated changes in vasa recta diameter in a live kidney slice model from rat are elicited in response to several vasoactive compounds (noradrenaline, endothelin-1, angiotensin-II and prostaglandin E₂). (Crawford *et al.*, 2012) Similar findings were observed in a murine kidney slice model developed by Lilley (Lilley, unpublished work). These vasoactive agents are also present in physiological and pathological conditions in the bladder, as briefly reviewed below. This chapter will also elucidate whether these agents act to regulate pericyte-mediated diameter changes in the bladder as observed in the kidney.

5.1.2.1 Angiotensin II (Ang II)

Angiotensin II (Ang II) is the key mediator of the renin-angiotensin system, with important functions on the modulation of water-salt balance, regulation of vascular smooth muscle tone and stimulation of aldosterone secretion. (Nishimura, 2017) Ang II receptors (AT-1 and AT-2) are expressed in both mucosa and detrusor of the urinary bladder (Tanabe, Ueno and Tsujimoto, 1993; Tobu *et al.*, 2012; Mori *et al.*, 2016) Ang II can be synthesised in the detrusor muscle layer (Waldeck *et al.*, 1997) and its secretion is increased by repetitive stretch stimulation of bladder smooth muscle cells (Park *et al.*, 1998). Exogenous addition of Ang II evokes contraction of detrusor muscle strips of human (Erspamer, Ronzoni and Falconieri Erspamer, 1981; Andersson, Hedlund and Stahl, 1992; Saito *et al.*, 1993; Lam *et al.*, 2000) canine (Steidle, Cohen and Neubauer, 1990), rabbit (Anderson *et al.*, 1984) and rat (Tanabe, Ueno and Tsujimoto, 1993; Hadzhibozheva *et al.*, 2019) urinary bladder, mediated through AT-1 receptors (Tanabe, Ueno and Tsujimoto, 1993). Angiotensin II also acts locally as a trophic factor to regulate smooth muscle growth and increase collagen production in the bladder wall. (Cheng, Decker and Lee, 1999) Bladder dysfunction has been associated with changes in expression of angiotensin receptors and functional response to angiotensin. As such, contractile response to angiotensin II is reduced in neurogenic bladders (Saito *et al.*, 1993). Moreover, age-related changes in bladder function in a rat model were associated with overexpression of AT-1 (Mori *et al.*, 2016). It was also reported change in expression of AT-1 receptors on rats with bladder outlet obstruction (Yamada *et al.*, 2009; Cho, Park and Kim, 2012; Tobu *et al.*, 2012) and induced inflammatory bladder (Tobu *et al.*, 2013).

5.1.2.2 Endothelin-1 (ET-1)

Endothelin-1 (ET-1) is a potent endogenous vasoconstrictor peptide, which was first isolated from the culture supernatant of porcine aortic vascular endothelial cells. (Yanagisawa *et al.*, 1988) It evokes a long-lasting contraction in vascular and non-vascular smooth muscle. (Borges, Von Grafenstein and Knight, 1989; Bolger *et al.*, 1990) Various ET-1 biological functions are mediated by interaction with ET_A and ET_B receptors (Sakurai *et al.*, 1990). In the human and rabbit bladder ET-1 is produced by vascular endothelial cells, urothelial cells, fibroblasts, non-vascular smooth muscle and serosal

mesothelium (De Tejada *et al.*, 1992) Moreover, ET_A and ET_B receptors are present in the in smooth muscle and urothelium of the urinary bladder, with an overall predominance of ET_A receptors. (Bolger *et al.*, 1990; Afiatpour *et al.*, 2003; Osano *et al.*, 2014). These findings are suggestive of an autocrine and paracrine regulatory role of ET-1 in this organ. ET-1 elicits concentration-dependent contractions of pig vesical arterial muscle.(Persson *et al.*, 1992) Furthermore, ET-1 has been shown to have a potent contractile activity, mediated through ET_A receptors, in isolated smooth muscle strips of urinary bladder of several species. (Maggi *et al.*, 1989; Garcia-Pascual, Larsson and Andersson, 1990; De Tejada *et al.*, 1992; Persson *et al.*, 1992; Donoso *et al.*, 1994)

5.1.2.3. Noradrenaline (NA)

Noradrenaline (NA) is released from sympathetic nerves innervating the bladder wall. NA action is elicited through α_1 , α_2 and β_{1-3} adrenoceptors. Detrusor muscle has a low expression of α_1 -adrenoceptors (more pronounced in rats than humans) associated to a limited functional role in the bladder wall, which can produce a weak muscle contraction and facilitate the release of noradrenaline and acetylcholine. However, a greater density α_1 -adrenoceptors (predominately α_{1A} -adrenoceptors) is present in the bladder neck region and urethra and mediates relevant muscle contraction. α_2 - adrenoceptors are also present in the bladder wall and mediate post-junctional inhibition off neurotransmitter release from post-ganglionic sympathetic and parasympathetic nerve terminals. β -adrenoceptors (particularly β_3 subtype) elicit smooth muscle relaxation in the bladder. This lead recently to the development of a β_3 -adrenoceptor agonist, mirabegron, with indication for the treatment of OAB. (Michel and Vrydag, 2006)

Adrenergic receptors (α_{1A} , α_{1D} and β_{1-3}) are also expressed in the urothelium layer. (Walden *et al.*, 1997; Ishihama *et al.*, 2006; Otsuka *et al.*, 2008; Moro, Tajouri and Chess-Williams, 2013) Exogenous addition of NA inhibited the spontaneous contractile activity of bladder mucosa preparations, mediated through β -adrenoceptors. Agonist interaction with α_1 -adrenoceptor in the mucosa, however, has been found to increase the frequency of spontaneous contractions in this tissue preparation. (Moro, Tajouri and Chess-Williams, 2013) Additional studies have shown NA evokes release of nitric oxide (NO) from bladder urothelium (Birder, Gerard Apodaca, *et al.*, 1998; Lori A. Birder *et al.*, 2002).

Furthermore, sympathetic nerves release NA that interacts with α_{1A} -adrenoceptors to mediate constriction of suburothelial arterioles. (Hashitani *et al.*, 2011) Hashitani *et al.* have suggested α_1 -adrenoceptor antagonists might improve bladder circulation, therefore preventing ischemic injury of urothelium and suburothelial cells. α_1 -adrenoceptor antagonists have been also suggested to improve bladder storage function by acting in afferent C-fibres (Yokoyama *et al.*, 2006, 2007), urothelium (Sun *et al.*, 2002) or detrusor (Bouchelouche *et al.*, 2005).

5.1.2.4. Prostaglandin E_2 (PGE_2)

PGE_2 is a cyclooxygenase (COX) product derived from arachidonic acid that modulates vascular tone (Audoly *et al.*, 1999), contractibility of non-vascular smooth muscle and is involved in sensitization of nociceptive afferent nerves (Cheng and Ji, 2008) and inflammatory response. PGE_2 effect is mediated through four G protein-coupled receptors, EP_1 - EP_4 . (Narumiya, Sugimoto and Ushikubi, 1999; Breyer *et al.*, 2001) Interaction with EP_2 and EP_4 leads to muscle relaxation and vasodilation, whereas EP_1 and EP_3 receptors have been found to mediate smooth muscle contraction vasoconstriction. (Narumiya, Sugimoto and Ushikubi, 1999; Van Rodijnen *et al.*, 2007) Although PGE_2 mediates mostly vasodilation (Edwards, 1985; Imig, Breyer and Breyer, 2002; Attwell *et al.*, 2010; Murrant *et al.*, 2014), vasoconstriction in response to this agent has also been reported (Haylor and Towers, 1982; Edwards, 1985; Inscho, Carmines and Navar, 1990; Van Rodijnen *et al.*, 2007).

Prostaglandins (PGs) play an important role in bladder normal function and in pathological states. (Rahnama'i *et al.*, 2012) PGE_2 is synthesised in the bladder in the mucosa (Brown, Zenser and Davis, 1980; Downie and Karmazyn, 1984; Jeremy *et al.*, 1987; Pinna, Zanardo and Puglisi, 2000; Nile, de Vente and Gillespie, 2010; Nile and Gillespie, 2012) and detrusor muscle (Abrams *et al.*, 1979; Brown, Zenser and Davis, 1980) and inhibited in the presence of indomethacin (COX inhibitor) (Abrams *et al.*, 1979; Downie and Karmazyn, 1984; Pinna, Zanardo and Puglisi, 2000). COX-I and COX-II have been found expressed in mice bladder in different developmental stages, but an increased expression was found in foetal mice and in response to induced bladder obstruction outlet. (Park *et al.*, 1997) Urothelial expression of EP_1 has been also reported in mice and this receptor has been shown to facilitate the micturition reflex in this specie

(Wang *et al.*, 2008). A study using EP₁ receptor knockout mice evidenced however that this receptor is not essential for normal micturition but has a role in the development of detrusor overactivity in response to intravesical PGE₂ and induced bladder outlet obstruction. (Schröder, Newgreen and Andersson, 2004) EP-4 and COX-II were found expressed in the rat bladder and their expression was significantly increased in cyclophosphamide-induced cystitis. (Chuang *et al.*, 2009) In the guinea pig bladder, COX-I has been found expressed in basal and intermediate cells in the urothelium and in interstitial cells (IC) in the lamina propria and detrusor muscle (de Jongh *et al.*, 2007, 2009; Nile, de Vente and Gillespie, 2010; Rahnama'i *et al.*, 2010), whereas COX-2 is expressed in IC and in some umbrella cells (Nile, de Vente and Gillespie, 2010) Moreover, in the guinea pig bladder EP-1 is expressed weakly in the urothelium and is present in the detrusor muscle and interstitial cells (vimentin⁺), that in some cases co-express COX-I. (Rahnama'i *et al.*, 2010, 2011) ET-2 is strongly expressed in the urothelium and suburothelium layers of guinea pig bladder. (Rahnama'i *et al.*, 2010) Exogenous PGE₂ increases detrusor contractibility in several species, and spontaneous detrusor contractions are attenuated in the presence of indomethacin. (Hills, 1976; Andersson, Ek and Persson, 1977; Choo and Mitchelson, 1977; Andersson, Husted and Sjögren, 1980; Takeda *et al.*, 2002; Rahnama'i *et al.*, 2013) Intravesical administration of PGE₂ induces C-fibre hyperactivity and stimulates the micturition reflex in the rat bladder (Ishizuka, Mattiasson and Andersson, 1995; Takeda *et al.*, 2002; Yokoyama *et al.*, 2007; Aizawa *et al.*, 2009) Intravesical administration of PGE₂ was beneficial in patients with urinary retention in some studies, but produce no therapeutic effect in others. (Andersson and Sjögren, 1982) Changes in COX-2 expression have been also implicated in bladder dysfunction - OAB, bladder inflammation, IC/BPS and KIC (Rahnama'i *et al.*, 2012; Lin *et al.*, 2015). Urinary PGE₂ was found increased in patients with OAB and IC/BPS (Kim *et al.*, 2005, 2006; Abrams *et al.*, 2010)

There is some evidence for prostaglandin blood flow regulation in the bladder. Distension of dog bladder has been associated with release of prostaglandins to the pelvic venous blood (Gilmore and Vane, 1971; Ghoneim *et al.*, 1976; Khalaf *et al.*, 1979) Vasodilation in the feline bladder in response to distension was unaffected by alpha-adrenoceptor blockade, beta-adrenoceptor blockade and muscarinic acetylcholine

receptor blockade, but was inhibited in the presence of indomethacin. Local release of prostaglandin with effect in vasculature tone was therefore hypothesised (Andersson *et al.*, 1985). However, the effect of cyclooxygenase system in bladder blood flow was studied in a rabbit model, but there were no significant differences between animals treated with PGE₂, indomethacin or controls. (Murrant *et al.*, 2014)

5.1.3. Hypothesis and aims

It was hypothesised that pericytes can mediate diameter changes of suburothelial capillaries of the bladder to modulate microvascular blood flow. The aim of the present section of work was to develop a viable *ex-vivo* bladder tissue model from male C57BL/6J mice to investigate blood flow regulation through capillaries. To develop this model the key objectives were:

1. Assess tissue viability over time
2. Using DIC imaging, investigate whether pericytes mediate diameter changes of suburothelial capillaries of the mouse bladder in response to vasoactive compounds – Ang II, ET-1, NA, PGE₂, and indomethacin.

5.2. Methods

5.2.1. Tissue preparation

Tissue was prepared as described in 2.2.1. Tissue preparation

5.2.2. Tissue viability

Tissue viability was assessed using propidium iodide and Hoechst co-staining protocol as described in 2.2.2. Tissue viability.

5.2.3. DIC imaging and pericyte functional experiments

DIC imaging and pericyte functional experiments were conducted as described in

2.2.3. DIC imaging and functional experiments. For this chapter the following vasoactive agents were used to evoke diameter changes: Ang-II (10 nM, 100 nM and 300 nM), indomethacin (30 µM and 100 µM), ET-1 (1 nM and 10 nM), NA (10 nM), PGE₂ (10 µM, 30 µM and 100 µM).

5.2.4. α -SMA and NG2 immunoreactivity of perivascular cells

Immunohistochemical staining to identify the expression of α -SMA and NG2 in perivascular cells and the nucleus of all cells (stained with Hoechst) in the suburothelial microvasculature was performed as described in 2.2.4.1 α -SMA/NG2/Hoechst immunohistochemical staining.

5.2.5. Statistical analysis

Mean % of tissue viability calculated for different time points was compared with ANOVA, followed by Tukey's multiple comparisons test, to determine possible statistically significant differences. Although it was not possible to confirm a normal distribution of the data due to the small sample size, normality of cell viability has been previously described in the literature (Gasparini *et al.*, 2017; Kang *et al.*, 2019). Statistical difference of diameter changes at pericyte and non-pericyte sites in responsive capillaries were calculated with paired *t*-tests for each concentration of vasoactive drug. Values of $p < 0.05$ were considered statistically significant. Paired *t*-test was used considering that for each capillary tested the diameter change was determined at a pericyte site and non-pericyte site, therefore considered a paired observation. Although normality was not confirmed for this data, due to the small sample size, this statistical test was conducted in agreement with previous studies (Crawford *et al.*, 2012).

5.3. Results

5.3.1. Tissue viability

Bladder mucosal preparations from mice and rat have been previously used to study the microvasculature in this organ. (Hashitani *et al.*, 2011, 2018; Mitsui and Hashitani, 2013; Krska, 2017) Previous work from Krska suggested that dissection of mucosa from detrusor can have an extensive detrimental effect in tissue viability, as maximal viability of 13.7% was reported in this mucosal preparation. (Krska, 2017) In the present study full-thickness bladder samples were used, thereby reducing tissue handling. Tissue viability was assessed at different time-points from dissection as described in 2.2.2. Tissue viability.

A substantial background noise was observed during imaging (Figure 36) and signal intensity was not uniform throughout each slide, presumably as a result of the thickness of the samples imaged (mouse bladder wall is ~350 μm thick (Leiria *et al.*, 2011)). Although these limitations have been recognised, it was still possible to identify and count all cells (which nuclei were labelled with Hoechst 33342) and dead cells (which nuclei were labelled with PI), to calculate the % of cell viability. Figure 37 (a-e) shows representative fluorescence images of bladder tissue labelled with Hoechst 33342 and PI at different time points from animal dissection (45 min, 1 h 45 min, 2 h 45 min, 3 h 45, 4 h45min). In these images the background was uniformly subtracted using Fiji software and brightness and contrast adjusted to better discern individual cells. Please note that unprocessed images were always used as reference during analysis to prevent bias. Mean average of cell viability was superior to 60% for all time points (Figure 37 [f]) and there was not a significant difference amongst time points as calculated by one-way ANOVA ($n = 3$ animals for each time point), followed by Tukey's multiple comparisons test.

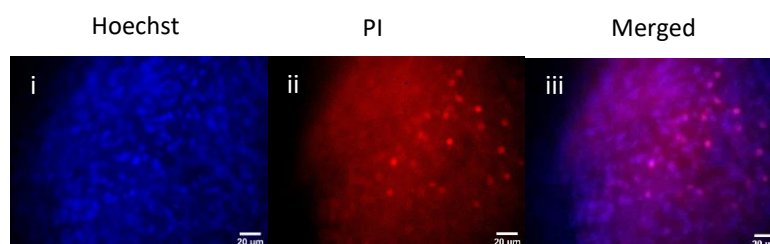


Figure 36 Fluorescence images of bladder tissue labelled with Hoechst 33342 and propidium iodide (PI) to identify the nuclei of all (i) and dead (ii) cells, respectively. Merged images show the ratio of total cell count:dead cells (ii). Substantial background noise can be observed.

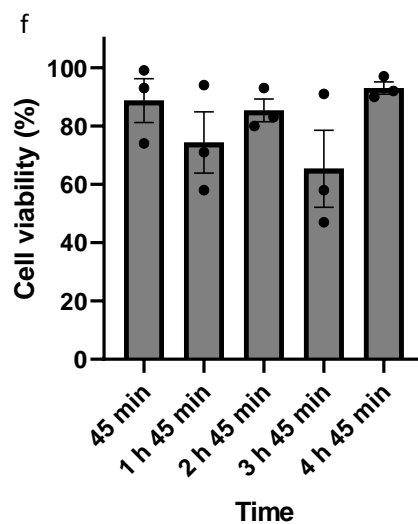
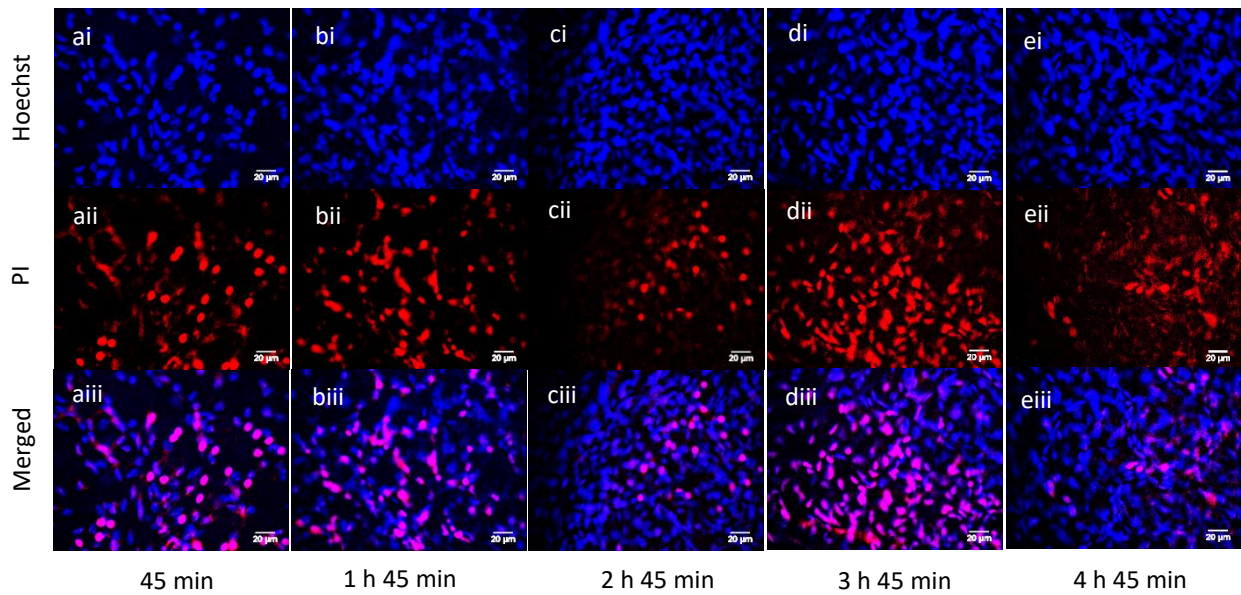


Figure 37 Representative fluorescence images of bladder tissue stained at different time points after animal dissection: 45 min (a), 1 h 45 min (b), 2 h 45 min (c), 3 h 45 min (d), 4 h 45 min (e). Tissue was labelled with Hoechst 33342 and propidium iodide (PI) to identify the nuclei of all (ai, bi, ci, di, ei) and dead (aii, bii, cii, dii, eii) cells, respectively, Merged images show the ratio of total cell count:dead cells (aiii, biii, ciii, diii, eiii). The background was uniformly subtracted using Fiji software and brightness and contrast adjusted to better discern individual cells. Mean % of cell viability (\pm SEM) for each time point is presented in (f). Mean % of cell viability was not statistically different amongst time-points, as calculated by one-way ANOVA ($n = 3$ animals for each time point), followed by Tukey's multiple comparisons test.

5.3.2. DIC imaging and pericyte functional experiments

5.3.2.1. Angiotensin II (Ang II)

The effect of angiotensin II (Ang II; 10 nM, 100 nM and 300 nM) in the suburothelial capillaries of the bladder was assessed in time series experiments (Figure 38). Table 5 summarizes the main data from DIC functional experiments where tissue was exposed to Ang II. Ang II 10 nM had no effect in the 7 capillaries (n = 6 animals) imaged and analysed. Ang II 100 nM evoked a pericyte mediated constriction of $17.9 \pm 3.1\%$ (from a resting diameter of $4.11 \pm 0.38 \mu\text{m}$) in 6 of 16 capillaries tested (n = 16 animals), which was significantly greater than at non-pericyte sites ($3.2 \pm 1.1\%$), from an initial diameter of $4.80 \pm 0.25 \mu\text{m}$), $p < 0.05$ determined with a paired *t*-test. At the end of the video, capillary diameter at pericyte sites had returned to $-7.7 \pm 0.9\%$ from baseline. Ang II 300 nM induced a vasoconstriction at pericyte sites of $30.0 \pm 12.6\%$ (from a resting diameter of $4.22 \pm 0.32 \mu\text{m}$) in 5 of 12 capillaries tested (n = 12 animals) that was not statistically different from constriction at non-pericyte sites ($5.6 \pm 1.3\%$, from an initial diameter of $5.30 \pm 0.39 \mu\text{m}$), $p > 0.05$ determined with a paired *t*-test. The response of capillaries to Ang II 100 nM was more variable: 3 capillaries returned to initial diameter (~4% of change from baseline), whereas other 2 capillaries exhibited maximum vasoconstriction even after a wash-out period of 10 min. Time to induce vasoconstriction and maximum vasoconstriction was comparable in response to Ang II 100 nM and 300 nM.

Table 5 DIC imaging of live bladder tissue demonstrates pericyte-mediated regulation of capillary diameter in response to angiotensin II (Ang II; 10 nM, 100 nM and 300 nM). Response rate and mean values \pm SEM of time to induce (t_{ind}) vasoconstriction, time to maximum (t_{max}) constriction from addition of Ang II, % of maximum (max) constriction at pericyte site and non-pericyte, and % change from baseline (% Δ vessel diameter) at the end of the video are provided. No response was observed for capillaries exposed to Ang II 10nM. Higher concentrations of Ang II (100nM and 300nM) produced a similar response rate, t_{ind} constriction, t_{max} constriction. Although % max constriction at pericytes sites was higher on average in response to Ang II 300nM, the response was also substantially more variable. Capillaries exposed to Ang II 100 returned to values closer to baseline, whereas not all capillaries returned to initial diameter when exposed to Ang II 300nM. [Ang II] – angiotensin II concentration.

[Ang II]	Response rate	t_{ind} constriction	t_{max} constriction	% max constriction pericyte sites	% max constriction non-pericyte sites	% Δ vessel diameter at the end of video
10 nM	0/6 (0%)	-	-	-	-	-
100 nM	6/16 (37.5%)	138 \pm 25 s	506 \pm 93 s	17.9 \pm 3.1%	3.2 \pm 2.7%	-7.7 \pm 0.9%
300 nM	5/12 (41.2%)	119 \pm 50 s	524 \pm 200 s	30.0 \pm 12.6%	5.6 \pm 1.3%	-25.1 \pm 14.3%

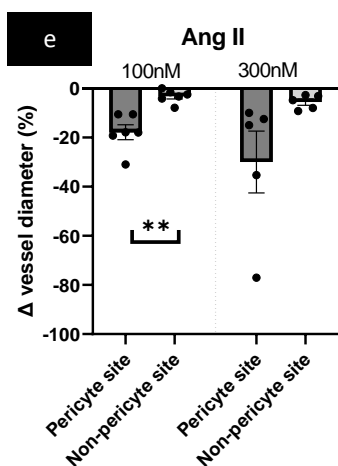
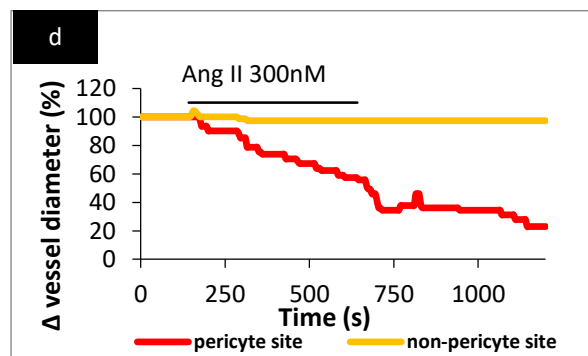
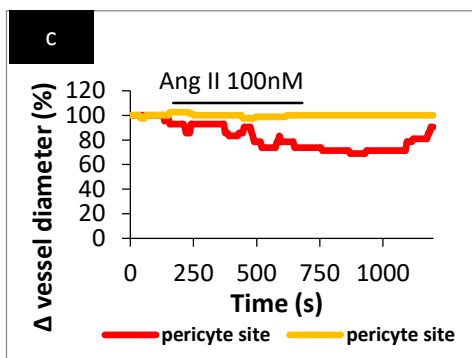
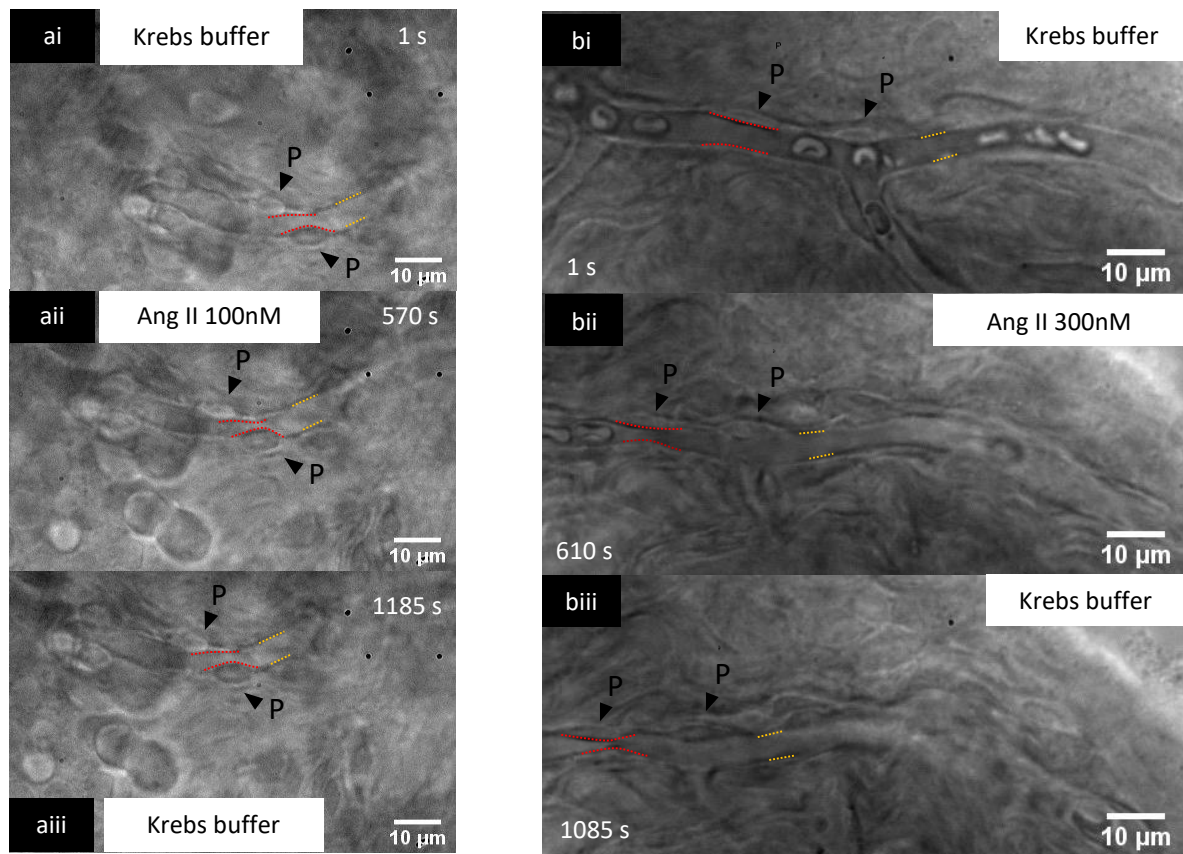


Figure 38–Functional experiments - Angiotensin II (Ang II) DIC images taken from a time series experiment showing pericyte-mediated constriction (a,b) of *in situ* bladder capillaries following exposure of tissue to Ang II 100 nM (a) and 300 nM. Pericytes are located on the abluminal side of the capillary (arrowheads). Red and yellow dotted lines highlight the areas where capillary diameters were measured at pericyte and non-pericyte sites, respectively. Tissue was superfused with Krebs buffer (ai,bi), followed by Ang II (aii,bii) to evoke vasoconstriction. Ang II 100nM evoked changes in capillary diameter that were reversible (aiii). Ang II 300 nM changes were not always reversible after a wash-out period of 10 min (biii). Representative traces of % of change in capillary diameter at a pericyte site (red trace) and non-pericyte site (yellow trace), is shown for tissue exposed to Ang II 100 nM (c) and 300 nM (d). Mean (\pm SEM) and individual data (dots) for maximum vasoconstriction (% change from baseline) in these experiments are shown in e. In responsive

capillaries, Ang II 100nM evoked significantly greater vasoconstriction at pericyte sites compared with

non-pericyte sites $**p < 0.01$, whereas Ang II 30 nM did not evoke a significantly greater vasoconstriction at pericyte sites compared with non-pericyte sites, $p > 0.05$ (calculated with paired t -tests).

5.3.2.2. Endothelin-1 (ET-1)

The effect of ET-1 (1 nM and 10 nM) in the suburothelial capillaries of the bladder was studied in time series experiments. Table 6 summarizes main data from DIC functional experiments where tissue was exposed to ET-1. An initial concentration of 10 nM of ET-1 was used to produce vasoconstriction. However, ET-1 induced a strong constriction in the two capillaries tested (~64 and 80% change in diameter) that was accompanied of endothelial swelling and presumably of non-vascular smooth muscle contraction, which severely affected imaging and subsequent analysis. Therefore, a concentration of 1 nM of ET-1 was used in the following experiments. ET-1 1 nM evoked a pericyte mediated constriction of $22.0 \pm 4.0\%$ (from an initial diameter of $4.59 \pm 0.36\mu\text{m}$) in 6 of 13 capillaries tested ($n = 13$ animals), which was significantly greater than at non-pericyte sites ($6.0 \pm 1.4\%$, from a resting diameter of 5.42 ± 1.25), $p < 0.01$ determined with a paired t -test (Figure 39). Vasoconstriction was not reversible for the duration of experiment.

Table 6 Summary of main findings from DIC experiments to study capillary functional responses to endothelin-1 (ET-1; 1 nM, 10 nM). Response rate and mean values \pm SEM of time to induce (t_{ind}) vasoconstriction, time to maximum (t_{max}) constriction from addition of ET-1, % of maximum (max) constriction at pericyte site and non-pericyte, and % change from baseline ($\% \Delta$ vessel diameter) at the end of the video are provided. Only two bladder samples ($n = 2$ animals) were superfused with ET-10 nM. Strong vasoconstriction was observed in response to ET-1 10 nM, however this was possibly accompanied by non-vascular smooth muscle contraction, causing severe changes of focus that impaired imaging and subsequent analysis. ET-1 1 nM produced a pericyte mediated vasoconstriction that was not reversible. [ET-1] – endothelin-1 concentration.

[ET-1]	Response rate	t_{ind} constriction	t_{max} constriction	% max constriction pericyte sites	% max constriction non-pericyte sites	$\% \Delta$ vessel diameter at the end of video
1 nM	6/13 (46.2%)	152 ± 41 s	604 ± 87 s	$-22.0 \pm 4.0\%$	$6.0 \pm 1.4\%$	$-18.1 \pm 4.4\%$
10 nM	2/2 (100%)	110 ± 10 s	N/A	$\sim 72 \pm 11\%$	N/A	N/A

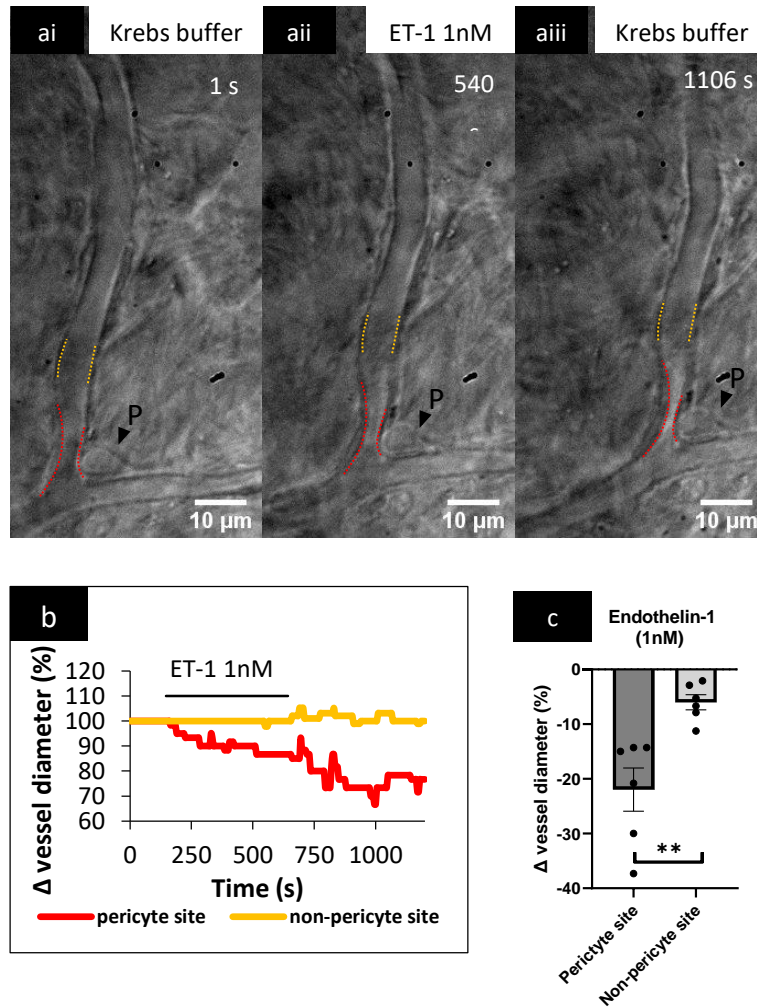


Figure 39 Functional experiments – Endothelin-1 (ET-1) DIC images taken from a time series experiment showing pericyte-mediated constriction (a) of an *in situ* bladder capillary following exposure of bladder tissue to ET-1 1nM. A pericyte is located on the capillary wall at a branch site (arrowhead) and red and yellow dotted lines highlight the areas where capillary diameter was measured at pericyte and non-pericyte sites, respectively. Tissue was superfused with Krebs buffer (ai), followed by ET-1 (aii) to evoke vasoconstriction. ET-1 evoked changes in vessel diameter that were not reversible (aiii). A representative trace (b) of % change in capillary diameter at a pericyte site (red trace), and non-pericyte site (yellow trace), is shown for tissue exposed to ET-1. Mean (\pm SEM) and individual data (dots) for maximum vasoconstriction (% change from baseline) in these experiments are shown in c. In responsive capillaries, ET-1 evoked a significantly greater vasoconstriction at pericyte sites compared with non-pericyte sites (c) $**p < 0.01$ (calculated with a paired *t*-test).

5.3.2.3. Noradrenaline (NA)

The effect of noradrenaline (NA;10nM) in the suburothelial capillaries of the bladder was assessed in time series experiments (Figure 40). Table 7 summarizes main data from DIC functional experiments where tissue was exposed to NA. NA 10nM evoked a pericyte mediated constriction of $17.2\pm 5.3\%$ (from a resting diameter of $5.28\pm 0.63\ \mu\text{m}$) in 5 of 19 capillaries tested (n=19 animals), which was significantly greater than at non-pericyte sites ($5.9\pm 6.2\%$), from an initial diameter of $5.17\pm 0.53\ \mu\text{m}$), $p<0.05$, determined with a paired *t*-test. Vasoconstriction at pericyte-sites was only reversible in two capillaries after NA was washed-out for 10 min with Krebs buffer.

Table 7 Summary of main findings from DIC experiments to study capillary functional responses to noradrenaline (NA; 10nM). Response rate and mean values \pm SEM of time to induce (t_{ind}) vasoconstriction, time to maximum (t_{max}) constriction from addition of NA 10nM, % of maximum (max) constriction at pericyte site and non-pericyte, and % change from baseline (% Δ vessel diameter) at the end of the video are provided. NA 10nM evoked a pericyte-mediated vasoconstriction that was only reversible in 2 capillaries (n=2 animals) of 5 responsive. [NA] – noradrenaline concentration

[NA]	Response rate	t_{ind} constriction	t_{max} constriction	% max constriction pericyte sites	% max constriction non-pericyte sites	% Δ vessel diameter at the end of video
10nM	5/19 (26.3%)	212 \pm 61 s	575 \pm 175 s	17.2 \pm 5.3%	5.9 \pm 1.6%	-15 \pm 6.2%

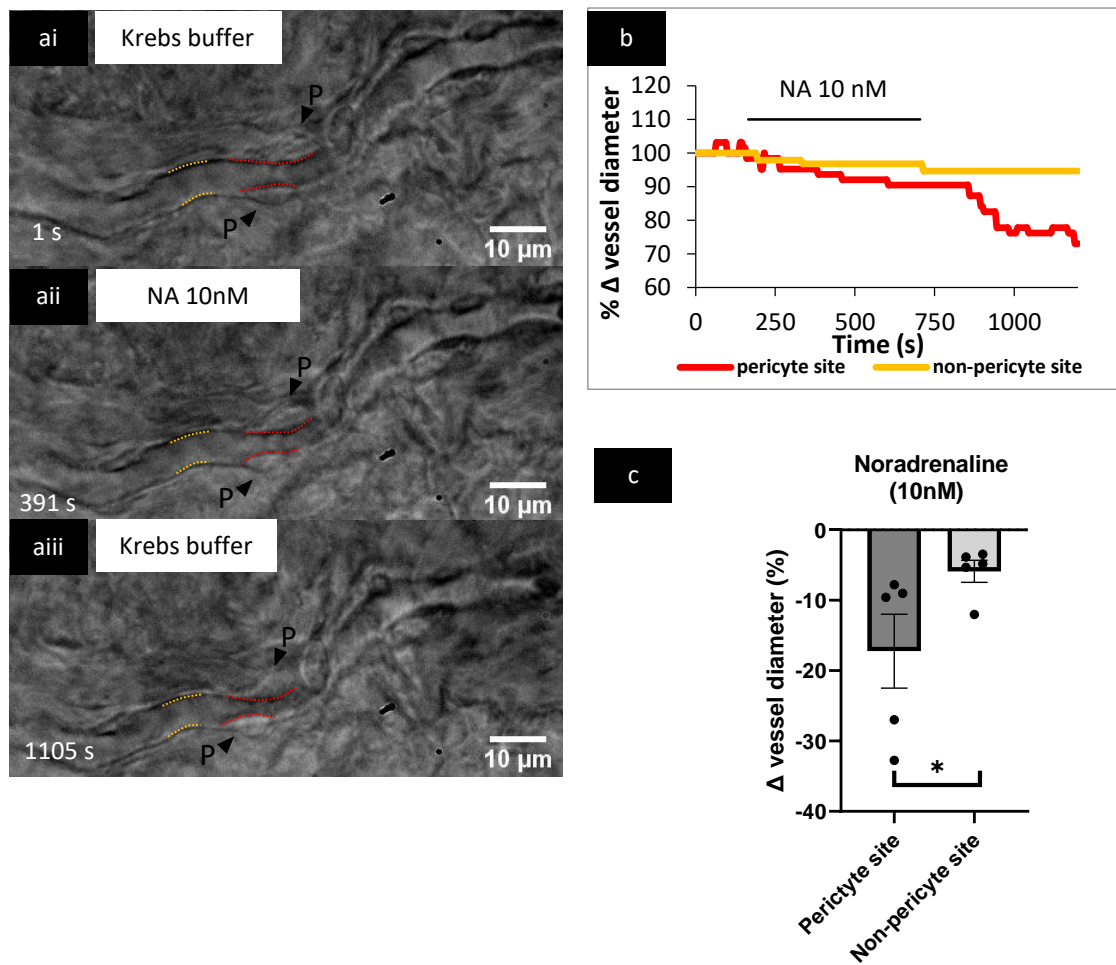


Figure 40 Functional experiments – Noradrenaline (NA) DIC images taken from a time series experiment showing pericyte-mediated constriction (a) of an *in situ* bladder capillaries following exposure of tissue to NA 10 nM. Pericytes are located on the capillary wall and red and yellow dotted lines highlight the areas where capillary diameter was measured at pericyte and non-pericyte sites, respectively. Tissue was superfused with Krebs buffer (ai), followed by NA (aii) to evoke vasoconstriction. NA evoked changes in vessel diameter that were not reversible (aiii). A representative trace (b) of % change in capillary diameter at a pericyte site (red trace), and non-pericyte site (yellow trace), is shown for tissue exposed to NA. Mean (\pm SEM) and individual data (dots) for maximum vasoconstriction (% change from baseline) in these experiments are shown in c. In responsive capillaries, NA evoked significantly greater vasoconstriction at pericyte sites compared with non-pericyte sites (c) * $p < 0.05$ (calculated with a paired *t*-test).

5.3.2.4. Prostaglandin E₂ (PGE₂)

The effect of prostaglandin E₂ (PGE₂; 10 μM, 30 μM and 100 μM) in the suburothelial capillaries of the bladder was assessed in time series experiments (Figures 41 and 42). Table 8 summarize main data from DIC functional experiments where tissue was exposed to PGE₂. PGE₂ 10μM had no effect in the 5 capillaries (n = 5 animals) tested. PGE₂ 30 μM elicited a pericyte-mediated dilation of $12.1 \pm 1.5\%$ (from a resting diameter of $4.83 \pm 0.39 \mu\text{m}$) in 3 of 17 capillaries tested (n = 17 animals), which was significantly greater than at non-pericyte sites ($3.68 \pm 1.21\%$, from an initial diameter of $5.61 \pm 0.33 \mu\text{m}$), $p < 0.05$ determined with a paired *t*-test. Vasodilation was reversible. Vasoconstriction was also observed in 3 capillaries exposed to PGE₂ 30 μM, however maximal constriction at pericyte sites ($12.6 \pm 6.7\%$, from a resting diameter of $4.00 \pm 0.38 \mu\text{m}$) was not statistically different from constriction at non-pericyte sites ($6.69 \pm 2.05\%$, from a resting diameter of $4.04 \pm 0.37 \mu\text{m}$), $p > 0.05$ determined with a paired *t*-test. At the end of the video, capillary diameter at pericyte sites had returned to $-6.0 \pm 2.1 \%$ from baseline. Contraction of non-vascular smooth muscle was apparent in these cases. PGE₂ evoked a vasoconstriction of $22.8 \pm 8.8\%$ at pericyte sites (from a resting diameter of $4.16 \pm 0.69 \mu\text{m}$) in 4 of 6 capillaries tested (n = 6 animals) that was not statistically different from constriction at non-pericyte sites ($6.6 \pm 1.7\%$, from a resting diameter of $5.16 \pm 0.60 \mu\text{m}$), $p > 0.05$ calculated with a paired *t*-test. Vasoconstriction was reversible. Some degree of non-vascular smooth muscle contraction was apparent.

Table 8 Summary of main findings from DIC experiments to study capillary functional responses to Prostaglandin E₂ (PGE₂; 10 μM, 30 μM and 100 μM). Vasodilation and vasoconstriction are represented separately in [A] and [B]. Response rate and mean values ± SEM of time to induce (t_{ind}) a response, time to maximum (t_{max}) constriction [A] or dilation [B] from addition of PGE₂, % of maximum (max) response at pericyte site and non-pericyte, and % change from baseline (% Δ vessel diameter) at the end of the video are provided. No response was observed for capillaries exposed to PGE₂ 10 μM. PGE₂ produced vasodilation in 3 capillaries and vasoconstriction 3 capillaries, but non-vascular smooth muscle contraction was apparent. A higher concentration, PGE₂ 100 μM produced vasoconstriction in 4 capillaries. Response rate and % maximum vasoconstriction were superior for this concentration, but non-vascular smooth muscle contraction seemed to occur. Response tends to be reversible with removal of PGE₂. [PGE₂] –PGE₂ concentration.

[A] Vasodilation

[PGE ₂]	Dilation Response rate	t _{ind} dilation	t _{max} dilation	% max dilation pericyte sites	% max dilation non-pericyte sites	%Δ vessel diameter at the end of video
10 μM	0/5 (0%)	-	-	-	-	-
30 μM	3/17 (17.6%)	137 ± 78 s	219 ± 41 s	12.10 ± 1.48%	2.34 ± 1.30%	3.68 ± 1.21%
100 μM	0/6 (0%)	-	-	-	-	-

[B] Vasoconstriction

[PGE ₂]	Constriction Response rate	t _{ind} constriction	t _{max} constriction	% max constriction pericyte sites	% max constriction non-pericyte sites	%Δ vessel diameter at the end of video
10 μM	0/5 (0%)	-	-	-	-	-
30 μM	3/17 (17.6%)	293 ± 58 s	435 ± 65 s	12.6 ± 2.7%	6.7 ± 2.1%	-6.0 ± 2.1%
100 μM	4/6 (66.6%)	156 ± 75 s	337 ± 77 s	22.8 ± 8.8%	6.6 ± 1.7%	-1.7 ± 2.2%

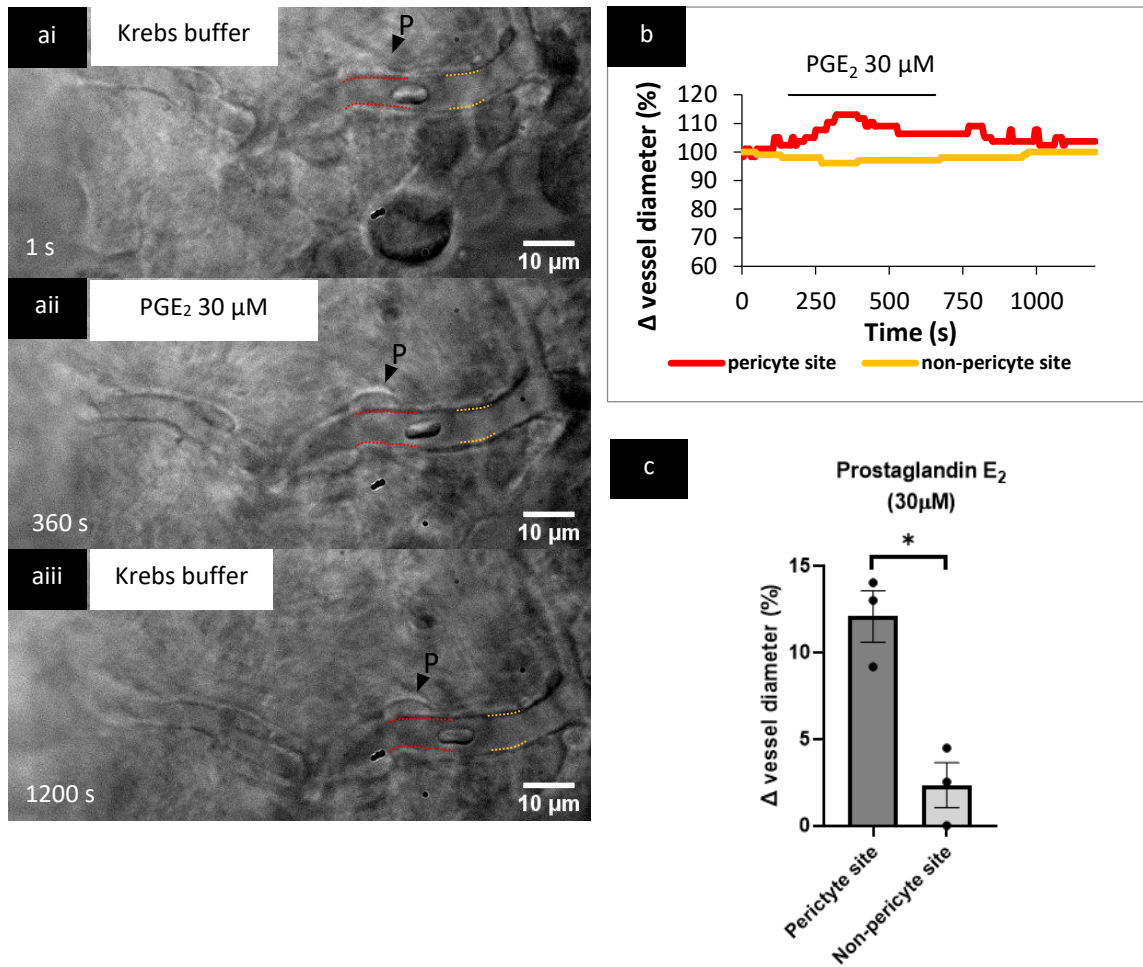


Figure 41 Functional experiments – Prostaglandin E₂ (PGE₂) DIC images taken from a time series experiment showing pericyte-mediated dilation (a) of an *in situ* bladder capillary following exposure of tissue to PGE₂ 30 μM. Pericytes are located on the capillary wall (arrowheads) and red and yellow dotted lines highlight the areas where capillary diameter was measured at pericyte and non-pericyte sites, respectively. Tissue was superfused with Krebs buffer (ai), followed by PGE₂ (aii) to evoke vasodilation. PGE₂ evoked changes in capillary diameter that were reversible (aiii). A trace (b) of % change in capillary diameter at a pericyte site (red trace), and non-pericyte site (yellow trace), is shown for tissue exposed to PGE₂ that responded with vasodilation. Mean (±SEM) and individual data (dots) for maximum vasodilation (% change from baseline) in these experiments are shown in (c). In responsive capillaries, PGE₂ evoked significantly greater vasodilation at pericyte sites compared with non-pericyte sites (c) $p < 0.05$ (calculated with paired *t*-tests).

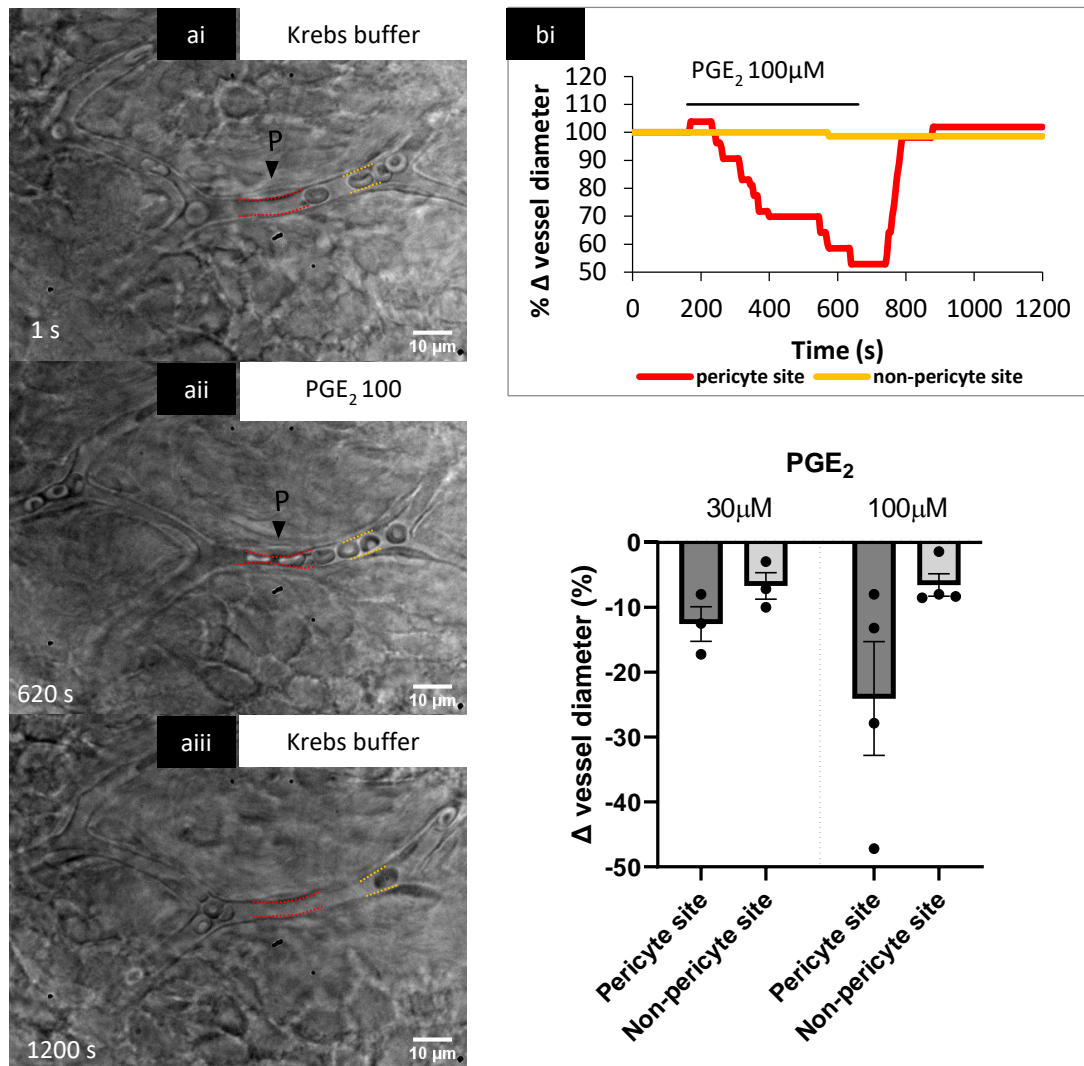


Figure 42 Functional experiments – Prostaglandin E₂ (PGE₂) DIC images taken from a time series experiment showing vasoconstriction (a) of an *in situ* bladder capillary following exposure of tissue to PGE₂ 100 μM. A pericyte is located on the capillary wall (arrowhead) and red and yellow dotted lines highlight the areas where capillary diameter was measured at pericyte and non-pericyte sites, respectively. Tissue was superfused with Krebs buffer (ai), followed by PGE₂ (a ii) that evoked vasoconstriction PGE₂ evoked changes in capillary diameter that were reversible (a iii). A trace (b) of % change in capillary diameter at a pericyte site (red trace), and non-pericyte site (yellow trace), is shown for tissue exposed to PGE₂ that responded with vasoconstriction. Mean (±SEM) and individual data (dots) for maximum vasoconstriction (% change from baseline) in these experiments are shown in c. In responsive capillaries, PGE₂ evoked vasoconstriction that was not statistically different at pericyte sites and non-pericyte sites (c) $p > 0.05$ (calculated with paired *t*-tests).

5.3.2.5. Indomethacin

The effect of indomethacin (30 and 100 μM) in the suburothelial capillaries of the bladder was assessed in time series experiments. Indomethacin 30 μM did not evoke a response in 6 capillaries tested (n = 6 animals). When applying a higher concentration, 100 μM , no response was observed in 11 of 13 capillaries (n = 13 animals). However, vasoconstriction in two capillaries (Figure 43) was observed during wash-out with Krebs buffer, ~6 min after indomethacin had been removed from the bath. Vasoconstriction was maximal at the end of the video (~55 and 23% change from baseline at pericyte sites). No statistical analysis was performed considering the limited response rate.

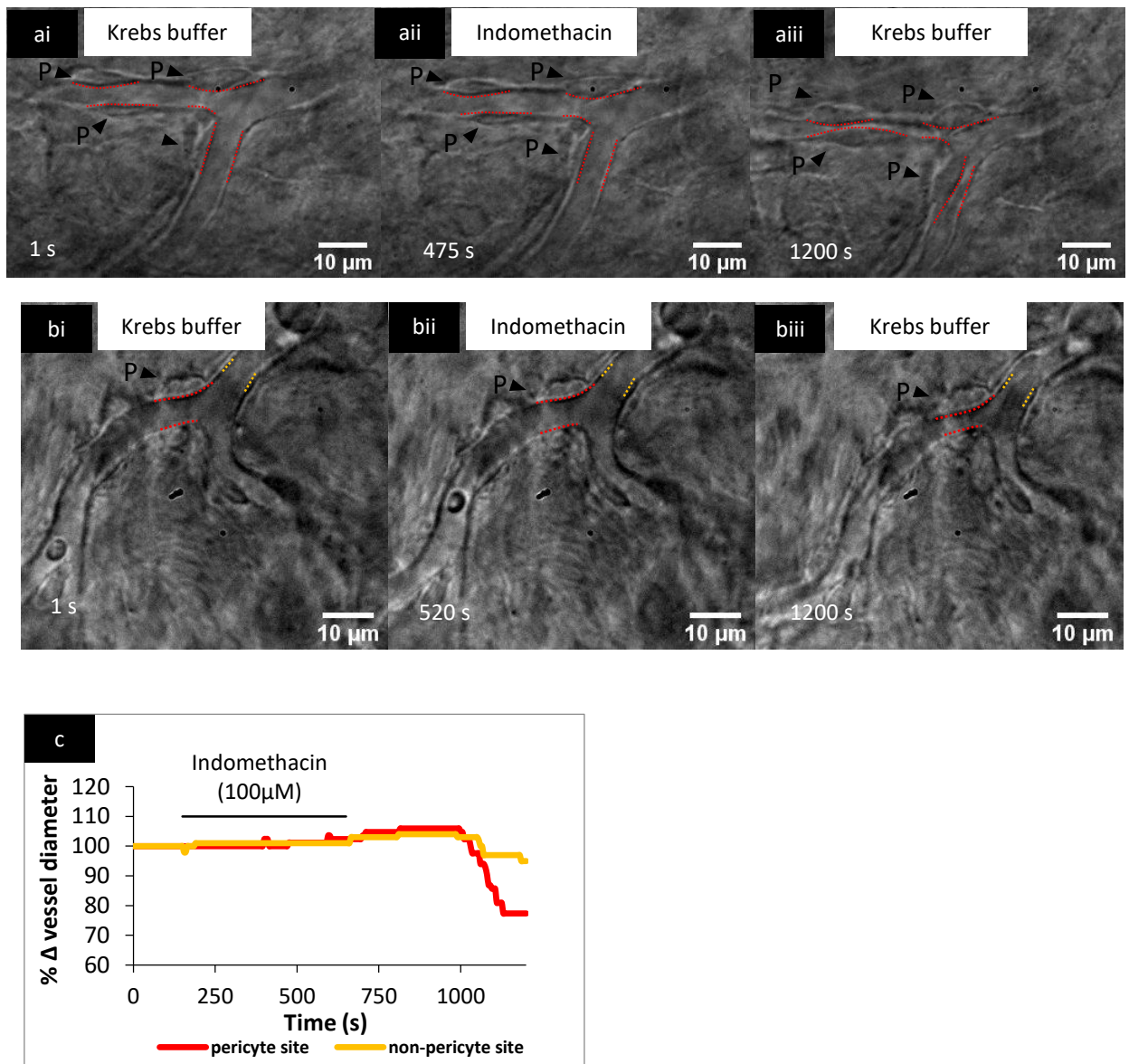


Figure 43 Functional experiments – Indomethacin DIC images taken from a time series experiment showing of pericyte-mediated late constriction (a,b) of *in situ* bladder capillaries following exposure of tissue to indomethacin (100 μM). Pericytes are located on the capillary wall (arrowheads, a and b) and red and yellow dotted lines (b) highlight the areas where capillary diameter was measured at pericyte and non-pericyte sites, respectively. Capillaries were superfused with Krebs buffer (ai, bi), followed by indomethacin (a ii, b ii) without change in vessel diameter. A late constriction was observed during the wash-out period (a iii, b iii). A representative trace (c) of % change in capillary diameter at a pericyte site (red trace) and non-pericyte site (yellow trace) is shown for tissue exposed to indomethacin that exhibited late constriction. Mean data for these experiments is not provided as capillaries from only 2 samples of bladder tissue were responsive (out of 13 samples of bladder imaged [n=13 mice]).

5.3.3. α -SMA and NG2 immunoreactivity of perivascular cells

Pericytes in capillaries and vascular smooth muscle cells were visualised by NG2-immunoreactivity (Figure 44). Vascular smooth muscle cells were arranged circumferentially in arterioles whereas pericytes in capillaries presented a typical 'bump-on-a-log' cell body and bipolar processes. Although the aim was to detect mural cells in the microvasculature expressing α -SMA, inconsistent results for the expression of α -SMA were obtained. Using the protocol described in 2.2.4.1 α -SMA/NG2/Hoechst immunohistochemical staining it was not possible to detect α -SMA in pericytes, but detection in arterioles was also erratic, being detectable in some smooth muscle cells but not all. Given these results, kidney slices from C57black/6J mice, obtained following an established protocol (Lilley, unpublished work), were also incubated with goat polyclonal anti- α -SMA and donkey anti-goat IgG (H+L), Alexa Fluor® 488 following the same protocol. It was not possible to detect α -SMA in these slices (results not shown). Both primary and secondary antibodies were purchased shortly before conducting this protocol and supplier instructions regarding aliquoting, storage and concentration were followed, however a poor quality of the antibody cannot be disregarded.

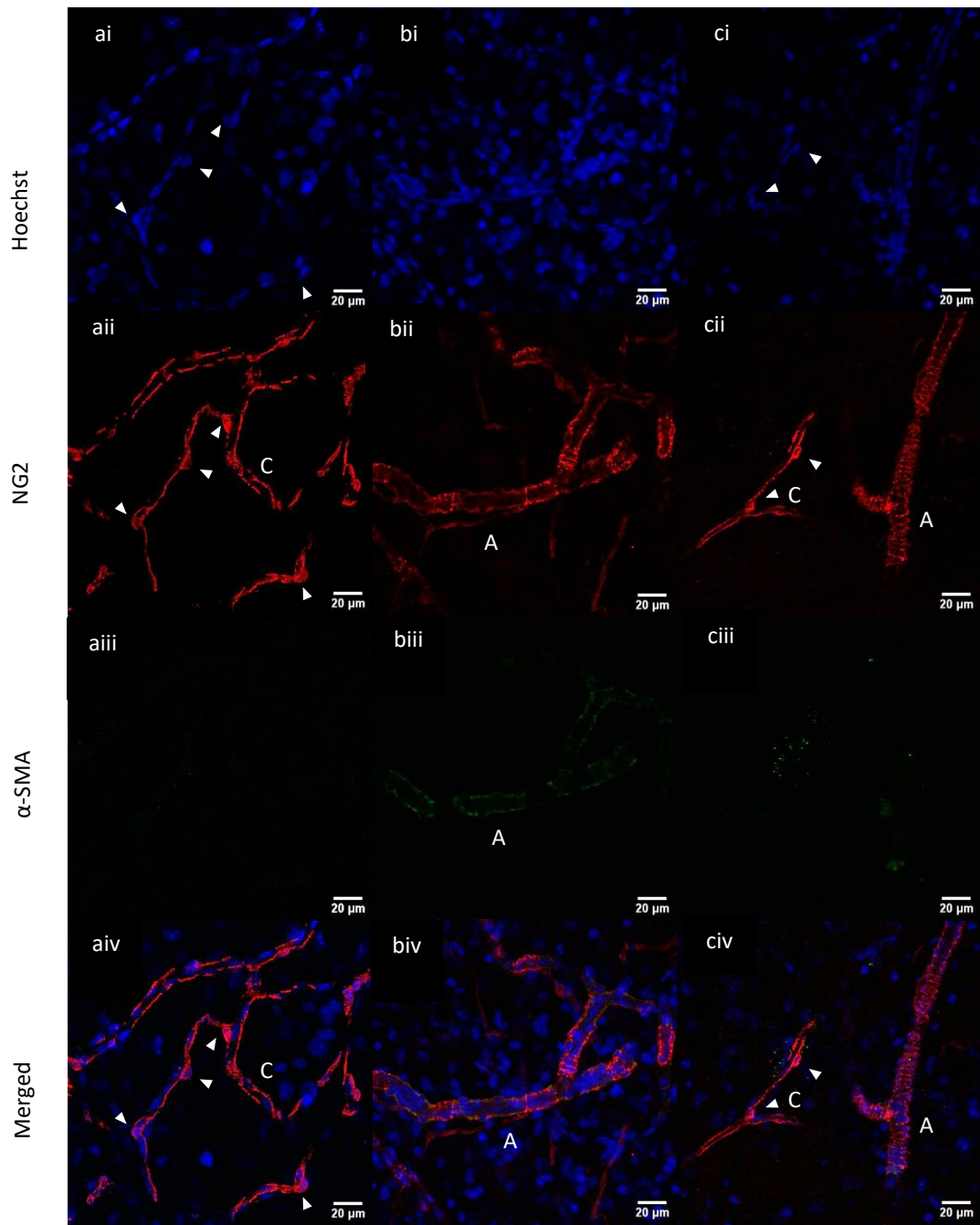


Figure 44 α -SMA/NG2/Hoechst immunohistochemical staining of the suburothelial microvasculature of the bladder) Pericytes in capillaries (C) and vascular smooth muscle cells in arterioles (A) were visualised by NG2-immunoreactivity (aii, bii and cii). Pericytes in capillaries present a typical 'bump-on-a-log' cell body (arrowheads) and bipolar processes and vascular smooth muscle cells are arranged circumferentially in arterioles. Nuclei of all cells were revealed by Hoechst staining (ai, bi, ci). α -SMA was not detected in capillary pericytes (aiii and ciii) and was detected in vascular smooth cells of some arterioles (biii) but not others (ciii). Detection of α -SMA was inconsistent and expression of α -SMA cannot be interpreted with confidence from the present study.

5.4. Discussion

The purpose of this study was to develop a viable full-thickness bladder tissue model to investigate suburothelial capillary properties and regulation *in situ*. Although it had been discussed the possibility to use porcine bladder tissue some difficulties were anticipated. These included the long distance from the closest abattoir to the laboratory in Medway School of Pharmacy (where functional experiments were conducted) and the need to section bladder tissue which due to its viscoelastic properties can be challenging and plausibly affect tissue viability. Mouse tissue, on the other hand, was possible to use in full-thickness. Keeping the tissue in full-thickness minimizes handling and potentially damaging effect of separation of mucosa from detrusor. Also, it might preserve the cellular communication that occurs within and between the different layers that constitute the bladder wall. Moreover, rodent models have been commonly used to investigate capillary regulation of blood flow. (Kawamura *et al.*, 2004; Peppiatt *et al.*, 2006; Fernandez-Klett *et al.*, 2010; Crawford *et al.*, 2012, 2013; Hall *et al.*, 2014; Hashitani *et al.*, 2015; Bertlich *et al.*, 2017; Canis *et al.*, 2017) C57BL/6J mice were used as this inbred strain is the most widely used in biomedical research (Bryant, 2011), and the first to have its genome sequenced, being a very commonly cited and well-characterized laboratory strain. Also, this mice strain had been used in our laboratory to characterise the microvasculature and pericyte function of the kidney (Lilley, 2019 unpublished work), which was compared with a well-established kidney slice model from rat. (Crawford *et al.*, 2012)

This model can, therefore, be useful to elucidate the role of pericytes in regulating capillary diameter in the lamina propria of the urinary bladder and to investigate the effect of vasoactive agents applied exogenously.

5.4.1. Tissue viability

To assess tissue viability co-staining with propidium iodide and Hoechst was employed. Propidium iodide binds to dsDNA but only penetrates dead cells, with compromised cell membrane, allowing their identification by red-fluorescent nuclear staining. On the other hand, Hoechst 3342 is permeant to all cells and stains the nucleus by emitting blue fluorescence when bound to dsDNA. (Ciancio *et al.*, 1988)

Cell viability was superior to 60% up to 5h from dissection. Tissue viability after 5 h was not investigated. Tissue samples from bladder were imaged with mucosa facing up in an upright fluorescent microscope and tissue viability here reported is likely to reflect viability at the surface area. Tissue viability of full-thickness bladder samples was superior to what was described for a mucosal preparation from mice (Krska, 2017). Similar tissue viability was reported for kidney slice preparations from rat (Crawford *et al.*, 2012), healthy rat kidneys (Dunn *et al.*, 2002) and brain slice preparations from rat (Peppiatt *et al.*, 2006). The present data indicate tissue is viable to conduct functional experiments.

5.4.2. DIC imaging and pericyte functional experiments

Diameter changes in capillaries were observed in response to vasoactive compounds applied exogenously. These changes were possible to measure off-line. In most cases, changes at pericyte sites were superior to changes at non-pericyte sites, suggesting pericytes are involved in the regulation of vessel diameter. Pericyte response to vasoactive compounds was observed both at branches sites and along the vessels and a difference in response rate was not established in this study. It is important to note that measurements at pericyte sites are performed where the cell body with a typical “bump-on-a-log” morphology is located. However, processes extend from the cell body along the vessel and those might contribute for some of the response measured at designated non-pericyte sites. Also, when applying exogenous compounds to the full thickness tissue, non-vascular smooth muscle tone can also be altered during imaging and affect vessel diameter to some extent. Using a micropipette to locally apply vasoactive compounds to the region surrounding the pericyte or directly into the lumen of the capillary could prevent extravascular events, however this might be practically challenging to achieve. Similar strategies have been previously described. (Pallone, 1994; Dunn *et al.*, 2002; Peppiatt *et al.*, 2006; Cai *et al.*, 2018) The response rate varied with vasoactive compound applied and concentration used. Overall, approximately 30% of the capillaries were responsive in the present model. The response rate for an established rat slice model was 51% (Crawford *et al.*, 2012). A recent adaptation of this kidney slice model to C57black/6J mice reported an overall response rate of 30-40% and varied from 14 to 67% depending on the agonist (Lilley, 2019 unpublished work). The

latter is comparable to the values in this study and suggests interspecies variation, with a lower response rate and magnitude of response on mice models. In addition, it was observed that in capillaries where more than one pericyte was present vessel diameter changes did not always occur in all pericytes. This observation suggests pericytes are functionally heterogeneous and is in line with what was described for pericytes localized in the microvasculature of kidney (Crawford *et al.*, 2012), retina (Kawamura *et al.*, 2004) and brain. Crawford *et al.*, 2012 have suggested that a simultaneous constriction of all pericytes would result in a severe vasoconstriction, potentially resulting in tissue hypoxia and subsequent detrimental effects. As such, pericytes are believed to regulate capillary diameter and mediate regional redistribution of blood flow with small adjustments to blood flow. (Crawford *et al.*, 2012)

Ang II 10 nM was ineffective in this murine bladder model, however it elicited a pericyte mediated vasoconstriction of 12 and 18% in mice (46% response rate) and rat kidney models, respectively. In isolated medullary vasa recta from rat kidney vasoconstriction of ~50% was described in response to Ang II 10 nM.(Pallone, 1994) This concentration of Ang II also elicited contraction of ~15% of pericytes monitored in isolated microvessels from rat retina (Kawamura *et al.*, 2004). On the other hand, Ang 100nM evoked a pericyte mediated constriction (~18%) in this model that was higher in magnitude than the effect measured in the murine kidney slice model (~10%) (Lilley, 2019 unpublished work). but lower than in the rat kidney slice model (~30%)(Crawford *et al.*, 2012). The response rate was equivalent to the murine kidney slice model for this concentration (37.5% in bladder and 35.7 % in kidney). A higher concentration, 300 nM, produced in average 30% of vasoconstriction in this bladder model, with a response rate of 41.2%. However, the magnitude of constriction evoked varied greatly and there was no statistical difference between pericyte and non-pericyte sites. This concentration has been shown to produce a ~14% pericyte mediated vasoconstriction in the murine kidney slice model, associated to 60% response rate. Ang II induced vasoconstriction was reversible with compound removal from the bath in the kidney models, but in the bladder model was reversible with Ang 100 nM II but not always with Ang II 300 nM. Moreover, reversible contractions were induced by Ang II 500 nM in ~34 % of pericytes with reduction of retina microvessel diameter of 54 %. (Kawamura *et al.*, 2004)

ET-1 10 nM elicited strong vasoconstriction (superior to 60% in 2 capillaries) in the present model. This was considerably higher than values reported for murine (30%) and rat (10%) kidney slice models (Crawford *et al.*, 2012). A lower concentration, 1nM, evoked a pericyte-mediated reduction in capillary diameter of 22% in this model, but fail to elicit a significant response in the murine kidney slice model. This data suggests an increased sensitivity of the microvasculature of the bladder to ET-1, plausibly with relevant differences in receptor expression. Vasoconstriction was long-lasting and not reversible for the duration of the experiment. This effect is well described for several vascular beds (Borges, Von Grafenstein and Knight, 1989; Bolger *et al.*, 1990; Crawford *et al.*, 2012) Pericytes in cell culture have also been shown to contract in response to ET-1 and express ET-1 receptors (Lee *et al.*, 1989; Neuhaus *et al.*, 2017)

NA 10nM evoked a pericyte-mediated capillary constriction of ~18% in the present model with a low response rate (~26%). A similar maximal constriction (~21%) was evoked in response to NA 10 nM in the rat kidney slice model (Crawford *et al.*, 2012).but this concentration had no effect in the murine kidney slice model (Lilley, 2019 unpublished work). In the latter, NA 30 nM, 100 nM and 300 nM were also tested but only a 300 nM concentration resulted vasoconstriction (~15%). NA (0.3–10 μ M) constricted pericytes on only 5% retinal capillaries from rat, whereas NA (1-2.5 μ M) constricted 50% of capillaries with ~60% diameter reduction in cerebellar slices from rat. (Peppiatt *et al.*, 2006) This data shows response to NA varies greatly depending on the capillary bed.

Vasoconstriction elicited by Ang II 100 nM (18%), ET-1 1nM (22%) and NA 10nM (18%) would increase blood flow resistance by approximately 2-2.5 fold, as predicted using Poiseuille's law, assuming laminar flow and absence of red blood cells (Landis, 1933; Hamilton, Attwell and Hall, 2010)

PGE₂ 10 μ M did not evoke a response in the capillaries tested. However this concentration has been shown to evoke a modest dilation, ~9% and 7%, in vasa recta capillaries of a murine (Lilley, 2019 unpublished work) and rat (Crawford *et al.*, 2012) kidney slice model. PGE₂ evoked a reversible pericyte-mediated dilation of 12% in 18% of the capillaries tested and a non-significant constriction (when compared to non-pericyte sites) of 13% in 18% of the capillaries. An involvement of non-vascular smooth

muscle contraction on this vasoconstriction is plausible. A higher concentration, 100 μM , did not evoke dilation in this model but elicited an 11% vasodilation in the murine kidney slice model (Lilley, 2019 unpublished work). However, in this bladder model vasoconstriction was observed in 67% of the capillaries but there was no statistical difference between diameter change at pericyte sites and non-pericyte sites. Non-vascular smooth muscle contraction appeared to be involved in part of the response, however it was noted that in some capillaries the response in pericyte sites was considerably higher than at non-pericyte sites. PGE_2 has been found to induce mostly vasodilation but in some cases vasoconstriction has been also documented (Haylor and Towers, 1982; Edwards, 1985; Inscho, Carmines and Navar, 1990; Imig, Breyer and Breyer, 2002; Van Rodijnen *et al.*, 2007; Attwell *et al.*, 2010; Murrant *et al.*, 2014). Heterogeneity in receptor expression may explain the distinct profile of responses. Also, it is important to note that the higher concentrations here used (30 and 100 μM) are above the EC_{50} and concentrations of PGE_2 that show a biological effect in bladder and other tissues (Choo and Mitchelson, 1977; Nakahata, Ono and Nakanishi, 1987; de Jongh *et al.*, 2007; Granato *et al.*, 2015) and are not expected *in vivo*, therefore the physiological relevance is questionable, therefore the physiological relevance is questionable. Indomethacin (30 and 100 μM) was applied to the bladder tissue to inhibit endogenous production of PGE_2 , however failed to produce diameter changes in most suburothelial capillaries. Only two capillaries exhibited a severe late constriction with indomethacin 100 μM , during the wash-out period. Whether that response resulted from a delayed effect of indomethacin inhibition of endogenous prostaglandins or from an increased release of endogenous prostaglandins (able to elicit vasoconstriction in suburothelial capillaries) with removal of indomethacin is inconclusive. Indomethacin 30 μM elicited a $\sim 14\%$ and $\sim 10\%$ reversible pericyte mediated constriction in the vasa recta in murine and rat kidney slice models, respectively. (Crawford *et al.*, 2012)

Overall, this data suggests pericytes residing in the suburothelial capillaries of the bladder are contractile and act to regulate vessel diameter in response to several vasoactive compounds. This is in line with observations in other organ tissues that evidence pericyte regulation of capillary diameter (Peppiatt *et al.*, 2006; Fernandez-Klett *et al.*, 2010; Crawford *et al.*, 2012; Hall *et al.*, 2014). Also, this data poses against the

argument that pericytes in capillaries of the bladder are not contractile, based on immunohistochemical studies that fail to detect α -SMA in these cells. (Mitsui and Hashitani, 2013; Hashitani *et al.*, 2018)

5.4.3. α -SMA and NG2 immunoreactivity of perivascular cells

It was possible to visualize pericytes and vascular smooth muscle cells, residing in capillaries and arterioles respectively, by their NG2-immunoreactivity. Morphological features were similar to what was previously described for bladder tissue (Mitsui and Hashitani, 2013; Hashitani *et al.*, 2018). Detection of α -SMA was inconsistent in the present study. Given these results, kidney slices from C57black/6J mice, obtained following an established protocol (Lilley, unpublished work), were also incubated with goat polyclonal anti- α -SMA and donkey anti-goat IgG (H+L), Alexa Fluor® 488 following the same protocol. It was not possible to detect α -SMA in these slices (results not shown). Both primary and secondary antibodies were purchased shortly before conducting this protocol and supplier instructions regarding aliquoting, storage and concentration were followed, however a poor quality of the antibody cannot be disregarded. Poor sensitivity of primary antibody or depolymerization of α -SMA might justify these results. (Alarcon-Martinez *et al.*, 2018) Most studies use mouse monoclonal antibody for α -smooth muscle actin (Mitsui and Hashitani, 2013; Alarcon-Martinez *et al.*, 2018) but that option was not considered to avoid non-specific binding. Further optimization of the protocol was not possible due to time constraints. However, it was recognised as an important line of future work to clarify expression pattern of α -SMA in bladder microvasculature. Using ice-cold methanol as a fixative to reduce depolymerization of α -SMA (Alarcon-Martinez *et al.*, 2018) and/or changing primary antibody might improve detection.

5.5. Conclusions

An *ex-vivo* bladder tissue model from mice to investigate blood flow regulation through capillaries was developed. Cell viability was superior to 60% up to 5h from dissection, suggesting that tissue was viable to conduct functional experiments during that time frame. DIC images of *ex-vivo* bladder tissue samples were obtained for experiments in which tissue was stimulated with vasoactive agents applied exogenously (angiotensin II, endothelin-1, noradrenaline, prostaglandin E2 and indomethacin) and pericyte-mediated changes of capillary diameter were observed in approximately 30% of the capillaries investigated. Therefore, this study evidences that suburothelial capillary pericytes in the bladder act to modulate capillary diameter in response to vasoactive agents previously reported to regulate capillary beds of other organs (Crawford *et al.*, 2012). The current model can be further used to study the effect of potential therapeutic or noxious compounds in the microvasculature. As such, using the present model the effect of ketamine in the microvasculature will be investigated in chapter 6 to help elucidate the pathological mechanism leading to KIC.

Chapter 6 – Ketamine effect in microvasculature

6.1 Introduction

6.1.1. Pharmacodynamics of ketamine

Ketamine is a non-competitive N-Methyl-D-Aspartate receptor (NMDAR) antagonist, which inhibits the receptor with concentrations from 2 to 50 μM . (Mion and Villevieille, 2013) Analgesic and anaesthetic, as well as antidepressant and psychotomimetic actions, are thought to be primarily mediated via NMDAR inhibition. However, ketamine interacts with various other binding sites. These include dopamine, serotonin, opioid and cholinergic receptors as well as sodium, potassium, L-type calcium and hyperpolarization-activated cyclic nucleotide-gated (HCN) channels. Nevertheless, ketamine has a lower affinity for these receptors than for NMDARs and their role *in vivo* is poorly understood. (Mion and Villevieille, 2013; Zanos et al., 2018)

6.1.1.1 NMDA receptor

NMDAR is widely present on the CNS, particularly in structures of nociception. (Mion and Villevieille, 2013) All NMDAR subunits have been identified in the male human and rat urinary bladder. (Gonzalez-Cadavid *et al.*, 2000) NR1 (NMDAR subunit) is expressed in the vascular endothelium of microvessels residing in the lamina propria of the human urinary bladder (Lin *et al.*, 2016), however NMDAR it is not expressed in the bladder urothelium (Baker *et al.*, 2016).

NMDAR is an ionotropic (*i.e.* ligand-gated ion channel) glutamate receptor permeable particularly to calcium, but also involved in the exchange of sodium and potassium. This receptor is a heteromeric multimer assembled by different arrangements of subunits (NR1, NR2A–D and NR3A and B). Commonly, NMDARs have a tetrameric structure. composed by two dimeric subunits of NR1 and NR2A or NR2B. Other combinations of two NR1 subunits and NR2C, NR2D, NR3A, or NR3B have also been reported. (LeMaistre *et al.*, 2012; Mion and Villevieille, 2013; Zanos *et al.*, 2018)

The activation of NMDAR is complex, involving various agonists interacting in cooperation and regulatory mechanisms (Figure 45). Glutamate and NMDA bind to the agonist binding domain of the GluN2 subunit. Glycine and D-serine bind to a glycine modulatory site on GluN1 subunit of the NMDA receptors. Glycine or D-serine and

glutamate are considered co-agonists of NMDAR, as simultaneous binding of one molecule of glycine or D-serine and one molecule of glutamate are needed for NMDAR activation, resulting in opening of the channel. However, magnesium (Mg^{2+}) blocks NMDAR in a voltage sensitive manner. At the resting membrane potential, Mg^{2+} blocks these channels tonically. Membrane depolarization and co-agonist activation are required for displacing Mg^{2+} and opening the channel. Phencyclidine (PCP), ketamine and dizocilpine are NMDAR antagonists that bind to the PCP binding site located within the channel pore of the NMDAR. (Mion and Villevieille, 2013; Zanos *et al.*, 2018)

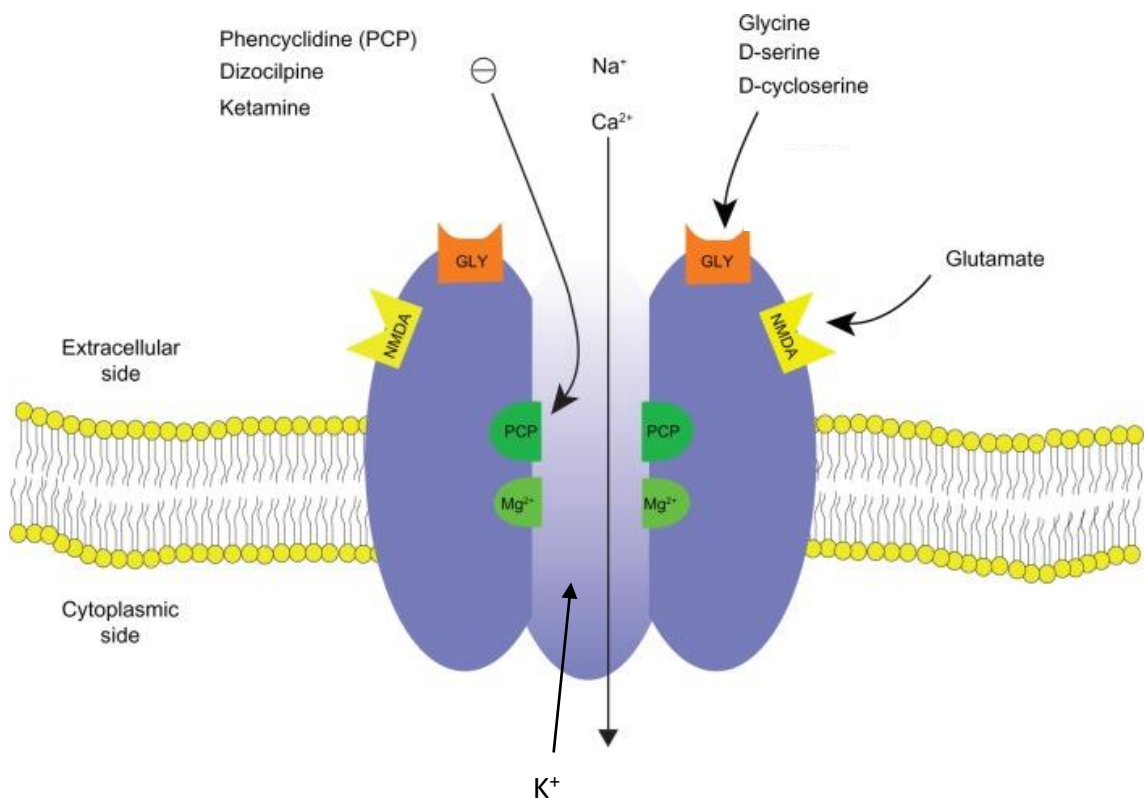


Figure 45 NMDA receptor The N-methyl-D-aspartate receptor (NMDAR) is a glutamate ionotropic receptor. Glutamate and NMDA interact with the agonist site on the NMDA receptors whereas glycine and D-serine bind to a glycine agonist binding site on the NMDA receptors. At a resting state, NMDAR is blocked by magnesium (Mg^{2+}) in a voltage-sensitive way. Co-activation by glutamate and glycine and/or D-serine and membrane depolarization are required to displace Mg^{2+} and open the channel. Upon NMDAR channel opening, calcium (Ca^{2+}) and sodium (Na^+) enter the cell whereas potassium (K^+) exits the cell. Phencyclidine (PCP), ketamine and dizocilpine bind to the PCP receptor in the inside of the NMDA receptors, blocking the channel in a non-competitive way. The symbol (-) represents inhibitory effect. glutamate receptor and nonselective cation channel with many ligands. (Li *et al.*, 2011)

6.1.1.2. Ketamine effect on vascular reactivity or tone

Ketamine administration has been reported to increase cardiac output, arterial blood pressure and heart rate. These effects are believed to be a consequence of direct stimulation of the central nervous system and subsequent increment of sympathetic nervous system outflow. Moreover, it has been suggested that inhibition of catecholamines (e.g. noradrenaline) uptake into postganglionic sympathetic nerve endings, depression of baroreceptor reflex activity, and adrenocortical stimulation also play a role. (Lundy and Frew, 1981; Akata, Izumi and Nakashima, 2001)

Nonetheless, in several *in vitro* and *in situ* studies ketamine has been shown to affect vasoconstrictor and vasodilator responses to pharmacologic stimuli. Ketamine enhances or attenuates these responses, depending on the blood vessel and vascular bed, animal species used, concentrations employed or experimental setup – e.g. the presence or absence of endothelium. (Akata, 2007)

Most experiments are conducted on isolated arteries or veins and show a direct effect on vascular smooth muscle cells (VSMC) and/or endothelial cells. Vascular smooth muscle contraction induced by various vasoactive agents (e.g. histamine, noradrenaline and K^+) can be inhibited in presence of ketamine using concentrations superior to those used in clinical practice ($\geq 100 \mu M$) (Kanmura, Yoshitake and Casteels, 1989; Kang *et al.*, 1990; Chung *et al.*, 1992; Ratz, Callahan and Lattanzio, 1993; Kanmur *et al.*, 1993; Abdalla, Laravuso and Will, 1994; Yamazaki *et al.*, 1995; Akata, Izumi and Nakashima, 2001; Ding, Damron and Murray, 2005; Klockgether-Radke *et al.*, 2005; Ibeawuchi, Ajayi and Ebeigbe, 2008; Jung and Jung, 2012) or potentiated with concentrations within the clinical range (Lundy and Frew, 1981; Fukuda, Su and Lee, 1986; Akata, Izumi and Nakashima, 2001; Klockgether-Radke *et al.*, 2005; Park *et al.*, 2016). Vasodilatory action is endothelium-independent and has been associated to a reduction of intracellular Ca^{2+} , resulting from decreased transmembrane Ca^{2+} influx through L-type Ca^{2+} channels and Ca^{2+} release from the internal stores of smooth muscle. (Yamazaki *et al.*, 1992; Ratz, Callahan and Lattanzio, 1993; Kanmura, Missiaen and Casteels, 1996; Akata, Izumi and Nakashima, 2001) Furthermore, it has been suggested that arterial vasodilation elicited by ketamine is NMDAR-independent, although the binding site remains unclear. Possible alternative targets are ion channels and G-protein-coupled receptors (GPCRs) (Noh *et*

al., 2009). In contrast, potentiation of vasoconstriction has been related with inhibition of extraneuronal uptake of catecholamines (Lundy and Frew, 1981) and facilitation of 5-HT_{2A} receptors. (Park *et al.*, 2016) On the other hand, ketamine attenuates induced relaxation by other vasoactive agents (Ogawa, Tanaka and Murray, 2001; Dojo *et al.*, 2002; Sohn and Murray, 2003). The mechanism involves inhibition of both the NO and endothelium-derived hyperpolarizing factors (EDHF) components of the vasodilatory response and reduction in endothelial [Ca²⁺]_i (Ogawa, Tanaka and Murray, 2001) and inhibition of K⁺_{ATP} channel activation in an endothelium-independent manner. (Sohn and Murray, 2003)

The effect of ketamine on microvascular reactivity or tone has been less studied. Asher *et al.* demonstrated that the vasoconstrictor effect of 5-HT in rat first-order cremasteric arterioles was enhanced when the animals were anaesthetized with ketamine. Also, third-order arterioles dilation evoked by 5-HT was attenuated in the presence of ketamine. (Asher *et al.*, 1992) On the other hand, the vasoconstrictor response to haemorrhage in rats was attenuated in cremasteric arterioles during ketamine-induced anaesthesia (Longnecker, Ross and Silver, 1982). Uhl and colleagues have shown a 73-83% reduction of baseline values in microvascular perfusion in mice ears skin after anaesthesia induced by ketamine. (Uhl *et al.*, 1994) In addition, Brookes *et al.* demonstrated changes evoked by ketamine in skeletal muscle microcirculation of normotensive and hypertensive rats, with reduction in diameter of arterioles and venules during maintenance of anaesthesia. (Brookes, Reilly and Brown, 2004)

6.1.2. Hypotheses and aims

It was hypothesised that ketamine can evoke microvascular changes in the bladder plausibly leading to, or contributing to, the unfavourable outcomes of ketamine-induced cystitis. The aims of the present section of work were to study ketamine effects on capillary diameter, pericyte morphology and density and further investigate if the ketamine effect in the microvasculature is NMDAR dependent. In this context, using the murine live bladder tissue model discussed in chapter 5, the key objectives were:

1. Assess if ketamine elicits pericyte-mediated changes in diameter of bladder capillaries during acute exposure.

2. Investigate if NMDAR agonists (glycine and L-glutamate) evoke pericyte-mediated changes in diameter of bladder capillaries. If an agonistic effect is observed, investigate if this effect is inhibited in presence of ketamine (NMDAR antagonist).
3. Study the effect of a longer exposure of bladder tissue to ketamine on capillary diameter, pericyte morphology and density.

6.2. Methods

6.2.1. Tissue preparation

Tissue was prepared as described in 2.2.1. Tissue preparation.

6.2.2. DIC imaging and pericyte functional experiments

DIC imaging and pericyte functional experiments were conducted as described in 2.2.3. DIC imaging and functional experiments.

For this chapter the following agents were used: Ketamine (10 µg/mL [\sim 36.47 µM], 30 µg/mL [\sim 109.42 µM] and 100 µg/mL [364.72 µM]), glycine (10 µM and 1mM) and L-glutamate (10 µM and 1mM).

6.2.3 NG2/GS-IB4 co-staining

Immunohistochemical staining to identify pericytes immunoreactive to NG2 and microvasculature was performed as described in 2.2.4.2 NG2/GS-IB4 co-staining.

6.2.4 Statistical analysis

Statistical difference of diameter changes at pericyte and non-pericyte sites in responsive capillaries were calculated with paired *t*-tests for each concentration of drug, as described in 5.2.5. Statistical analysis. Mean pericyte density (number of perivascular NG2⁺ cells / 10,000 µm²), number of pericytes along 100 µm of capillary, distance between pericyte cell bodies, height and width of pericyte cell body and length of processes along the capillaries after treatment with Krebs buffer or ketamine (10 µg/mL, 30 µg/mL or 100 µg/mL) were compared using repeated measures one-way ANOVA. Values of $p < 0.05$ were considered statistically significant. This test was selected as measurements are made under different conditions (treatments) for each bladder. This means that for each bladder four samples were obtained and exposed to one of the treatments with Krebs buffer or ketamine (10 µg/mL, 30 µg/mL or 100 µg/mL) each. This can increase the power of the test to detect significant differences between means. Normality was not determined, considering the small sample size, however normal distribution was assumed in agreement to observations of previous studies. (Crawford *et al.*, 2012; Hashitani *et al.*, 2018)

6.3. Results

6.3.1. Functional experiments

6.3.1.1. Ketamine

The effect of ketamine hydrochloride (KH; 10, 30 and 100 $\mu\text{g}/\text{mL}$) in the suburothelial capillaries of the bladder was investigated using the model described in chapter 5. Table 9 summarizes main data from DIC functional experiments where tissue was exposed to KH. KH 10 $\mu\text{g}/\text{mL}$ showed no effect in the diameter of 10 capillaries ($n = 10$ animals) tested. KH 30 $\mu\text{g}/\text{mL}$ evoked a pericyte mediated constriction of $15.6 \pm 2.3\%$ (from a resting diameter of $4.84 \pm 0.19 \mu\text{m}$) in 8 of 26 capillaries tested ($n = 26$ animals), which was significantly greater than at non-pericyte sites ($4.0 \pm 1.73\%$, from an initial diameter of $5.3 \pm 0.29 \mu\text{m}$), $p < 0.05$, determined with a paired t -test. Dilation was only observed once and it was unclear whether it occurred at a pericyte site (Figure 46). Interestingly, constriction was observed in a pericyte site in the same capillary. KH 100 $\mu\text{g}/\text{mL}$ induced a vasoconstriction at pericyte sites of $27.1 \pm 7.2\%$ (from a resting diameter of $3.95 \pm 0.27 \mu\text{m}$) in 6 of 15 capillaries tested ($n=15$ animals), which was significantly greater than at non-pericyte sites ($5.3 \pm 1.8\%$, from an initial diameter $4.82 \pm 0.35 \mu\text{m}$), $p < 0.05$. Time to induce vasoconstriction and maximum constriction was not statistically different between tissue exposed to KH 30 and 100 $\mu\text{g}/\text{mL}$. However, response rate was superior using KH 100 $\mu\text{g}/\text{mL}$ (40%) than 30 $\mu\text{g}/\text{mL}$ (30.8%). Vasoconstriction evoked by these concentrations of KH was not reversible in most responsive capillaries.

Table 9 Summary of main findings from DIC experiments to study capillary functional responses to ketamine (KH; 10 µg/mL, 100 µg/mL and 300 µg/mL) . Response rate and mean values ± SEM of time to induce (t_{ind}) vasoconstriction, time to maximum (t_{max}) constriction from addition of KH, % of maximum (max) constriction at pericyte site and non-pericyte, and % change from baseline (%Δ vessel diameter) at the end of the video are provided. No response was observed for capillaries exposed to KH 10 µg/mL. Higher concentrations of KH (30 and 100 µg/mL) produced a non-reversible vasoconstriction that was greater at pericyte-sites than at non pericyte-sites. t_{ind} constriction and % max constriction were not statistically different between KH 30 and 100 µg/mL, however t_{max} constriction was superior for the higher concentration. Response rate was superior for tissue exposed to KH 100 µg/mL (40%) than to KH 30 µg/mL. [KH] – ketamine concentration.

[KH]	Response rate	t_{ind} constriction n	t_{max} constriction n	% max constriction pericyte sites	% max constriction non-pericyte sites	%Δ vessel diameter at the end of video
10 µg/mL	0/10 (0%)	-	-	-	-	-
30 µg/mL	8/26 (30.8%)	161 ± 48 s	455 ± 67 s	15.6 ± 2.3 %	4.0 ± 1.73%	-13.6 ± 2.0%
100 µg/mL	6/15 (40%)	191 ± 68 s	716 ± 38 s	27.1 ± 7.2 %	5.3 ± 1.8%	-24.8 ± 7.2%

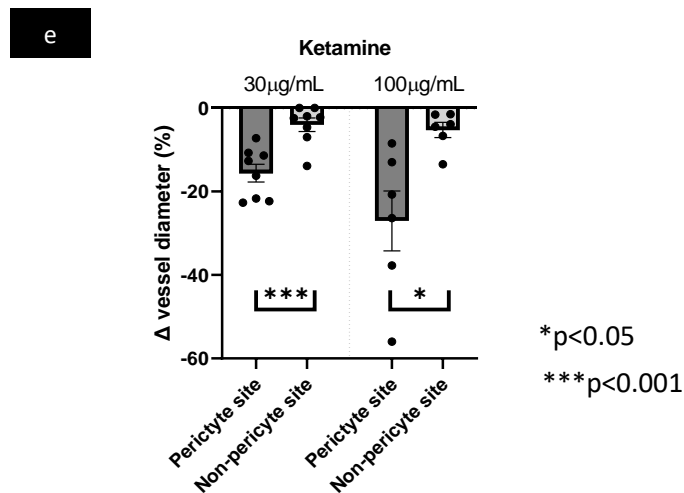
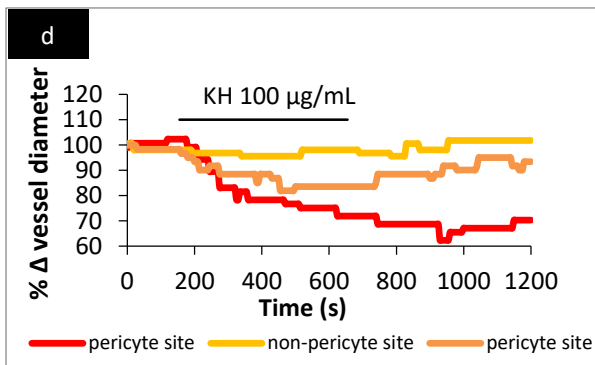
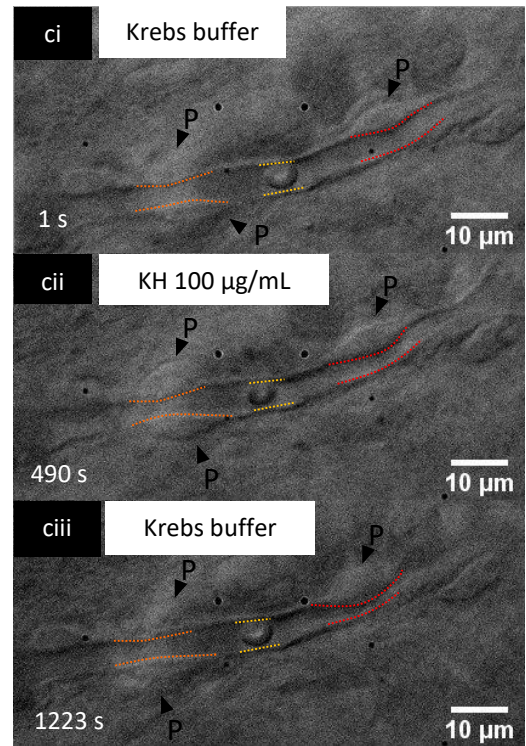
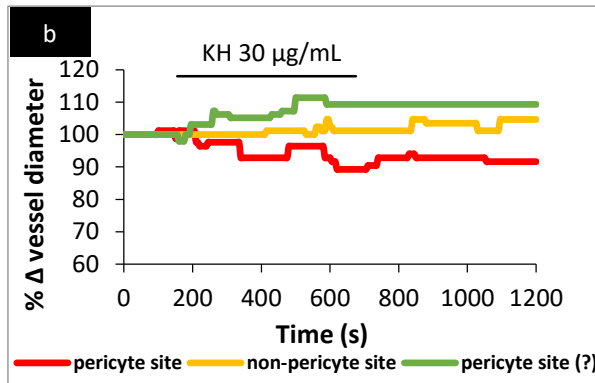
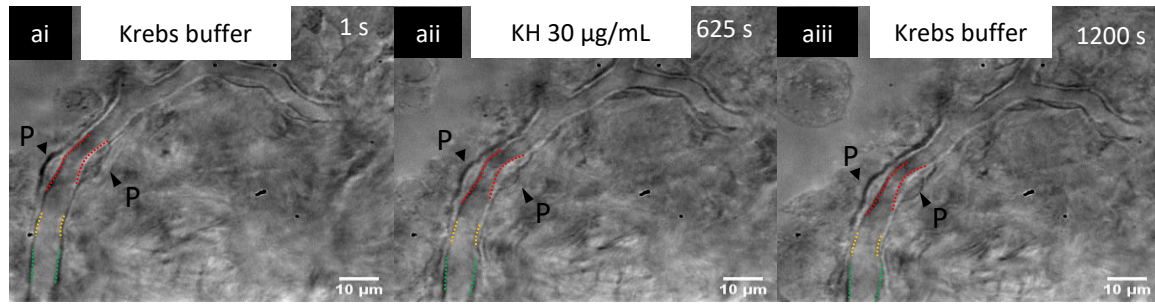


Figure 46 Functional experiments – Ketamine (KH) DIC images taken from a time series experiment showing pericyte-mediated diameter changes of *in situ* bladder capillaries following exposure of tissue to KH 30 µg/mL (a) and 100 µg/mL (c). Pericytes are located on the abluminal side of the capillaries (arrowheads) (a): Red, yellow and green dotted lines highlight the areas where capillary diameter was measured at pericyte, non-pericyte and undetermined sites, respectively. Tissue was superfused with Krebs buffer (ai), followed by KH 30 µg/mL (aii) which evoked constriction (red) and dilation (green). KH

evoked changes in vessel diameter that were not reversible (aiii). Traces (b) of % change in capillary diameter at a pericyte site (red trace), non-pericyte site (yellow trace) and undetermined site (green trace) are shown for tissue exposed to KH. Dilation was not a common occurrence and was only observed in this experiment, whereas vasoconstriction was observed in 30.8% of capillaries tested with KH 30 $\mu\text{g}/\text{mL}$. (c): Red and orange dotted lines highlight the areas where capillary diameter was measured at pericyte sites and yellow at a non-pericyte site. Tissue was superfused with Krebs buffer (ci), followed by KH 100 $\mu\text{g}/\text{mL}$ (cii) which evoked constriction. KH evoked changes in vessel diameter that were reversible and not reversible at different pericytes (aiii - orange trace and red trace respectively). Overall, maximum vasoconstriction was not reversible. A representative trace (d) of % change in capillary diameter at two pericyte sites (red and orange traces) and non-pericyte site (yellow trace) is shown for tissue exposed to KH. Mean ($\pm\text{SEM}$) and individual data (dots) for maximum vasoconstriction (% change from baseline) in these experiments are shown in (e). In responsive capillaries, KH 30 $\mu\text{g}/\text{mL}$ (n=8) and 100 $\mu\text{g}/\text{mL}$ (n=6) evoked a significantly greater vasoconstriction at pericyte sites compared with non-pericyte sites (e) $p<0.05$. Vasoconstriction elicited by KH 30 $\mu\text{g}/\text{mL}$ and 100 $\mu\text{g}/\text{mL}$ was not statistically different.

6.3.1.2. L-glutamate

The effect of L-glutamate (GLU; 10 μM and 1 mM) in the suburothelial capillaries of the bladder was assessed in time series experiments. GLU 10 μM evoked a dilation ($\sim 8\%$) in one of 14 capillaries tested (n=9 animals). GLU 1mM evoked a dilation in 1 of 6 capillaries tested (n = 6 mice). No statistical analysis was performed considering the limited response rate.

6.3.1.3. Glycine

The effect of glycine (GLY; 10 μM and 1 mM) in the suburothelial capillaries of the bladder was assessed in time series experiments. GLY 10 μM did not elicit a response in 4 capillaries tested (n=4 animals). GLY 1mM evoked a dilation (Figure 47) in 2 of 17 capillaries tested (n = 12 mice). No statistical analysis was performed considering the limited response rate.

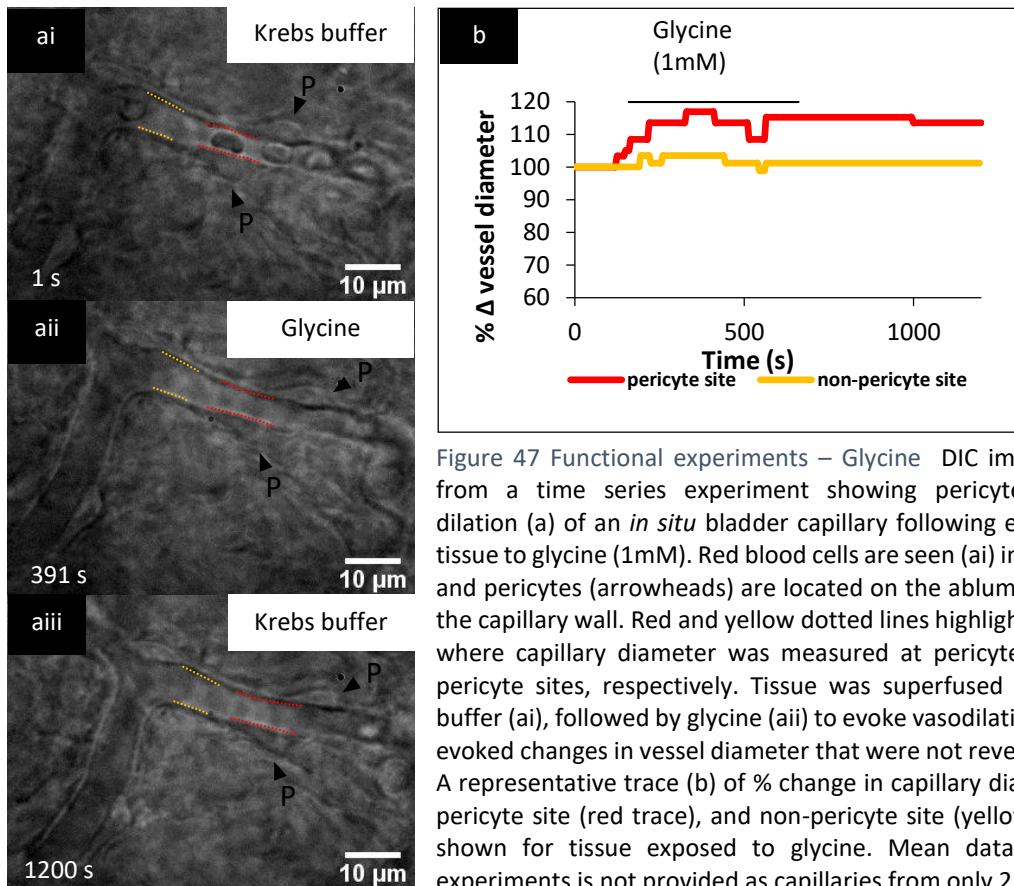


Figure 47 Functional experiments – Glycine DIC images taken from a time series experiment showing pericyte-mediated dilation (a) of an *in situ* bladder capillary following exposure of tissue to glycine (1mM). Red blood cells are seen (ai) in the lumen and pericytes (arrowheads) are located on the abluminal side of the capillary wall. Red and yellow dotted lines highlight the areas where capillary diameter was measured at pericyte and non-pericyte sites, respectively. Tissue was superfused with Krebs buffer (ai), followed by glycine (a_{ii}) to evoke vasodilation. Glycine evoked changes in vessel diameter that were not reversible (a_{iii}). A representative trace (b) of % change in capillary diameter at a pericyte site (red trace), and non-pericyte site (yellow trace), is shown for tissue exposed to glycine. Mean data for these experiments is not provided as capillaries from only 2 samples of bladder tissue were responsive (out of 17 samples of bladder imaged [n=12 mice]).

6.3.1.3. Glycine and L-glutamate

A potential synergistic effect of glycine (GLY, 1 mM) and L-glutamate (GLU, 1 mM) in the suburothelial capillaries of the bladder was investigated in time series experiments. When applied together, GLY (1 mM) and GLU (1 mM) elicited no effect in 6 capillaries tested (n=6 animals).

6.3.2 Immunohistochemical features (NG2/IB4)

Lamina propria preparations labelled with Alexa-488-conjugated IB4 and anti-NG2 (probed with Alexa 555 secondary antibody) allowed identification of capillaries and pericytes residing in the capillary network (Figure 48). In preliminary work it was observed that urothelial cells of the mouse bladder are strongly stained by GS-IB4 conjugated with Alexa Fluor® 488 (Figure 43), reason why urothelium was removed from tissue preparations in following work.

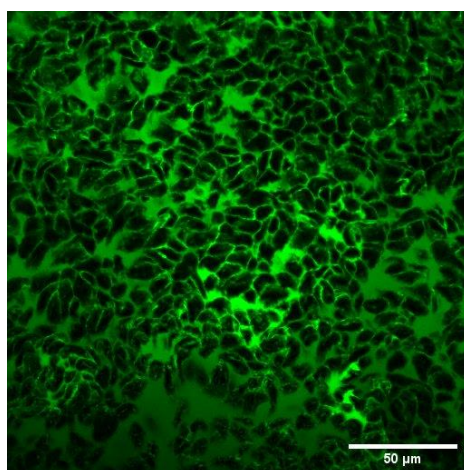


Figure 48 Confocal image of a mouse bladder mucosa preparation (where urothelium was not removed) stained with GS-IB4 conjugated with Alexa Fluor® 488. Urothelial cells can be easily identified in this mucosal preparation however, prevents appropriate detection of suburothelial microvasculature.

It was observed that morphologically NG2⁺ pericyte cells laying in the suburothelial capillaries of the murine bladder have a typical bump-on-a-log appearance, with an oval cell body and processes running along the capillaries. Pericytes can be found at branch sites (Figure .49 f) and between branch sites along the capillary (Figure 49 e).

Lamina propria preparations were incubated for 4 h with Krebs buffer, KH 10 μg/mL, 30 μg/mL and 100 μg/mL to investigate microvascular changes evoked by KH. Pericyte density (Figure 50 a) was not statistically different ($p > 0.05$) between treatments, with a mean of 3 to 4 pericytes per 10 000 μm². Distance between pericytes (Figure 50 b) was roughly 30 μm for all treatments, no statistical difference was observed ($p > 0.05$). Capillary diameter at pericyte sites and non-pericyte sites was not statistically different (for each treatment and between treatments, with values varying in average between 4.04 and 4.46 μm (Figure 50 c). Regarding pericyte morphology, cell body width (Figure

50 e) was not statistically different ($p > 0.05$) between treatments and varied in average between 9.66 and 10.64 μm . Also, pericyte cell body height (Figure 50 d) was not statistically different ($p > 0.05$) between treatments and varied in average between 4.20 and 4.82. The length of processes along vessels (Figure 50 f) was not statistically different ($p > 0.05$) amongst treatments, with averages varying between 19.00 and 21.42 μm . Please note that was often difficult to perceive where a process of a pericyte ended when in close contact with a process of another pericyte.

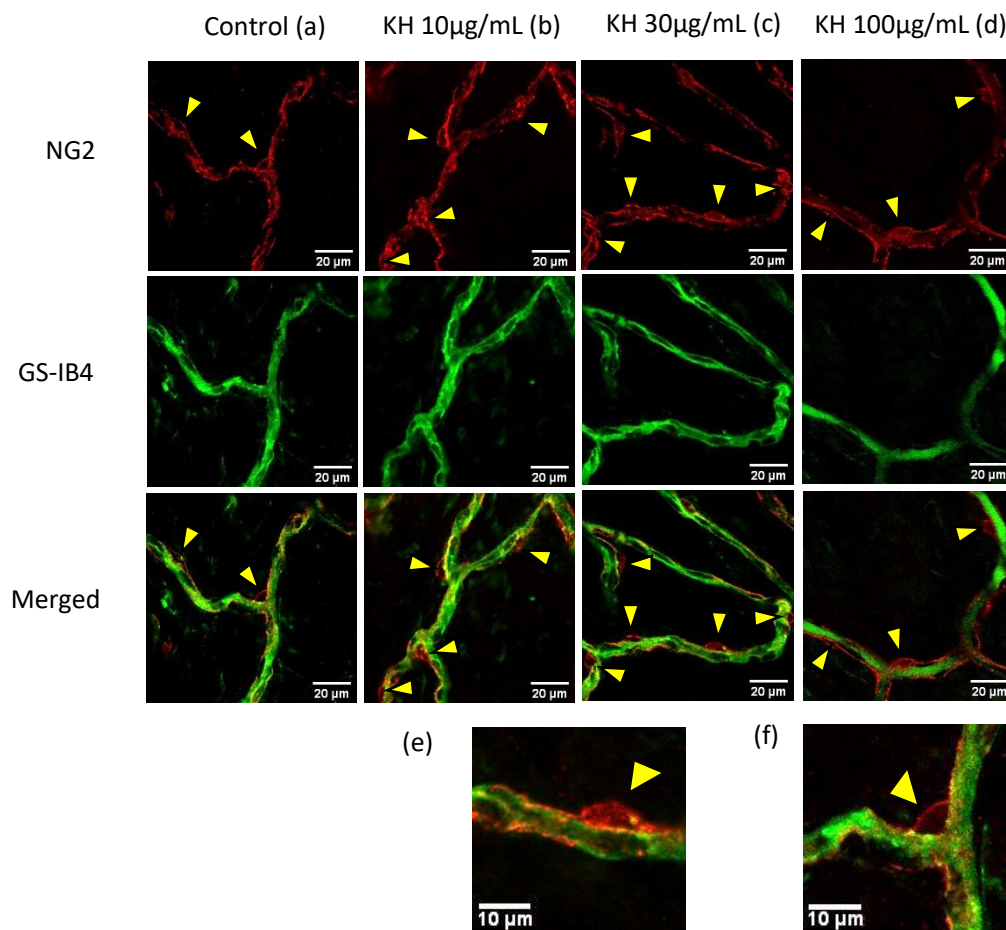


Figure 49 Representative confocal images of the capillary network in the lamina propria of the bladder after incubation for 4 h with Krebs buffer (a), KH 10 $\mu\text{g}/\text{mL}$ (b), 30 $\mu\text{g}/\text{mL}$ (c) and 100 $\mu\text{g}/\text{mL}$ (d). Bladder tissue samples were labelled with Alexa-488-conjugated IB₄ and anti-NG₂ (probed with Alexa 555 secondary antibody) to identify capillaries (green) and pericytes (red), respectively. Pericyte cell bodies (arrowheads) are located on the abluminal side of the capillary at branch places (e) and along capillaries (f). Processes extend from the cell body to run along the capillary.

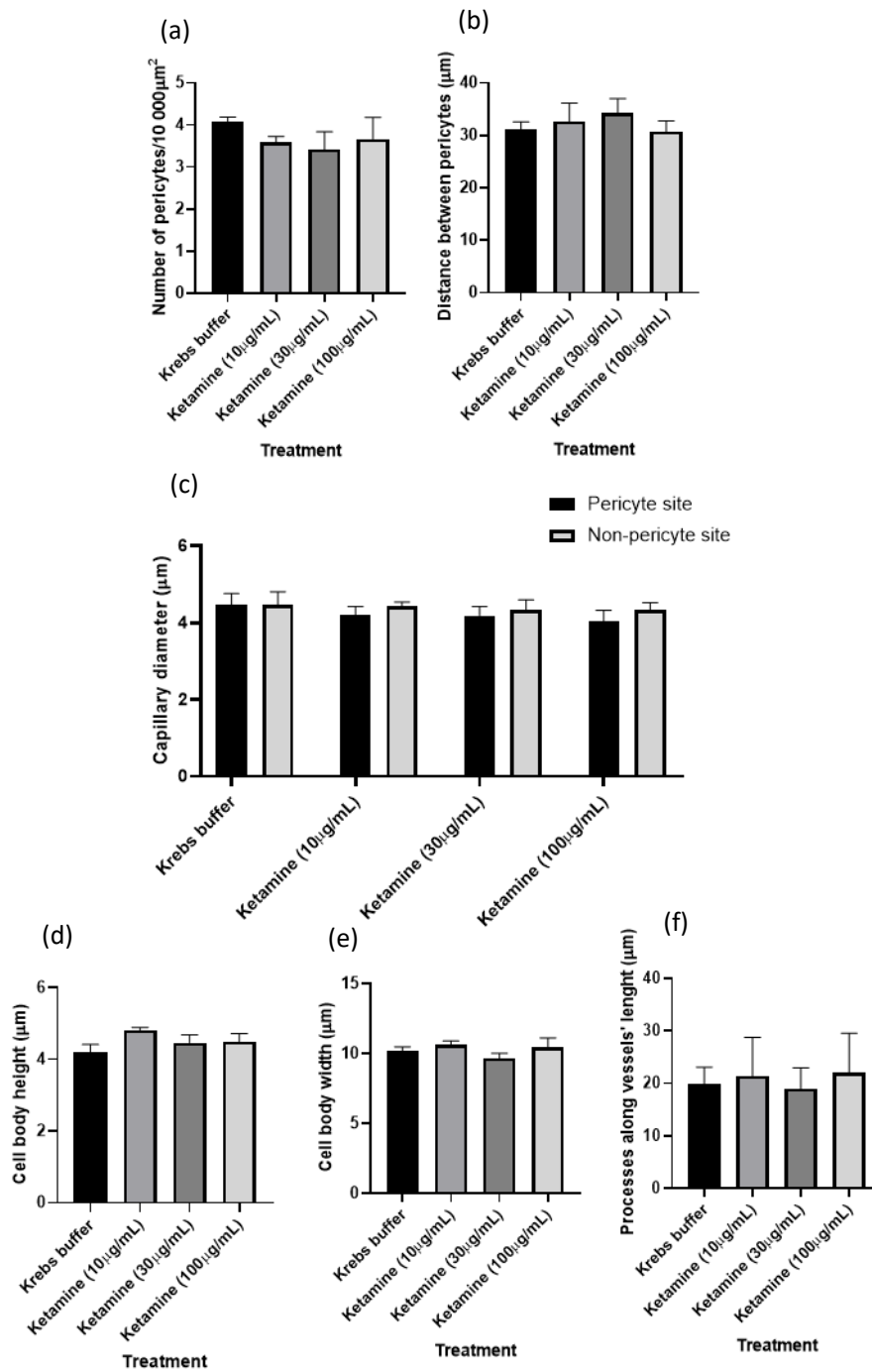


Figure 50 Pericyte density (number of pericytes/10 000 µm², a), distance between pericytes (b), capillary diameter at pericyte sites (c) and non-pericyte sites (d) and pericyte morphology (cell body height, e), width, f) and processes along vessel's length (g) after incubation for 4 h with Krebs buffer, KH 10 µg/mL, 30 µg/mL and 100 µg/mL. No statistical differences were observed in pericyte density (number of pericytes/10 000 µm², a), distance between pericytes (b), capillary diameter at pericyte sites and non-pericyte sites (c), cell and height (d) body width (e) and processes along vessel's length (f) (p > 0.05 per treatment).

6.4 Discussion

This section of work aimed to understand the effect of KH on the microvasculature of the bladder, using the live murine bladder tissue model described in chapter 5.

6.4.1. DIC imaging and pericyte functional experiments

To investigate if ketamine evokes pericyte-mediated changes in diameter during acute exposure, functional experiments were conducted as previously described in chapter 5.

Three concentrations were used - 10 µg/mL (~36.47 µM), 30 µg/mL (~109.42 µM) and 100 µg/mL (364.72 µM). Clinically relevant plasmatic concentrations of ketamine are usually below 100 µM (Domino *et al.*, 1982). Higher circulatory concentrations are expectable following recreational use of ketamine, associated with higher doses. (Wood *et al.*, 2011) Moreover, as discussed in chapter 4, ketamine accumulated in urine can penetrate into the bladder wall and achieve approximately a concentration of 10 µg/mL (estimated for a ketamine dose of 1 g) in the lamina propria, where the capillary network resides.

KH 10 µg/mL had no effect on the suburothelial capillaries, whereas KH 30 µg/mL and KH 100 µg/mL elicited a pericyte-mediated constriction. Vasoconstriction evoked by KH (~15-30%) could result in reduction of flow by approximately 50-70%, as predicted using Poiseuille's law, assuming laminar flow and absence of red blood cells (Landis, 1933; Hamilton, Attwell and Hall, 2010) This reduction in blood flow to bladder tissue might be linked to the unfavourable bladder outcome associated with abuse of ketamine. For these experiments, capillaries were not pre-constricted or dilated and the effect of ketamine alone on the basal diameter of capillaries was investigated. Ketamine alone had no effect on the basal tone of arteries (Lundy and Frew, 1981; Ogawa, Tanaka and Murray, 2001; Ding, Damron and Murray, 2005) or slightly reduced basal tension (Jung and Jung, 2012) in other studies.

As previously described, ketamine is a non-competitive antagonist of NMDAR and its analgesic and anaesthetic effects are mediated through this receptor. (Peltoniemi *et al.*, 2016). To investigate whether the vasoconstrictor response observed was mediated via NMDAR, L-glutamate and glycine were applied exogenously to the tissue alone or in association.

Endogenous concentrations of glutamate depend on the biological compartment, with plasmatic concentrations around 150 μM and concentration in the synaptic cleft following neuronal release superior to 1mM for less than 10 ms and, subsequently, less than 20 nM. Moreover, tonic basal concentration within the extracellular space varies between 0.02 and 30 μM (Moussawi *et al.*, 2011) In the present study, exogenous concentration of 10 μM and 1mM were used, however capillaries exhibited a low response rate to both concentrations. Capillary response appears to depend on the vascular bed. Peppiatt *et al* has reported that glutamate (500 μM) did not elicit a response in retinal capillaries from rat. On the other hand, pre-constricted cerebellar capillaries dilated in response to glutamate (100-500 μM), but glutamate had no effect in basal diameter of capillaries.(Peppiatt *et al.*, 2006) Hall *et al* have shown that glutamate (500 μM) dilates murine brain capillaries at pericyte sites, mediated by prostaglandin E_2 . This mechanism also involves nitric oxide release to inhibit synthesis of vasoconstricting 20-HETE. (Hall *et al.*, 2014) Moreover, superfusion of live kidney slices of rat with glutamate (10 μM) elicited a pericyte-mediated dilation of vasa recta (~16%). Glutamate-evoked dilation was attenuated in presence of dizocilpine (also designated MK-801; NMDAR antagonist), suggesting an NMDAR-dependent mechanism. (Wildman *et al.*, 2020)

A previous study from LeMaistre *et al.* has shown that glutamate or NMDA applied to isolated brain arteries and arterioles in association with D-serine elicited vasodilation, however not when glutamate or NMDA (0.1 μM to 100 mM) was applied alone. (LeMaistre *et al.*, 2012) It was hypothesised that co-activation of glutamate with glycine (or D-serine that act in the same modulatory binding site) could be necessary to observe a response in this bladder preparation.

First, the effect of glycine alone was investigated. Plasmatic concentrations of glycine vary between 170 and 330 μM (Petrat *et al.*, 2012).In the present study, glycine 10 μM and 1mM were used, as per glutamate. In these experiments, capillaries were mostly non responsive to glycine alone (response rate 0-16%). Glycine caused pericyte-mediated dilation of vasa recta in live kidney slices of rat. However, co-application with dizocilpine resulted in pericyte-mediated vasoconstriction, which suggests a NMDAR-dependent mechanism. (Wildman *et al.*, 2020)

In the present study, when applied together, glutamate (1 mM) and glycine (1 mM) showed no effect on 6 capillaries. Considering the overall limited response, no more experiments were conducted with these NMDAR co-agonists. If an agonistic effect had been clearly observed the next step would have been to investigate if that effect was inhibited in presence of ketamine. *Per se*, these results do not indicate that ketamine vasoconstriction is not mediated by NMDAR. Future studies to investigate whether dizocilpine, a high affinity site antagonist of NMDAR, has a similar effect to ketamine are needed. Moreover, pre-constriction of capillaries before applying glutamate and glycine could have provided more clear responses. This, however, would require a significantly higher number of capillaries, to account for the response rate of the vasoconstrictor and response rate of the co-agonists of NMDAR. As previously described, ketamine can interact with other receptors and channels that can be involved in the vasoconstriction observed. Future studies are therefore essential to elucidate the mechanism of action of ketamine in the microvasculature.

6.4.2. Immunohistochemical features (NG2/IB4)

The morphological features of capillary pericytes of the murine bladder observed in this study were similar to those described in Hashitani *et al.* studies. (Hashitani *et al.*, 2018)

As mentioned in the results section 6.3.2. Immunohistochemical features (NG2/IB4), it became evident in preliminary work that urothelial cells of the mouse bladder are strongly stained by GS-IB4 conjugated with Alexa Fluor® 488. Previous studies have shown that isolectin from *Griffonia simplicifolia* binds not only to endothelial cells of blood vessels but also to some epithelial cells in the mouse tissues (Laitinen, 1987). The additional step to remove urothelium improved image quality and made possible to observe the microvasculature.

Pericyte density was investigated following prolonged exposure (4 h) to ketamine. Changes in pericyte density have been reported in pathological states including in diabetic retinopathy tumoral development and sepsis induced by LPS, associated with a loss in pericytes. (Bergers and Song, 2005; Zeng *et al.*, 2016; Rudziak, Ellis and Kowalewska, 2019) However, prolonged exposure (4 h) of lamina propria preparations to ketamine 10, 30 and 100 µg/mL did not result in significant difference in pericyte density or distance between pericytes when compared to control (Krebs buffer alone).

It is plausible that the concentration and period of incubation in this experimental setting are insufficient to affect pericyte distribution/migration.

Also, capillary diameter at pericyte sites and non-pericyte sites was not statistically different, for each treatment and between treatments, although it shows a tendency to reduce diameter as ketamine concentration increases. These results should however not be interpreted as contradicting those obtained in pericyte functional experiments, where each capillary acts as its own control and only responsive capillaries are included in statistical analysis to compare diameter change at pericyte site and non-pericyte site. A statistical difference in this experimental setting is therefore more difficult to perceive and a larger sample size may be necessary to detect it, which was not possible due to time constraints.

Morphologically, no statistical difference was observed between height, width or length of processes of pericytes exposed to KH (10 µg/mL, 30 µg/mL and 100 µg/mL) and control (Krebs buffer). However, a general trend in increase in cell body height average can be observed, when comparing the treated groups to control. It has been reported that activated pericytes during angiogenesis increase their cell body volume and reduce the length of processes. Changes in morphology can also be observed in response to cytokines. (Díaz-Flores *et al.*, 2009)

Overall, the immunohistochemical features were similar for control group and lamina preparations treated with ketamine. It is possible that the small sample size (n=4), incubation time and concentrations used were not enough to detect differences.

The model employed is a useful tool to observe acute changes evoked by ketamine in the microvasculature, which would be otherwise be difficult to observe using *in vivo* models. The effect of ketamine metabolites was not studied although it has been suggested that their activity is a contributing factor for ketamine induced-cystitis. (Chu *et al.*, 2008) Another limitation of this study is that longer incubations than 4 h were not performed. Ketamine-induced cystitis is associated with prolonged abuse and high doses of ketamine (Winstock *et al.*, 2012), therefore chronic exposure might be an important factor for the development of the pathology. Complementary studies using *in vivo* models of ketamine-induced cystitis may help elucidating the effect of this drug

on the microvasculature. Tissue from such models can also be easily used to visualise the microvasculature as hereby described to either compare to the functional responses of microvasculature of healthy tissue or to test different drugs with therapeutic potential acting on the microvasculature.

6.5. Conclusions

In the present study the effect of ketamine on the microvasculature was investigated, as changes in the microvasculature were hypothesised to be involved in the pathological mechanism leading to ketamine-induced cystitis. Acute exposure of suburothelial capillaries to ketamine (30 $\mu\text{g}/\text{mL}$ and 100 $\mu\text{g}/\text{mL}$) evoked pericyte-mediated constriction. This effect may translate *in vivo* into reduction of blood flow to the tissue and subsequently affect bladder function. Considering most ketamine actions, including anaesthetic and analgesic, are primarily mediated via non-competitive antagonism of NMDAR, this receptor was considered a plausible molecular target involved in the vasoconstrictive effect. However, glutamate and glycine, which are co-agonists of NMDAR, elicited a negligible effect on the basal diameter of suburothelial capillaries when applied to the tissue, alone or in association. As such, the molecular target(s) of ketamine responsible for this vasoconstrictive effect need to be further investigated.

The effect of incubation with ketamine for a longer period (4h) on the suburothelial capillaries and pericytes of the bladder was also studied. However, changes in all parameters measured (e.g. pericyte density, diameter at pericytes and non-pericyte sites and cell morphology) were not statistically different. It should be noted that the small sample size ($n=4$ bladders) reduced the power of the study and therefore its ability to detect an effect. However, it was observed a general trend for a greater cell body height in tissue treated with ketamine, when compared to tissue treated with Krebs buffer alone, which may suggest morphological changes at an early stage of ketamine-induced cystitis.

The current study shows that ketamine has a direct effect on the bladder microvasculature, plausible to affect tissue perfusion and function. Informed by this current data, future studies looking at the molecular mechanism of ketamine in the bladder microvasculature are needed, as understanding the pathological mechanism of ketamine is essential for the development of efficient therapies.

GENERAL OVERVIEW OF THE THESIS

The present chapter aims to summarize the main findings of this thesis as well as identify limitations of the studies and potential future areas of research informed by the present data.

The bladder wall acts as an exceptional barrier to prevent cross movement of water, ions, toxins and other substances between the urine and bloodstream. Intravesical drug delivery is a method that provides direct delivery of drugs into the bladder, minimizing systemic side effects. (GuhaSarkar and Banerjee, 2010) This therapeutic strategy can be employed to help treat or ameliorate symptoms associated with different bladder pathologies, including IC/BPS (Zhang *et al.*, 2016), OAB (Evans, 2005) and KIC (Meng *et al.*, 2015). However, the efficacy is limited by the progressive dilution of the instilled drug by urine, which also affects drug residence time, dependent on voiding frequency. Moreover, urothelium low permeability can present a challenge when the drug target is localised in a deeper layer of the bladder. (GuhaSarkar and Banerjee, 2010) Currently, most therapeutic regimens using intravesical drug delivery remain empirically designed and therefore their potential is underachieved. Information regarding concentrations achieved within the bladder wall following intravesical drug delivery is often non-existent and minimum effective tissue concentrations in the target layer largely unknown.

The initial focus of this project was to investigate the efficacy of second line pharmacological treatments for OAB and IC/BPS through drug delivery studies, alongside investigations to elucidate the mechanism of action, to help maximise the potential of intravesical drug delivery.

In chapter 3, an *ex-vivo* whole bladder model from pig was used to compare delivery profiles of clinically relevant solutions of lidocaine (LH 2% saline. LH 4% and LH 2% alkalinised) instilled intravesically. Drug distribution into the urothelium, lamina propria and detrusor after 60 min from instillation was investigated and concentration – depth profiles were determined. Concentrations within the bladder wall were largely dependent on the concentration and pH of the instilled solution. As such, bladders instilled with LH 4% saline had approximately the double concentration within all layers

of the bladder when compared to those instilled with LH 2% saline, which was in agreement with Fick's first law.(Fick, 1995) Intravesical delivery of LH 2% alkalised also resulted in concentrations within the bladder twice higher to those resultant from LH 2% saline. An increased absorption was to be expected as a higher pH increases the non-ionized fraction of lidocaine, able to penetrate into the tissue. (Henry *et al.*, 2001) However, histological analysis revealed that the urothelium of bladders treated with alkalised lidocaine was severely affected, whereas normal urothelium was observed for bladders treated with saline solutions of lidocaine or saline solution alone. These urothelial changes are likely to have a damaging effect on the barrier function of the bladder and increase the absorption of lidocaine. These results were surprising as to my knowledge no similar findings have been reported in clinical studies, although histological data is absent. (Henry *et al.*, 2001; Nguan *et al.*, 2005; Parsons, 2005; Nickel *et al.*, 2009; Parsons *et al.*, 2012) Urine production was simulated to account for the dilution effect on drug dose instilled and to mimic the pH environment inside the bladder in physiological conditions. The alkalised solution was less affected by urine flow when compared to LH 2% saline. In part, this can be explained by the buffering effect of sodium bicarbonate; the increment in pH increases the non-ionized fraction of lidocaine which is capable of penetrating into the tissue as previously mentioned. On the other hand, the histological changes observed can also increase the absorption of lidocaine. It is not clear whether the histological findings here reported can also develop in the human bladder when exposed to a bicarbonate solution and that is an important question that should be addressed in future research. If that were to be the case other questions arise: Would a lower volume of bicarbonate show a better safety profile and still improve lidocaine absorption? If not, would a higher dose of lidocaine be a better option to ensure efficient absorption? Clarifying these questions is important to inform clinical decisions and to ensure safe administration of lidocaine in human patients. A detailed profile of the drug distribution within the bladder following intravesical delivery, as described in this study, can be extremely useful when optimising therapeutics and can be a helpful tool in future research.

At an early stage it had been envisioned to study the intravesical delivery of other clinically relevant drugs in addition to lidocaine, such as capsaicin analogues, DMSO and

botulinum toxin-A. However, the project took a different trajectory as I became more aware of the impact of ketamine-induced cystitis (KIC) and the big gap in knowledge regarding the pathological mechanism, which is understandable as KIC was only identified in 2007.(Shahani *et al.*, 2007) This condition has been associated with ketamine drug abuse, particularly in situations of high frequency and dose. Nevertheless, there is a growing interest in ketamine as a treatment option for depression, likely to involve multiple and repeated doses for a long period of time. Although low ketamine doses have been used in depression studies the potential for developing urological toxicity and other side effects described for this substance (e.g. gastrointestinal and cognitive) need to be carefully investigated. Most studies failed to assess adequately long-term side effects resulting from ketamine use in depression. (Short *et al.*, 2018)

Although some studies (Bureau *et al.*, 2015; Baker *et al.*, 2016) suggest that the effect of ketamine on the mucosa is resultant from exposure to urinary ketamine stored in the bladder, there was insufficient urinary data to support the concentrations used. Therefore, in chapter 4 the porcine whole bladder model was adapted to investigate whether urinary ketamine accumulated and stored in the bladder following drug abuse can penetrate into the bladder and achieve potential noxious concentrations. The accumulation of ketamine in the bladder was predicted, based in pharmacokinetic data available in the literature (Pai and Heining, 2007; Peltoniemi *et al.*, 2016; Zanos *et al.*, 2018). This was a simple estimation to be used as a starting point for this study and is not expected to have the same accuracy or precision of more complex pharmacokinetic models. For these experiments, ketamine was prepared in artificial urine, to ensure that the pH and salt environment was comparable to the content of the bladder in physiological conditions. As described for lidocaine, concentrations within the bladder following intravesical delivery will depend on the concentration of the solution instilled. As such, ketamine 6 mM retained for 1 h inside the bladder resulted in concentrations in every layer that were roughly twice as those determined for ketamine 3 mM. More concentrations would be required to accurately determine if the concentration of the instilled solution and concentration achieved within the bladder are directly proportional. Problems were observed with detection of ketamine for lower

concentrations of instilled solution. For a concentration of 0.3 mM retained for 4 h inside the bladder was not possible to establish a concentration-depth profile as for previous instilled solutions, considering some lidocaine peaks fell below the LOQ when sections were grouped in the same manner. Nevertheless, concentration per layer was determined. Having in consideration this issue, it was decided that gradient concentrations ten times higher than those initially estimated would be instilled to the bladder. Additional adjustments to the volume were necessary to prevent outflow of the instilled solution as described in the respective chapter. If a ten-fold less concentrated solution had been administered, as initially estimated, expected concentrations within the bladder wall would be roughly ten-fold less ($\sim 10 \mu\text{g/g}$ of wet tissue). One limitation of the model used is that it does not account for systemic blood concentrations of ketamine. Regardless, these results evidence that penetration of ketamine into the bladder wall occurs and concentrations determined can support future research. Urothelial damage was observed in bladders exposed for longer to higher concentrations of ketamine ($\sim 3 \text{ mM}$ for 4 h) and to a less extent for lower concentrations, which is agreement with observations of other studies. (Bureau et al., 2015) This supports the hypothesis that urinary ketamine has a direct cytotoxic effect in the mucosa, which appear to be time and dose dependent.

In addition to a direct cytotoxic effect of ketamine on the urothelium it has also been proposed that changes in the microvasculature are involved in the development of KIC. (Chu *et al.*, 2008; Lin *et al.*, 2016) Associated with vascular changes, ischemia and subsequent tissue hypoxia can lead to structural, molecular and functional changes in the bladder, which can have a critical impact in the development of LUTs. To investigate the direct effect of ketamine in the microvasculature it was essential to develop a bladder tissue model to observe changes elicited by ketamine *in situ*.

The regulation of blood flow has been investigated in several capillary beds, including from CNS and kidney (Peppiatt *et al.*, 2006; Fernandez-Klett *et al.*, 2010; Crawford *et al.*, 2012; Hall *et al.*, 2014) A lamina propria preparation from mice bladder had been previously reported. (Krska, 2017) However, in this study reduced tissue viability was described, offering concerns in regard to validity of results. Therefore, in chapter 5 a full thickness tissue model from murine bladder was developed to investigate pericyte

regulation in the suburothelial capillaries of the bladder. Preserving the tissue in full-thickness improved tissue viability when compared to a murine lamina propria preparation (Krska, 2017), suggesting that the tissue model is adequate to conduct functional experiments. Various vasoactive agents were applied exogenously and elicited pericyte-mediated changes in the diameter of suburothelial capillaries, evidencing that pericytes residing in the capillary bed of the mucosa of the bladder are contractile and have a regulatory role in the microvascular blood flow. This suggests pericyte cells as potential therapeutic targets in pathologies secondary to microvascular changes. Future work is required to clarify pericytes content of α -SMA or other contractile filaments, such as vimentin and desmin. (Bandopadhyay *et al.*, 2001) In addition, intracellular calcium imaging would allow to visualise calcium transients in the microvasculature in response to vasoactive agents.

In chapter 6 the murine bladder tissue model was used to investigate the effect of ketamine on the microvasculature. Acute exposure of suburothelial capillaries to ketamine evoked pericyte-mediated constriction, which may result in reduced tissue perfusion and plausibly affect bladder function. This finding evidences that pericyte cells may be involved in the pathological mechanism of ketamine and that these cells should be further investigated as potential therapeutic targets for KIC. To understand if the molecular mechanism leading to vasoconstriction was mediated through NMDAR antagonism, tissue was exposed to NMDAR co-agonists, glycine and glutamate. However, the low response rate made impossible to test an antagonistic effect of ketamine after observing an agonistic effect. Therefore, the molecular target(s) of ketamine leading to microvascular changes remains to be elucidated. However, longer incubation (4h) with ketamine has shown no statistical differences in several parameters (e.g. pericyte density, diameter at pericytes and non-pericyte sites and pericyte morphology) when compared to control. Nevertheless, an overall greater cell body height was observed for tissue treated with ketamine which may suggest morphological changes at an early stage of ketamine-induced cystitis. A greater sample size could improve the statistical power, increasing the chance of detecting a true effect. Cell death and expression changes in pericytes (e.g. change in expression of α -SMA) were not determined in this study but would be relevant to investigate in the future.

Taken together these findings suggest that ketamine has a direct cytotoxic effect in the urothelium and can evoke changes in the microvasculature of the bladder, which are likely to affect bladder function and contribute to the development of ketamine-induced cystitis.

REFERENCES

- A. L. Dalmose, J. J. Hvistendahl, L. (2000) 'Surgically induced urologic models in swine', *Journal of Investigative Surgery*. Taylor & Francis, 13(3), pp. 133–145. doi: 10.1080/08941930050075829.
- Abdalla, S. S., Laravuso, R. B. and Will, J. A. (1994) 'Mechanisms of the inhibitory effect of ketamine on guinea pig isolated main pulmonary artery.', *Anesthesia and analgesia*, 78(1), pp. 17–22. doi: 10.1213/00000539-199401000-00005.
- Abrams, P. *et al.* (2003) 'The standardisation of terminology in lower urinary tract function: report from the standardisation sub-committee of the International Continence Society', *Urology*. Elsevier, 61(1), pp. 37–49. doi: 10.1016/S0090-4295(02)02243-4.
- Abrams, P. *et al.* (2010) 'Urinary prostaglandin E2 levels are elevated in patients with overactive bladder and painful bladder syndrome and correlate with bladder diary symptoms', *European Urology Supplements*. Elsevier, 9(2), p. 252. doi: 10.1016/S1569-9056(10)60766-X.
- Abrams, P. H. *et al.* (1979) 'The synthesis and release of prostaglandins by human urinary bladder muscle in vitro.', *Investigative urology*, 16(5), pp. 346–8. Available at: <http://www.ncbi.nlm.nih.gov/pubmed/429129> (Accessed: 18 June 2019).
- Adamowicz, P. and Kala, M. (2005) 'Urinary excretion rates of ketamine and norketamine following therapeutic ketamine administration: method and detection window considerations', *Journal of Analytical Toxicology*, 29(5), pp. 376–382. doi: 10.1093/jat/29.5.376.
- Afiatpour, P. *et al.* (2003) 'Developmental changes in the functional, biochemical and molecular properties of rat bladder endothelin receptors', *Naunyn-Schmiedeberg's Archives of Pharmacology*. Springer-Verlag, 367(5), pp. 462–472. doi: 10.1007/s00210-003-0715-6.
- Aizawa, N. *et al.* (2009) 'Effects of CL316,243, a β 3-adrenoceptor agonist, and intravesical prostaglandin E2 on the primary bladder afferent activity of the rat', *Neurourology and Urodynamics*. John Wiley & Sons, Ltd, 29(5), pp. 771–776. doi:

10.1002/nau.20826.

Aizawa, N. and Wyndaele, J.-J. (2010) 'Effects of phenazopyridine on rat bladder primary afferent activity, and comparison with lidocaine and acetaminophen', *Neurourology and Urodynamics*. Wiley Subscription Services, Inc., A Wiley Company, 29(8), pp. 1445–1450. doi: 10.1002/nau.20886.

Akata, T. (2007) 'General anesthetics and vascular smooth muscle', *Anesthesiology*. American Society of Anesthesiologists, 106(2), pp. 365–391. doi: 10.1097/00000542-200702000-00026.

Akata, T., Izumi, K. and Nakashima, M. (2001) 'Mechanisms of direct inhibitory action of ketamine on vascular smooth muscle in mesenteric resistance arteries', *Anesthesiology*. American Society of Anesthesiologists, 95(2), pp. 452–462. doi: 10.1097/00000542-200108000-00030.

Alarcon-Martinez, L. *et al.* (2018) 'Capillary pericytes express α -smooth muscle actin, which requires prevention of filamentous-actin depolymerization for detection', *eLife*. eLife Sciences Publications, Ltd, 7. doi: 10.7554/eLife.34861.

Anderson, G. F. *et al.* (1984) 'Evidence for angiotensin II receptors in the urinary bladder of the rabbit', *Canadian Journal of Physiology and Pharmacology*. NRC Research Press Ottawa, Canada, 62(4), pp. 390–395. doi: 10.1139/y84-062.

Andersson, K.-E. and Arner, A. (2004) 'Urinary bladder contraction and relaxation: physiology and pathophysiology.', *Physiological reviews*. American Physiological Society, 84(3), pp. 935–86. doi: 10.1152/physrev.00038.2003.

Andersson, K.-E., Boedtkjer, D. B. and Forman, A. (2017) 'The link between vascular dysfunction, bladder ischemia, and aging bladder dysfunction.', *Therapeutic advances in urology*. SAGE Publications, 9(1), pp. 11–27. doi: 10.1177/1756287216675778.

Andersson, K.-E., Ek, A. and Persson, C. G. A. (1977) 'Effects of prostaglandins on the isolated human bladder and urethra', *Acta Physiologica Scandinavica*. John Wiley & Sons, Ltd (10.1111), 100(2), pp. 165–171. doi: 10.1111/j.1748-1716.1977.tb05933.x.

Andersson, K.-E., Hedlund, H. and Stahl, M. (1992) 'Contractions induced by angiotensin

I, angiotensin II and bradykinin in isolated smooth muscle from the human detrusor', *Acta Physiologica Scandinavica*. John Wiley & Sons, Ltd (10.1111), 145(3), pp. 253–259. doi: 10.1111/j.1748-1716.1992.tb09362.x.

Andersson, K.-E. and McCloskey, K. D. (2014) 'Lamina propria: The functional center of the bladder?', *Neurourology and Urodynamics*. Wiley-Blackwell, 33(1), pp. 9–16. doi: 10.1002/nau.22465.

Andersson, K.-E. and Sjögren, C. (1982) 'Aspects on the physiology and pharmacology of the bladder and urethra', *Progress in Neurobiology*. Pergamon, 19(1–2), pp. 71–89. doi: 10.1016/0301-0082(82)90021-1.

Andersson, K. E., Husted, S. and Sjögren, C. (1980) 'Contribution of prostaglandins to the adenosine triphosphate-induced contraction of rabbit urinary bladder.', *British journal of pharmacology*. Wiley-Blackwell, 70(3), pp. 443–52. doi: 10.1111/j.1476-5381.1980.tb08722.x.

Andersson, P.-O. *et al.* (1985) 'Changes in vascular resistance in the feline urinary bladder in response to bladder filling', *Journal of Urology*, 134(5), pp. 1041–1046. doi: 10.1016/S0022-5347(17)47584-7.

Apodaca, G. (2004) 'The uroepithelium: not just a passive barrier', *Traffic*. Wiley/Blackwell (10.1111), 5(3), pp. 117–128. doi: 10.1046/j.1600-0854.2003.00156.x.

Arentsen, H. C. *et al.* (2011) 'Pharmacokinetics and toxicity of intravesical TMX-101: a preclinical study in pigs', *BJU International*. John Wiley & Sons, Ltd (10.1111), 108(7), pp. 1210–1214. doi: 10.1111/j.1464-410X.2010.10055.x.

Asher, E. F. *et al.* (1992) 'Alteration of arteriolar responses to serotonin by two intravenous anesthetics', *Journal of Vascular Research*. Karger Publishers, 29(4), pp. 322–329. doi: 10.1159/000158947.

Attwell, D. *et al.* (2010) 'Glial and neuronal control of brain blood flow', *Nature*. Nature Publishing Group, 468(7321), pp. 232–243. doi: 10.1038/nature09613.

Attwell, D. *et al.* (2016) 'What is a pericyte?', *Journal of cerebral blood flow and metabolism : official journal of the International Society of Cerebral Blood Flow and*

Metabolism. SAGE Publications, 36(2), pp. 451–5. doi: 10.1177/0271678X15610340.

Audoly, L. P. *et al.* (1999) 'Identification of specific EP receptors responsible for the hemodynamic effects of PGE₂', *American Journal of Physiology-Heart and Circulatory Physiology*. American Physiological Society Bethesda, MD, 277(3), pp. H924–H930. doi: 10.1152/ajpheart.1999.277.3.H924.

Azadzi, K. M. *et al.* (2003) 'Increased leukotriene and prostaglandin release, and overactivity in the chronically ischemic bladder', *Journal of Urology*, 169(5), pp. 1885–1891. doi: 10.1097/01.ju.0000048668.97821.f4.

Azadzi, K. M. *et al.* (2004) 'Alteration of urothelial-mediated tone in the ischemic bladder: Role of eicosanoids', *Neurourology and Urodynamics*. John Wiley & Sons, Ltd, 23(3), pp. 258–264. doi: 10.1002/nau.20029.

Azadzi, K. M. *et al.* (2010) 'Oxidative modification of mitochondrial integrity and nerve fiber density in the ischemic overactive bladder', *Journal of Urology*, 183(1), pp. 362–369. doi: 10.1016/j.juro.2009.08.103.

Azadzi, K. M. *et al.* (2011) 'Molecular reactions and ultrastructural damage in the chronically ischemic bladder', *Journal of Urology*, 186(5), pp. 2115–2122. doi: 10.1016/j.juro.2011.06.047.

Azadzi, K. M., Radisavljevic, Z. M. and Siroky, M. B. (2008) 'Effects of ischemia on tachykinin-containing nerves and neurokinin receptors in the rabbit bladder', *Urology*. Elsevier, 71(5), pp. 979–983. doi: 10.1016/J.UROLOGY.2007.11.012.

Bade, J. J. *et al.* (1997) 'A placebo-controlled study of intravesical pentosanpolysulphate for the treatment of interstitial cystitis', *British Journal of Urology*, 79(2), pp. 168–171. doi: 10.1046/j.1464-410X.1997.03384.x.

Baker, S. C. *et al.* (2013) 'Nerve hyperplasia: a unique feature of ketamine cystitis.', *Acta neuropathologica communications*. BioMed Central, 1, p. 64. doi: 10.1186/2051-5960-1-64.

Baker, S. C. *et al.* (2016) 'Ketamine-induced apoptosis in normal human urothelial cells', *The American Journal of Pathology*, 186(5), pp. 1267–1277. doi:

10.1016/j.ajpath.2015.12.014.

Bandopadhyay, R. *et al.* (2001) 'Contractile proteins in pericytes at the blood-brain and blood-retinal barriers', *Journal of Neurocytology*. Kluwer Academic Publishers, 30(1), pp. 35–44. doi: 10.1023/A:1011965307612.

Beckel, J. M. *et al.* (2006) 'Expression of functional nicotinic acetylcholine receptors in rat urinary bladder epithelial cells.', *American journal of physiology. Renal physiology*. NIH Public Access, 290(1), pp. F103-10. doi: 10.1152/ajprenal.00098.2005.

Bergers, G. and Song, S. (2005) 'The role of pericytes in blood-vessel formation and maintenance.', *Neuro-oncology*. Oxford University Press, 7(4), pp. 452–64. doi: 10.1215/S1152851705000232.

Bertlich, M. *et al.* (2017) 'Role of capillary pericytes and precapillary arterioles in the vascular mechanism of betahistine in a guinea pig inner ear model', *Life Sciences*. Pergamon, 187, pp. 17–21. doi: 10.1016/J.LFS.2017.08.015.

Biers, S. M. *et al.* (2006) 'The functional effects of a c-kit tyrosine inhibitor on guinea-pig and human detrusor', *BJU International*, 97(3), pp. 612–616. doi: 10.1111/j.1464-410X.2005.05988.x.

Birch, B. R. and Miller, R. A. (1994) 'Absorption characteristics of lignocaine following intravesical instillation', *Scandinavian Journal of Urology and Nephrology*, 28(4), pp. 359–364. doi: 10.3109/00365599409180513.

Birder, L. A., Apodaca, G, *et al.* (1998) 'Adrenergic- and capsaicin-evoked nitric oxide release from urothelium and afferent nerves in urinary bladder.', *The American journal of physiology*, 275(2), pp. F226-9. doi: 10.1152/ajprenal.1998.275.2.F226.

Birder, L. A., Apodaca, Gerard, *et al.* (1998) 'Adrenergic- and capsaicin-evoked nitric oxide release from urothelium and afferent nerves in urinary bladder', *American Journal of Physiology-Renal Physiology*. American Physiological Society Bethesda, MD, 275(2), pp. F226–F229. doi: 10.1152/ajprenal.1998.275.2.F226.

Birder, L. A. *et al.* (2001) 'Vanilloid receptor expression suggests a sensory role for urinary bladder epithelial cells.', *Proceedings of the National Academy of Sciences of the*

United States of America. National Academy of Sciences, 98(23), pp. 13396–401. doi: 10.1073/pnas.231243698.

Birder, L.A. *et al.* (2002) 'Altered urinary bladder function in mice lacking the vanilloid receptor TRPV1', *Nature Neuroscience*. Nature Publishing Group, 5(9), pp. 856–860. doi: 10.1038/nn902.

Birder, Lori A. *et al.* (2002) ' β -adrenoceptor agonists stimulate endothelial nitric oxide synthase in rat urinary bladder urothelial cells', *Journal of Neuroscience*. Society for Neuroscience, 22(18), pp. 8063–8070. doi: 10.1523/JNEUROSCI.22-18-08063.2002.

Birder, L. A. and Andersson, K.-E. (2013) 'Urothelial signaling', *Physiological Reviews*. American Physiological Society Bethesda, MD, 93(2), pp. 653–680. doi: 10.1152/physrev.00030.2012.

Birder, L. and Andersson, K.-E. (2018) 'Animal modelling of interstitial cystitis/bladder pain syndrome.', *International neurourology journal*. Korean Continence Society, 22(Suppl 1), pp. S3-9. doi: 10.5213/inj.1835062.531.

Bolger, G. T. *et al.* (1990) 'Tissue specificity of endothelin binding sites', *Journal of Cardiovascular Pharmacology*, 16(3), pp. 367–375. doi: 10.1097/00005344-199009000-00004.

Borges, R., Von Grafenstein, H. and Knight, D. E. (1989) 'Tissue selectivity of endothelin', *European Journal of Pharmacology*. Elsevier, 165(2–3), pp. 223–230. doi: 10.1016/0014-2999(89)90716-4.

Borysova, L. *et al.* (2013) 'How calcium signals in myocytes and pericytes are integrated across in situ microvascular networks and control microvascular tone.', *Cell calcium*. Elsevier, 54(3), pp. 163–74. doi: 10.1016/j.ceca.2013.06.001.

Borysova, L. and Dora, K. A. (2018) 'The three faces of pericytes', *The Journal of Physiology*. Wiley/Blackwell (10.1111), 596(16), pp. 3453–3454. doi: 10.1111/JP276534.

Bouchelouche, K. *et al.* (2005) 'Increased contractile response to phenylephrine in detrusor patients with bladder outlet obstruction: effect of the α 1A and α 1D-adrenergic receptor antagonist tamsulosin', *Journal of Urology*, 173(2), pp. 657–661. doi:

10.1097/01.ju.0000143198.16610.84.

Bourne, D. (2016) *Chapter 5 - Analysis of urine data*. Available at: <https://www.boomer.org/c/p4/c05/c0503.php> (Accessed: 30 July 2019).

Brading, A. F. (1997) 'A myogenic basis for the overactive bladder', *Urology*. Elsevier, 50(6), pp. 57–67. doi: 10.1016/S0090-4295(97)00591-8.

Breyer, R. M. *et al.* (2001) 'Prostanoid receptors: subtypes and signaling', *Annual Review of Pharmacology and Toxicology*. Annual Reviews 4139 El Camino Way, P.O. Box 10139, Palo Alto, CA 94303-0139, USA, 41(1), pp. 661–690. doi: 10.1146/annurev.pharmtox.41.1.661.

Brookes, Z. L., Reilly, C. S. and Brown, N. J. (2004) 'Differential effects of propofol, ketamine, and thiopental anaesthesia on the skeletal muscle microcirculation of normotensive and hypertensive rats in vivo.', *British journal of anaesthesia*. Elsevier, 93(2), pp. 249–56. doi: 10.1093/bja/ae190.

Brown, W. W., Zenser, T. V and Davis, B. B. (1980) 'Prostaglandin E2 production by rabbit urinary bladder.', *The American journal of physiology*. American Physiological Society Bethesda, MD, 239(5), pp. F452-8. doi: 10.1152/ajprenal.1980.239.5.F452.

Bryant, C. D. (2011) 'The blessings and curses of C57BL/6 substrains in mouse genetic studies', *Annals of the New York Academy of Sciences*. Blackwell Publishing Inc., 1245(1), pp. 31–33. doi: 10.1111/j.1749-6632.2011.06325.x.

Bschleipfer, T. *et al.* (2015) 'Systemic atherosclerosis causes detrusor overactivity: functional and morphological changes in hyperlipoproteinemic apoE^{-/-}LDLR^{-/-} mice', *The Journal of Urology*. No longer published by Elsevier, 193(1), pp. 345–351. doi: 10.1016/J.JURO.2014.08.098.

Bureau, M. *et al.* (2015) 'Demonstration of the direct impact of ketamine on urothelium using a tissue engineered bladder model.', *Canadian Urological Association journal = Journal de l'Association des urologues du Canada*. Canadian Medical Association, 9(9–10), pp. E613-7. doi: 10.5489/cuaj.2899.

Burmester, A. G. *et al.* (2008) 'Electromotive drug administration for treatment of

therapy-refractory overactive bladder', *International braz j urol*. Sociedade Brasileira de Urologia, 34(6), pp. 758–764. doi: 10.1590/S1677-55382008000600011.

Burnstock, G. (2013) 'Purinergetic signalling in the lower urinary tract', *Acta Physiologica*. John Wiley & Sons, Ltd (10.1111), 207(1), pp. 40–52. doi: 10.1111/apha.12012.

Cahill, D. J., Fry, C. H. and Foxall, P. J. D. (2003) 'Variation in urine composition in the human urinary tract: evidence of urothelial function in situ?', *The Journal of Urology*. Elsevier, 169(3), pp. 871–874. doi: 10.1097/01.JU.0000052404.42651.55.

Cai, C. *et al.* (2018) 'Stimulation-induced increases in cerebral blood flow and local capillary vasoconstriction depend on conducted vascular responses.', *Proceedings of the National Academy of Sciences of the United States of America*. National Academy of Sciences, 115(25), pp. E5796–E5804. doi: 10.1073/pnas.1707702115.

Camões, J. *et al.* (2015) 'Lower urinary tract symptoms and aging: the impact of chronic bladder ischemia on overactive bladder syndrome', *Urologia Internationalis*. Karger Publishers, 95(4), pp. 373–379. doi: 10.1159/000437336.

Canis, M. B. *et al.* (2017) 'Cochlear pericytes are capable of reversibly decreasing capillary diameter in vivo after tumor necrosis factor exposure', *Otology & amp*, 38(10), pp. e545–e550. doi: 10.1097/mao.0000000000001523.

Chapple, C. (2014) 'Chapter 2: Pathophysiology of neurogenic detrusor overactivity and the symptom complex of "Overactive bladder"', *Neurourology and Urodynamics*. John Wiley & Sons, Ltd, 33(S3), pp. S6–S13. doi: 10.1002/nau.22635.

Chaux, A. (2011) *Pathology Outlines - Normal histology*. Available at: <http://www.pathologyoutlines.com/topic/bladderhistology.html> (Accessed: 8 May 2018).

Chen, D. *et al.* (2003) 'Effect of dimethyl sulfoxide on bladder tissue penetration of intravesical paclitaxel', *Clinical Cancer Research*, 9(1). Available at: <https://clincancerres.aacrjournals.org/content/9/1/363.long> (Accessed: 6 February 2017).

Chen, I.-C. *et al.* (2017) 'Risk Factors of Lower Urinary Tract Syndrome among Ketamine

Users', *LUTS: Lower Urinary Tract Symptoms*. Blackwell Publishing Asia Pty Ltd. doi: 10.1111/luts.12178.

Chen, M.-H. *et al.* (2018) 'Rapid inflammation modulation and antidepressant efficacy of a low-dose ketamine infusion in treatment-resistant depression: A randomized, double-blind control study', *Psychiatry Research*. Elsevier, 269, pp. 207–211. doi: 10.1016/J.PSYCHRES.2018.08.078.

Cheng, E. Y., Decker, R. S. and Lee, C. (1999) 'Role of angiotensin II in bladder smooth muscle growth and function', in *Advances in experimental medicine and biology*, pp. 183–191. doi: 10.1007/978-1-4615-4737-2_14.

Cheng, J.-K. and Ji, R.-R. (2008) 'Intracellular signaling in primary sensory neurons and persistent pain.', *Neurochemical research*. NIH Public Access, 33(10), pp. 1970–8. doi: 10.1007/s11064-008-9711-z.

Cho, S. T., Park, E. Y. and Kim, J. C. (2012) 'Effect of angiotensin II receptor antagonist telmisartan on detrusor overactivity in rats with bladder outlet obstruction', *Urology*. Elsevier, 80(5), pp. 1163.e1-1163.e7. doi: 10.1016/J.UROLOGY.2012.05.002.

Choo, L. K. and Mitchelson, F. (1977) 'The role of prostaglandins in the excitatory innervation of the rat urinary bladder', *Prostaglandins*, 13(5), pp. 917–926. doi: 10.1016/0090-6980(77)90221-0.

Chu, P. S.-K. *et al.* (2008) 'The destruction of the lower urinary tract by ketamine abuse: a new syndrome?', *BJU International*. Wiley/Blackwell (10.1111), 102(11), pp. 1616–1622. doi: 10.1111/j.1464-410X.2008.07920.x.

Chuang, S.-M. *et al.* (2013) 'Dual involvements of cyclooxygenase and nitric oxide synthase expressions in ketamine-induced ulcerative cystitis in rat bladder', *Neurourology and Urodynamics*, 32(8), pp. 1137–1143. doi: 10.1002/nau.22367.

Chuang, Y.-C. *et al.* (2009) 'Intravesical Botulinum Toxin A administration inhibits COX-2 and EP4 expression and suppresses bladder hyperactivity in cyclophosphamide-induced cystitis in rats', *European Urology*. Elsevier, 56(1), pp. 159–167. doi: 10.1016/j.eururo.2008.05.007.

Chung, H. C. *et al.* (1992) 'Partially endothelium-dependent relaxing effect of ketamine on the canine basilar artery in vitro.', *Ma zui xue za zhi = Anaesthesiologica Sinica*, 30(1), pp. 1–6. Available at: <http://www.ncbi.nlm.nih.gov/pubmed/1608313> (Accessed: 13 August 2019).

Ciancio, G. *et al.* (1988) 'Measurement of cell-cycle phase-specific cell death using Hoechst 33342 and propidium iodide: preservation by ethanol fixation.', *Journal of Histochemistry & Cytochemistry*, 36(9), pp. 1147–1152. doi: 10.1177/36.9.2457047.

Clemens, J. Q. *et al.* (2005) 'Prevalence and incidence of interstitial cystitis in a managed care population', *The Journal of Urology*. Elsevier, 173(1), pp. 98–102. doi: 10.1097/01.JU.0000146114.53828.82.

ClinicalTrials.gov (2018) *Identifier NCT02395042 - A safety and efficacy study of LiRIS® in females with interstitial cystitis with hunner's lesions*. Available at: <https://clinicaltrials.gov/ct2/show/study/NCT02395042> (Accessed: 11 October 2018).

Contreras-Sanz, A. *et al.* (2016) 'Altered urothelial ATP signalling in major subset of human overactive bladder patients with pyuria.', *American journal of physiology. Renal physiology*, p. ajprenal.00339.2015. doi: 10.1152/ajprenal.00339.2015.

Corcos, J. *et al.* (2017) 'CUA guideline on adult overactive bladder.', *Canadian Urological Association journal = Journal de l'Association des urologues du Canada*. Canadian Medical Association, 11(5), pp. E142–E173. doi: 10.5489/cuaj.4586.

Crawford, C. *et al.* (2012) 'An intact kidney slice model to investigate vasa recta properties and function in situ.', *Nephron. Physiology*. Karger Publishers, 120(3), pp. p17-31. doi: 10.1159/000339110.

Crawford, C. *et al.* (2013) 'Sympathetic nerve-derived ATP regulates renal medullary vasa recta diameter via pericyte cells: a role for regulating medullary blood flow?', *Frontiers in physiology*. Frontiers Media SA, 4, p. 307. doi: 10.3389/fphys.2013.00307.

Crowe, R. and Burnstock, G. (1989) 'A histochemical and immunohistochemical study of the autonomic innervation of the lower urinary tract of the female pig. Is the pig a good model for the human bladder and urethra?', *The Journal of urology*, 141(2), pp. 414–22. doi: 10.1016/s0022-5347(17)40785-3.

Curhan, G. C. *et al.* (1999) 'Epidemiology of interstitial cystitis: a population based study', *The Journal of Urology*. Elsevier, 161(2), pp. 549–552. doi: 10.1016/S0022-5347(01)61947-5.

Daly, D. *et al.* (2007) 'Bladder afferent sensitivity in wild-type and TRPV1 knockout mice.', *The Journal of physiology*. Wiley-Blackwell, 583(Pt 2), pp. 663–74. doi: 10.1113/jphysiol.2007.139147.

Damiano, R. *et al.* (2011) 'Prevention of recurrent urinary tract infections by intravesical administration of hyaluronic acid and chondroitin sulphate: a placebo-controlled randomised trial', *European Urology*. Elsevier, 59(4), pp. 645–651. doi: 10.1016/J.EURURO.2010.12.039.

Das, A. K. *et al.* (2002) 'Effect of Doxazosin on rat urinary bladder function after partial outlet obstruction', *Neurourology and Urodynamics*. John Wiley & Sons, Ltd, 21(2), pp. 160–166. doi: 10.1002/nau.10045.

Dasgupta, P., Fowler, C. J. and Stephen, R. L. (1998) 'Electromotive drug administration of lidocaine to anesthetize the bladder before intravesical capsaicin.', *The Journal of urology*, 159(6), pp. 1857–61. doi: 10.1016/S0022-5347(01)63176-8.

Davis, N. F., Brady, C. M. and Creagh, T. (2014) 'Interstitial cystitis/painful bladder syndrome: epidemiology, pathophysiology and evidence-based treatment options.', *European journal of obstetrics, gynecology, and reproductive biology*. Elsevier, 175, pp. 30–7. doi: 10.1016/j.ejogrb.2013.12.041.

Díaz-Flores, L. *et al.* (2009) 'Pericytes. Morphofunction, interactions and pathology in a quiescent and activated mesenchymal cell niche', *Histology and Histopathology*, pp. 909–969. doi: 10.14670/HH-24.909.

Ding, X., Damron, D. S. and Murray, P. A. (2005) 'Ketamine attenuates acetylcholine-induced contraction by decreasing myofilament Ca²⁺ sensitivity in pulmonary veins', *Anesthesiology*. American Society of Anesthesiologists, 102(3), pp. 588–596. doi: 10.1097/00000542-200503000-00018.

Dixon, J. S. and Gilpin, C. J. (1987) 'Presumptive sensory axons of the human urinary bladder: a fine structural study.', *Journal of anatomy*. Wiley-Blackwell, 151, pp. 199–207.

Available at: <http://www.ncbi.nlm.nih.gov/pubmed/3654351> (Accessed: 13 June 2018).

Djavan, B. and Marberger, M. (1999) 'A meta-analysis on the efficacy and tolerability of α 1-adrenoceptor antagonists in patients with lower urinary tract symptoms suggestive of benign prostatic obstruction', *European Urology*, 36(1), pp. 1–13. doi: 10.1159/000019919.

Dojo, M. *et al.* (2002) 'Ketamine stereoselectively affects vasorelaxation mediated by ATP-sensitive K⁺ channels in the rat aorta', *Anesthesiology*. American Society of Anesthesiologists, 97(4), pp. 882–886. doi: 10.1097/00000542-200210000-00020.

Domino, E. F. *et al.* (1982) 'Plasma levels of ketamine and two of its metabolites in surgical patients using a gas chromatographic mass fragmentographic assay.', *Anesthesia and analgesia*, 61(2), pp. 87–92. doi: 10.1213/00000539-198202000-00004.

Donoso, M. V *et al.* (1994) 'Involvement of ETA receptors in the facilitation by endothelin-1 of non-adrenergic non-cholinergic transmission in the rat urinary bladder.', *British journal of pharmacology*. Wiley-Blackwell, 111(2), pp. 473–82. doi: 10.1111/j.1476-5381.1994.tb14761.x.

Downie, J. W. and Karmazyn, M. (1984) 'Mechanical trauma to bladder epithelium liberates prostanoids which modulate neurotransmission in rabbit detrusor muscle.', *The Journal of pharmacology and experimental therapeutics*, 230(2), pp. 445–9. Available at: <http://www.ncbi.nlm.nih.gov/pubmed/6146713> (Accessed: 17 June 2019).

Drake, M. J. *et al.* (2005) 'Localized contractions in the normal human bladder and in urinary urgency', *BJU International*. John Wiley & Sons, Ltd (10.1111), 95(7), pp. 1002–1005. doi: 10.1111/j.1464-410X.2005.05455.x.

DrugWise (2017) *Highways and buyways: A snapshot of UK drug scenes 2016*. Available at: www.drugwise.org.uk (Accessed: 17 July 2019).

Duan, Q. *et al.* (2017) 'Changes to the bladder epithelial barrier are associated with ketamine-induced cystitis.', *Experimental and therapeutic medicine*. Spandidos Publications, 14(4), pp. 2757–2762. doi: 10.3892/etm.2017.4913.

Dunn, K. W. *et al.* (2002) 'Functional studies of the kidney of living animals using

multicolor two-photon microscopy', *American Journal of Physiology-Cell Physiology*. American Physiological Society Bethesda, MD, 283(3), pp. C905–C916. doi: 10.1152/ajpcell.00159.2002.

Edwards, R. M. (1985) 'Effects of prostaglandins on vasoconstrictor action in isolated renal arterioles.', *The American journal of physiology*, 248(6 Pt 2), pp. F779-84. doi: 10.1152/ajprenal.1985.248.6.F779.

Engelhardt, P. F. *et al.* (2011) 'Long-term results of intravesical hyaluronan therapy in bladder pain syndrome/interstitial cystitis', *International Urogynecology Journal*. Springer-Verlag, 22(4), pp. 401–405. doi: 10.1007/s00192-010-1294-y.

Erman, A. and Veranič, P. (2011) 'Time- and temperature-dependent autolysis of urinary bladder epithelium during ex vivo preservation', *Protoplasma*, 248(3), pp. 541–550. doi: 10.1007/s00709-010-0201-1.

Erspamer, V., Ronzoni, G. and Falconieri Erspamer, G. (1981) 'Effects of active peptides on the isolated muscle of the human urinary bladder.', *Investigative urology*, 18(4), pp. 302–4. Available at: <http://www.ncbi.nlm.nih.gov/pubmed/7451095> (Accessed: 11 June 2019).

Evans, R. J. (2005) 'Intravesical therapy for overactive bladder', *Current Urology Reports*, 6(6), pp. 429–433. doi: 10.1007/s11934-005-0037-y.

F. Brading, J. E. Greenland, I. W., A. (1999) 'Blood supply to the bladder during filling', *Scandinavian Journal of Urology and Nephrology*, 33(201), pp. 25–31. doi: 10.1080/00365599950510012.

Fan, G.-Y. *et al.* (2017) 'The immunomodulatory imbalance in patients with ketamine cystitis.', *BioMed research international*. Hindawi Limited, 2017, p. 2329868. doi: 10.1155/2017/2329868.

Ferguson, D. R., Kennedy, I. and Burton, T. J. (1997) 'ATP is released from rabbit urinary bladder epithelial cells by hydrostatic pressure changes--a possible sensory mechanism?', *The Journal of physiology*. Wiley-Blackwell, 505 (Pt 2(Pt 2)), pp. 503–11. doi: 10.1111/j.1469-7793.1997.503bb.x.

Fernandez-Klett, F. *et al.* (2010) 'Pericytes in capillaries are contractile in vivo, but arterioles mediate functional hyperemia in the mouse brain', *Proceedings of the National Academy of Sciences*. National Academy of Sciences, 107(51), pp. 22290–22295. doi: 10.1073/pnas.1011321108.

Fick, A. (1995) 'On liquid diffusion', *Journal of Membrane Science*, 100(1), pp. 33–38. doi: 10.1016/0376-7388(94)00230-V.

Fontanella, U. A., Rossi, C. A. and Stephen, R. L. (1992) 'Iontophoretic local anaesthesia for bladder dilatation in the treatment of interstitial cystitis', *British Journal of Urology*. John Wiley & Sons, Ltd (10.1111), 69(6), pp. 662–663. doi: 10.1111/j.1464-410X.1992.tb15647.x.

Fowler, C. J., Griffiths, D. and de Groat, W. C. (2008) 'The neural control of micturition.', *Nature reviews. Neuroscience*. NIH Public Access, 9(6), pp. 453–66. doi: 10.1038/nrn2401.

Frazier, K. S. *et al.* (2012) 'Proliferative and nonproliferative lesions of the rat and mouse urinary system', *Toxicologic Pathology*. SAGE PublicationsSage CA: Los Angeles, CA, 40(4_suppl), pp. 14S-86S. doi: 10.1177/0192623312438736.

Fry, C. H. and Vahabi, B. (2016) 'The role of the mucosa in normal and abnormal bladder function', *Basic & Clinical Pharmacology & Toxicology*, 119(S3), pp. 57–62. doi: 10.1111/bcpt.12626.

Fukuda, S., Su, C. and Lee, T. J. (1986) 'Potentiation of pressor responses to serotonin by ketamine in isolated perfused rat mesentery.', *Journal of cardiovascular pharmacology*, 8(4), pp. 765–70. Available at: <http://www.ncbi.nlm.nih.gov/pubmed/2427816> (Accessed: 13 August 2019).

Gabella, G. (1995) 'The structural relations between nerve fibres and muscle cells in the urinary bladder of the rat', *Journal of Neurocytology*. Kluwer Academic Publishers, 24(3), pp. 159–187. doi: 10.1007/BF01181533.

Gabella, G. and Davis, C. (1998) 'Distribution of afferent axons in the bladder of rats', *Journal of Neurocytology*. Kluwer Academic Publishers, 27(3), pp. 141–155. doi: 10.1023/A:1006903507321.

Garcia-Pascual, A., Larsson, B. and Andersson, K.-E. (1990) 'Contractile effects of endothelin-I and localization of endothelin binding sites in rabbit lower urinary tract smooth muscle', *Acta Physiologica Scandinavica*. John Wiley & Sons, Ltd (10.1111), 140(4), pp. 545–555. doi: 10.1111/j.1748-1716.1990.tb09032.x.

Gasparini, L. *et al.* (2017) 'In vitro cell viability by CellProfiler[®] software as equivalent to MTT assay', *Pharmacognosy Magazine*. Medknow Publications, 13(50), p. 365. doi: 10.4103/0973-1296.210176.

Gevaert, T. *et al.* (2017) 'Comparative study of the organisation and phenotypes of bladder interstitial cells in human, mouse and rat', *Cell and Tissue Research*. Springer Berlin Heidelberg, 370(3), pp. 403–416. doi: 10.1007/s00441-017-2694-9.

Ghoneim, M. A. *et al.* (1976) 'The influence of vesical distension on the urethral resistance to flow: a possible role for prostaglandins?', *The Journal of urology*, 116(6), pp. 739–43. doi: 10.1016/s0022-5347(17)58993-4.

Giannantoni, A. *et al.* (2006) 'New frontiers in intravesical therapies and drug delivery', *European Urology*, 50(6), pp. 1183–1193. doi: 10.1016/j.eururo.2006.08.025.

Giglio, D. *et al.* (2005) 'Altered muscarinic receptor subtype expression and functional responses in cyclophosphamide induced cystitis in rats', *Autonomic Neuroscience*. Elsevier, 122(1–2), pp. 9–20. doi: 10.1016/J.AUTNEU.2005.07.005.

Gilmore, N. J. and Vane, J. R. (1971) 'Hormones released into the circulation when the urinary bladder of the anaesthetized dog is distended.', *Clinical science*. Portland Press Limited, 41(1), pp. 69–83. doi: 10.1042/CS0410069.

Goepel, M. *et al.* (1998) 'Muscarinic receptor subtypes in porcine detrusor: comparison with humans and regulation by bladder augmentation.', *Urological research*, 26(2), pp. 149–54. doi: 10.1007/s002400050038.

Goi, Y. *et al.* (2016) 'Silodosin, an α 1A-adrenoceptor antagonist, may ameliorate ischemia-induced bladder denervation and detrusor dysfunction by improving bladder blood flow', *Pharmacology*. Karger Publishers, 97(3–4), pp. 161–170. doi: 10.1159/000443965.

Golzari, S. E. J. *et al.* (2014) 'Lidocaine and pain management in the emergency department: A review article', *Anesthesiology and Pain Medicine*. Kowsar Medical Publishing Company. doi: 10.5812/aapm.15444.

Gonzalez-Cadavid, N. F. *et al.* (2000) 'Presence of NMDA Receptor Subunits in the Male Lower Urogenital Tract', *Journal of Andrology*. John Wiley & Sons, Ltd, 21(4), pp. 566–578. doi: 10.1002/J.1939-4640.2000.TB02122.X.

Gonzalez, E. J., Arms, L. and Vizzard, M. A. (2014) 'The role(s) of cytokines/chemokines in urinary bladder inflammation and dysfunction.', *BioMed research international*. Hindawi Limited, 2014, p. 120525. doi: 10.1155/2014/120525.

Gormley, E. A. *et al.* (2012) 'Diagnosis and treatment of overactive bladder (non-neurogenic) in adults: AUA/SUFU guideline', *The Journal of Urology*. Elsevier, 188(6), pp. 2455–2463. doi: 10.1016/j.juro.2012.09.079.

Gosling, J. A. and Dixon, J. S. (1974) 'Sensory nerves in the mammalian urinary tract. An evaluation using light and electron microscopy.', *Journal of anatomy*. Wiley-Blackwell, 117(Pt 1), pp. 133–44. Available at: <http://www.ncbi.nlm.nih.gov/pubmed/4844655> (Accessed: 13 June 2018).

Grabnar, I. *et al.* (2006) 'Kinetic model of drug distribution in the urinary bladder wall following intravesical instillation', *International Journal of Pharmaceutics*, 322(1), pp. 52–59. doi: 10.1016/j.ijpharm.2006.05.026.

Grabnar, I., Bogataj, M. and Mrhar, A. (2003) 'Influence of chitosan and polycarbophil on permeation of a model hydrophilic drug into the urinary bladder wall', *International Journal of Pharmaceutics*. Elsevier, 256(1–2), pp. 167–173. doi: 10.1016/S0378-5173(03)00074-7.

Granato, C. *et al.* (2015) 'Prostaglandin E2 excitatory effects on rat urinary bladder: a comparison between the β -adrenoceptor modulation of non-voiding activity in vivo and micro-contractile activity in vitro', *Naunyn-Schmiedeberg's Archives of Pharmacology*. Springer Berlin Heidelberg, 388(7), pp. 727–735. doi: 10.1007/s00210-015-1139-9.

Grant, R. I. *et al.* (2019) 'Organizational hierarchy and structural diversity of microvascular pericytes in adult mouse cortex', *Journal of Cerebral Blood Flow &*

Metabolism. SAGE PublicationsSage UK: London, England, 39(3), pp. 411–425. doi: 10.1177/0271678X17732229.

Greenland, J. E. *et al.* (2000) 'The effect of bladder outlet obstruction on tissue oxygen tension and blood flow in the pig bladder', *BJU International*. John Wiley & Sons, Ltd (10.1111), 85(9), pp. 1109–1114. doi: 10.1046/j.1464-410x.2000.00611.x.

Greenland, J. E. and Brading, A. F. (2001) 'The effect of bladder outflow obstruction on detrusor blood flow changes during the voiding cycle in conscious pigs', *The Journal of Urology*. No longer published by Elsevier, 165(1), pp. 245–248. doi: 10.1097/00005392-200101000-00072.

Gu, D. *et al.* (2014) 'Long-term ketamine abuse induces cystitis in rats by impairing the bladder epithelial barrier', *Molecular Biology Reports*. Springer Netherlands, 41(11), pp. 7313–7322. doi: 10.1007/s11033-014-3616-5.

GuhaSarkar, S. and Banerjee, R. (2010) 'Intravesical drug delivery: Challenges, current status, opportunities and novel strategies', *Journal of Controlled Release*, 148(2), pp. 147–159. doi: 10.1016/j.jconrel.2010.08.031.

Gürpınar, T., Wong, H. Y. and Griffith, D. P. (1996) 'Electromotive administration of intravesical lidocaine in patients with interstitial cystitis.', *Journal of endourology*, 10(5), pp. 443–7. doi: 10.1089/end.1996.10.443.

Hadzhibozheva, P. *et al.* (2019) 'Analysis of angiotensin II-Induced rat urinary bladder contractions in the presence of angiotensin II receptors blockers', *Archives of Physiology and Biochemistry*. Taylor & Francis, pp. 1–5. doi: 10.1080/13813455.2018.1555669.

Hakenberg, O. W. *et al.* (2000) 'Bladder wall thickness in normal adults and men with mild lower urinary tract symptoms and benign prostatic enlargement.', *Neurourology and urodynamics*, 19(5), pp. 585–93. doi: 10.1002/1520-6777(2000)19:5<585::aid-nau5>3.0.co;2-u.

Hall, C. N. *et al.* (2014) 'Capillary pericytes regulate cerebral blood flow in health and disease', *Nature*. Europe PMC Funders, 508(7494), pp. 55–60. doi: 10.1038/nature13165.

Hamilton, N. B., Attwell, D. and Hall, C. N. (2010) 'Pericyte-mediated regulation of capillary diameter: a component of neurovascular coupling in health and disease.', *Frontiers in neuroenergetics*. Frontiers Media SA, 2. doi: 10.3389/fnene.2010.00005.

Hanna-Mitchell, A. T. *et al.* (2007) 'Non-neuronal acetylcholine and urinary bladder urothelium', *Life Sciences*. Pergamon, 80(24–25), pp. 2298–2302. doi: 10.1016/J.LFS.2007.02.010.

Harrison, K. A. *et al.* (1996) 'Radiolabeled iododeoxyuridine: safety evaluation.', *Journal of nuclear medicine : official publication, Society of Nuclear Medicine*, 37(4 Suppl), pp. 13S-16S. Available at: <http://www.ncbi.nlm.nih.gov/pubmed/8676196> (Accessed: 29 May 2019).

Hartmann, D. A. *et al.* (2015) 'Pericyte structure and distribution in the cerebral cortex revealed by high-resolution imaging of transgenic mice.', *Neurophotonics*. Society of Photo-Optical Instrumentation Engineers, 2(4), p. 041402. doi: 10.1117/1.NPh.2.4.041402.

Hashim, H. and Abrams, P. (2006) 'Is the bladder a reliable witness for predicting detrusor overactivity?', *Journal of Urology*, 175(1), pp. 191–194. doi: 10.1016/S0022-5347(05)00067-4.

Hashitani, H. *et al.* (2011) 'Functional properties of suburothelial microvessels in the rat bladder', *The Journal of Urology*. Elsevier, 185(6), pp. 2382–2391. doi: 10.1016/J.JURO.2011.02.046.

Hashitani, H. *et al.* (2012) 'Functional and morphological properties of pericytes in suburothelial venules of the mouse bladder.', *British journal of pharmacology*. Wiley-Blackwell, 167(8), pp. 1723–36. doi: 10.1111/j.1476-5381.2012.02125.x.

Hashitani, H. *et al.* (2015) 'Pacemaker role of pericytes in generating synchronized spontaneous Ca²⁺ transients in the myenteric microvasculature of the guinea-pig gastric antrum', *Cell Calcium*. Churchill Livingstone, 58(5), pp. 442–456. doi: 10.1016/J.CECA.2015.06.012.

Hashitani, H. *et al.* (2018) 'Role of capillary pericytes in the integration of spontaneous Ca²⁺ transients in the suburothelial microvasculature *in situ* of the mouse bladder', *The*

Journal of Physiology. Wiley/Blackwell (10.1111), 596(16), pp. 3531–3552. doi: 10.1113/JP275845.

Hashitani, H. and Lang, R. J. (2016) 'Spontaneous activity in the microvasculature of visceral organs: role of pericytes and voltage-dependent Ca(2+) channels.', *The Journal of physiology*. Wiley-Blackwell, 594(3), pp. 555–65. doi: 10.1113/JP271438.

Haylen, B. T. *et al.* (2009) 'An international urogynecological association (IUGA)/international continence society (ICS) joint report on the terminology for female pelvic floor dysfunction', *Neurourology and Urodynamics*. Wiley Subscription Services, Inc., A Wiley Company, 29(1), p. n/a-n/a. doi: 10.1002/nau.20798.

Haylor, J. and Towers, J. (1982) 'Renal vasodilator activity of prostaglandin E2 in the rat anaesthetized with pentobarbitone.', *British journal of pharmacology*. Wiley-Blackwell, 76(1), pp. 131–7. doi: 10.1111/j.1476-5381.1982.tb09198.x.

Henry, R. *et al.* (2001) 'Absorption of alkalized intravesical lidocaine in normal and inflamed bladders: a simple method for improving bladder anesthesia', *The Journal of Urology*, 165(6), pp. 1900–1903. doi: 10.1016/S0022-5347(05)66238-6.

Henry, R. A., Morales, A. and Cahill, C. M. (2015) 'Beyond a simple anesthetic effect: lidocaine in the diagnosis and treatment of interstitial cystitis/bladder pain syndrome', *Urology*, 85(5), pp. 1025–1033. doi: 10.1016/j.urology.2015.01.021.

Higson, R. H., Smith, J. C. and Hills, W. (1979) 'Intravesical lignocaine and detrusor instability.', *British journal of urology*, 51(6), pp. 500–3. doi: 10.1111/j.1464-410x.1979.tb03587.x.

Hill, R. A. *et al.* (2015) 'Regional blood flow in the normal and ischemic brain is controlled by arteriolar smooth muscle cell contractility and not by capillary pericytes.', *Neuron*. NIH Public Access, 87(1), pp. 95–110. doi: 10.1016/j.neuron.2015.06.001.

Hill, W. G. (2015) 'Control of urinary drainage and voiding', *Clinical Journal of the American Society of Nephrology*, 10(3), pp. 480–492. doi: 10.2215/CJN.04520413.

Hills, N. H. (1976) 'Prostaglandins and tone in isolated strips of mammalian bladder [proceedings].', *British journal of pharmacology*. Wiley-Blackwell, 57(3), pp. 464P-465P.

Available at: <http://www.ncbi.nlm.nih.gov/pubmed/974355> (Accessed: 18 June 2019).

Hollmann, M. W. and Durieux, M. E. (2000) 'Local anesthetics and the inflammatory response', *Anesthesiology*. [American Society of Anesthesiologists, etc.], 93(3), pp. 858–875. doi: 10.1097/00000542-200009000-00038.

Holmäng, S., Aldenborg, F. and Hedelin, H. (1994) 'Multiple bladder biopsies under intravesical lignocaine anaesthesia.', *British journal of urology*, 73(2), pp. 160–3. doi: 10.1111/j.1464-410x.1994.tb07485.x.

Home Office (2018) *Drug Misuse: Findings from the 2017/18 Crime Survey for England and Wales Further information*. Available at: <https://www.gov.uk/government/statistics/announcements> (Accessed: 17 July 2019).

Home Office (2019) *Drugs misuse: findings from the 2018/19 crime survey for england and wales*. DANDY BOOKSELLERS LTD.

Hong, Y. *et al.* (2018) 'Management of complications of ketamine abuse: 10 years' experience in Hong Kong', *Hong Kong Medical Journal*. doi: 10.12809/hkmj177086.

Hossler, F. E. *et al.* (2013) 'Microvascular architecture of mouse urinary bladder described with vascular corrosion casting, light microscopy, SEM, and TEM', *Microscopy and Microanalysis*. Cambridge University Press, 19(06), pp. 1428–1435. doi: 10.1017/S143192761301341X.

Hossler, F. E. and Kao, R. L. (2007) 'Microvasculature of the urinary bladder of the dog: A study using vascular corrosion casting', *Microscopy and Microanalysis*. Cambridge University Press, 13(03), pp. 220–227. doi: 10.1017/S1431927607070249.

Hossler, F. E. and Monson, F. C. (1995) 'Microvasculature of the rabbit urinary bladder', *The Anatomical Record*. Wiley-Blackwell, 243(4), pp. 438–448. doi: 10.1002/ar.1092430406.

Hossler, F., Kao, R. and Monson, F. (2005) 'Microvasculature of the mammalian urinary bladder - A preliminary comparative study using corrosion casting', *Microscopy and Microanalysis*, 11(S02). doi: 10.1017/S1431927605502356.

Hsieh, J.-T. *et al.* (2011) 'R11, a novel cell-permeable peptide, as an intravesical delivery

vehicle', *BJU International*. John Wiley & Sons, Ltd (10.1111), 108(10), pp. 1666–1671. doi: 10.1111/j.1464-410X.2011.10185.x.

Huang, C.-J. *et al.* (2018) 'Clinical significance of interleukin-6 and inducible nitric oxide synthase in ketamine-induced cystitis.', *International journal of molecular medicine*. Spandidos Publications, 41(2), pp. 836–844. doi: 10.3892/ijmm.2017.3264.

Huang, L.-K. *et al.* (2014) 'Evaluation of the extent of ketamine-induced uropathy: the role of CT urography.', *Postgraduate medical journal*. BMJ Publishing Group, 90(1062), pp. 185–90. doi: 10.1136/postgradmedj-2013-131776.

Hunner, G. L. (1915) 'A rare type of bladder ulcer in women; report of cases', *The Boston Medical and Surgical Journal*, 172(18), pp. 660–664. doi: 10.1056/NEJM191505061721802.

Hwang, P. *et al.* (1997) 'Efficacy of pentosan polysulfate in the treatment of interstitial cystitis: A meta-analysis', *Urology*. Elsevier, 50(1), pp. 39–43. doi: 10.1016/S0090-4295(97)00110-6.

Hwang, T.-L. *et al.* (2009) 'Permeation enhancer-containing water-in-oil nanoemulsions as carriers for intravesical cisplatin delivery', *Pharmaceutical Research*. Springer US, 26(10), pp. 2314–2323. doi: 10.1007/s11095-009-9947-6.

Hypolite, J. A. *et al.* (1993) 'Metabolic studies on rabbit bladder smooth muscle and mucosa.', *Molecular and cellular biochemistry*, 125(1), pp. 35–42. doi: 10.1007/bf00926832.

Ibeawuchi, C. U., Ajayi, O. I. and Ebeigbe, A. B. (2008) 'Vascular effect of ketamine in isolated rabbit aortic smooth muscle.', *Nigerian journal of physiological sciences : official publication of the Physiological Society of Nigeria*, 23(1–2), pp. 85–8. doi: 10.4314/njps.v23i1-2.54935.

Ikeda, Y. *et al.* (2007) 'Role of gap junctions in spontaneous activity of the rat bladder.', *American journal of physiology. Renal physiology*. NIH Public Access, 293(4), pp. F1018–25. doi: 10.1152/ajprenal.00183.2007.

Imig, J. D., Breyer, M. D. and Breyer, R. M. (2002) 'Contribution of prostaglandin EP₂

receptors to renal microvascular reactivity in mice', *American Journal of Physiology-Renal Physiology*. American Physiological Society Bethesda, MD , 283(3), pp. F415–F422. doi: 10.1152/ajprenal.00351.2001.

Inoue, S. *et al.* (2012) 'Effect of silodosin on detrusor overactivity in the male spontaneously hypertensive rat', *BJU International*. John Wiley & Sons, Ltd (10.1111), 110(2b), pp. E118–E124. doi: 10.1111/j.1464-410X.2011.10814.x.

Inoue, T. and Gabella, G. (1991) 'A vascular network closely linked to the epithelium of the urinary bladder of the rat.', *Cell and tissue research*, 263(1), pp. 137–43. doi: 10.1007/bf00318409.

Inscho, E. W., Carmines, P. K. and Navar, L. G. (1990) 'Prostaglandin influences on afferent arteriolar responses to vasoconstrictor agonists.', *The American journal of physiology*, 259(1 Pt 2), pp. F157-63. doi: 10.1152/ajprenal.1990.259.1.F157.

Irwin, D. E. *et al.* (2006) 'Population-based survey of urinary incontinence, overactive bladder, and other lower urinary tract symptoms in five countries: results of the EPIC study', *European Urology*. Elsevier, 50(6), pp. 1306–1315. doi: 10.1016/j.eururo.2006.09.019.

Irwin, D. E. *et al.* (2011) 'Worldwide prevalence estimates of lower urinary tract symptoms, overactive bladder, urinary incontinence and bladder outlet obstruction', *BJU International*. Blackwell Publishing Ltd, 108(7), pp. 1132–1138. doi: 10.1111/j.1464-410X.2010.09993.x.

Ishihama, H. *et al.* (2006) 'Activation of α_{1D} Adrenergic Receptors in the Rat Urothelium Facilitates the Micturition Reflex', *Journal of Urology*, 175(1), pp. 358–364. doi: 10.1016/S0022-5347(05)00016-9.

Ishizuka, O., Mattiasson, A. and Andersson, K. E. (1995) 'Prostaglandin E2-induced bladder hyperactivity in normal, conscious rats: involvement of tachykinins?', *The Journal of urology*, 153(6), pp. 2034–8. doi: 10.1016/s0022-5347(01)67397-x.

lu, H.-T., Jiang, Y.-H. and Kuo, H.-C. (2015) 'Alteration of urothelial inflammation, apoptosis, and junction protein in patients with various bladder conditions and storage bladder symptoms suggest common pathway involved in underlying pathophysiology',

LUTS: Lower Urinary Tract Symptoms. Blackwell Publishing Asia Pty Ltd, 7(2), pp. 102–107. doi: 10.1111/luts.12062.

Janssen, D. A. W. *et al.* (2013) 'The distribution and function of chondroitin sulfate and other sulfated glycosaminoglycans in the human bladder and their contribution to the protective bladder barrier', *The Journal of Urology*. Elsevier, 189(1), pp. 336–342. doi: 10.1016/J.JURO.2012.09.022.

Jeremy, J. Y. *et al.* (1987) 'Eicosanoid synthesis by human urinary bladder mucosa: pathological implications.', *British journal of urology*, 59(1), pp. 36–9. doi: 10.1111/j.1464-410x.1987.tb04575.x.

Jhang, J.-F. *et al.* (2014) 'Elevated serum IgE may be associated with development of ketamine cystitis', *The Journal of Urology*. Elsevier, 192(4), pp. 1249–1256. doi: 10.1016/J.JURO.2014.05.084.

Jhang, J.-F. *et al.* (2016) 'The role of immunoglobulin E in the pathogenesis of ketamine related cystitis and ulcerative interstitial cystitis: an immunohistochemical study.', *Pain physician*, 19(4), pp. E581-7. Available at: <http://www.ncbi.nlm.nih.gov/pubmed/27228524> (Accessed: 1 August 2017).

Jhang, J.-F. *et al.* (2018) 'Histopathological characteristics of ketamine-associated uropathy and their clinical association', *Neurourology and Urodynamics*. Wiley-Blackwell, 37(5), pp. 1764–1772. doi: 10.1002/nau.23514.

Jhang, J.-F., Hsu, Y.-H. and Kuo, H.-C. (2015) 'Possible pathophysiology of ketamine-related cystitis and associated treatment strategies', *International Journal of Urology*, 22(9), pp. 816–825. doi: 10.1111/iju.12841.

de Jongh, R. *et al.* (2007) 'The effects of exogenous prostaglandins and the identification of constitutive cyclooxygenase I and II immunoreactivity in the normal guinea pig bladder', *BJU International*. John Wiley & Sons, Ltd (10.1111), 100(2), pp. 419–429. doi: 10.1111/j.1464-410X.2007.07011.x.

de Jongh, R. *et al.* (2009) 'The localization of cyclo-oxygenase immuno-reactivity (COX I-IR) to the urothelium and to interstitial cells in the bladder wall.', *Journal of cellular and molecular medicine*. Wiley-Blackwell, 13(9B), pp. 3069–81. doi: 10.1111/j.1582-

4934.2008.00475.x.

Juan, Y.-S. *et al.* (2009) 'The Effect of ischemia/reperfusion on rabbit bladder—role of Rho-kinase and smooth muscle regulatory proteins', *Urology*. Elsevier, 73(5), pp. 1126–1130. doi: 10.1016/J.UROLOGY.2008.02.063.

Juan, Y.-S. *et al.* (2015) 'Translocation of NF-κB and expression of cyclooxygenase-2 are enhanced by ketamine-induced ulcerative cystitis in rat bladder', *The American Journal of Pathology*, 185(8), pp. 2269–2285. doi: 10.1016/j.ajpath.2015.04.020.

Jung, I. and Jung, S. H. (2012) 'Vasorelaxant mechanisms of ketamine in rabbit renal artery', *Korean Journal of Anesthesiology*, 63(6), p. 533. doi: 10.4097/kjae.2012.63.6.533.

Juszczak, K. *et al.* (2009) 'Urodynamic effects of the bladder C-fiber afferent activity modulation in chronic model of overactive bladder in rats.', *Journal of physiology and pharmacology : an official journal of the Polish Physiological Society*, 60(4), pp. 85–91. doi: 10.1016/S1569-9056(09)74822-5.

Kang, B. S. *et al.* (1990) 'Effects of ketamine on contractile responses in vascular smooth muscle', *Yonsei Medical Journal*, 31(4), p. 325. doi: 10.3349/ymj.1990.31.4.325.

Kang, S. H. *et al.* (2019) 'Assessment of stem cell viability in the initial healing period in rabbits with a cranial bone defect according to the type and form of scaffold', *Journal of Periodontal and Implant Science*. Korean Academy of Periodontology, 49(4), pp. 258–267. doi: 10.5051/jpis.2019.49.4.258.

Kanmur, Y. *et al.* (1993) 'Effects of ketamine on contraction and synthesis of inositol 1,4,5-trisphosphate in smooth muscle of the rabbit mesenteric artery', *Anesthesiology*. [American Society of Anesthesiologists, etc.], 79(3), pp. 571–579. doi: 10.1097/00000542-199309000-00022.

Kanmura, Y., Missiaen, L. and Casteels, R. (1996) 'The effects of ketamine on Ca²⁺ movements in A7r5 vascular smooth muscle cells.', *Anesthesia and analgesia*, 83(5), pp. 1105–9. doi: 10.1097/00000539-199611000-00036.

Kanmura, Y., Yoshitake, J. and Casteels, R. (1989) 'Ketamine-induced relaxation in intact

and skinned smooth muscles of the rabbit ear artery.', *British journal of pharmacology*. Wiley-Blackwell, 97(2), pp. 591–7. doi: 10.1111/j.1476-5381.1989.tb11990.x.

Karavana, S. Y. *et al.* (2018) 'Gemcitabine hydrochloride microspheres used for intravesical treatment of superficial bladder cancer: a comprehensive in vitro/ex vivo/in vivo evaluation.', *Drug design, development and therapy*. Dove Press, 12, pp. 1959–1975. doi: 10.2147/DDDT.S164704.

Kawamura, H. *et al.* (2004) 'Effects of angiotensin II on the pericyte-containing microvasculature of the rat retina', *The Journal of Physiology*. Wiley-Blackwell, 561(3), pp. 671–683. doi: 10.1113/jphysiol.2004.073098.

Ke, X. *et al.* (2018) 'The profile of cognitive impairments in chronic ketamine users', *Psychiatry Research*. Elsevier, 266, pp. 124–131. doi: 10.1016/J.PSYCHRES.2018.05.050.

Keay, S. *et al.* (2003) 'Changes in human bladder epithelial cell gene expression associated with interstitial cystitis or antiproliferative factor treatment', *Physiological Genomics*. American Physiological Society, 14(2), pp. 107–115. doi: 10.1152/physiolgenomics.00055.2003.

Kerec, M. *et al.* (2002) 'The enhancement of pipemidic acid permeation into the pig urinary bladder wall', *International Journal of Pharmaceutics*. Elsevier, 240(1–2), pp. 33–36. doi: 10.1016/S0378-5173(02)00108-4.

Kershen, R. T., Azadzo, K. M. and Siroky, M. B. (2002) 'Blood flow, pressure and compliance in the male human bladder', *Journal of Urology*, 168(1), pp. 121–125. doi: 10.1016/S0022-5347(05)64843-4.

Khalaf, I. M. *et al.* (1979) 'Release of prostaglandins into the pelvic venous blood of dogs in response to vesical distension and pelvic nerve stimulation.', *Investigative urology*, 17(3), pp. 244–7. Available at: <http://www.ncbi.nlm.nih.gov/pubmed/500325> (Accessed: 19 June 2019).

Kidger, E. *et al.* (2016) 'A rare urachal cyst in a case of ketamine-induced cystitis provides mechanistic insights', *Urology*, 90, pp. 223.e1–223.e7. doi: 10.1016/j.urology.2015.12.015.

Kim, A. *et al.* (2016) 'Mesenchymal stem cells protect against the tissue fibrosis of ketamine-induced cystitis in rat bladder.', *Scientific reports*. Nature Publishing Group, 6, p. 30881. doi: 10.1038/srep30881.

Kim, J. C. *et al.* (2005) 'Changes of urinary nerve growth factor and prostaglandins in male patients with overactive bladder symptom', *International Journal of Urology*. John Wiley & Sons, Ltd (10.1111), 12(10), pp. 875–880. doi: 10.1111/j.1442-2042.2005.01140.x.

Kim, J. C. *et al.* (2006) 'Nerve growth factor and prostaglandins in the urine of female patients with overactive bladder', *Journal of Urology*, 175(5), pp. 1773–1776. doi: 10.1016/S0022-5347(05)00992-4.

Kim, J. W. *et al.* (2013) 'Effects of coenzyme Q10 on bladder dysfunction induced by chronic bladder ischemia in a rat model', *Journal of Urology*, 189(6), pp. 2371–2376. doi: 10.1016/j.juro.2012.12.101.

Klockgether-Radke, A. P. *et al.* (2005) 'Ketamine enantiomers differentially relax isolated coronary artery rings.', *European journal of anaesthesiology*, 22(3), pp. 215–21. doi: 10.1017/s0265021505000372.

Kobayashi, E. *et al.* (2012) 'The pig as a model for translational research: overview of porcine animal models at Jichi Medical University.', *Transplantation research*. BioMed Central, 1(1), p. 8. doi: 10.1186/2047-1440-1-8.

Kopacz, D. J. and Bernards, C. M. (2001) 'Effect of clonidine on lidocaine clearance in vivo', *Anesthesiology*. [American Society of Anesthesiologists, etc.], 95(6), pp. 1371–1376. doi: 10.1097/00000542-200112000-00015.

Kornfield, T. E. and Newman, E. A. (2014) 'Regulation of blood flow in the retinal trilaminar vascular network.', *The Journal of neuroscience : the official journal of the Society for Neuroscience*. Society for Neuroscience, 34(34), pp. 11504–13. doi: 10.1523/JNEUROSCI.1971-14.2014.

Koroäec, P. and Jezernik, K. (2000) 'Early cellular and ultrastructural response of the mouse urinary bladder urothelium to ischemia', *Virchows Archiv*. Springer-Verlag, 436(4), pp. 377–383. doi: 10.1007/s004280050462.

Krska, L. (2017) 'The role of the bladder microbiome in lower urinary tract disorders'. Available at: <https://kar.kent.ac.uk/73522/> (Accessed: 5 June 2019).

Kumar, V. *et al.* (2010) 'In vitro release of adenosine triphosphate from the urothelium of human bladders with detrusor overactivity, both neurogenic and idiopathic', *European Urology*. Elsevier, 57(6), pp. 1087–1092. doi: 10.1016/J.EURURO.2009.11.042.

Kumar, V., Chapple, C. C. and Chess-Williams, R. (2004) 'Characteristics of adenosine triphosphatase release from porcine and human normal bladder', *Journal of Urology*, 172(2), pp. 744–747. doi: 10.1097/01.ju.0000131244.67160.f4ABSTRACT.

Kur, J., Newman, E. A. and Chan-Ling, T. (2012) 'Cellular and physiological mechanisms underlying blood flow regulation in the retina and choroid in health and disease.', *Progress in retinal and eye research*, 31(5), pp. 377–406. doi: 10.1016/j.preteyeres.2012.04.004.

Kushida, N. and Fry, C. H. (2016) 'On the origin of spontaneous activity in the bladder', *BJU International*. John Wiley & Sons, Ltd (10.1111), 117(6), pp. 982–992. doi: 10.1111/bju.13240.

Kuzmuk, K. N. and Schook, L. B. (2010) 'Pigs as a model for biomedical sciences.', in *The genetics of the pig*. 2nd edn. Wallingford: CABI, pp. 426–444. doi: 10.1079/9781845937560.0426.

Lai, Y. *et al.* (2012) 'Ketamine-associated urinary tract dysfunction: an underrecognized clinical entity.', *Urologia internationalis*. Karger Publishers, 89(1), pp. 93–6. doi: 10.1159/000338098.

Laitinen, L. (1987) 'Griffonia simplicifolia lectins bind specifically to endothelial cells and some epithelial cells in mouse tissues.', *The Histochemical journal*, 19(4), pp. 225–34. doi: 10.1007/bf01680633.

Lam, D. S. H. *et al.* (2000) 'Angiotensin II in child urinary bladder: functional and autoradiographic studies', *BJU International*. John Wiley & Sons, Ltd (10.1111), 86(4), pp. 494–501. doi: 10.1046/j.1464-410X.2000.00771.x.

Landis, E. M. (1933) 'Factors controlling the movement of fluid through the human

capillary wall.', *The Yale journal of biology and medicine*, 5(3), pp. 201–25. Available at: <https://www.ncbi.nlm.nih.gov/pmc/articles/PMC2606466/pdf/yjbm00565-0001.pdf> (Accessed: 1 July 2019).

Lapointe, S. P. *et al.* (2001) 'The effects of intravesical lidocaine on bladder dynamics of children with myelomeningocele', *The Journal of Urology*, 165(6 Pt 2), pp. 2380–2382. doi: 10.1097/00005392-200106001-00041.

Lawrence, J. M. *et al.* (2008) 'Prevalence and co-occurrence of pelvic floor disorders in community-dwelling women', *Obstetrics & Gynecology*, 111(3), pp. 678–685. doi: 10.1097/AOG.0b013e3181660c1b.

Leakakos, T. *et al.* (2003) 'Intravesical administration of doxorubicin to swine bladder using magnetically targeted carriers.', *Cancer chemotherapy and pharmacology*, 51(6), pp. 445–50. doi: 10.1007/s00280-003-0597-9.

Lee, C.-L., Jiang, Y.-H. and Kuo, H.-C. (2013) 'Increased apoptosis and suburothelial inflammation in patients with ketamine-related cystitis: a comparison with non-ulcerative interstitial cystitis and controls', *BJU International*. Wiley/Blackwell (10.1111), 112(8), pp. 1156–1162. doi: 10.1111/bju.12256.

Lee, H. and Cima, M. J. (2011) 'An intravesical device for the sustained delivery of lidocaine to the bladder', *Journal of Controlled Release*, 149(2), pp. 133–139. doi: 10.1016/j.jconrel.2010.10.016.

Lee, H. Y., Bardini, M. and Burnstock, G. (2000) 'Distribution of P2X receptors in the urinary bladder and in the ureter of the rat', *The Journal of Urology*. Elsevier, 163(6), pp. 2002–2007. doi: 10.1016/S0022-5347(05)67618-5.

Lee, S. W. *et al.* (2018) 'The therapeutic effect of human embryonic stem cell-derived multipotent mesenchymal stem cells on chemical-induced cystitis in rats.', *International neurourology journal*. Korean Continence Society, 22(Suppl 1), pp. S34-45. doi: 10.5213/inj.1836014.007.

Lee, T. S. *et al.* (1989) 'Characterization of endothelin receptors and effects of endothelin on diacylglycerol and protein kinase C in retinal capillary pericytes.', *Diabetes*. American Diabetes Association, 38(12), pp. 1643–6. doi: 10.2337/diab.38.12.1643.

Lee, W.-C. *et al.* (2018) 'Potential orphan drug therapy of intravesical liposomal onabotulinumtoxin-A for ketamine-induced cystitis by mucosal protection and anti-inflammation in a rat model.', *Scientific reports*. Nature Publishing Group, 8(1), p. 5795. doi: 10.1038/s41598-018-24239-9.

Lee, Y.-L. *et al.* (2017) 'Elucidating mechanisms of bladder repair after hyaluronan instillation in ketamine-induced ulcerative cystitis in animal model', *The American Journal of Pathology*, 187(9), pp. 1945–1959. doi: 10.1016/j.ajpath.2017.06.004.

Leiria, L. O. S. *et al.* (2011) 'Functional, morphological and molecular characterization of bladder dysfunction in streptozotocin-induced diabetic mice: evidence of a role for L-type voltage-operated Ca²⁺ channels.', *British journal of pharmacology*. Wiley-Blackwell, 163(6), pp. 1276–88. doi: 10.1111/j.1476-5381.2011.01311.x.

LeMaistre, J. L. *et al.* (2012) 'Coactivation of NMDA receptors by glutamate and -serine induces dilation of isolated middle cerebral arteries', *Journal of Cerebral Blood Flow & Metabolism*. SAGE Publications, 32(3), p. 537. doi: 10.1038/JCBFM.2011.161.

Leppilahti, M. *et al.* (2002) 'Prevalence of symptoms related to interstitial cystitis in women: a population based study in finland', *The Journal of Urology*. Elsevier, 168(1), pp. 139–143. doi: 10.1016/S0022-5347(05)64847-1.

Lewis, S. A. (2000) 'Everything you wanted to know about the bladder epithelium but were afraid to ask', *American Journal of Physiology-Renal Physiology*, 278(6), pp. F867–F874. doi: 10.1152/ajprenal.2000.278.6.F867.

Lewis, S. A. and Lewis, J. R. (2006) 'Kinetics of urothelial ATP release', *American Journal of Physiology-Renal Physiology*. American Physiological Society, 291(2), pp. F332–F340. doi: 10.1152/ajprenal.00340.2005.

Li, C.-C. *et al.* (2019) 'A survey for ketamine abuse and its relation to the lower urinary tract symptoms in Taiwan.', *Scientific reports*. Nature Publishing Group, 9(1), p. 7240. doi: 10.1038/s41598-019-43746-x.

Li, C. *et al.* (2014) 'Quantitative elasticity measurement of urinary bladder wall using laser-induced surface acoustic waves.', *Biomedical optics express*. Optical Society of America, 5(12), pp. 4313–28. doi: 10.1364/BOE.5.004313.

- Li, J.-H. *et al.* (2011) 'To use or not to use: an update on licit and illicit ketamine use', *Substance Abuse and Rehabilitation*. Dove Medical Press Ltd., p. 11. doi: 10.2147/sar.s15458.
- Li, N. *et al.* (2010) 'mTOR-dependent synapse formation underlies the rapid antidepressant effects of NMDA antagonists.', *Science (New York, N.Y.)*. NIH Public Access, 329(5994), pp. 959–64. doi: 10.1126/science.1190287.
- Liao, Y., Tang, Y. and Hao, W. (2017) 'Ketamine and international regulations', *The American Journal of Drug and Alcohol Abuse*. Taylor & Francis, 43(5), pp. 495–504. doi: 10.1080/00952990.2016.1278449.
- Lin, C.-C. *et al.* (2016) 'Microvascular injury in ketamine-induced bladder dysfunction', *PLOS ONE*. Edited by J. Kim. Public Library of Science, 11(8), p. e0160578. doi: 10.1371/journal.pone.0160578.
- Lin, C.-C., Yang, A.-H. and Lin, A. T.-L. (2017) 'Activation of the mTOR dependent signaling pathway underlies ketamine-induced uropathy', *Neurourology and Urodynamics*. doi: 10.1002/nau.23234.
- Lin, H.-C. *et al.* (2015) 'Histopathological assessment of inflammation and expression of inflammatory markers in patients with ketamine-induced cystitis.', *Molecular medicine reports*, 11(4), pp. 2421–8. doi: 10.3892/mmr.2014.3110.
- Liu, K.-M. *et al.* (2015) 'Ketamine-induced ulcerative cystitis and bladder apoptosis involve oxidative stress mediated by mitochondria and the endoplasmic reticulum', *American Journal of Physiology-Renal Physiology*, 309(4), pp. F318–F331. doi: 10.1152/ajprenal.00607.2014.
- Liu, S. Y. W. *et al.* (2017) 'Clinical pattern and prevalence of upper gastrointestinal toxicity in patients abusing ketamine', *Journal of Digestive Diseases*. Wiley/Blackwell (10.1111), 18(9), pp. 504–510. doi: 10.1111/1751-2980.12512.
- Lokeshwar, V. B. *et al.* (2005) 'Urinary uronate and sulfated glycosaminoglycan levels: markers for interstitial cystitis severity', *The Journal of Urology*. Elsevier, 174(1), pp. 344–349. doi: 10.1097/01.JU.0000161599.69942.2E.

Longnecker, D. E., Ross, D. C. and Silver, I. A. (1982) 'Anesthetic influence on arteriolar diameters and tissue oxygen tension in hemorrhaged rats', *Anesthesiology*, 57(3), pp. 177–182. doi: 10.1097/00000542-198209000-00006.

Lugnani, F. *et al.* (2008) 'Iontophoresis of drugs in the bladder wall: equipment and preliminary studies', *Artificial Organs*. John Wiley & Sons, Ltd (10.1111), 17(1), pp. 8–17. doi: 10.1111/j.1525-1594.1993.tb00378.x.

Lukacz, E. S. *et al.* (2011) 'A healthy bladder: a consensus statement.', *International journal of clinical practice*. Wiley-Blackwell, 65(10), pp. 1026–36. doi: 10.1111/j.1742-1241.2011.02763.x.

Lundy, P. M. and Frew, R. (1981) 'Ketamine potentiates catecholamine responses of vascular smooth muscle by inhibition of extraneuronal uptake', *Canadian Journal of Physiology and Pharmacology*. NRC Research Press Ottawa, Canada, 59(6), pp. 520–527. doi: 10.1139/y81-078.

Lv, Y.-S. *et al.* (2012) 'Intravesical hyaluronic acid and alkalinized lidocaine for the treatment of severe painful bladder syndrome/interstitial cystitis', *International Urogynecology Journal*. Springer-Verlag, 23(12), pp. 1715–1720. doi: 10.1007/s00192-012-1802-3.

Maggi, C. A. *et al.* (1989) 'Potent contractile activity of endothelin on the human isolated urinary bladder.', *British journal of pharmacology*. Wiley-Blackwell, 96(4), pp. 755–7. doi: 10.1111/j.1476-5381.1989.tb11879.x.

Mak, S. K. *et al.* (2011) 'Lower urinary tract changes in young adults using ketamine', *Journal of Urology*, 186(2), pp. 610–614. doi: 10.1016/j.juro.2011.03.108.

Malde, S. *et al.* (2018) 'Guideline of guidelines: bladder pain syndrome', *BJU International*. Wiley/Blackwell (10.1111), 122(5), pp. 729–743. doi: 10.1111/bju.14399.

Mansfield, K. J. *et al.* (2005) 'Muscarinic receptor subtypes in human bladder detrusor and mucosa, studied by radioligand binding and quantitative competitive RT-PCR: changes in ageing.', *British journal of pharmacology*. Wiley-Blackwell, 144(8), pp. 1089–99. doi: 10.1038/sj.bjp.0706147.

Mason, K. *et al.* (2010) 'Ketamine-associated lower urinary tract destruction: a new radiological challenge', *Clinical Radiology*. W.B. Saunders, 65(10), pp. 795–800. doi: 10.1016/J.CRAD.2010.05.003.

Matsuoka, P. K. *et al.* (2012) 'Intravesical treatment of painful bladder syndrome: a systematic review and meta-analysis', *International Urogynecology Journal*. Springer-Verlag, 23(9), pp. 1147–1153. doi: 10.1007/s00192-012-1686-2.

Mazzoni, J., Cutforth, T. and Agalliu, D. (2015) 'Dissecting the role of smooth muscle cells versus pericytes in regulating cerebral blood flow using in vivo optical imaging', *Neuron*. Cell Press, 87(1), pp. 4–6. doi: 10.1016/J.NEURON.2015.06.024.

Meng, E. *et al.* (2011) 'Involvement of purinergic neurotransmission in ketamine induced bladder dysfunction', *The Journal of Urology*. Elsevier, 186(3), pp. 1134–1141. doi: 10.1016/j.juro.2011.04.102.

Meng, E. *et al.* (2015) 'Intravesical hyaluronic acid treatment for ketamine-associated cystitis: Preliminary results', *Urological Science*. No longer published by Elsevier, 26(3), pp. 176–179. doi: 10.1016/J.UROLS.2015.07.001.

Merrill, L. *et al.* (2016) 'Receptors, channels and signalling in the urothelial sensory system in the bladder', *Nature Reviews Urology*. Nature Publishing Group, 13(4), pp. 193–204. doi: 10.1038/nrurol.2016.13.

Michel, M. C. and Vrydag, W. (2006) ' α 1-, α 2- and β -adrenoceptors in the urinary bladder, urethra and prostate', *British Journal of Pharmacology*. Wiley-Blackwell, 147(Suppl 2), p. S88. doi: 10.1038/SJ.BJP.0706619.

Middela, S. and Pearce, I. (2011) 'Ketamine-induced vesicopathy: a literature review', *International Journal of Clinical Practice*. Wiley/Blackwell (10.1111), 65(1), pp. 27–30. doi: 10.1111/j.1742-1241.2010.02502.x.

Miftahof, R. N. and Nam, H. G. (2013) *Biomechanics of the human urinary bladder*. Berlin, Heidelberg: Springer Berlin Heidelberg. doi: 10.1007/978-3-642-36146-3.

Mills, I. W. *et al.* (2000) 'Studies of the pathophysiology of idiopathic detrusor instability: the physiological properties of the detrusor smooth muscle and its pattern of

innervation.', *The Journal of urology*, 163(2), pp. 646–51. doi: 10.1016/s0022-5347(05)67951-7.

Milsom, I. *et al.* (2014) 'Global prevalence and economic burden of urgency urinary incontinence: a systematic review.', *European urology*. Elsevier, 65(1), pp. 79–95. doi: 10.1016/j.eururo.2013.08.031.

Miodoński, A. J. and Litwin, J. A. (1999) 'Microvascular architecture of the human urinary bladder wall: a corrosion casting study.', *The Anatomical record*, 254(3), pp. 375–81. doi: 10.1002/(SICI)1097-0185(19990301)254:3<375::AID-AR8>3.0.CO;2-R.

Mion, G. (2017) 'History of anaesthesia: The ketamine story - past, present and future.', *European journal of anaesthesiology*, 34(9), pp. 571–575. doi: 10.1097/EJA.0000000000000638.

Mion, G. and Villeveille, T. (2013) 'Ketamine pharmacology: An update (pharmacodynamics and molecular aspects, recent findings)', *CNS Neuroscience and Therapeutics*, pp. 370–380. doi: 10.1111/cns.12099.

Mitsui, R. and Hashitani, H. (2013) 'Immunohistochemical characteristics of suburothelial microvasculature in the mouse bladder', *Histochemistry and Cell Biology*. Springer Berlin Heidelberg, 140(2), pp. 189–200. doi: 10.1007/s00418-012-1074-5.

Mitsui, R. and Hashitani, H. (2015) 'Functional properties of submucosal venules in the rat stomach', *Pflügers Archiv - European Journal of Physiology*. Springer Berlin Heidelberg, 467(6), pp. 1327–1342. doi: 10.1007/s00424-014-1576-1.

Mitsui, R. and Hashitani, H. (2016) 'Mechanisms underlying spontaneous constrictions of postcapillary venules in the rat stomach', *Pflügers Archiv - European Journal of Physiology*. Springer Berlin Heidelberg, 468(2), pp. 279–291. doi: 10.1007/s00424-015-1752-y.

Moch, C. *et al.* (2014) 'Bladder tissue permeability and transport modelling of intravesical alum, lidocaine hydrochloride, methylprednisolone hemisuccinate and mitomycin C', *International Journal of Pharmaceutics*, 464(1), pp. 91–103. doi: 10.1016/j.ijpharm.2014.01.021.

Moore, K. A. *et al.* (2001) 'Urine concentrations of ketamine and norketamine following illegal consumption.', *Journal of analytical toxicology*, 25(7), pp. 583–8. doi: 10.1093/jat/25.7.583.

Morales, A. *et al.* (1996) 'Intravesical hyaluronic acid in the treatment of refractory interstitial cystitis', *The Journal of Urology*. Elsevier, 156(1), pp. 45–48. doi: 10.1016/S0022-5347(01)65933-0.

Mori, K. *et al.* (2016) 'Age-related changes in bladder function with altered angiotensin II receptor mechanisms in rats', *Neurourology and Urodynamics*. John Wiley & Sons, Ltd, 35(8), pp. 908–913. doi: 10.1002/nau.22849.

Moro, C. and Chess-Williams, R. (2012) 'Non-adrenergic, non-cholinergic, non-purinergeric contractions of the urothelium/lamina propria of the pig bladder', *Autonomic and Autacoid Pharmacology*. John Wiley & Sons, Ltd (10.1111), 32(3–4), pp. 53–59. doi: 10.1111/aap.12000.

Moro, C., Leeds, C. and Chess-Williams, R. (2012) 'Contractile activity of the bladder urothelium/lamina propria and its regulation by nitric oxide', *European Journal of Pharmacology*. Elsevier, 674(2–3), pp. 445–449. doi: 10.1016/j.ejphar.2011.11.020.

Moro, C., Tajouri, L. and Chess-Williams, R. (2013) 'Adrenoceptor function and expression in bladder urothelium and lamina propria', *Urology*. Elsevier, 81(1), pp. 211.e1-211.e7. doi: 10.1016/j.urology.2012.09.011.

Moussawi, K. *et al.* (2011) 'Extracellular glutamate: Functional compartments operate in different concentration ranges', *Frontiers in Systems Neuroscience*, (NOVEMBER 2011). doi: 10.3389/fnsys.2011.00094.

Muetzelfeldt, L. *et al.* (2008) 'Journey through the K-hole: Phenomenological aspects of ketamine use', *Drug and Alcohol Dependence*. Elsevier, 95(3), pp. 219–229. doi: 10.1016/J.DRUGALCDEP.2008.01.024.

Murrant, C. L. *et al.* (2014) 'Prostaglandins induce vasodilatation of the microvasculature during muscle contraction and induce vasodilatation independent of adenosine.', *The Journal of physiology*. Wiley-Blackwell, 592(6), pp. 1267–81. doi: 10.1113/jphysiol.2013.264259.

Nakahata, N., Ono, T. and Nakanishi, H. (1987) 'Contribution of prostaglandin E2 to bradykinin-induced contraction in rabbit urinary detrusor.', *The Japanese Journal of Pharmacology*. The Japanese Pharmacological Society, 43(4), pp. 351–359. doi: 10.1254/jjp.43.351.

Nambiar, A. K. *et al.* (2016) 'Alkalinized lidocaine versus lidocaine gel as local anesthesia prior to intra-vesical botulinum toxin (BoNTA) injections: A prospective, single center, randomized, double-blind, parallel group trial of efficacy and morbidity', *Neurourology and Urodynamics*, 35(4), pp. 522–527. doi: 10.1002/nau.22750.

Narumiya, S., Sugimoto, Y. and Ushikubi, F. (1999) 'Prostanoid receptors: structures, properties, and functions', *Physiological Reviews*. American Physiological Society Bethesda, MD, 79(4), pp. 1193–1226. doi: 10.1152/physrev.1999.79.4.1193.

National Center for Biotechnology Information (no date) *Ketamine hydrochloride* / *C13H17Cl2NO* - *PubChem*. Available at: <https://pubchem.ncbi.nlm.nih.gov/compound/Ketamine-hydrochloride> (Accessed: 29 July 2019).

National Institute for Health and Care Excellence (2014) *Interstitial cystitis: dimethyl sulfoxide bladder instillation*. Available at: <https://www.nice.org.uk/advice/esuom26/chapter/Key-points-from-the-evidence> (Accessed: 12 November 2018).

Negrete, H. O. *et al.* (1996) 'Permeability properties of the intact mammalian bladder epithelium', *American Journal of Physiology-Renal Physiology*, 271(4), pp. F886–F894. doi: 10.1152/ajprenal.1996.271.4.F886.

Nehls, V. (1991) 'Heterogeneity of microvascular pericytes for smooth muscle type alpha-actin', *The Journal of Cell Biology*. The Rockefeller University Press, 113(1), pp. 147–154. doi: 10.1083/jcb.113.1.147.

Neuhaus, A. A. *et al.* (2017) 'Novel method to study pericyte contractility and responses to ischaemia in vitro using electrical impedance.', *Journal of cerebral blood flow and metabolism: official journal of the International Society of Cerebral Blood Flow and Metabolism*. SAGE Publications, 37(6), pp. 2013–2024. doi:

10.1177/0271678X16659495.

Neuhaus, J. *et al.* (2018) '3D-electron microscopic characterization of interstitial cells in the human bladder upper lamina propria', *Neurourology and Urodynamics*. John Wiley & Sons, Ltd, 37(1), pp. 89–98. doi: 10.1002/nau.23270.

Ng, S. H. *et al.* (2010) 'Emergency department presentation of ketamine abusers in Hong Kong: a review of 233 cases.', *Hong Kong medical journal = Xianggang yi xue za zhi*, 16(1), pp. 6–11. Available at: <http://www.ncbi.nlm.nih.gov/pubmed/20124567> (Accessed: 22 January 2019).

Nguan, C. *et al.* (2005) 'A prospective, double-blind, randomized cross-over study evaluating changes in urinary pH for relieving the symptoms of interstitial cystitis', *BJU International*. John Wiley & Sons, Ltd (10.1111), 95(1), pp. 91–94. doi: 10.1111/j.1464-410X.2004.05257.x.

NICE (2013) 'Urinary incontinence in women: management | Guidance and guidelines | NICE'. NICE. Available at: <https://www.nice.org.uk/guidance/cg171> (Accessed: 21 February 2018).

Nickel, J. C. *et al.* (2009) 'Intravesical alkalinized lidocaine (PSD597) offers sustained relief from symptoms of interstitial cystitis and painful bladder syndrome.', *BJU international*, 103(7), pp. 910–8. doi: 10.1111/j.1464-410X.2008.08162.x.

Nickel, J. C. *et al.* (2012) 'Continuous intravesical lidocaine treatment for interstitial cystitis/bladder pain syndrome: safety and efficacy of a new drug delivery device', *Science Translational Medicine*, 4(143).

Nile, C. J. and Gillespie, J. I. (2012) 'Interactions between cholinergic and prostaglandin signaling elements in the urothelium: role for muscarinic type 2 receptors', *Urology*. Elsevier, 79(1), pp. 240.e17–240.e23. doi: 10.1016/j.urology.2011.08.029.

Nile, C. J., de Vente, J. and Gillespie, J. I. (2010) 'Stretch independent regulation of prostaglandin E 2 production within the isolated guinea-pig lamina propria', *BJU International*. John Wiley & Sons, Ltd (10.1111), 105(4), pp. 540–548. doi: 10.1111/j.1464-410X.2009.08705.x.

Nishimura, H. (2017) 'Renin-angiotensin system in vertebrates: phylogenetic view of structure and function', *Anatomical Science International*. Springer Japan, 92(2), pp. 215–247. doi: 10.1007/s12565-016-0372-8.

Noh, H. J. *et al.* (2009) 'The vasodilatory effect of ketamine is independent of the N-methyl-D-aspartate receptor: lack of functional N-methyl-D-aspartate receptors in rat mesenteric artery smooth muscle', *European Journal of Anaesthesiology*, 26(8), pp. 676–682. doi: 10.1097/EJA.0b013e32832a1704.

Nomiya, M. *et al.* (2012) 'The effect of atherosclerosis-induced chronic bladder ischemia on bladder function in the rat', *Neurourology and Urodynamics*. John Wiley & Sons, Ltd, 31(1), pp. 195–200. doi: 10.1002/nau.21073.

Nomiya, M., Burmeister, D. M., Sawada, N., Campeau, L., Zarifpour, M., Yamaguchi, O., *et al.* (2013) 'Effect of melatonin on chronic bladder-ischaemia-associated changes in rat bladder function', *BJU International*. John Wiley & Sons, Ltd (10.1111), 112(2), pp. E221–E230. doi: 10.1111/j.1464-410X.2012.11746.x.

Nomiya, M., Burmeister, D. M., Sawada, N., Campeau, L., Zarifpour, M., Keys, T., *et al.* (2013) 'Prophylactic effect of tadalafil on bladder function in a rat model of chronic bladder ischemia', *The Journal of Urology*. No longer published by Elsevier, 189(2), pp. 754–761. doi: 10.1016/J.JURO.2012.07.141.

Nomiya, M. *et al.* (2014) 'Progressive vascular damage may lead to bladder underactivity in rats', *Journal of Urology*, 191(5), pp. 1462–1469. doi: 10.1016/j.juro.2013.10.097.

Nomiya, M., Andersson, K.-E. and Yamaguchi, O. (2015) 'Chronic bladder ischemia and oxidative stress: New pharmacotherapeutic targets for lower urinary tract symptoms', *International Journal of Urology*. John Wiley & Sons, Ltd (10.1111), 22(1), pp. 40–46. doi: 10.1111/iju.12652.

Ogawa, K., Tanaka, S. and Murray, P. A. (2001) 'Inhibitory effects of etomidate and ketamine on endothelium-dependent relaxation in canine pulmonary artery', *Anesthesiology*. [American Society of Anesthesiologists, etc.], 94(4), pp. 668–677. doi: 10.1097/00000542-200104000-00022.

Oh, S.-J. *et al.* (2005) 'Effects of local anesthetics on human bladder contractility',

Neurourology and Urodynamics. Wiley Subscription Services, Inc., A Wiley Company, 24(3), pp. 288–294. doi: 10.1002/nau.20113.

Oravisto, K. J. (1975) 'Epidemiology of interstitial cystitis.', *Annales chirurgiae et gynaecologiae Fenniae*, 64(2), pp. 75–7. Available at: <http://www.ncbi.nlm.nih.gov/pubmed/1137336> (Accessed: 31 August 2018).

Osano, A. *et al.* (2014) 'Bladder endothelin-1 receptor binding of bosentan and ambrisentan', *Journal of Pharmacological Sciences*, 124(1), pp. 86–91. doi: 10.1254/jphs.13198FP.

Otsuka, A. *et al.* (2008) 'Expression and functional role of β -adrenoceptors in the human urinary bladder urothelium', *Naunyn-Schmiedeberg's Archives of Pharmacology*. Springer-Verlag, 377(4–6), pp. 473–481. doi: 10.1007/s00210-008-0274-y.

Oxford Health NHS Foundation Trust (no date) *Ketamine treatment service*. Available at: <https://www.oxfordhealth.nhs.uk/ketamine-service/> (Accessed: 29 July 2019).

Oxley, J. D. *et al.* (2009) 'Ketamine cystitis as a mimic of carcinoma in situ', *Histopathology*. Wiley/Blackwell (10.1111), 55(6), pp. 705–708. doi: 10.1111/j.1365-2559.2009.03437.x.

Pai, A. and Heining, M. (2007) 'Ketamine', *Continuing Education in Anaesthesia, Critical Care & Pain*. Oxford University Press, 7(2), pp. 59–63. doi: 10.1093/bjaceaccp/mkm008.

Pallone, T. L. (1994) 'Vasoconstriction of outer medullary vasa recta by angiotensin II is modulated by prostaglandin E₂.', *The American journal of physiology*. American Physiological Society Bethesda, MD, 266(6 Pt 2), pp. F850-7. doi: 10.1152/ajprenal.1994.266.6.F850.

Pan, Y. *et al.* (2017) 'In vivo biodistribution and toxicity of intravesical administration of quantum dots for optical molecular imaging of bladder cancer.', *Scientific reports*. Nature Publishing Group, 7(1), p. 9309. doi: 10.1038/s41598-017-08591-w.

Park, J. M. *et al.* (1997) 'Cyclooxygenase-2 is expressed in bladder during fetal development and stimulated by outlet obstruction', *American Journal of Physiology-Renal Physiology*. American Physiological Society Bethesda, MD, 273(4), pp. F538–F544.

doi: 10.1152/ajprenal.1997.273.4.F538.

Park, J. M. *et al.* (1998) 'Stretch activates heparin-binding EGF-like growth factor expression in bladder smooth muscle cells', *American Journal of Physiology-Cell Physiology*. American Physiological Society Bethesda, MD , 275(5), pp. C1247–C1254. doi: 10.1152/ajpcell.1998.275.5.C1247.

Park, S. W. *et al.* (2016) 'Facilitation of serotonin-induced contraction of rat mesenteric artery by ketamine', *The Korean Journal of Physiology & Pharmacology : Official Journal of the Korean Physiological Society and the Korean Society of Pharmacology*. Korean Physiological Society and Korean Society of Pharmacology, 20(6), p. 605. doi: 10.4196/KJPP.2016.20.6.605.

Parkin, M. C. *et al.* (2008) 'Detection of ketamine and its metabolites in urine by ultra high pressure liquid chromatography–tandem mass spectrometry', *Journal of Chromatography B*, 876(1), pp. 137–142. doi: 10.1016/j.jchromb.2008.09.036.

Parsons, B. A. and Drake, M. J. (2011) 'Animal models in overactive bladder research', in. Springer, Berlin, Heidelberg, pp. 15–43. doi: 10.1007/978-3-642-16499-6_2.

Parsons, C. L. *et al.* (1994) 'Abnormal sensitivity to intravesical potassium in interstitial cystitis and radiation cystitis', *Neurourology and Urodynamics*. Wiley-Blackwell, 13(5), pp. 515–520. doi: 10.1002/nau.1930130503.

Parsons, C. L. (2005) 'Successful downregulation of bladder sensory nerves with combination of heparin and alkalized lidocaine in patients with interstitial cystitis', *Urology*, 65(1), pp. 45–48. doi: 10.1016/j.urology.2004.08.056.

Parsons, C. L. (2007) 'The role of the urinary epithelium in the pathogenesis of interstitial cystitis/prostatitis/urethritis', *Urology*. Elsevier, 69(4), pp. S9–S16. doi: 10.1016/j.urology.2006.03.084.

Parsons, C. L. (2011) 'The role of a leaky epithelium and potassium in the generation of bladder symptoms in interstitial cystitis/overactive bladder, urethral syndrome, prostatitis and gynaecological chronic pelvic pain', *BJU International*. Wiley/Blackwell (10.1111), 107(3), pp. 370–375. doi: 10.1111/j.1464-410X.2010.09843.x.

Parsons, C. L. *et al.* (2012) 'Alkalinized lidocaine and heparin provide immediate relief of pain and urgency in patients with interstitial cystitis', *The Journal of Sexual Medicine*. Blackwell Publishing Inc, 9(1), pp. 207–212. doi: 10.1111/j.1743-6109.2011.02542.x.

Peeker, R. *et al.* (2000) 'Intravesical bacillus calmette-guerin and dimethyl sulfoxide for treatment of classic and nonulcer interstitial cystitis:: a prospective, randomized double-blind study', *The Journal of Urology*. Elsevier, 164(6), pp. 1912–1916. doi: 10.1016/S0022-5347(05)66916-9.

Peltoniemi, M. A. *et al.* (2016) 'Ketamine: a review of clinical pharmacokinetics and pharmacodynamics in anesthesia and pain therapy', *Clinical Pharmacokinetics*. Springer International Publishing, 55(9), pp. 1059–1077. doi: 10.1007/s40262-016-0383-6.

Peng, M. *et al.* (2016) 'High efficacy of intravesical treatment of metformin on bladder cancer in preclinical model.', *Oncotarget*. Impact Journals, LLC, 7(8), pp. 9102–17. doi: 10.18632/oncotarget.6933.

Peppiatt, C. M. *et al.* (2006) 'Bidirectional control of CNS capillary diameter by pericytes.', *Nature*. Europe PMC Funders, 443(7112), pp. 700–4. doi: 10.1038/nature05193.

Perez-Marrero, R., Emerson, L. E. and Feltis, J. T. (1988) 'A controlled study of dimethyl sulfoxide in interstitial cystitis', *The Journal of Urology*. Elsevier, 140(1), pp. 36–39. doi: 10.1016/S0022-5347(17)41478-9.

Perlman, R. L. (2016) 'Mouse models of human disease An evolutionary perspective', *Evolution*, pp. 170–176. doi: 10.1093/emph/eow014.

Persson, K. *et al.* (1992) 'Endothelin-1-induced contractions of isolated pig detrusor and vesical arterial smooth muscle: Calcium dependence and phosphoinositide hydrolysis', *General Pharmacology: The Vascular System*. Pergamon, 23(3), pp. 445–453. doi: 10.1016/0306-3623(92)90110-6.

Petrat, F. *et al.* (2012) 'Glycine, a simple physiological compound protecting by yet puzzling mechanism(s) against ischaemia-reperfusion injury: Current knowledge', *British Journal of Pharmacology*, pp. 2059–2072. doi: 10.1111/j.1476-5381.2011.01711.x.

Petrou, S. P. *et al.* (2009) 'Botulinum a toxin/dimethyl sulfoxide bladder instillations for women with refractory idiopathic detrusor overactivity: a phase 1/2 study.', *Mayo Clinic proceedings*. Mayo Foundation, 84(8), pp. 702–6. doi: 10.1016/S0025-6196(11)60520-X.

Pharmacopeial Convention, I. (ed.) (2016) *United States Pharmacopoeia-National Formulary*. Rockville, Md. Available at: USP-39 NF - 34.

Pinggera, Germar-Michael *et al.* (2008) 'Association of lower urinary tract symptoms and chronic ischaemia of the lower urinary tract in elderly women and men: assessment using colour Doppler ultrasonography', *BJU International*. John Wiley & Sons, Ltd (10.1111), 102(4), pp. 470–474. doi: 10.1111/j.1464-410X.2008.07587.x.

Pinggera, Germar-M. *et al.* (2008) 'α-blockers improve chronic ischaemia of the lower urinary tract in patients with lower urinary tract symptoms', *BJU International*. John Wiley & Sons, Ltd (10.1111), 101(3), pp. 319–324. doi: 10.1111/j.1464-410X.2007.07339.x.

Pinggera, G.-M. *et al.* (2014) 'Effect of tadalafil once daily on prostate blood flow and perfusion in men with lower urinary tract symptoms secondary to benign prostatic hyperplasia: a randomized, double-blind, multicenter, placebo-controlled trial.', *Urology*. Elsevier, 84(2), pp. 412–9. doi: 10.1016/j.urology.2014.02.063.

Pinna, C., Zanardo, R. and Puglisi, L. (2000) 'Prostaglandin-release impairment in the bladder epithelium of streptozotocin-induced diabetic rats', *European Journal of Pharmacology*. Elsevier, 388(3), pp. 267–273. doi: 10.1016/S0014-2999(99)00833-X.

Pode, D., Zylber-Katz, E. and Shapiro, A. (1992) 'Intravesical lidocaine: topical anesthesia for bladder mucosal biopsies.', *The Journal of urology*, 148(3), pp. 795–6. doi: 10.1016/s0022-5347(17)36722-8.

Ponholzer, A. *et al.* (2006) 'The association between vascular risk factors and lower urinary tract symptoms in both sexes', *European Urology*. Elsevier, 50(3), pp. 581–586. doi: 10.1016/j.eururo.2006.01.031.

Radu, F. *et al.* (2011) 'The effect of antioxidants on the response of the rabbit urinary bladder to in vitro ischemia/reperfusion', *Molecular and Cellular Biochemistry*. Springer

US, 355(1–2), pp. 65–73. doi: 10.1007/s11010-011-0839-9.

Rahnama'i, M. S. *et al.* (2010) 'Prostaglandin receptor EP1 and EP2 site in guinea pig bladder urothelium and lamina propria', *Journal of Urology*, 183(3), pp. 1241–1247. doi: 10.1016/j.juro.2009.11.004.

Rahnama'i, M. S. *et al.* (2011) 'The relationship between prostaglandin E receptor 1 and cyclooxygenase I expression in guinea pig bladder interstitial cells: proposition of a signal propagation system', *Journal of Urology*, 185(1), pp. 315–322. doi: 10.1016/j.juro.2010.09.005.

Rahnama'i, M. S. *et al.* (2012) 'The role of prostanoids in urinary bladder physiology', *Nature Reviews Urology*. Nature Publishing Group, 9(5), pp. 283–290. doi: 10.1038/nrurol.2012.33.

Rahnama'i, M. S. *et al.* (2013) 'The effect of indomethacin on the muscarinic induced contractions in the isolated normal guinea pig urinary bladder', *BMC Urology*. BioMed Central, 13, p. 8. doi: 10.1186/1471-2490-13-8.

Rajandram, R. *et al.* (2016) 'Intact urothelial barrier function in a mouse model of ketamine-induced voiding dysfunction.', *American journal of physiology. Renal physiology*. American Physiological Society, 310(9), pp. F885-94. doi: 10.1152/ajprenal.00483.2015.

Rajandram, R. *et al.* (2017) 'Oral ketamine induced pathological changes of the urinary tract in a rat model.', *The Malaysian journal of pathology*, 39(1), pp. 47–53. Available at: <http://www.ncbi.nlm.nih.gov/pubmed/28413205> (Accessed: 14 September 2018).

Ratz, P. H., Callahan, P. E. and Lattanzio, F. A. (1993) 'Ketamine relaxes rabbit femoral arteries by reducing [Ca²⁺]_i and phospholipase C activity', *European Journal of Pharmacology*. Elsevier, 236(3), pp. 433–441. doi: 10.1016/0014-2999(93)90482-W.

Reckler, J. *et al.* (1986) 'Urothelial injury to the rabbit bladder from various alkaline and acidic solutions used to dissolve kidney stones.', *The Journal of urology*, 136(1), pp. 181–3. doi: 10.1016/s0022-5347(17)44767-7.

Ren, L. *et al.* (2016) 'Evaluation of Su Fu'ning lotion's inhibitory effects on bladder cancer

cells in vitro and in vivo by intravesical instillation.', *Integrative cancer therapies*. SAGE Publications, 15(1), pp. 80–6. doi: 10.1177/1534735415596569.

Riedl, C. R. *et al.* (1997) 'Intravesical electromotive drug administration for the treatment of non-infectious chronic cystitis.', *International urogynecology journal and pelvic floor dysfunction*, 8(3), pp. 134–7. doi: 10.1007/bf02764844.

Riedl, C. R. *et al.* (2008) 'Hyaluronan treatment of interstitial cystitis/painful bladder syndrome', *International Urogynecology Journal*, 19(5), pp. 717–721. doi: 10.1007/s00192-007-0515-5.

Roberts, R. O. *et al.* (2003) 'Incidence of physician-diagnosed interstitial cystitis in Olmsted County: a community-based study', *BJU International*. Wiley/Blackwell (10.1111), 91(3), pp. 181–185. doi: 10.1046/j.1464-410X.2003.04060.x.

Van Rodijnen, W. F. *et al.* (2007) 'Direct vasoconstrictor effect of prostaglandin E 2 on renal interlobular arteries: role of the EP3 receptor', *Am J Physiol Renal Physiol*, 292(5), pp. 1094–1101. doi: 10.1152/ajprenal.00351.2005.-Evidence.

Roosen, A. *et al.* (2009) 'Suburothelial myofibroblasts in the human overactive bladder and the effect of Botulinum Neurotoxin type A treatment', *European Urology*. Elsevier, 55(6), pp. 1440–1449. doi: 10.1016/J.EURURO.2008.11.009.

Rosamilia, A., Dwyer, P. L. and Gibson, J. (1997) 'Electromotive drug administration of lidocaine and dexamethasone followed by cystodistension in women with interstitial cystitis', *International Urogynecology Journal*. Springer-Verlag, 8(3), pp. 142–145. doi: 10.1007/BF02764846.

Rosen, R. *et al.* (2003) 'Lower urinary tract symptoms and male sexual dysfunction: the multinational survey of the aging male (MSAM-7)', *European Urology*. Elsevier, 44(6), pp. 637–649. doi: 10.1016/j.eururo.2003.08.015.

Rossi, C. *et al.* (2001) 'α-blockade improves symptoms suggestive of bladder outlet obstruction but fails to relieve it', *Journal of Urology*, 165(1), pp. 38–41. doi: 10.1097/00005392-200101000-00010.

Rudziak, P., Ellis, C. G. and Kowalewska, P. M. (2019) 'Role and molecular mechanisms

of pericytes in regulation of leukocyte diapedesis in inflamed tissues', *Mediators of inflammation*. NLM (Medline), p. 4123605. doi: 10.1155/2019/4123605.

Sadananda, P. *et al.* (2009) 'Release of ATP from rat urinary bladder mucosa: role of acid, vanilloids and stretch.', *British journal of pharmacology*. Wiley-Blackwell, 158(7), pp. 1655–62. doi: 10.1111/j.1476-5381.2009.00431.x.

Sadananda, P., Chess-Williams, R. and Burcher, E. (2008) 'Contractile properties of the pig bladder mucosa in response to neurokinin A: a role for myofibroblasts?', *British journal of pharmacology*. Wiley-Blackwell, 153(7), pp. 1465–73. doi: 10.1038/bjp.2008.29.

Sairanen, J. *et al.* (2009) 'Evaluation of health-related quality of life in patients with painful bladder syndrome/interstitial cystitis and the impact of four treatments on it', *Scandinavian Journal of Urology and Nephrology*. Taylor & Francis, 43(3), pp. 212–219. doi: 10.1080/00365590802671031.

Saito, M. *et al.* (1993) 'Response of the human urinary bladder to angiotensins: a comparison between neurogenic and control bladders.', *The Journal of urology*, 149(2), pp. 408–11. doi: 10.1016/s0022-5347(17)36105-0.

Sakurai, T. *et al.* (1990) 'Cloning of a cDNA encoding a non-isopeptide-selective subtype of the endothelin receptor', *Nature*. Nature Publishing Group, 348(6303), pp. 732–735. doi: 10.1038/348732a0.

Sant, G. R. *et al.* (2003) 'A pilot clinical trial of oral pentosan polysulfate and oral hydroxyzine in patients with interstitial cystitis.', *The Journal of urology*, 170(3), pp. 810–5. doi: 10.1097/01.ju.0000083020.06212.3d.

Sant, G. R. *et al.* (2007) 'The mast cell in interstitial cystitis: role in pathophysiology and pathogenesis', *Urology*. Elsevier, 69(4), pp. S34–S40. doi: 10.1016/J.UROLOGY.2006.08.1109.

Sawada, N. *et al.* (2013) 'Protective effect of a β 3-adrenoceptor agonist on bladder function in a rat model of chronic bladder ischemia', *European Urology*. Elsevier, 64(4), pp. 664–671. doi: 10.1016/j.eururo.2013.06.043.

Schifano, F. *et al.* (2008) 'Trapped in the "K-hole": Overview of deaths associated with ketamine misuse in the UK (1993-2006)', *Journal of Clinical Psychopharmacology*, pp. 114–116. doi: 10.1097/JCP.0b013e3181612cdc.

Scholz, A. *et al.* (1998) 'Complex blockage of TTX-Resistant Na⁺ Currents by lidocaine and bupivacaine reduce firing frequency in DRG Neurons', *Journal of Neurophysiology*. American Physiological Society Bethesda, MD, 79(4), pp. 1746–1754. doi: 10.1152/jn.1998.79.4.1746.

Schröder, A., Newgreen, D. and Andersson, K.-E. (2004) 'Detrusor responses to prostaglandin E2 and bladder outlet obstruction in wild-type and EP1 receptor knockout mice', *The Journal of Urology*. No longer published by Elsevier, 172(3), pp. 1166–1170. doi: 10.1097/01.JU.0000134186.58854.2C.

See, W. A. and Xia, Q. (1992) 'Regional chemotherapy for bladder neoplasms using continuous intravesical infusion of doxorubicin: impact of concomitant administration of dimethyl sulfoxide on drug absorption and antitumor activity.', *Journal of the National Cancer Institute*, 84(7), pp. 510–5. doi: 10.1093/jnci/84.7.510.

De Sèze, M. *et al.* (2004) 'Intravesical capsaicin versus resiniferatoxin for the treatment of detrusor hyperreflexia in spinal cord injured patients: a double-blind, randomized, controlled study', *The Journal of Urology*, 171(1), pp. 251–255. doi: 10.1097/01.ju.0000100385.93801.d4.

Shahani, R. *et al.* (2007) 'Ketamine-associated ulcerative cystitis: A new clinical entity', *Urology*, 69(5), pp. 810–812. doi: 10.1016/j.urology.2007.01.038.

Shan, Z. *et al.* (2018) 'Ketamine induces reactive oxygen species and enhances autophagy in SV-HUC-1 human uroepithelial cells', *Journal of Cellular Physiology*. Wiley-Blackwell. doi: 10.1002/jcp.27094.

Shen, C.-H. *et al.* (2015) 'Biological effect of ketamine in urothelial cell lines and global gene expression analysis in the bladders of ketamine-injected mice.', *Molecular medicine reports*. Spandidos Publications, 11(2), pp. 887–95. doi: 10.3892/mmr.2014.2823.

Shenfeld, O. Z. *et al.* (2005) 'Do atherosclerosis and chronic bladder ischemia really play

a role in detrusor dysfunction of old age?', *Urology*. Elsevier, 65(1), pp. 181–184. doi: 10.1016/J.UROLOGY.2004.08.055.

Shimizu, Y. *et al.* (2014) 'Neurohumoral regulation of spontaneous constrictions in suburothelial venules of the rat urinary bladder', *Vascular Pharmacology*. Elsevier, 60(2), pp. 84–94. doi: 10.1016/J.VPH.2014.01.002.

Short, B. *et al.* (2018) 'Side-effects associated with ketamine use in depression: a systematic review.', *The lancet. Psychiatry*. Elsevier, 5(1), pp. 65–78. doi: 10.1016/S2215-0366(17)30272-9.

Sibley, G. N. (1985) 'An experimental model of detrusor instability in the obstructed pig.', *British journal of urology*, 57(3), pp. 292–8. doi: 10.1111/j.1464-410x.1985.tb06347.x.

Sihra, N., Ockrim, J. and Wood, D. (2018) 'The effects of recreational ketamine cystitis on urinary tract reconstruction - a surgical challenge', *BJU International*. Wiley/Blackwell (10.1111), 121(3), pp. 458–465. doi: 10.1111/bju.14094.

Simonato, A. *et al.* (2003) 'Laparoscopic radical cystoprostatectomy: A technique illustrated step by step', *European Urology*. Elsevier, 44(1), pp. 132–138. doi: 10.1016/S0302-2838(03)00214-8.

Singh, P. and Roberts, M. S. (1994) 'Dermal and underlying tissue pharmacokinetics of lidocaine after topical application', *Journal of Pharmaceutical Sciences*. Elsevier, 83(6), pp. 774–782. doi: 10.1002/JPS.2600830604.

Smith, S. D. *et al.* (1996) 'Urinary nitric oxide synthase activity and cyclic GMP levels are decreased with interstitial cystitis and increased with urinary tract infections', *The Journal of Urology*. Elsevier, 155(4), pp. 1432–1435. doi: 10.1016/S0022-5347(01)66301-8.

Sohn, J.-T. and Murray, P. A. (2003) 'Inhibitory effects of etomidate and ketamine on adenosine triphosphate-sensitive potassium channel relaxation in canine pulmonary artery', *Anesthesiology: The Journal of the American Society of Anesthesiologists*. The American Society of Anesthesiologists, 98(1), pp. 104–113. doi: 0000542-200301000-00019.

Soler, R. *et al.* (2013) 'Future direction in pharmacotherapy for non-neurogenic male lower urinary tract symptoms', *European Urology*. Elsevier, 64(4), pp. 610–621. doi: 10.1016/j.eururo.2013.04.042.

Song, D., Wientjes, M. G. and Au, J. L.-S. (1997) 'Bladder tissue pharmacokinetics of intravesical taxol', *Cancer Chemotherapy and Pharmacology*. Springer-Verlag, 40(4), pp. 285–292. doi: 10.1007/s002800050660.

Song, M. *et al.* (2016) 'The fibrosis of ketamine, a noncompetitive N -methyl- d -aspartic acid receptor antagonist dose-dependent change in a ketamine-induced cystitis rat model', *Drug and Chemical Toxicology*. Taylor & Francis, 39(2), pp. 206–212. doi: 10.3109/01480545.2015.1079916.

Di Stasi, Savino M. *et al.* (1997) 'Electromotive administration of oxybutynin into the human bladder wall', *The Journal of Urology*. Elsevier, 158(1), pp. 228–233. doi: 10.1097/00005392-199707000-00076.

Di Stasi, S M *et al.* (1997) 'Electromotive delivery of mitomycin C into human bladder wall.', *Cancer research*. American Association for Cancer Research, 57(5), pp. 875–80. Available at: <http://www.ncbi.nlm.nih.gov/pubmed/9041189> (Accessed: 12 November 2018).

Di Stasi, S. M. *et al.* (2003) 'The stability of lidocaine and epinephrine solutions exposed to electric current and comparative administration rates of the two drugs into pig bladder wall', *Urological Research*, 31(3), pp. 169–176. doi: 10.1007/s00240-003-0310-9.

Steidle, C. P., Cohen, M. L. and Neubauer, B. L. (1990) 'Bradykinin-induced contractions of canine prostate and bladder: effect of angiotensin-converting enzyme inhibition.', *The Journal of urology*, 144(2 Pt 1), pp. 390–2. doi: 10.1016/s0022-5347(17)39467-3.

Stein, P., Rajasekaran, M. and Parsons, C. L. (2005) 'Tamm-Horsfall protein protects urothelial permeability barrier', *Urology*. Elsevier, 66(4), pp. 903–907. doi: 10.1016/J.UROLOGY.2005.05.021.

Steiner, C. *et al.* (2018) 'Comparative immunohistochemical characterization of interstitial cells in the urinary bladder of human, guinea pig and pig', *Histochemistry and*

Cell Biology. Springer Berlin Heidelberg, 149(5), pp. 491–501. doi: 10.1007/s00418-018-1655-z.

Steinhoff, G., Ittah, B. and Rowan, S. (2002) 'The efficacy of chondroitin sulfate 0.2% in treating interstitial cystitis.', *The Canadian journal of urology*, 9(1), pp. 1454–8. Available at: <http://www.ncbi.nlm.nih.gov/pubmed/11886599>.

Storr, T. and Quibell, R. (2009) 'Can ketamine prescribed for pain cause damage to the urinary tract?', *Palliative Medicine*. SAGE PublicationsSage UK: London, England, 23(7), pp. 670–672. doi: 10.1177/0269216309106828.

Sui, G.-P. *et al.* (2008) 'Modulation of bladder myofibroblast activity: implications for bladder function.', *American journal of physiology. Renal physiology*. American Physiological Society, 295(3), pp. F688-97. doi: 10.1152/ajprenal.00133.2008.

Sui, G. P. *et al.* (2002) 'Gap junctions and connexin expression in human suburothelial interstitial cells', *BJU International*. Wiley/Blackwell (10.1111), 90(1), pp. 118–129. doi: 10.1046/j.1464-410X.2002.02834.x.

Sun, Y. *et al.* (2002) 'Effect of doxazosin on stretch-activated adenosine triphosphate release in bladder urothelial cells from patients with benign prostatic hyperplasia', *Urology*. Elsevier, 60(2), pp. 351–356. doi: 10.1016/S0090-4295(02)01710-7.

Sunagawa, M. *et al.* (2015) 'Urinary bladder mucosal responses to ischemia.', *World journal of urology*. NIH Public Access, 33(2), pp. 275–80. doi: 10.1007/s00345-014-1298-1.

Takeda, H. *et al.* (2002) 'Effects of B3-adrenoceptor stimulation on prostaglandin E2-induced bladder hyperactivity and on the cardiovascular system in conscious rats', *Neurourology and Urodynamics*. John Wiley & Sons, Ltd, 21(6), pp. 558–565. doi: 10.1002/nau.10034.

Tam, Y. *et al.* (2016) 'Population-based survey of the prevalence of lower urinary tract symptoms in adolescents with and without psychotropic substance abuse', *Hong Kong Medical Journal*. doi: 10.12809/hkmj154806.

Tammela, T. *et al.* (1993) 'Urothelial permeability of the isolated whole bladder',

Neurourology and Urodynamics. Wiley Subscription Services, Inc., A Wiley Company, 12(1), pp. 39–47. doi: 10.1002/nau.1930120106.

Tanabe, N., Ueno, A. and Tsujimoto, G. (1993) 'Angiotensin II Receptors in the rat urinary bladder smooth muscle: Type 1 subtype receptors mediate contractile responses', *The Journal of Urology*. No longer published by Elsevier, 150(3), pp. 1056–1059. doi: 10.1016/S0022-5347(17)35685-9.

Tanaka, E. *et al.* (2016) 'Lidocaine concentration in oral tissue by the addition of epinephrine.', *Anesthesia progress*, 63(1), pp. 17–24. doi: 10.2344/15-00003R2.1.

Taneja, R. (2010) 'Intravesical lignocaine in the diagnosis of bladder pain syndrome.', *International urogynecology journal*, 21(3), pp. 321–4. doi: 10.1007/s00192-009-1045-0.

Tarcan *et al.* (1998) 'Age-related erectile and voiding dysfunction: the role of arterial insufficiency', *BJU International*. John Wiley & Sons, Ltd (10.1111), 82(S1), pp. 26–33. doi: 10.1046/j.1464-410X.1998.0820s1026.x.

Tatematsu, M. *et al.* (1978) *Neovascularization in benign and malignant urinary bladder epithelial proliferative lesions of the rat observed in situ by scanning electron microscopy and autoradiography* 1. Available at: <http://cancerres.aacrjournals.org/content/38/6/1792.full-text.pdf> (Accessed: 1 August 2018).

Teichman, J. M., Nielsen-Omeis, B. J. and McIver, B. D. (1997) 'Modified urodynamics for interstitial cystitis.', *Techniques in urology*, 3(2), pp. 65–8. Available at: <http://www.ncbi.nlm.nih.gov/pubmed/9297763> (Accessed: 8 July 2019).

De Tejada, I. S. *et al.* (1992) 'Endothelin in the urinary bladder. i. synthesis of endothelin-1 by epithelia, smooth muscle and fibroblasts suggests autocrine and paracrine cellular regulation', *The Journal of Urology*, 148(4), pp. 1290–1298. doi: 10.1016/S0022-5347(17)36895-7.

Templeman, L. *et al.* (2003) 'Investigation of neurokinin-2 and -3 receptors in the human and pig bladder', *BJU International*. John Wiley & Sons, Ltd (10.1111), 92(7), pp. 787–792. doi: 10.1046/j.1464-410X.2003.04458.x.

Theoharides, T. C., Kempuraj, D. and Sant, G. R. (2001) 'Mast cell involvement in interstitial cystitis: a review of human and experimental evidence', *Urology*. Elsevier, 57(6), pp. 47–55. doi: 10.1016/S0090-4295(01)01129-3.

Thrasher, J. B. *et al.* (1993) 'Lidocaine as topical anesthesia for bladder mappings and cold-cup biopsies.', *The Journal of urology*, 150(2 Pt 1), pp. 335–6. doi: 10.1016/s0022-5347(17)35477-0.

Tobu, S. *et al.* (2012) 'Changes in angiotensin II type 1 receptor expression in the rat bladder by bladder outlet obstruction', *Urologia Internationalis*. Karger Publishers, 89(2), pp. 241–245. doi: 10.1159/000339373.

Tobu, S. *et al.* (2013) 'Upregulation of angiotensin II receptor and connexin 43 in increased suburothelial myofibroblasts in the rat inflammatory bladder', *LUTS: Lower Urinary Tract Symptoms*, 5(2), pp. 90–95. doi: 10.1111/j.1757-5672.2012.00167.x.

Tringali, G. *et al.* (2008) 'The in vitro rabbit whole bladder as a model to investigate the urothelial transport of anticancer agents: The ONCOFID-P® paradigm', *Pharmacological Research*. Academic Press, 58(5–6), pp. 340–343. doi: 10.1016/J.PHRS.2008.09.008.

Tsai, T.-H. *et al.* (2009) 'Ketamine-associated bladder dysfunction', *International Journal of Urology*. Wiley/Blackwell (10.1111), 16(10), pp. 826–829. doi: 10.1111/j.1442-2042.2009.02361.x.

Tsai, Y. C., Birder, L. and Kuo, H.-C. (2016) 'Abnormal sensory protein expression and urothelial dysfunction in ketamine-related cystitis in humans.', *International neurourology journal*. Korean Continence Society, 20(3), pp. 197–202. doi: 10.5213/inj.1632634.317.

Tsai, Y. C. and Kuo, H.-C. (2015) 'Ketamine cystitis: Its urological impact and management', *Urological Science*, 26(3), pp. 153–157. doi: 10.1016/J.UROLS.2014.11.003.

Tsallas, A., Jackson, J. and Burt, H. (2011) 'The uptake of paclitaxel and docetaxel into ex vivo porcine bladder tissue from polymeric micelle formulations', *Cancer Chemotherapy and Pharmacology*. Springer-Verlag, 68(2), pp. 431–444. doi: 10.1007/s00280-010-1499-2.

Tyagi, P. *et al.* (2006) 'Local drug delivery to bladder using technology innovations', *Urologic Clinics of North America*. Elsevier, 33(4), pp. 519–530. doi: 10.1016/J.UCL.2006.06.012.

Tyagi, P. *et al.* (2009) 'Investigations into the presence of functional Beta1, Beta2 and Beta3-adrenoceptors in urothelium and detrusor of human bladder.', *International braz j urol: official journal of the Brazilian Society of Urology*, 35(1), pp. 76–83. doi: 10.1590/s1677-55382009000100012.

Tyagi, P. *et al.* (2016) 'Advances in intravesical therapy for urinary tract disorders', *Expert Opinion on Drug Delivery*, 13(1), pp. 71–84. doi: 10.1517/17425247.2016.1100166.

Tyagi, S. *et al.* (2006) 'Qualitative and quantitative expression profile of muscarinic receptors in human urothelium and detrusor', *The Journal of Urology*. Elsevier, 176(4), pp. 1673–1678. doi: 10.1016/J.JURO.2006.06.088.

Tyler, M. W. *et al.* (2017) 'Classics in chemical neuroscience: Ketamine', *ACS Chemical Neuroscience*. American Chemical Society, 8(6), pp. 1122–1134. doi: 10.1021/acscchemneuro.7b00074.

U.S. Food and Drug Administration (no date) *FDA approves new nasal spray medication for treatment-resistant depression; available only at a certified doctor's office or clinic | FDA*. Available at: <https://www.fda.gov/news-events/press-announcements/fda-approves-new-nasal-spray-medication-treatment-resistant-depression-available-only-certified> (Accessed: 29 July 2019).

Uhl, E. *et al.* (1994) 'Influence of ketamine and pentobarbital on microvascular perfusion in normal skin and skin flaps.', *International journal of microcirculation, clinical and experimental*, 14(5), pp. 308–12. doi: 10.1159/000178847.

United States Pharmacopeia and National Formulary (2006) *United States Pharmacopeia and National Formulary (USP 29-NF 24)*. Available at: http://www.pharmacopeia.cn/v29240/usp29nf24s0_m43960.html (Accessed: 4 December 2019).

Uzun, H. *et al.* (2013) 'Increased pulse-wave velocity and carotid intima–media thickness in patients with lower urinary tract symptoms', *Scandinavian Journal of Urology*. Taylor

& Francis, 47(5), pp. 393–398. doi: 10.3109/21681805.2013.780185.

Vickers, B. A., Lee, W. and Hunsberger, J. (2017) 'A case report: subanesthetic ketamine infusion for treatment of cancer-related pain produces urinary urge incontinence.', *A & A case reports*, 8(9), pp. 219–221. doi: 10.1213/XAA.0000000000000472.

Vij, M., Srikrishna, S. and Cardozo, L. (2012) 'Interstitial cystitis: diagnosis and management', *European Journal of Obstetrics & Gynecology and Reproductive Biology*, 161(1), pp. 1–7. doi: 10.1016/j.ejogrb.2011.12.014.

Vouri, S. M. *et al.* (2017) 'Adverse events and treatment discontinuations of antimuscarinics for the treatment of overactive bladder in older adults: A systematic review and meta-analysis', *Archives of Gerontology and Geriatrics*, 69, pp. 77–96. doi: 10.1016/j.archger.2016.11.006.

Wakabayashi, Y. *et al.* (1993) 'Substance P-containing axon terminals in the mucosa of the human urinary bladder: pre-embedding immunohistochemistry using cryostat sections for electron microscopy.', *Histochemistry*, 100(6), pp. 401–7. doi: 10.1007/bf00267819.

Waldeck, K. *et al.* (1997) 'Characterization of angiotensin II formation in human isolated bladder by selective inhibitors of ACE and human chymase: a functional and biochemical study.', *British journal of pharmacology*. Wiley-Blackwell, 121(6), pp. 1081–6. doi: 10.1038/sj.bjp.0701240.

Walden, P. D. *et al.* (1997) 'Localization of mRNA and receptor binding sites for the alpha 1a-adrenoceptor subtype in the rat, monkey and human urinary bladder and prostate.', *The Journal of urology*, 157(3), pp. 1032–8. doi: [https://doi.org/10.1016/S0022-5347\(01\)65136-X](https://doi.org/10.1016/S0022-5347(01)65136-X).

Wang, Q. *et al.* (2017) 'Ketamine analog methoxetamine induced inflammation and dysfunction of bladder in rats.', *International journal of molecular sciences*. Multidisciplinary Digital Publishing Institute (MDPI), 18(1). doi: 10.3390/ijms18010117.

Wang, X. *et al.* (2008) 'Urothelium EP1 receptor facilitates the micturition reflex in mice.', *Biomedical research (Tokyo, Japan)*, 29(2), pp. 105–11. doi: 10.2220/biomedres.29.105.

Wein, A. *et al.* (2003) 'Prevalence and burden of overactive bladder in the United States', *World J Urol.* Springer-Verlag. doi: 10.1007/s00345-002-0301-4.

Welk, B. K. and Teichman, J. M. H. (2008) 'Dyspareunia response in patients with interstitial cystitis treated with intravesical lidocaine, bicarbonate, and heparin', *Urology.* Elsevier, 71(1), pp. 67–70. doi: 10.1016/J.UROLOGY.2007.09.067.

Westropp, J. L. and Buffington, C. A. T. (2002) 'In vivo models of interstitial cystitis.', *The Journal of urology*, 167(2 Pt 1), pp. 694–702. doi: 10.1097/00005392-200202000-00068.

Wildman, S. S. *et al.* (2020) 'A novel functional role for the classic CNS neurotransmitters, GABA, glycine and glutamate, in the kidney: potent and opposing regulators of renal blood flow', *under review*.

Williams, N. A. *et al.* (2014) 'An ex vivo investigation into the transurothelial permeability and bladder wall distribution of the nonsteroidal anti-inflammatory ketorolac', *Molecular Pharmaceutics*, 11(3), pp. 673–682. doi: 10.1021/mp400274z.

Williams, N. A. *et al.* (2015) 'Investigating detrusor muscle concentrations of oxybutynin after intravesical delivery in an ex vivo porcine model', *Journal of Pharmaceutical Sciences*, 104(7), pp. 2233–2240. doi: 10.1002/jps.24471.

Williams, N. A. *et al.* (2016) 'Evidence of nonuniformity in urothelium barrier function between the upper urinary tract and bladder.', *The Journal of urology*, 195(3), pp. 763–770. doi: 10.1016/j.juro.2015.10.066.

Winstock, A. R. *et al.* (2012) 'The prevalence and natural history of urinary symptoms among recreational ketamine users', *BJU International.* Blackwell Publishing Ltd, 110(11), pp. 1762–1766. doi: 10.1111/j.1464-410X.2012.11028.x.

Winstock, A. R. (2019) *Global Drug Survey - Key Findings report.* Available at: <https://www.globaldrugsurvey.com/> (Accessed: 17 July 2019).

Wiseman, O. J. *et al.* (2002) 'The ultrastructure of bladder lamina propria nerves in healthy subjects and patients with detrusor hyperreflexia', *The Journal of Urology.* Elsevier, 168(5), pp. 2040–2045. doi: 10.1016/S0022-5347(05)64291-7.

Wiseman, O. J., Fowler, C. J. and Landon, D. N. (2003) 'The role of the human bladder

lamina propria myofibroblast', *BJU International*. Wiley/Blackwell (10.1111), 91(1), pp. 89–93. doi: 10.1046/j.1464-410X.2003.03802.x.

Wood, D. *et al.* (2011) 'Recreational ketamine: from pleasure to pain', *BJU International*. Blackwell Publishing Ltd, 107(12), pp. 1881–1884. doi: 10.1111/j.1464-410X.2010.10031.x.

World Drug Report (2019). Available at: <https://wdr.unodc.org/wdr2019/> (Accessed: 17 July 2019).

Wyndaele, J. . and Wachter, S. D. (2002) 'Cystometrical sensory data from a normal population: comparison of two groups of young healthy volunteers examined with 5 years interval', *European Urology*. Elsevier, 42(1), pp. 34–38. doi: 10.1016/S0302-2838(02)00221-X.

Xiao, Z. *et al.* (2014) 'Somatic modulation of spinal reflex bladder activity mediated by nociceptive bladder afferent nerve fibers in cats.', *American journal of physiology. Renal physiology*. American Physiological Society, 307(6), pp. F673-9. doi: 10.1152/ajprenal.00308.2014.

Xu, D. *et al.* (2018) 'Ketamine delays progression of oxidative and damaged cataract through regulating HMGB-1/NF-κB in lens epithelial cells', *Immunopharmacology and Immunotoxicology*. Taylor & Francis, pp. 1–6. doi: 10.1080/08923973.2018.1478851.

Yamada, S. *et al.* (2009) 'Bladder angiotensin-II receptors: characterization and alteration in bladder outlet obstruction.', *European urology*. Elsevier, 55(2), pp. 482–9. doi: 10.1016/j.eururo.2008.03.015.

Yamazaki, M. *et al.* (1992) 'Effects of ketamine on voltage-dependent Ca²⁺ currents in single smooth muscle cells from rabbit portal vein', *Pharmacology*. Karger Publishers, 45(3), pp. 162–169. doi: 10.1159/000138994.

Yamazaki, M. *et al.* (1995) 'The vasodilatory effects of ketamine on isolated rabbit portal veins', *Pharmacology & Toxicology*. John Wiley & Sons, Ltd (10.1111), 76(1), pp. 3–8. doi: 10.1111/j.1600-0773.1995.tb00094.x.

Yanagisawa, M. *et al.* (1988) 'A novel potent vasoconstrictor peptide produced by

vascular endothelial cells', *Nature*. Nature Publishing Group, 332(6163), pp. 411–415. doi: 10.1038/332411a0.

Yanase, H. *et al.* (2008) 'The involvement of urothelial α 1A adrenergic receptor in controlling the micturition reflex', *Biomedical Research*. Biomedical Research Press, 29(5), pp. 239–244. doi: 10.2220/biomedres.29.239.

Yang, H.-H., Zhai, W.-J. and Kuo, H.-C. (2017) 'The putative involvement of actin-binding proteins and cytoskeleton proteins in pathological mechanisms of ketamine cystitis- Revealed by a prospective pilot study using proteomic approaches', *PROTEOMICS - Clinical Applications*, 11(3–4), p. 1600085. doi: 10.1002/prca.201600085.

Yee, C.-H. *et al.* (2017) 'The risk of upper urinary tract involvement in patients with ketamine-associated uropathy.', *International neurourology journal*. Korean Continence Society, 21(2), pp. 128–132. doi: 10.5213/inj.1732704.352.

Yee, C. *et al.* (2015) 'Clinical outcome of a prospective case series of patients with ketamine cystitis who underwent standardized treatment protocol', *Urology*. Elsevier, 86(2), pp. 236–243. doi: 10.1016/J.UROLOGY.2015.05.003.

Yee, C. *et al.* (2016) 'Ketamine-associated uropathy: from presentation to management', *Current Bladder Dysfunction Reports*. Springer US, 11(3), pp. 266–271. doi: 10.1007/s11884-016-0380-5.

Yeung, L. Y. *et al.* (2009) 'Mice are prone to kidney pathology after prolonged ketamine addiction', *Toxicology Letters*. Elsevier, 191(2–3), pp. 275–278. doi: 10.1016/J.TOXLET.2009.09.006.

Yokoyama, O. *et al.* (1997) 'Urodynamic effects of intravesical instillation of lidocaine in patients with overactive detrusor', *The Journal of Urology*. Elsevier, 157(5), pp. 1826–1830. doi: 10.1016/S0022-5347(01)64870-5.

Yokoyama, O. *et al.* (2000) 'Diagnostic value of intravesical lidocaine for overactive bladder', *The Journal of Urology*. Elsevier, 164(2), pp. 340–343. doi: 10.1016/S0022-5347(05)67355-7.

Yokoyama, O. *et al.* (2006) 'Improvement of bladder storage function by α 1-blocker

depends on the suppression of C-fiber afferent activity in rats', *Neurourology and Urodynamics*. John Wiley & Sons, Ltd, 25(5), pp. 461–467. doi: 10.1002/nau.20253.

Yokoyama, O. *et al.* (2007) 'Improvement in bladder storage function by tamsulosin depends on suppression of c-fiber urethral afferent activity in rats', *Journal of Urology*, 177(2), pp. 771–775. doi: 10.1016/j.juro.2006.09.076.

Yoshida, M. *et al.* (2006) 'Non-neuronal cholinergic system in human bladder urothelium', *Urology*. Elsevier, 67(2), pp. 425–430. doi: 10.1016/J.UROLOGY.2005.08.014.

Yoshida, M. *et al.* (2010) 'The effects of chronic hyperlipidemia on bladder function in myocardial infarction-prone Watanabe heritable hyperlipidemic (WHHLMI) rabbits', *Neurourology and Urodynamics*. John Wiley & Sons, Ltd, 29(7), pp. 1350–1354. doi: 10.1002/nau.20843.

Zanos, P. *et al.* (2018) 'Ketamine and ketamine metabolite pharmacology: insights into therapeutic mechanisms.', *Pharmacological reviews*. American Society for Pharmacology and Experimental Therapeutics, 70(3), pp. 621–660. doi: 10.1124/pr.117.015198.

Zeng, H. *et al.* (2016) 'LPS causes pericyte loss and microvascular dysfunction via disruption of Sirt3/angiopoietins/Tie-2 and HIF-2 α /Notch3 pathways', *Scientific Reports*. Nature Publishing Group, 6. doi: 10.1038/srep20931.

Zhang, C.-O. *et al.* (2005) 'Regulation of tight junction proteins and bladder epithelial paracellular permeability by an antiproliferative factor from patients with interstitial cystitis', *The Journal of Urology*. Elsevier, 174(6), pp. 2382–2387. doi: 10.1097/01.JU.0000180417.11976.99.

Zhang, Q. *et al.* (2014) 'Effects of ischemia and oxidative stress on bladder purinoceptors expression', *Urology*. Elsevier, 84(5), pp. 1249.e1-1249.e7. doi: 10.1016/J.UROLOGY.2014.07.023.

Zhang, W. *et al.* (2016) 'Intravesical treatment for interstitial cystitis/painful bladder syndrome: a network meta-analysis', *International Urogynecology Journal*. Springer London, pp. 1–11. doi: 10.1007/s00192-016-3079-4.

Zhao, Z. *et al.* (2016) 'Progressive changes in detrusor function and micturition patterns with chronic bladder ischemia', *Investigative and Clinical Urology*. Korean Urological Association, 57(4), p. 249. doi: 10.4111/ICU.2016.57.4.249.